



The University of
Nottingham

UNITED KINGDOM • CHINA • MALAYSIA

A New Classification System for Biomass and
Waste Materials for their use in Combustion

Philip Jenkinson BSc (Hons)

Thesis submitted to the University of Nottingham
for the degree of Doctor of Engineering

September 2015

Abstract

The use of biomass derived solid fuels for electricity generation in combustion, gasification and pyrolysis plant has received increasing levels of interest for commercial operation in recent years. However, there are limited tools available which allow a prediction of the performance of these fuels during thermochemical transformation given an understanding of their original chemical structure.

As such, this investigation has concentrated on the derivation of a simply utilised classification system able to predict a series of important fuel combustion characteristics given an understanding of both the organic and inorganic chemical and structural composition of any lignocellulosic biomass fuel. A prediction of volatile matter content and char yields during pyrolysis has been made using correlation with aromatic carbon, potassium and calcium contents using both thermogravimetric slow heating and simulated pulverised fuel (PF) entrained flow rapid heating. Alongside this, investigation of the impact of biomass composition, namely aromaticity and alkali/alkaline earth metal concentrations, on char structure and oxidative char reactivity of simulated PF chars has been conducted.

Experimental investigation has involved the pre-treatment of a wide range of commercially available biomass fuels including softwood, hardwood, herbaceous and agricultural waste materials to remove both lignin and ion exchangeable mineral species. In addition to this, torrefaction has been utilised to increase the aromatic character of chosen fuels. This has allowed a quantification of the impact of aromaticity and mineral matter concentration on pyrolysis and char combustion reactions to be derived for a wide range of fuel aromaticity and mineral matter contents.

Considerable success has been achieved in the classification of an array of lignocellulosic biomass. Accurate prediction of pyrolysis char and volatile matter yields under both slow and rapid entrained flow drop tube heating conditions have been attained using simple empirical correlations with fuel aromatic carbon and alkali/alkaline earth mineral species concentrations (K+Ca being utilised here).

This classification system has relied upon the clear linear correlation observed between aromatic carbon content and char yield in the absence of mineral matter influences (R^2 of 0.98 and 0.95 being observed for demineralised biomass under slow and rapid heating pyrolysis respectively). In addition to this, the relative enhancement of char yield due to mineral matter interaction with varying concentration of K and Ca within the fuel has been quantified and is used to calculate total char yields. The empirical relationship derived under slow heating takes the following form:

$$\text{Slow Heating Char Yield} = (1 \times \text{Aromatic Carbon}) + (16.1 \times (K + Ca))$$

Where slow heating char yield is the char yield wt% on a dry ash free basis (daf), aromatic carbon is the wt% daf aromatic carbon content of the biomass and K+Ca is the wt% K+Ca content of the raw fuel on a dry basis.

This relationship applies below K+Ca contents of 0.6 wt% db, beyond this a fixed additional char yield of 9.76 wt% daf can be applied as a quantification of the influence of enhanced char yield due to mineral activity as the second term in the above equation.

For rapid heating entrained flow pyrolysis the empirical prediction of char yield is conducted as follows:

$$\text{Rapid Heating Char Yield} = (0.58 \times \text{Aromatic Carbon}) + (2.43 \times (K + Ca))$$

Strong linear correlations of predicted vs. observed char yield have been derived with correlation coefficient $R^2 = 0.96$ and 0.99 with mean relative errors of 7.8 and 8.4% for slow and rapid heating pyrolysis respectively.

Furthermore, the influence of biomass aromaticity and active mineral content on char formation processes, the form of chars generated under PF like devolatilisation conditions and their subsequent oxidation reactivity has been studied in detail. Both alkali/alkaline earth mineral matter content (primarily K and Ca) and aromaticity are instrumental in determining the porosity, morphology and surface area of simulated PF chars. Due to its tendency to soften during heat treatment lignin is shown to produce low surface area, non-porous chars under slow heating and this behaviour drives a reduction in char surface area and combustion reactivity with increasing aromatic carbon content. Although char surface areas have been seen to be negatively correlated with increasing potassium and calcium content this may be due to ash blockage of char pore structures. However, the likelihood of a negative impact of mineral enhanced charring has been discussed. K catalysis of combustion reactions is clearly evident in apparent and inherent char reactivities; however, easy quantitative assessment of this influence has been prevented by the clear complexity of mineral behaviour during the pyrolysis process. The development of char structure and reactivity as a function of char combustion degree has also been investigated under entrained flow combustion conditions.

The results of this study indicate that by accurately quantifying aromatic carbon, potassium and calcium contents, all lignocellulosic fuels can be classified in terms of their behaviour during pyrolysis (volatile matter and char yields), the form of char structures generated (surface area and porosity) and char combustion reactivity. It is hoped that this relative classification will shed light on the predicted performance of

biomass fuels for use in combustion driven power generation infrastructure, especially in pulverised fuel applications.

Acknowledgements

The production of this body of work has most certainly not been achieved in isolation and this leaves many varied parties to thank for all their help on this long road of discovery.

I would first and foremost like to thank my beautiful and supportive wife Nicola for her support over the past four years, her constant encouragement and open ears (there is not much she doesn't know about the char combustion processes of solid fuels!). I much appreciate the support of the rest of my family in getting me here.

I would like to thank all of my friends at the Engineering Doctoral Training Centre in Efficient Fossil Energy Technologies (affectionately known as EFET) at the University of Nottingham for their varied insights into my work and unending interest – I wish all of you the best of luck in the future. Special thanks must go to Dr Umair Hussain who aided me in the preparation of torrefied fuel samples and SEM image capturing.

Thanks must also go to my hard working supervisory team without whose broad knowledge and hard earned experience this work would never have taken the form it does today, this is with special regard to Professor Colin E. Snape, Professor John W. Patrick and Mr. Karl Bindemann.

I must also extend my gratitude to the rest of the scientific community with interest in coal and biomass combustion for the varied opportunities you have offered me to learn from others whilst presenting my work to a wider audience. My sponsors BF2RA have been indispensable in this regard.

Contents

ABSTRACT	I
ACKNOWLEDGEMENTS	V
CHAPTER 1: INTRODUCTION	1
1.1. BACKGROUND	1
1.2. RATIONALE	3
CHAPTER 2: LITERATURE REVIEW	6
2.1. SOLID FUEL COMBUSTION PROCESSES AND THEIR IMPORTANCE	6
2.1.1. DEVOLATILISATION	8
2.1.2. CHAR FORMATION	11
2.1.3. CHAR OXIDATION	13
2.2. COAL: ITS NATURE, COMBUSTION BEHAVIOUR AND CLASSIFICATION	16
2.2.1. THE NATURE OF COAL	16
2.2.2. THE MACERAL CONCEPT	18
2.2.3. CLASSIFICATION OF COAL COMBUSTION	19
2.2.4. THE IMPORTANCE OF AROMATIC CARBON CONTENT	22
2.3. REQUIREMENT FOR A NEW CLASSIFICATION SYSTEM FOR BIOMASS AND WASTE	
MATERIALS FOR USE IN COMBUSTION	24
2.4. BIOMASS; ITS NATURE, COMBUSTION BEHAVIOUR AND CLASSIFICATION	25
2.4.1. THE NATURE OF BIOMASS	25
2.4.2. CELLULOSE:	30
2.4.3. HEMICELLULOSE:	32
2.4.4. LIGNIN:	33
2.5. THERMOCHEMICAL CONVERSION PROCESSES OF BIOMASS	36
2.5.1. HEMICELLULOSE PYROLYSIS	36

2.5.2.	CELLULOSE PYROLYSIS.....	37
2.5.3.	LIGNIN PYROLYSIS.....	39
2.5.4.	SUMMARY.....	42
2.6.	BIOMASS CHAR FORMATION AND COMBUSTION	43
2.6.1.	BIOMASS CHAR FORMATION.....	43
2.6.2.	EVOLUTION OF FLUIDITY.....	48
2.7.	BIOMASS UPGRADING AND COMPOSITION (TORREFACTION AND HYDROTHERMAL UPGRADING)	51
2.8.	INORGANIC MATTER AND ITS IMPACT	53
2.8.1.	AAEM INFLUENCE ON DEVOLATILISATION PROCESSES	53
2.8.2.	AAEM INFLUENCE ON CHAR FORMATION AND OXIDATION	55
2.8.3.	INORGANIC CONSTITUENT DYNAMICS AND THEIR IMPACT.....	58
2.9.	SUMMARY OF FINDINGS	61
2.10.	PROJECT AIMS AND OBJECTIVES	62
	CHAPTER 3: MATERIALS AND METHODOLOGY	64
3.1.	FUEL SELECTION AND PREPARATION	64
3.1.1	RAW FUEL SELECTION	65
3.1.2	CHEMICAL DELIGNIFICATION.....	69
3.1.3	DEMINERALISATION	72
3.1.4	TORREFACTION	73
3.1.5.	MILLING AND SIZING.....	74
3.2.	FUEL CHARACTERISATION	75
3.2.1.	ELEMENTAL ANALYSIS	75
3.2.2.	MINERAL MATTER QUANTIFICATION.....	77
3.2.3.	AROMATICITY BY SOLID STATE CP-MAS ¹³ C NMR	78

3.3. CHAR GENERATION AND COMBUSTION ANALYSIS.....	82
3.3.1. THERMOGRAVIMETRIC ANALYSIS (TGA)	82
3.3.1.1. TGA Slow Pyrolysis Char Preparation	82
3.3.1.2. Non-isothermal Combustion Profiling	84
3.3.2. HTF CHAR GENERATION	84
3.3.3. ENTRAINED FLOW DROP TUBE FURNACE (DTF)	85
3.3.3.1. Gas Supply System	87
3.3.3.2. Heating System	90
3.3.3.3. Water Cooled Feeder and Collector Probes	91
3.3.4. DTF CHAR GENERATION.....	92
3.3.5. DTF CHAR RE-FIRING.....	94
3.4. CHAR CHARACTERISATION	96
3.4.1. CHAR REACTIVITY	96
3.4.2. BET SURFACE AREA ANALYSIS	100
3.4.3. CHAR MORPHOLOGY ASSESSMENT BY OPTICAL MICROSCOPY	102
CHAPTER 4: BASIC FUEL CHARACTERISATION	104
4.1. ELEMENTAL ANALYSIS (C, H, N, O).....	104
4.1.1. IMPACT OF ORGANOSOLV DELIGNIFICATION ON ELEMENTAL COMPOSITION	107
4.1.2. IMPACT OF ACID DEMINERALISATION ON ELEMENTAL COMPOSITION	111
4.1.3. IMPACT OF TORREFACTION ON ELEMENTAL COMPOSITION.....	112
4.2. ASH CONTENT AND SPECIATION	114
4.2.1. IMPACT OF ORGANOSOLV DELIGNIFICATION ON INORGANIC CHEMICAL COMPOSITION	115
4.2.2. IMPACT OF ACID DEMINERALISATION ON INORGANIC CHEMICAL COMPOSITION	116
4.2.3. IMPACT OF TORREFACTION ON INORGANIC CHEMICAL COMPOSITION	116
4.3. AROMATIC CARBON CONTENT BY ¹³C NMR SPECTROSCOPY	117
4.3.1. IMPACT OF ORGANOSOLV DELIGNIFICATION ON AROMATIC CARBON CONTENT	119

4.3.2.	IMPACT OF ACID DEMINERALISATION ON AROMATIC CARBON CONTENT	119
4.3.3.	IMPACT OF TORREFACTION ON AROMATIC CARBON CONTENT	120
4.4.	SUMMARY	120
CHAPTER 5: BIOMASS SAMPLE PREPARATION METHODS.....		122
5.1.	ORGANOSOLV DELIGNIFICATION	122
5.1.1.	AROMATIC CARBON BALANCES OF ORGANOSOLV FRACTIONATION USING ¹³ C NMR	123
5.2.	TORREFACTION	129
5.3.	HCL WASHING AND PARTIAL DEMINERALISATION	144
5.4.	SUMMARY	145
CHAPTER 6: PREDICATION OF PYROLYSIS CHAR YIELDS		147
6.1.	TGA SLOW HEATING PYROLYSIS CHAR YIELD.....	147
6.2.	DTF RAPID HEATING PYROLYSIS CHAR YIELD.....	164
6.3.	SUMMARY	179
CHAPTER 7: CHAR CHARACTERISATION		181
7.1.	HTF CHAR MORPHOLOGY AND SURFACE AREA	181
7.2.	DTF CHAR MORPHOLOGY AND BET SURFACE AREA	183
7.3.	SUMMARY	207
CHAPTER 8: COMBUSTION BEHAVIOUR AND CHAR REACTIVITY		211
8.1.	NON-ISOTHERMAL COMBUSTION TGA.....	211
8.2.	ISOTHERMAL CHAR REACTIVITY OF HTF CHARS AND ASSESSMENT OF LIGNIN REACTIVITY.....	231
8.3.	ISOTHERMAL CHAR REACTIVITY OF RAPID HEATING DTF CHARS.....	234
8.3.1.	THE INFLUENCE OF AROMATIC CARBON AND MINERAL MATTER CONTENT ON APPARENT CHAR COMBUSTION REACTION RATE.....	245

8.3.2.	THE INFLUENCE OF TORREFACTION ON APPARENT CHAR COMBUSTION REACTION RATE.....	249
8.3.3.	INTRINSIC CHAR COMBUSTION REACTION RATES	250
8.4.	DTF CHAR RE-FIRING	257
8.5.	SUMMARY	274
CHAPTER 9: CONCLUSIONS AND FUTURE WORK.....		277
9.1.	FUTURE WORK	280
9.1.1.	IGNITION AND FLAME STABILITY STUDY.....	280
9.1.2.	COMPUTERISED MODELLING STUDIES	281
CHAPTER 10: REFERENCES		282

List of Figures

<i>Figure 2-1 Three Fold Char Morphology Classification, 12</i>	<i>Figure 2-13 Broido-Shafizadeh Model for Cellulose Devolatilisation, 39</i>
<i>Figure 2-2 Reactivity and Combustion Properties of Maceral Groups (Su et al. 2001), 20</i>	<i>Figure 2-14: Proposed Lignin Pyrolysis Pathway, 41</i>
<i>Figure 2-3 Fixed Carbon Yield vs. Aromatic Carbon Content for a Range of Coals with Differing Rank (taken from Miknis et al., 1980), 23</i>	<i>Figure 2-15 Temperature Dependence of the ¹³C CPMAS NMR Spectra of Chars from Alkali Lignin, Prepared under Pyrolytic Conditions, 42</i>
<i>Figure 2-4 Breakdown of Biomass Composition, 28</i>	<i>Figure 2-16 Willow Particle Combustion Profile using Meker Burner, 56</i>
<i>Figure 2-5 Typical Plant Cell Wall Structure (Basu, 2010), 29</i>	<i>Figure 3-1 Organosolv Process Flow (adapted from Brosse et al., 2009, 72</i>
<i>Figure 2-6 Structure of plant cell walls, 30</i>	<i>Figure 3-2 Typical Slow Heating TGA Char Generation Experiment Profile, 83</i>
<i>Figure 2-7 Single Chain Cellulose Unit (Adapted from Harmsen et al., 2010), 31</i>	<i>Figure 3-3 Drop Tube Furnace Schematic, 86</i>
<i>Figure 2-8 Parallel Arrangement of Cellulose with H-Bonding, 32</i>	<i>Figure 3-4 Drop Tube Furnace, 87</i>
<i>Figure 2-9 Schematic Structure of Hemicellulose Structure of Arborescent Plants, 32</i>	<i>Figure 3-5 DTF Temperature Profiles, 91</i>
<i>Figure 2-10 Three primary lignin monomer units, 34</i>	<i>Figure 3-6 Arrhenius Plot for Corn Stover DTF Char under Varying Combustion Regime, 99</i>
<i>Figure 2-11 Proposed Poplar Lignin Structure Showing Linkages, 35</i>	<i>Figure 3-7 Adsorption Isotherm for BET Surface Area Analysis, 101</i>
<i>Figure 2-12 Common Lignin Linkages and Their Relative Contributions, 35</i>	<i>Figure 4-1 Van Krevelen Diagram (Atomic H:C vs. O:C Ratios), 107</i>
	<i>Figure 4-2 Raw Wheat Straw Pellet SEM Image, 109</i>

Figure 4-3 Delignified Wheat Straw Pellet SEM Image, 110

Figure 4-4 Raw Pine Woodchip SEM Image, 110

Figure 4-5 Delignified Pine Woodchip SEM Image, 111

Figure 4-6 Carbon Content vs. Torrefaction Temperature, 113

Figure 4-7 Column Plot of Aromatic Carbon Content, 118

Figure 5.1: Pine Ethanol Organosolv Mass Fractionation, 124

Figure 5.2: Wheat Straw Ethanol Organosolv Mass Fractionation, 124

Figure 5-3 ¹³C SS CPMAS NMR Spectra of Pine Ethanol Organosolv Fractions, 126

Figure 5-4 ¹³C SS CPMAS NMR Spectra of Wheat Straw Ethanol Organosolv Fractions, 127

Figure 5-5 Torrefaction Temperature Mass loss Differences, 132

Figure 5-6 ¹³C NMR Spectra of Raw and Torrefied Wheat Straw Pellets, 134

Figure 5-7 ¹³C NMR Spectra of Raw and Corn Stover Pellets, 135

Figure 5-8 ¹³C NMR Spectra of Raw and Torrefied Pine Woodchips, 136

Figure 5-9 ¹³C NMR Spectra of Raw and Torrefied Mixed Softwood Pellets, 137

Figure 5-10 Aromatic Carbon Mass Balance vs. Torrefaction Mass Loss, 140

Figure 5-11 SEM Images of Raw and Torrefied Mixed Softwood, 143

Figure 6-1 Column Plot of Slow Heating Pyrolysis Char Yields, 148

Figure 6-2 Slow Heating Pyrolysis Char Yield vs. K+Ca Content, 150

Figure 6-3 Slow Heating Pyrolysis Char Yield vs. Atomic O:C Ratio, 151

Figure 6-4 Slow Heating Pyrolysis Char Yield vs. Atomic H:C Ratio, 152

Figure 6-5 Slow Heating Pyrolysis Char Yield vs. Aromatic Carbon Content for all Non-Demineralised Biomass, 153

Figure 6-6 Slow Heating Char Yield vs. Aromatic Carbon Content for all Demineralised Biomass, 154

Figure 6-7 Theoretical Additional Char Yield under Slow Heating vs. K+Ca Content for Non-demineralised Biomass, 159

Figure 6-8 Calculated vs. Observed Slow Heating Pyrolysis Char Yield, 163

Figure 6-9 Error of Prediction for Slow Heating Pyrolysis Char Yield Calculation, 164

Figure 6-10 Column Plot of DTF Rapid Heating Pyrolysis Char Yields, 167

Figure 6-11 Rapid Heating Pyrolysis Char Yield vs. Atomic O:C Ratio, 168

Figure 6-12 Rapid Heating Pyrolysis Char Yield vs. Atomic H:C Ratio, 179

Figure 6-13 Rapid Heating Pyrolysis Char Yield vs. Aromatic Carbon Content for all Non-Demineralised Biomasses, 171

Figure 6-14 Rapid Heating Char Yield vs. Aromatic Carbon Content for all Demineralised Biomasses, 173

Figure 6-15 Theoretical Additional Char Yield under Rapid Heating vs. K+Ca Content for Non-demineralised Biomasses, 174

Figure 6-16 Calculated vs. Observed Rapid Heating Pyrolysis Char Yield, 177

Figure 6-17 Error of Prediction for Rapid Heating Pyrolysis Char Yield Calculation, 178

Figure 7-1 HTF Char Morphology, 181

Figure 7-2 Kellingley Coal DTF Char Morphology 1300°C 600 ms (50-75 µm), 188

Figure 7-3 Wheat Straw Pellet Fraction DTF Char Morphologies, 189

Figure 7-4 Corn Stover Pellet Fraction DTF Char Morphologies, 190

Figure 7-5 Pine Woodchip Fraction DTF Char Morphologies, 191

- Figure 7-6 Eucalyptus Pellet Fraction DTF Char Morphologies, 192*
- Figure 7-7 Miscanthus Pellet Fraction DTF Char Morphologies, 193*
- Figure 7-8 Miscanthus Pellet Fraction DTF Char Morphologies, 194*
- Figure 7-9 Torrefied Wheat Straw Pellets, 195*
- Figure 7-10 Torrefied corn Stover Pellets, 196*
- Figure 7-11 Torrefied Mixed Softwood Pellets, 197*
- Figure 7-12 Torrefied Pine Char Morphology, 198*
- Figure 7-13 Partially Swollen Char Retaining Part Cell Structure, 199*
- Figure 7-14 DTF Char BET Surface Area vs. % Thin Walled Chars, 202*
- Figure 7-15 DTF Char BET Surface Area vs. K+Ca Content for Non-demineralised Fuels, 203*
- Figure 7-16 DTF Char BET Surface Area vs. Aromatic Carbon Content for, 203*
- Figure 7-17 DTF Char BET Surface Area Suppression vs. Fuel K+Ca Content, 205*
- Figure 7-18 DTF Char BET Surface Area vs. Fuel Aromatic Carbon for All Samples, 207*
- Figure 8-1 Wheat Straw Pellet Fraction Non-isothermal Combustion Profiles, 212*
- Figure 8-2 Corn Stover Pellet Fraction Non-isothermal Combustion Profiles, 216*
- Figure 8-3 Pine Woodchip Fraction Non-isothermal Combustion Profiles, 221*
- Figure 8-4 Olive Cake Pellet Fraction Non-isothermal Combustion Profiles, 221*
- Figure 8-5 Eucalyptus Pellet Fraction Non-isothermal Combustion Profiles, 223*
- Figure 8-6 Mixed Softwood Pellet Fraction Non-isothermal Combustion Profiles, 225*
- Figure 8-7 Lignin Non-isothermal Combustion Profiles, 227*
- Figure 8-8 Reference Coal Non-isothermal Combustion Profiles, 228*
- Figure 8-9 Char Burnout Profiles for Demineralised Corn Stover Fraction HTF Chars, 231*
- Figure 8-10 Char Burnout Profiles for Demineralised Pine Woodchip Fraction HTF Chars, 232*
- Figure 8-11 Char Burnout Profiles for Wheat Straw Pellet Fraction DTF Chars, 235*
- Figure 8-12 Char Burnout Profiles for Corn Stover Pellet Fraction DTF Chars, 235*
- Figure 8-13 Char Burnout Profiles for Pine Woodchip Fraction DTF Chars, 236*
- Figure 8-14 Char Burnout Profiles for Miscanthus Pellet Fraction DTF Chars, 236*
- Figure 8-15 Char Burnout Profiles for Eucalyptus Pellet Fraction DTF Chars, 237*
- Figure 8-16 Char Burnout Profiles for Mixed Softwood Pellet Fraction DTF Chars, 237*
- Figure 8-17 Arrhenius Plots for Wheat Straw Pellet Fraction DTF Chars, 238*
- Figure 8-18 Arrhenius Plots for Corn Stover Pellet Fraction DTF Chars, 238*
- Figure 8-19 Arrhenius Plots for Pine Woodchip Fraction DTF Chars, 239*
- Figure 8-20 Arrhenius Plots for Miscanthus Pellet Fraction DTF Chars, 239*
- Figure 8-21 Arrhenius Plots for Eucalyptus Pellet Fraction DTF Chars, 240*
- Figure 8-22 Arrhenius Plots for Mixed Softwood Pellet Fraction DTF Chars, 240*
- Figure 8-23 Arrhenius Plots for Raw and Torrefied Wheat Straw Pellet DTF Chars, 241*
- Figure 8-24 Arrhenius Plots for Raw and Torrefied Corn Stover Pellet DTF Chars, 241*
- Figure 8-25 Arrhenius Plots for Raw and Torrefied Pine Woodchip DTF Chars, 242*
- Figure 8-26 Arrhenius Plots for Raw and Torrefied Mixed Softwood Pellet DTF Chars, 242*

- Figure 8-27 Arrhenius Plots for Steam Exploded Mixed Wood Pellet DTF Chars, 243*
- Figure 8-28 Arrhenius Plots for Kellingley Coal DTF Chars, 243*
- Figure 8-29 DTF Char k_a vs. K+Ca for Non-demineralised Samples, 246*
- Figure 8-30 DTF Char k_a vs. K for Non-demineralised Samples, 246*
- Figure 8-31 DTF Char k_a vs. BET Surface Area for Demineralised Samples, 247*
- Figure 8-32 DTF Char k_a vs. Biomass Aromatic Carbon Content, 248*
- Figure 8-33 DTF Char k_a vs. Aromatic Carbon Content of Torrefied Biomass Samples, 249*
- Figure 8-34 DTF Char k_i vs. K+Ca for Non-demineralised Samples, 252*
- Figure 8-35 DTF Char k_i vs. Biomass Aromatic Carbon Content, 252*
- Figure 8-36 Observed-Calculated k_i vs. Fuel K+Ca Content, 255*
- Figure 8-37 Torrefied Biomass DTF Char Combustion k_i vs. Fuel Aromatic Carbon, 256*
- Figure 8-38 Wheat Straw Fractions Char Re-firing Burnout vs. Re-firing Residence Time, 259*
- Figure 8-39 Eucalyptus Fractions Char Re-firing Burnout vs. Re-firing Residence Time, 259*
- Figure 8-40 Wheat Straw Pellet Fraction DTF Char Re-firing Char Conversion Rate vs., 263*
- Figure 8-41 Eucalyptus Pellet Fraction DTF Char Re-firing Char Conversion Rate vs., 263*
- Figure 8-42 Straw Pellet Fraction Char BET Surface Area vs. DTF Re-firing Char Conversion, 266*
- Figure 8-43 Ln[Char Remaining] vs. DTF Re-firing Time for Wheat Straw Pellet Fractions, 266*
- Figure 8-44 Ln[Char Remaining] vs. DTF Re-firing Time for Eucalyptus Pellet Fractions, 269*
- Figure 8-45 Delignified Wheat Straw Char Re-firing Arrhenius Plots, 271*
- Figure 8-46 Delignified Wheat Straw Char Re-firing Arrhenius Plots, 271*
- Figure 8-47 Demineralised Wheat Straw Char Re-firing Arrhenius Plots, 272*
- Figure 8-48 Demineralised Delignified Wheat Straw Char Re-firing Arrhenius Plots, 272*
- Figure 8-49 E_a vs. Char Conversion for Wheat Straw DTF Re-firing, 273*
- Figure 8-50 k_i vs. Char Conversion for Wheat Straw DTF Re-firing, 273*

Chapter 1: Introduction

1.1. Background

Growing realisation of the now widely recognised impacts of anthropogenically driven global warming has prompted many governments throughout the globe to commit to legislation which stipulates strict reductions in CO₂ emissions from the energy sector. As such, the UK government has pledged its adherence to a series of legally binding carbon budgets under the 2008 Climate Change Act. The act sets a target to cut CO₂ emissions by 34% on 1990 levels by 2020 and at least 80% by 2050 (HM Government, 2009).

Alongside these ambitious carbon reduction goals, the government also aims to increase renewable energy generation with the EU's Renewable Energy Directive requiring that 15% of the UK's primary energy demand comes from renewable energy sources in 2020. Estimates suggest that this translates to at least 30% of electricity generated that year by renewables (DECC, 2009). The chief burden of these objectives has been and will continue to be shouldered by the electricity generation sector, with renewable power production increasing from 8.39% during 2010 (DECC 2011(a)) to 30-40% by 2020. This must be achieved whilst cutting greenhouse-gas emissions by 22% on 2008 levels (DECC 2011(b)). Strong growth in UK renewable generation has already been seen with around 20% of total electricity generated in 2014 being produced using renewable technologies (60 TWh), up from 16% in 2013 (50 TWh) and 5% in 2007 (19 TWh) (CCC, 2015).

Considering that typical coal combustion systems emit around 872 gCO₂/kWh compared to the Committee on Climate Change's aim of 50gCO₂/kWh it is clear that significant contribution of unabated coal-fired power production will become an unacceptable

element of the future energy system and that a suitable, cost effective replacement for coal must be adopted over the coming decades.

Such concerns have driven wider, urgent consideration of alternative options for electrical power generation. As such the use of solid fuel sources with a reduced carbon intensity which can be utilised in a similar manner to coal, such as biomass and waste derived fuels, has received increasing interest in recent years as a possible option for the replacement of finite fossil fuel resources in power production. Biomass fuelled thermal generation is able to provide dispatchable, ostensibly carbon neutral electricity which is in stark contrast to the variable nature of power output from alternative renewable energy sources such as wind power, thus aiding in the provision of an effective counterbalance to increased penetration of intermittent renewable generation whilst improving energy security issues by providing a source of diversification in fuel supply.

The increased interest in a solid biomass fuel alternative to coal has seen biomass power generation become the greatest single contributor to UK renewable energy generation in 2014, providing 7% of UK generation (with 6% from onshore and 4% from offshore wind).

Although the above is true of the conversion of biomass at point of use there are carbon inputs into the cycle prior to utilisation which include agricultural propagation, fertilisation and harvesting practices, biomass processing (including drying, size reduction and pelletisation) and transportation. All of these activities have a negative impact on the achievable carbon savings to be made by displacing fossil fuels and this saving is thus wholly dependent upon the source and processing of the biomass in question; however, a recent report by DRAX Power Ltd. stated that the biomass sourced in 2014 for their on-going coal to biomass conversion of coal fired pulverised fuel (PF)

boilers provided an 87.86% reduction in carbon emissions per MJ of energy content on average when compared with coal (DRAX, 2015). This clearly demonstrates that considerable carbon emission reductions are achievable through the replacement of coal with sustainably sourced biomass materials even where the quantities of biomass being utilised is high (4.09 million tonnes in 2014) as is the case when considering 100% coal to biomass conversion projects.

In order to encourage the accelerated adoption of low carbon power generation alternatives the UK government have utilised a string of financial subsidy mechanisms. The most recent mechanism, Contracts for Difference (CFD), offers a guaranteed return of 105 £/MWhr for coal fired power plants which convert to 100% biomass combustion (DECC, 2013). Considering the current price of electricity in the UK (as of 2015) is stagnant at under 50 £/MWhr this offers considerable incentive to convert coal fired power plants to biomass firing. As such a number of coal to biomass combustion plant conversion projects have been completed both in the UK and abroad including three 500 MWe units of DRAX power station, Ironbridge, Tilbury, Thunder Bay, Atitokan and Gardanne power stations with Lynemouth and Uskmouth stations looking to convert to biomass fuels in the near future.

1.2. Rationale

It is clear that, given the financial incentives available, the on-going conversion of coal fired power plants to biomass derived fuels both in the UK and internationally, the relatively well developed nature of biofuel utilising power generating technologies, the wider interest in the use of biomass and waste derived fuels and the potential reductions in carbon dioxide emissions achievable that biomass utilisation is likely to play a growing role in the displacement of coal based generating capacity. As such, it has

become important to fully understand the nature of the wide ranging biomass available for utilisation as a fuel and their behaviour during conversion via thermochemical treatment used in combustion driven power generation infrastructure.

Given its long history of use, and the widespread adoption of coal for combustion and gasification driven power generation, a number of successful classification tools have been developed for differing coals that are able to characterise their performance during thermochemical conversion. Coal plant owners have been utilising relatively complex coal classification systems for many decades in order to predict the impact of individual fuels on plant operations. These systems typically utilise empirical knowledge of the impact of coal composition on their performance during combustion to predict performance in the plant during use using only basic characterisation of the fuels chemical and physical properties. Systems such as the Electrical Power Research Institutes Coal Quality Impact Model can be utilised to give an appreciation of the impact of coal characteristics on combustion performance (volatile matter yields, char reactivity and thus combustion efficiency), emissions generation (NO_x, CO, carbon in ash and dust emissions), ash behaviour (slagging, fowling and corrosion of heat exchange surfaces) and subsequent impact on plant efficiency, reliability and availability (Davidson et al., 1990). These tools provide an invaluable resource to electrical power utilities either in the forecasting the impact of changes in fuel purchasing strategies and thus avoiding costly plant performance issues, or in diagnosing existing plant issues believed to be caused by fuel quality issues in a cost effective manner.

To date some efforts have been made in this vane for biomass fuels, however, limited success has been achieved and no widely accepted predictive classification systems have yet been developed. This is especially true for pulverised fuel applications which are considerably under studied when compared to pyrolysis and gasification

technologies. It is for this reason that the current study has focussed upon the investigation of certain key thermochemical conversion processes undergone by biomass fuels in the specific context of PF combustion applications and aims to allow for a valid, reliable prediction of combustion behaviour based upon the inherent composition of the fuel in line with those tools previously derived to describe coal combustion dynamics. This research will investigate the influence of biomass fuel composition on devolatilisation and char combustion behaviour. From this analysis, it is hoped that a meaningful classification of the varied biomass fuel sources available can be made, providing power generators with an accurate prediction of fuel performance during combustion from a basic characterisation of their chemical and structural composition. Such a system can then be utilised to inform decision making during the procurement and use of wide range of biomass fuels in an efficient, economical and environmentally sustainable manner.

Chapter 2: Literature Review

2.1. Solid Fuel Combustion Processes and Their Importance

The combustion dynamics undergone by solid fuel particles within the boiler of PF fired power generation infrastructure are key in determining the performance, availability and reliability of the power plant and ultimately dictate the safe, efficient and economic operation of the power generation cycle as a whole. Variations in the combustion performance of differing fuels is able to significantly alter a number of parameters including: the efficiency of combustion and heat transfer processes in the boiler; the shape and stability of PF flames and thus their ability to provide continuous, reliable, safe and even heat input; the generation of both gaseous (CO, NO_x, SO₂) and solid (particulate matter and carbon in ash) pollutant species; boiler ash deposition slagging, fouling and corrosion; the design and operation of combustion infrastructure including burners, overfire air systems and emissions abatement plant.

The processes undergone during PF combustion are varied and complex, their individual dynamics being influenced by a large range of factors including the nature of the fuel and varied operating conditions. However, solid fuel combustion processes can be generally described to consist of several distinct yet interconnected processes which occur sequentially as the fuel particles pass through the boiler experiencing distinct regions of furnace temperature and gaseous environment (principally furnace gas oxygen content).

These general processes have been summarised as follows for both coal and biomass combustion (Ranzi et al., 2008; Smith, 2013; Smoot, 1993):

- ▶ Particle Drying: On initial introduction into the boiler any moisture remaining inherent within or adhered to the fuel particle following pulverisation and

conveyance in hot primary air is lost via evaporation on heating by the high intensity PF flame located at the mouth of the burner

- ▶ **Devolatilisation:** Thermal decomposition of the fuel on rapid heating within the flame which occurs over 30-100 ms and gives rise to the liberation of reactive organic structures as combustible, low molecular weight volatile gas species and condensable vapours accompanied by rapid development of the molecular structure and physical morphology of the solid char structures which remain following devolatilisation
- ▶ **Volatile Combustion:** Following the evolution of volatile matter from the particle the volatile gases undergo gas phase oxidation in a layer surrounding the devolatilising particle. Volatile matter combustion processes govern the near burner flame temperature and is critical for establishment of stable PF flames, this being largely dependent upon the rate of release, yield and composition of volatile gases (Fletcher 1989). These reactions are regulated primarily by the presence of reactive radical species, their reaction with original volatile gases, radical chain branching and ultimate recombination of radicals
- ▶ **Char Combustion:** Char structures which remain following the loss of volatile matter components and comprise the thermally stable components of the fuel not lost through pyrolysis undergo oxidation reactions as local oxygen availability increases. This typically occurs as the particle leaves the fuel rich flame core and volatile matter release subsides, secondary air streams are mixed with combustion products and introduction of overfire air above the burner belt creates a globally oxidising environment). These oxidation reactions occur over a considerably wider time window (especially char combustion) which is dependent upon the design of combustion

infrastructure and often requires the effective use of furnace volume to maximise the residence time allowed for combustion to proceed to completions, thus maximising combustion efficiency and minimising loss of unburned char particles in boiler flyash

Of the above processes undergone during PF combustion, the devolatilisation process is of elevated importance in determining the overall combustion performance of a potential fuel given the important role it plays in influencing both the release dynamics and volume of volatile gases produced in the PF flame and the physiochemical nature of char particles formed during pyrolysis. These factors have a deterministic influence on the formation and nature of the flame, the formation of gaseous pollutant species especially NO_x and CO and char oxidation reactivity which will ultimately dictate the efficacy of boiler combustion processes, study of fuel devolatilisation and its influence on char formation are thus believed to be most important in the characterisation of fuels for application in PF fired boilers (Williams et al., 2002). It is vital to assess the volatile matter yields obtained and the nature of the char produced with respect to chemical reactivity to oxygen and physical properties (principally surface area and porosity) under realistic boiler conditions in order to understand the potential impacts associated with the adoption of a certain fuel given their relative importance in determining the overall combustion performance of any individual fuel. Each of these processes is described in some detail in the following sections alongside the existing characterisation methods available in the context of the combustion of both pulverised coal and biomass fuels.

2.1.1. Devolatilisation

The decomposition of solid fuel particles to form gaseous volatile matter and solid char structures is known as devolatilisation. Devolatilisation under the environmental

conditions which prevail within PF fired boilers is generally assumed to proceed in the absence of any considerable availability of oxygen due to the rapid efflux of volatiles contained within the particle which form an oxygen deficient boundary layer around the particle (Senneca et al., 2004). In conjunction with this, operation of modern low NO_x burner equipment commonly used in PF utility boilers limits the introduction of air into the core of the flame during devolatilisation in order to reduce the conversion of volatile released nitrogen compounds to NO_x. As such the devolatilisation processes undergone during the early stages of combustion in low NO_x burner equipped coal fired power plants can be closely simulated experimentally through thermal decomposition under an inert (commonly nitrogenous) environment. This is commonly referred to as pyrolysis and in many instances there is no significant alteration of the yield or compositions of volatiles produced or the chemical and structural nature of chars compared to devolatilisation in air (British Coal Corporation, 1991; Hayhurst and Lawrence, 1995).

This assumption has led to the widespread use of experimental equipment able to simulate the rapid heating rates undergone by particles during combustion in an entrained flow (including the investigation described herein) to study the devolatilisation of solid fuels under an inert atmosphere and thus allow for comprehensive characterisation of the chars produced to give insight into both devolatilisation and char combustion dynamics.

Although studies of coal pyrolysis provide valuable information in the differing conversion behaviour of coals during PF devolatilisation, a number of studies have identified differences between coal conversion processes when performed under oxidative and inert atmospheres (Alonso et al., 2001(a); Davini et al., 1996). These studies generally evidence an increase in both the rate of peak volatile loss and the mass yield of volatile matter in the presence of oxygen. This is due to more aggressive

bond breaking by oxygen giving rise to lighter volatile gas species and a higher degree of surface area development of the char (Biagini and Tognotti, 2006). The effects of oxygen in the devolatilising environment is small however, and, on comparison with char samples collected from industrial pulverised fuel furnaces, chars generated under inert environments in the laboratory have been shown to more closely relate to industrially relevant chars than those produced under oxidising conditions (Davini et al., 1996). The differences in char conversion rates and surface area variations during combustion between entrained flow rapid heating rate pyrolysis generated and actual industrial PF chars has been shown to be insignificant (Hayhurst and Lawrence, 1995). It is under this assumption that both this investigation and the majority of such investigations under laboratory conditions have been conducted with chars having been generated under inert, pyrolytic conditions.

Typically devolatilisation of solid fuels proceeds via a three step process whereby the initial heating of the fuel induces a number of physical and structural transformations which may result in the reordering of the fuel and loss of some occluded gases. Beyond a critical temperature which is dependent upon the chemical structure and reactivity of the fuel components, rapid chemical decomposition reactions begin (Biagini et al., 2006; Solomon et al., 1992), with consequent losses in fuel mass, as reactive fuel species thermally decompose to form volatile gases and condensable light tars leaving a solid carbonaceous residue known as char. This process typically leads to high degree of hydrogen depletion and loss of some oxygenated functionalities which leaves char structures carbon rich, typically being characterised by a high degree of condensed aromatic functionality (Perry et al., 2000; Maroto-Valer et al., 1996).

2.1.2. Char Formation

Although both biomass and coal exhibit intrinsic pore structures within the raw material, the decomposition of the organic component of the fuel during devolatilisation leads to considerable re-ordering of both the physical and chemical structure of the solid char fraction which remains following the loss of volatile matter (Solomon et al., 1992). The nature of the char is thus largely determined by the behaviour of the fuel during devolatilisation which is heavily influenced by the original fuel composition and their thermal histories during pyrolysis.

Under PF like conditions of entrained flow rapid heating both coal and biomass fuels have been observed to undergo considerable fluidity developments and plasticisation during pyrolysis which enables the formation, coalescence and egression of volatile gas bubbles within the fuel structure during pyrolytic mass loss and essentially determines the form of the char produced (Avila et al., 2011; Borrego et al., 2009). The restructuring is more severe in high heating rate conversion cases such as PF devolatilisation where the total volatile matter yield is increased and the rate at which volatiles are expelled from the fuel is far higher (Guerrero et al., 2008).

The form of the pores developed in char structures are generally subdivided into macropores (>500 Å in diameter), mesopores (20-500 Å in diameter) and micropores (<20 Å in diameter) (Simons, 1983). Given that char surface area and pore diffusion processes can play a limiting role in the combustion rates of chars their importance cannot be underestimated.

There is continued conjecture within the scientific community as to the relative importance of each of the pore sizes in controlling oxidation reaction rates (Külaots et al., 2007) and a growing body of evidence appears to suggest that smaller micropores

are of reduced importance in determining oxidation rates as they are largely closed to oxidising agents (Aarna and Suuberg, 1998; Hurt et al., 1991; Radović et al., 1983)

Given the importance of char pore nature and distribution, a number of char characterisation systems have been developed to describe coal chars with regard to their shape, internal structure, wall thickness and anisotropy, and have played a key role in predicting the char burnout efficiency of specific coal chars (Bailey et al., 1990; Cloke et al., 2003; Rosenberg et al., 1996).

A three-fold char morphological characterisation system for high heating rate pulverised coal chars has been proposed by Bailey et al. (1990) and widely adopted by researchers in the field and is exemplified in Figure 2-1.

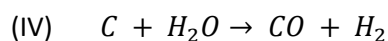
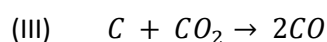
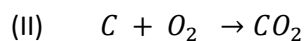
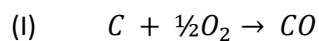
Char groups	Group I 	Group II 	Group III 
Char subtypes	Cenosphere tenuisphere, tenuinetwork	Crassisphere, crassinetwork, mesosphere, mixed porous, (mixed dense)	Inertoid, solid, fusinoid (mixed dense)
Char particle shape	Spheroidal	Spheroidal to irregular	Subspheroidal, rectangular or irregular
Porosity	> 80%	>50%	~50%
Pore shape	Spheroidal	Variable	Spheroidal to elongate and angular
Wall thickness	< 5 μm	Variable	> 5 μm
Dominant maceral components	Vitrinite	Vitrinite and inertinite	Inertinite
Swelling ratio	>1.3	<1.0	<0.9

Figure 2-1 Three Fold Char Morphology Classification

The form of the char is believed to largely dictate char combustion efficiencies by altering the available surface area, active site proliferation and intra-particle diffusion of oxygen (Oka et al., 1987; Smith, 1982). Generally speaking thin walled porous group I chars (tenuispheres having a thin walled bubble like structure and tenuinetwork presenting some internal char wall structure) are most open to oxygen diffusion into the internal pore structure and contain the largest surface area per unit mass of char and thus combust at the highest rates. Group II chars exhibit higher wall thicknesses and considerably reduced porosity and present reduced oxidation reactivity, while solid type group III chars are dense and show little internal pore structure and thus react more slowly and generally giving rise to the majority of unburned fuel particles in boiler flyash (Hurt et al., 1995; Oka et al., 1987). Considerable success also being seen on correlation of char morphotypes and petrographic maceral compositions of parent coals (Alonso et al., 2001(b)).

2.1.3. Char Oxidation

As the concentration of volatile gases surrounding the fuel particle become depleted through their gaseous combustion, solid carbonaceous char structures are exposed to the oxidising combustion air present in the furnace, allowing char oxidation to proceed. The primary chemical reactions undergone by the char matrix during combustive oxidation are summarised as follows (Lu et al., 2008; Sami et al., 2001):



These reactions involve a number of chemical and physical phenomenon including (Smith et al., 2013):

- (1) diffusion of gaseous oxidising agent species to the char surface
- (2) adsorption of these species to the solid surface
- (3) reaction of char with adsorbed oxidising species
- (4) desorption of combustion products
- (5) gas phase diffusion of products through the boundary layer into the free gas stream

Under normal combustion conditions where an abundance of oxygen is available reactions (I) and (II) dominate, however, reactions (III) and (IV) may become significant in widely utilised burner designs (including low NO_x burners) where the fuel particles are closely spaced and considerable quantities of H₂O are evolved during heating, resulting in reduced oxygen availability and higher vapour phase water concentrations around the combusting particles (Sami et al. 2001). These heterogeneous reactions are governed by a range of factors which include heat and mass transfer, gaseous diffusion through the boundary layer surrounding the particle (volatile boundary), gaseous turbulence, particle surface area, active site proliferation and inherent chemical reactivity of the char matrix (Smith, 1982). All of these factors are influenced by the chemical and physical nature of the char which is in turn largely determined by the original structural composition of the fuel, the rate of volatile release from the fuel, thermal history and the surrounding gaseous environment.

The rate of char oxidation can be limited either by chemical kinetics, mass transport processes, or a combination of the two, depending upon the temperature under which

the reactions take place (Essenhigh, 1989; Laurendeau, 1978; Young and Smith, 1989). At relatively low temperature the reactivity of the char toward oxygen is low and thus the overall rate of combustion is controlled by chemical kinetics (Regime I combustion). As the temperature increases, the chemical reactivity also increases to the point whereby oxygen is likely to be partially consumed as it diffuses into the internal structure of the char leading to mixed diffusion and chemical kinetic control of the combustion rate (Regime II combustion). Beyond these temperatures the rate of chemical char oxidation becomes extremely fast, under such conditions any oxygen reaching the external surface of the particle is rapidly consumed and combustion reactions are effectively restricted to this surface, under these conditions the overall rate of char conversion is determined by the bulk mass transfer of reactants (oxygen) to the char surface (Regime III combustion).

A number of studies of coal char oxidation have revealed that the combustion conditions prevailing during pulverised fuel firing give rise to the oxidation of char under largely regime II conditions (especially following the high temperature near burner zone) whereby both the surface area and the chemical kinetics of combustion play a role in determining the combustion rate (Gavalas, 1980). Given this observation the reactivity of the resultant chars are largely dependent upon the chemical makeup and level of condensation of the char as well as surface area and porosity development, both of which are influenced by the pyrolysis behaviour of the parent fuel, the thermal treatment it has undergone and the composition nature of the fuel prior to conversion.

During the oxidation of porous char particles the internal surface area available to reaction with oxygen can increase as a function of the degree of conversion due to the opening of sealed pores within the char and the growth of existing pores (Chan et al., 1999; Smith, 1982; Williams et al., 2001). This development of porosity will depend both

upon the rate of reaction of the char and its initial porosity characteristics. Given the complexity of the evolving porous structure and the potential depletion of more chemically active portions of the char (Lu et al., 2002; Wornat et al., 1996), which both influence the changing rate of char combustion, the expression of oxidation rate normalised to active surface area is often utilised to describe the intrinsic chemical reactivity of the char.

2.2. Coal: Its Nature, Combustion Behaviour and Classification

In devising a new classification scheme for solid biomass fuel combustion it is invaluable to review the current knowledge base which has been developed for coal and its combustion behaviour and assess the methods currently utilised to classify coals with regard to their performance during devolatilisation and char oxidation processes with considerable success. As such, the following sections will describe the nature of coal fuels and the influences their chemical and structural conformation have on combustion-related behaviour in the specific context of those existing classification systems used to predict combustion performance parameters using knowledge of the composition of the raw fuel.

2.2.1. The Nature of Coal

Coal is effectively an organic rock, derived through a complex series of peatification and coalification reactions (otherwise known as coal diagenesis). These processes give rise to a complex, heterogeneous organic matrix consisting of a wide variety of diverse chemical and structural components. The term maceral was first proposed by Marie Stopes (1935) in order to describe these structural components which consist of the macerated remains of an array of vegetation and plant materials and have since been

defined as an “organic substance, or optically homogenous aggregates of organic substances, possessing distinctive physical and chemical properties, and occurring naturally in the sedimentary, metamorphic, and igneous materials of the earth” (Spackman, 1958). These maceral fractions originate in the partial decomposition and maceration of a wide variety of biological units found in natural plant materials during coal formation. This process does not give rise to a uniform, homogenous product but instead forms a highly heterogeneous structure which retains a number of distinct sub-components which occupy distinct regions within the coal structure and differ greatly in both their chemical and physical characteristics. The properties of these fractions, known as macerals, which form the bulk constituents of coal, vary greatly and thus are known to undergo differing reaction dynamics during combustion. This high degree of variation stems from the vast chemical and morphological dissimilarities exhibited by individual plant materials from which the maceral fractions are derived and the numerous parameter known to effect the nature of coal forming reactions during coalification (including pressure, thermal history, deposition environment, geological forces, residence time etc.)(Orem and Finkelman, 2003). Because different plant components have different molecular structures, their chemical decomposition behaviours differ greatly during coal diagenesis on exposure to elevated temperature, pressure and chemical degradation. The original biological structures undergo considerable alteration during their transformation into coal and this too may give rise to differentiation between coal macerals. Conversion involves a range of biochemical processes which result in peatification of plant material, followed by burial diagenesis and coalification, all of which act to significantly alter the chemical, physical and morphological nature of the existing organic matter (Teichmuller, 1989). Overall these processes act to degrade the chemically reactive, aliphatic portions of coal precursors.

2.2.2. The Maceral Concept

Maceral components can be distinguished from one another primarily on the basis of their differing morphological properties, namely their morphological structure, internal texture and polishing relief with optical characteristics, with reflectance being an especially important analytical tool.

Maceral constituents have been observed to fall into three main maceral groups, being identified as either vitrinite, liptinite (formally exinite) or inertinite macerals. More sophisticated subsequent analysis has revealed that within these main maceral groups there exist an extensive range of maceral subgroups and individual maceral components all of which differ in their internal structure and chemical composition, significantly influencing the thermochemical reactions undergone during the combustion process.

The maceral classification as utilised by the International Committee of Coal and Organic Petrology (ICCP) can be seen in Table 2-1.

Grup Maceral	Sub Group Maceral	Maceral
Vitrinite	Telovitrinite	Tekstinite Tekto-ulminite Eu-ulminite Telocolinite
	Detrovitrinite	Attrinite Densinite Desmoccolinite
	Gelovitrinite	Corpogelinite Porigelinite Eugelinite
Liptinite		Sporinite Cutinite Resinite Liptodetrinite Alginite Suberinite Flourinite Eksudatinitite Bituminite
Inertinite	Telo-Inertinite	Fusinite Semi Fusinite Seklerotinitite
	Detro-Inertinite	Inertodetrinite Mikrinitite
	Gelo-Inertinite	Makrinitite

Table 2-1 Maceral Groups, Sub Groups and Individual Components (Suárez-Ruiz, 2012)

2.2.3. Classification of Coal Combustion

Maceral composition has an important influence on the combustion of pulverised coal due to the varying elemental, molecular and structural composition of maceral groups and the influence these differences have on the thermochemical decomposition processes encountered during combustion through devolatilisation and oxidation. These differences in chemical and physical properties, alongside their differing responses to thermal decomposition process conditions give rise to the generation of differing char in char yield and morphology during devolatilisation. Several studies (Lightman et al., 1968; Jones et al., 1985; Milligan et al., 1997) have demonstrated how different macerals behave under simulated PF combustion conditions and have shown the diverse morphologies of the char particles produced (Street et al., 1969; Hamilton, 1981).

The overall reactivity of the maceral groups has been widely considered, with Su et al., 2001 summarising the influence of individual maceral groups on the combustion behaviour of parent coals as shown in Figure 2-2.

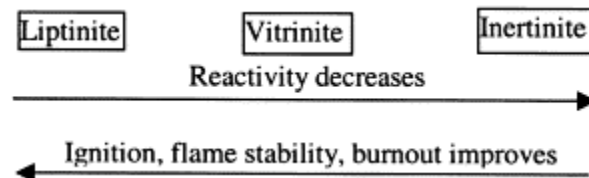


Figure 2-2 Reactivity and Combustion Properties of Maceral Groups (Su et al. 2001)

Although this correlation is based upon basic knowledge of the composition and reactivity of coal maceral groups only, and ignores the significant influence of char structural morphology, it is generally accepted to hold for most northern hemisphere coals.

Liptinite macerals generally form only a minor component in bituminous and higher rank coals due to their significant degradation during later coalification reactions.

Liptinite have by far the greatest hydrogen content of the maceral groups, containing a high proportion of aliphatic components. This lack of aromatic character makes liptinite highly reactive, producing the greatest yield of volatiles during devolatilisation- typically being twice that of associated vitrinites of similar rank (Crelling et al., 1988). Isolated liptinite macerals have been observed to pyrolyse rapidly, undergoing complete devolatilisation within 200 milliseconds during pilot scale PF boiler trials, leaving almost no carbonaceous char residue (Clove and Lester, 1994; Lee and Whaley 1983; Ottaway 1982). As such liptinite content has been used as a marker of the ability of a coal to establish an attached, stable volatile combustion flame at the burner in PF firing application.

Due to its largely unaltered nature when beginning the coalification process vitrinites are the most altered of all of the maceral groups during coal maturation. This means that vitrinite characteristics alter significantly with differing coal rank (Shibaoka et al., 1985). In general however vitrinites contain a somewhat higher degree of aromatic carbon than liptinites of similar rank, causing them to devolatilise at somewhat higher temperature and produce greater proportions of char than liptinite, this being largely dependent on rank.

Inertinite macerals have traditionally been considered as being largely inert during combustion, giving rise to low volatile matter yields and largely solid, unreactive type III chars, this behaviour being attributed primarily to its high level of aromatic character (Crelling et al., 1992; Milligan et al., 1997). More recent research has suggested however that part of the inertinite group, mainly low reflectance semifusinite, is far more reactive than previously thought (Vleeskens and Nandi, 1983); some southern hemisphere inertinites show reactivity close to that of vitrinite (Cai et al., 1998; Choudhury et al., 2008; Thomas et al., 1993). This has led to the inclusion of some “reactive inertinites” within the reactive coal maceral groups (Rentel et al., 1987), these being largely those which form fused chars, which have undergone fluidisation (Thomas et al., 1993), following which more valid prediction of unburned carbon emission from PF boiler plant was attained.

A number of studies have used the above correlations and have ranked the total yield of volatiles produced during pyrolysis for coal macerals of similar rank in the order liptinite > vitrinite > inertinite (Howard, 1981, Stach et al., 1982).

A raft of literature has aimed to develop of universal understanding of the form and thus oxidative reactivity of coal chars given understanding of their maceral composition with some considerable success having been achieved. In general, these studies (Jones

et al., 1985; Morrison, 1986; Lahaye and Prado, 1988; Oka et al., 1987) have shown that in general terms type I and II chars are predominantly generated from vitrinite rich coal fractions with very little or no solid character, thicker wall type II network structures and type III chars being attributed to inertinite macerals.

2.2.4. The Importance of Aromatic Carbon Content

A number of studies have utilised quantitative ^{13}C NMR techniques in an effort to fully understand the underlying chemical and structural forces driving the rank-dependent combustion performance of individual coal macerals. These reveal that the aromaticity of carbon within liptinite, vitrinite and inertinite maceral groups for a large range of coals of varying rank consistently show increasing aromaticity in the order liptinite < vitrinite < inertinite (Jones et al., 1986; Crelling, 1992; Choi et al., 1989; Zilm et al., 1981). As such it has been postulated that increasing aromatic carbon content gives rise to the increases in char yield observed between maceral groups and with increasing coal rank (Milligan et al., 1997). This has led to the utilisation of accurately determined aromatic carbon content as an indicator of potential char yield of coals such that a number of investigations have closely correlated aromatic carbon and char yield wt%'s on a dry ash free basis with correlation coefficients greater than 0.95 (Maciel et al., 1979; Miknis et al., 1981; Soloman, 1981) (Figure 2-3 is taken from Miknis et al., 1981 and includes results from both this study and that of Maciel et al., 1979).

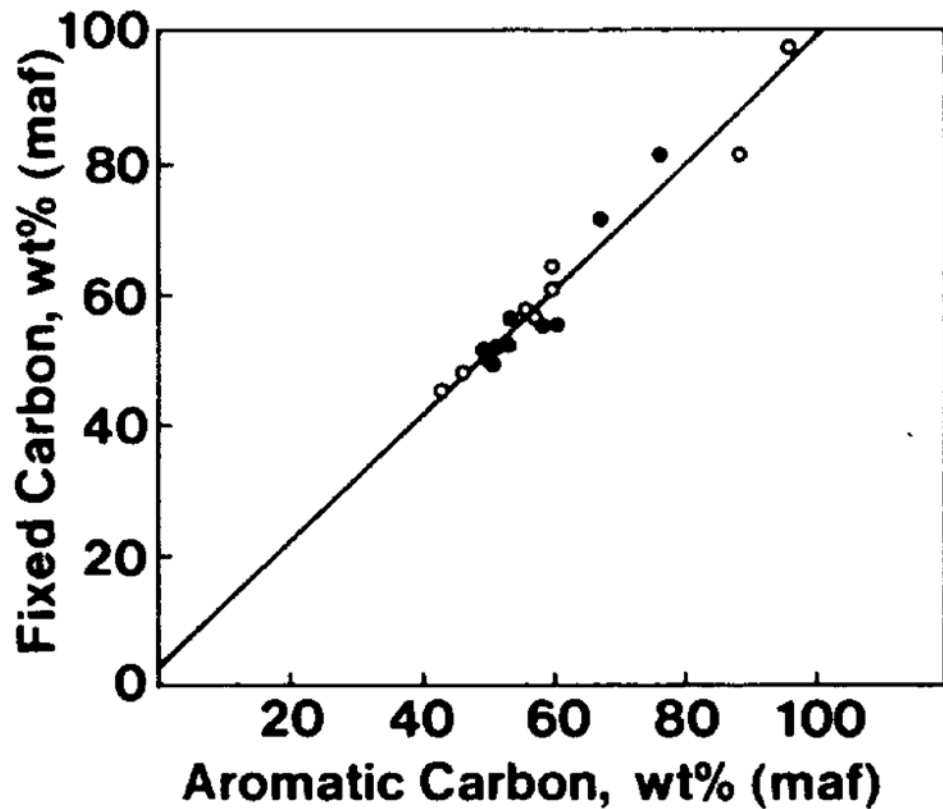


Figure 2-3 Fixed Carbon Yield vs. Aromatic Carbon Content for a Range of Coals with Differing Rank (taken from Miknis et al., 1980)

Given that biomass fuels likewise contain both aromatic and aliphatic components it is likely that the abundance of aromatic carbon structures in biomass fuels also plays a role in determining the char yield produced from these fuels. Although the influence of aromaticity of coals on char forming reactions of whole coals and their isolated maceral components is well established, very little research has been conducted in an effort to extend this knowledge to the charring of biomass fuels beyond the characterisation of the final char structures formed (Bourke et al., 2007; González-Vila et al., 2001; Apaydin-Varol and Putun, 2012) and analysis of biofuels at varying degrees of thermal treatment (Ben and Ragauskas, 2012; Melkior et al., 2012). Given the very strong influence of inherent aromatic carbon content on coal pyrolysis char yields and its recognised role in determining the relative reactivity of individual coal maceral chars further research is

warranted to determine the role of biomass aromaticity on their combustion characteristic during both devolatilisation and char oxidation.

2.3. Requirement for a New Classification System for Biomass and Waste Materials for use in Combustion

The understanding of coal chemical and structural composition and its influence on the combustion behaviour of differing coals is substantial. Such understanding has allowed for valid, reliable predictions of the performance of these fuels during thermochemical conversion. This understanding has been and remains invaluable in assessing the potential impacts of the utilisation of certain fuels in specific power generating infrastructure. This is evidenced by recent major fuel switching programmes undergone in the USA to adopt high volatile Powder River Basin coals, in the UK following privatisation of the electricity generating capacity and the adoption of world traded coals in preference to indigenous coal varieties and in South East Asia with the widespread adoption of Indonesian sub-bituminous and indigenous anthracite resources.

At present, however, no such system exists to describe the significant differences between biomass fuels and the consequent dissimilarities observed during their conversion via thermochemical means. The present investigation aims to close this gap through a study of the influence of key chemical components of a range of biomass fuels on their thermochemical conversion behaviour and the derivation and proposition of a new classification system for biomass and waste materials for their use in combustion. As such the following sections describe the chemical and structural nature of biomass fuels and the current understanding of how these factors influence their devolatilisation and char conversion behaviours.

2.4. Biomass; Its Nature, Combustion Behaviour and Classification

2.4.1. The Nature of Biomass

According to The United Nations Framework; Convention on Climate Change (UNFCCC, 2005) biomass materials can be defined as:

“non fossilized and biodegradable organic material originating from plants, animals and micro-organisms. This shall also include products, by-products, residues and waste from agriculture, forestry and related industries as well as the non fossilized and biodegradable organic fractions of industrial and municipal wastes.”

The massive diversity of the plant kingdom gives rise to a huge variety of potential biomass fuels, ranging from naturally and agriculturally sourced woody and herbaceous matter to industrial, agricultural and municipal waste by-products, being derived from a variety of different sources. Biomass feedstocks can be subdivided on a number of bases, with separation most commonly being conducted on the grounds of differing fuel origin, this being broken down into three principle groups (Vassilev et al. 2010).

Wood and Woody Biomass:

This group includes all coniferous or deciduous, gymnospermous or angiospermous hard and soft woody plant species and their components (barks, branches, stems, leaves etc.). By-products of wood processing industries such as sawdust, wood waste, mill scrap and timber slash also form part of this category due to their similar composition.

Herbaceous and Agricultural Biomass:

Comprising annual or perennial, arable or non-arable and process or field based biomass from a range of herbaceous plant species which lack a permanent woody stem. These commonly include a variety of grasses, flowers, straws, stalks, fibres, shells, pits and other residues which are often sourced as a waste product of agricultural harvesting activities.

Animal, Human, Industrial and Contaminated Biomass Wastes:

This category consists of a diverse range of waste derived materials including various manures, carcass residues (meat and bone wastes), municipal solid waste, sewage sludge, and contaminated industrial wastes such as demolition wood, hospital waste and paper-processing residues.

Similarly to coal, biomass can be regarded as a complex, heterogeneous mixture of three principle organic components being cellulose, hemicellulose and lignin (Figure 2-4) in association with varying abundances of other organic and inorganic compounds with varying solid and fluid phases, contents and origins (Vassilev et al., 2012)(Table 2-2).

Group	Subgroups
untreated wood	beech, birch, cork, fir/spruce/pine, oak, park waste wood, poplar, willow, tropical hard wood, other hard wood, other soft wood, bark, leaves, needles, others
treated wood	composted wood, demolition wood, org. preserved wood, salt-preserved wood, particle board, others
grass/plant	alfalfa, cattle feed (new), cotton, flax, flower/garden plants (new), fruit (new), hemp (previously group straw), jute, kenaf, miscanthus, reed, switch grass, vegetable, verge grass, other grass, other plants
straw (stalks, cobs, ears)	barley, maize/corn, rape, rice, rye, sorghum, sunflower, wheat, others
husk/shell/pit	almond, cacao, coconut, hazelnut, olive, peanut, potato, rice, sunflower, walnut, others
algae	others
organic residue/product	organic domestic waste food, industry waste, food industry product (new subdivision), bagasse, grain/meal, paper, paper pulp, slaughterhouse residue, black liquor, auction waste, agricultural/horticultural waste, textile waste, others
sludge	sewage, waste water treatment, food industry, paper sludge, drainage culvert, others
RDF and MSW	RDF with plastic, RDF without plastic, RDF unknown, MSW
non-organic residue	cables, car-shredder, electronic scrap, carpet waste, plastics, others

Table 2-2 Biomass Feedstock Type Categorisation (Bergman et al., 2005)

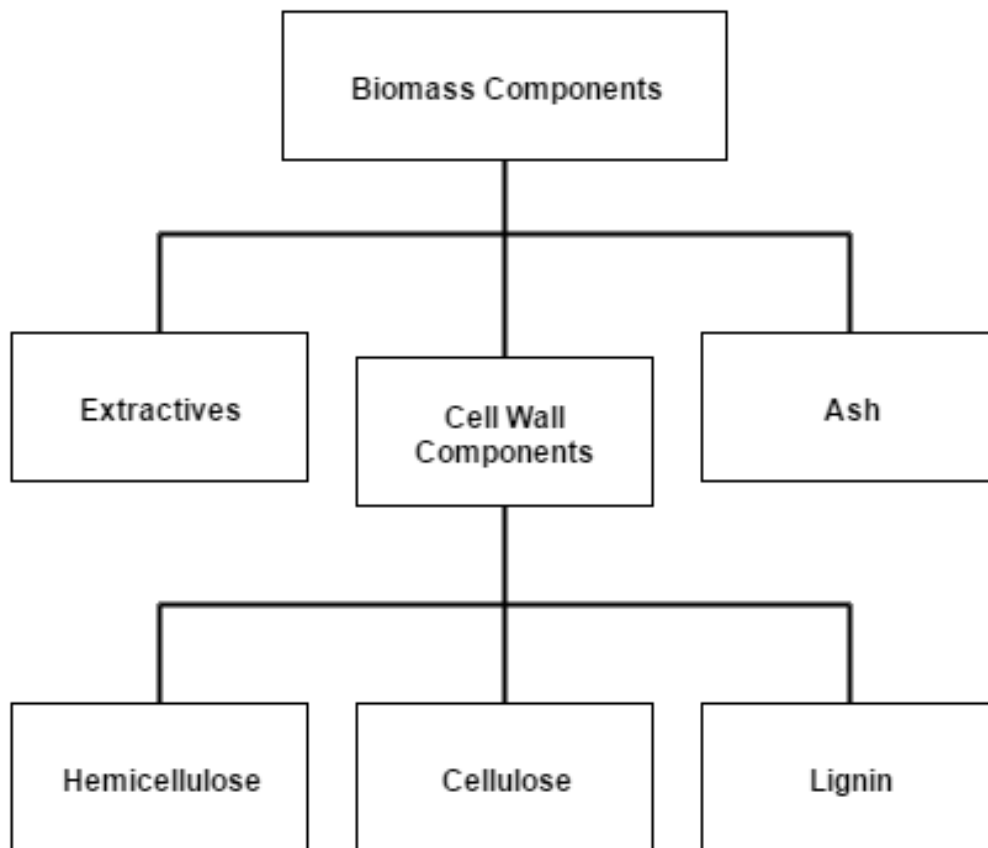


Figure 2-4 Breakdown of Biomass Composition

These three principle structural units combine closely within plant cell walls, exhibiting high degrees of inter-polymer cross linkage and close association of the three individual polymer units. Each of the main structural biopolymers has a unique chemical makeup, forming characteristic structures within the plant cell, each of which plays a distinct role in the mechanical stability and strength of biological systems.

A typical plant cell contains a primary and secondary cell wall, which is in turn composed of three distinct layers, as shown in Figure 2-5.

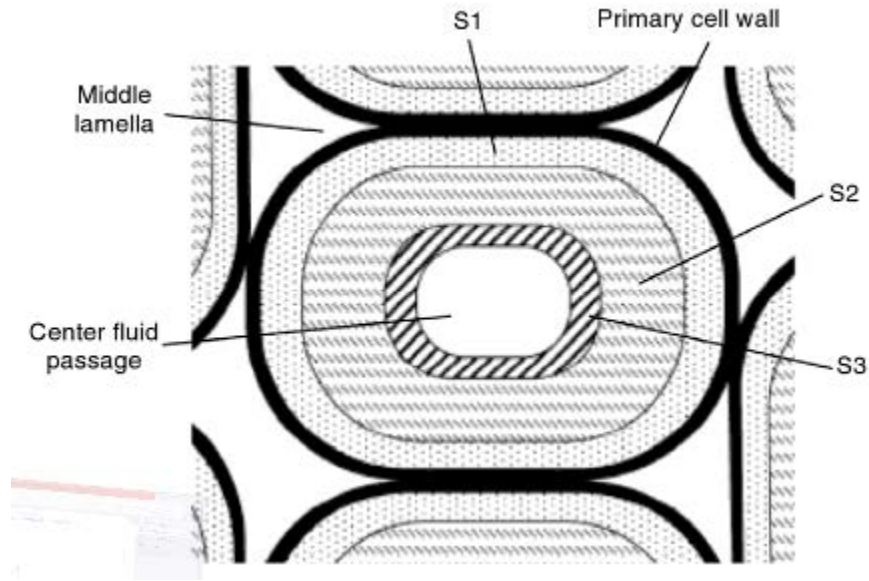


Figure 2-5 Typical Plant Cell Wall Structure (Basu, 2010)

Different fragments of the plant structure contain varying degrees of lignin, cellulose and hemicellulose depending upon the function of the plant component. The middle lamella between cells is highly enriched in lignin which acts to bind individual neighbouring cells together, effectively offering structural support to the plant. The central, S2 layer of the secondary cell wall is composed primarily of vertically orientated microfibril structures which comprise bundles of cellulose microfibrils bound together by a surrounding hemicellulose matrix. Whilst cellulose is found in the greatest concentration in the S2 layer, hemicellulose is most abundant in S3 where it acts as a coating layer for the central fluid passage.

Plant cell structure differs significantly depending on plant species and tissue type as shown in Figure 2-6. This differentiation between biological materials results in an alteration of the lignin, cellulose and hemicellulose content of the matter and accounts for the dramatic variation observed in biomass biopolymer compositions and subsequent dissimilarities in the thermochemical properties of different biomass feedstocks.

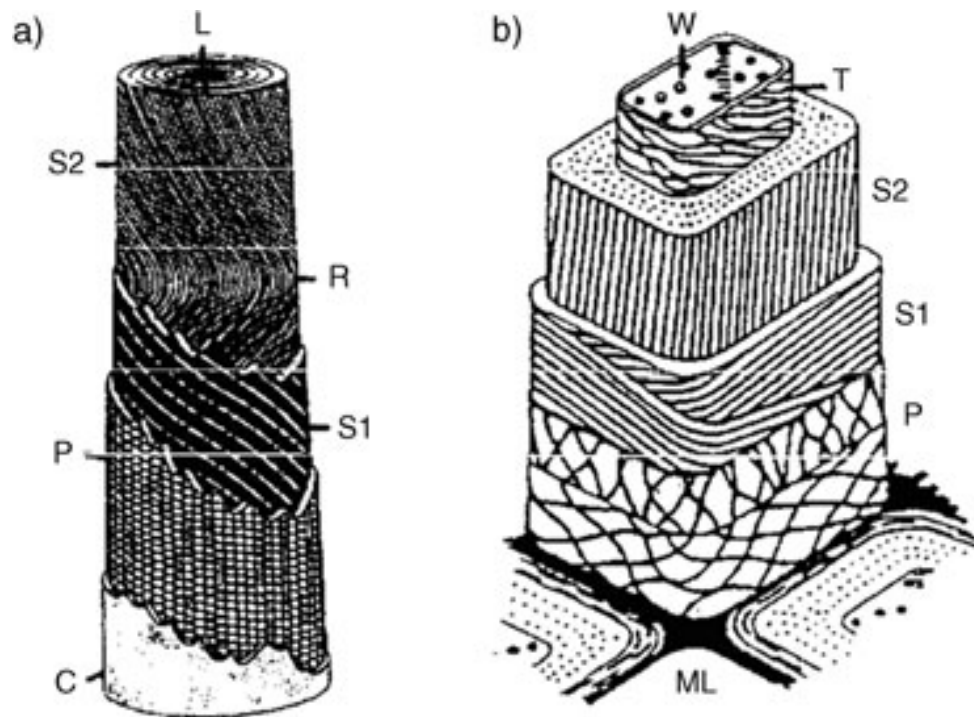


Figure 2-6 Structure of plant cell walls exemplified by a) cotton and b) wood fibres

C = cuticula layer, L = lumen, ML = middle lamella, P = primary cell wall layer,

R = reversing point,

S1 = secondary cell wall layer 1, S2 = secondary cell wall layer 2, T = tertiary cell wall,

W = wart layer.

(Klemm et al., 2005)

2.4.2. Cellulose:

Cellulose is a polysaccharide consisting of a saturated, straight chain of glucose sub-units linked by β -1,4 glucosidic bonds. These bonds allow for the formation of long, linear glucose polymer chains which, due to the even distribution of hydroxide

functionality on either side of the glucose monomer units, are able to form hydrogen bonds between cellulose molecules (Figure 2-7).

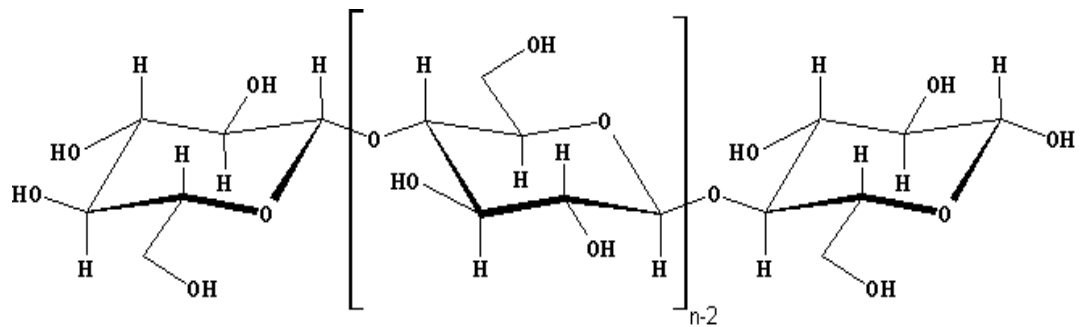


Figure 2-7 Single Chain Cellulose Unit (Adapted from Harmsen et al., 2010)

This hydrogen bonding results in the formation of a strongly bound structural polymer comprising a number of parallel cellulose chains chemically bound to one another with coalescence of several of levels of polymer chains within the plant cell wall leading to the formation of cellulose microfibrils (Figure 2-8 shows H-bonding between adjacent cellulose chains (red) and parallel levels of cellulose (blue) to form strong linear microfibril structures).

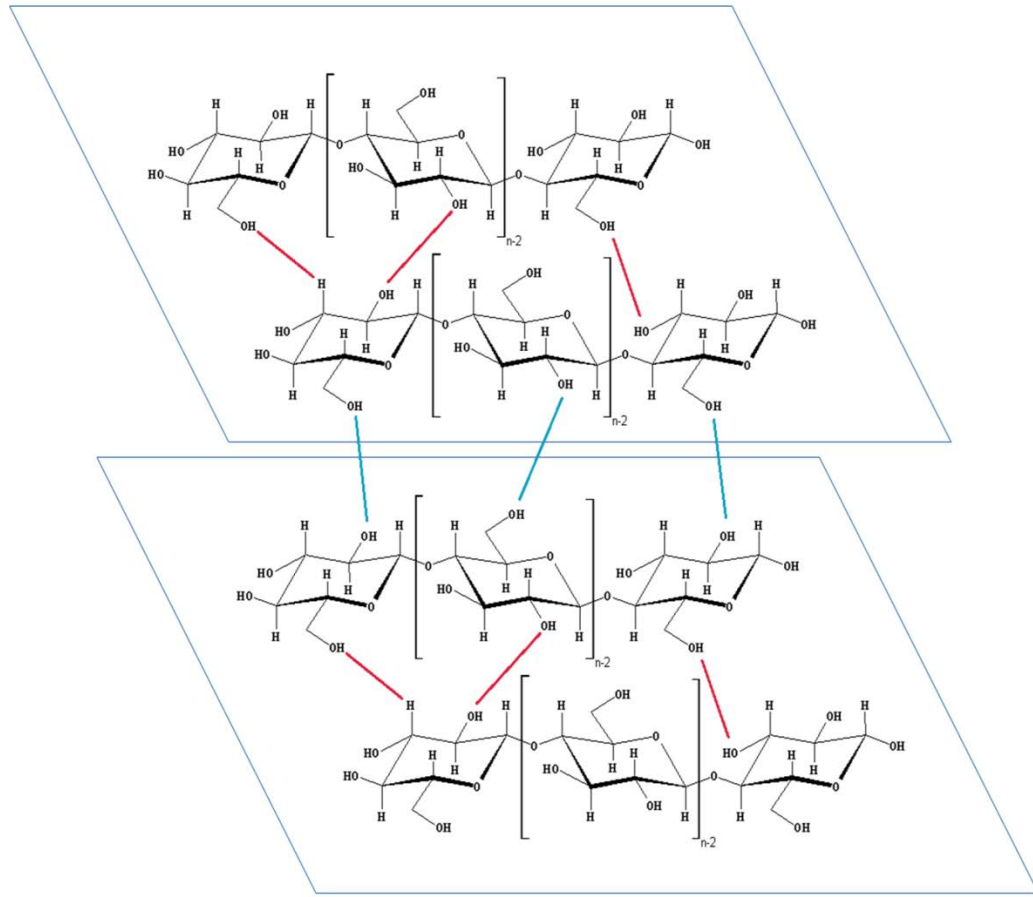


Figure 2-8 Parallel Arrangement of Cellulose with H-Bonding

(Adapted from Harmsen et al., 2010)

2.4.3. Hemicellulose:

Hemicellulose typically constitutes 15-30% of woody biomass and is composed primarily of a highly substituted, branched xylan and mannan pentose sugar polymer backbone. These bind tightly, yet non-covalently to the cellulose surface to form a microfibril coating within the cell wall. Xylan, the most abundant form of hemicellulose, consists of β -1,4 linked xylopyranosyl monomer units, varyingly substituted with a range of other sugars and functional groups (Figure 2-9)(Harmsen et al., 2010). This high degree of substitution of the 5-carbon xylose backbone gives rise to a highly heterogeneous

branched structure which is greatly dependent on biomass origin and varies extensively between softwood, hardwood and herbaceous plant species.

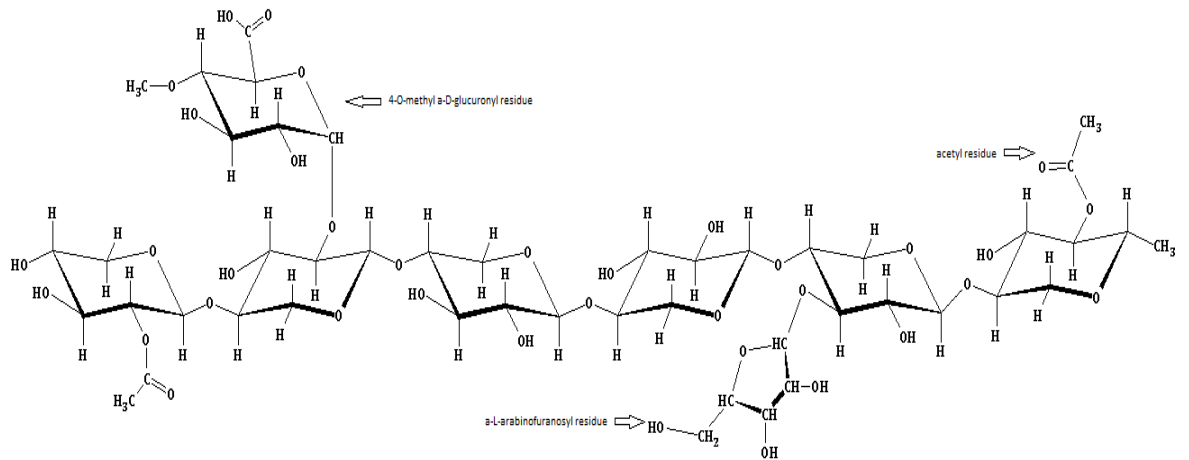


Figure 2-9 Schematic Structure of Hemicellulose Structure of Arborescent Plants

(Adapted from Harmsen et al., 2010)

2.4.4. Lignin:

Lignin is a highly complex 3-dimensional, cross-linked aromatic biopolymer with a high degree of substituted functionality, forming the skeletal structure of the plant structure whilst providing a binding agent between individual plant cells. Lignin is preferentially deposited between cell wall microfibrils, offering high structural rigidity to the interwoven lignocellulosic complex of the cell walls and cementing adjacent cells together. This leads to particular concentration of lignin in the middle lamellae between cells to ensure their close fixing. The composition of this aromatic polymer network is highly dependent on the plant species from which it is derived yet is predominantly made up of three phenyl propane monomers known as monolignols, namely syringyl, guaiacyl and p-hydroxyphenyl units (Figure 2-10). The fractions of these three units within the polymer network depend predominantly on the plant species and tissue type from which it is derived.

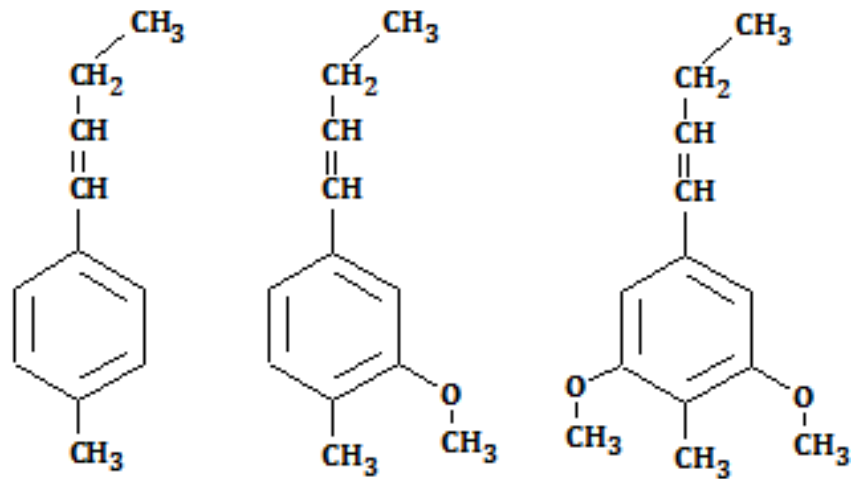


Figure 2-10 Three primary lignin monomer units from left to right *p*-hydroxyphenyl; guaiacyl and; syringyl monolignols (adapted from Harmsen et al., 2010)

Lignin polymerisation reactions result in the linkage of these monomer units to form an amorphous, highly branched 3 dimensional polymer matrix (Vanholme et al., 2010) (Figure 2-11). Several linkage types exist in native lignin compounds, ether bonding typically constituting around 70% of the total, this being dominated by the β -O-4 ether linkage which contributes around 45-50% to the total linkages between monolignols. The remaining 30% is comprised of covalent C-C bonding within the structure (Figure 2-12). Furthermore lignin aromatic units are highly substituted, containing a range of side chains with differing functionality. The primary functional groups encountered include methoxyl groups, phenolic hydroxyl groups, and few terminal carbonyl groups which all act to alter lignin reactivity, the relative contributions of these groups can be seen in Figure 2-12.

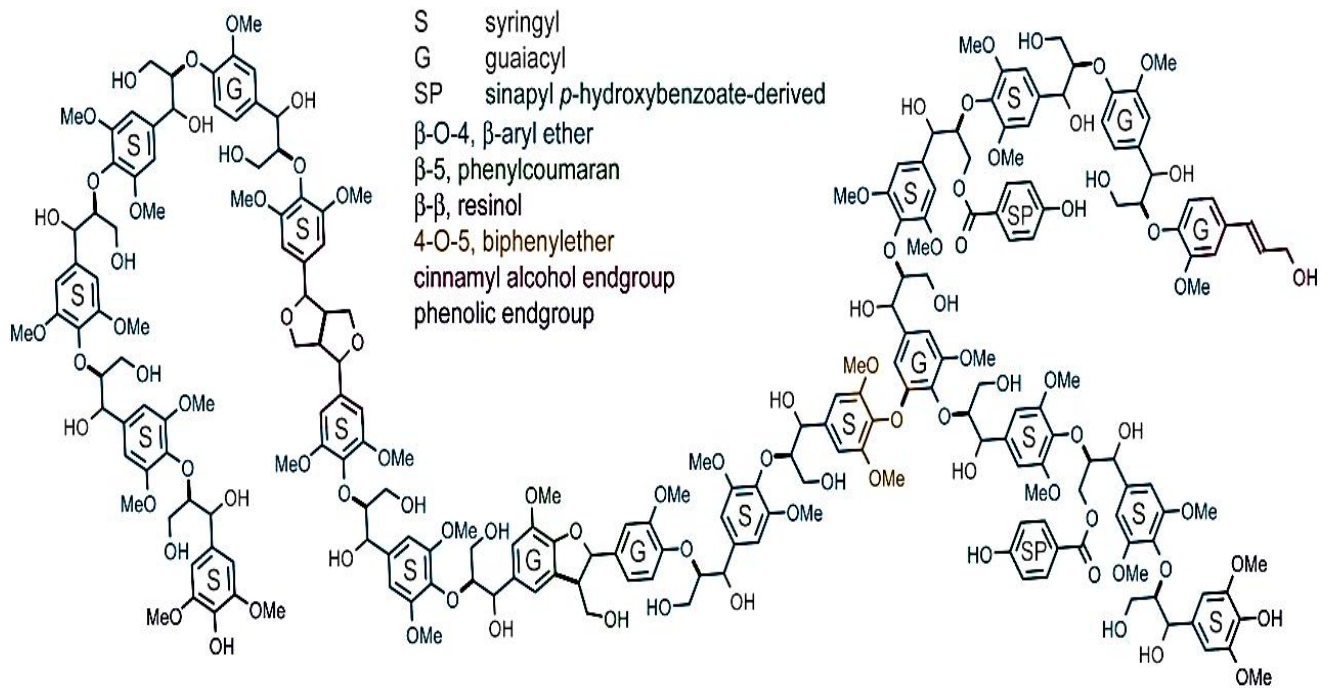


Figure 2-11 Proposed Poplar Lignin Structure Showing Linkages (Vanholme et al., 2010)

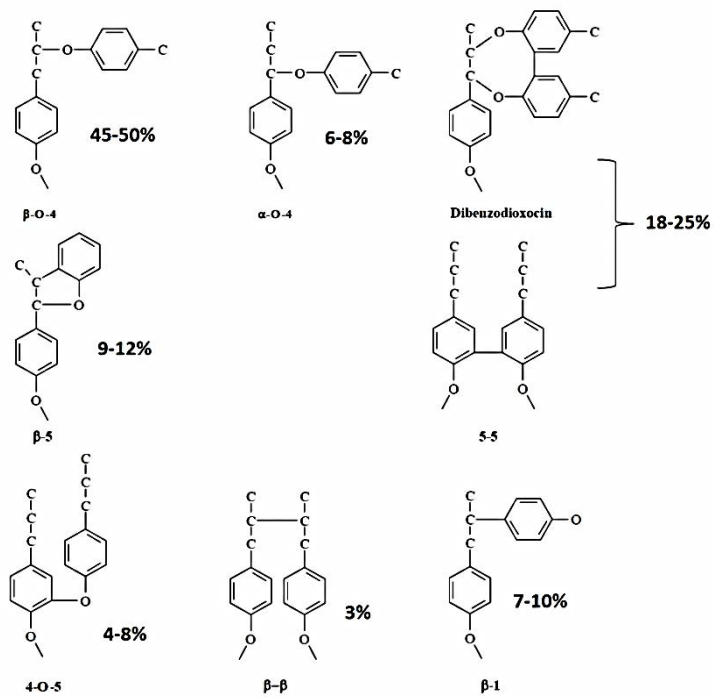


Figure 2-12 Common Lignin Linkages and Their Relative Contributions

(Adapted from Argyropoulos et al., 2002 and Ragauskas et al., 2006)

2.5. Thermochemical Conversion Processes of Biomass

Given their differing chemical composition, each of the biomass pseudo-components exhibit individual behaviours during thermochemical decomposition reactions. In addition, the active mineral content of biomass fuels is well evidenced to have a significant impact on devolatilisation and combustion pathways of fuel components. This subsequently influences the nature of the chars produced and their combustion reactivity. Given the importance of both organic chemical structure and inorganic mineral interactions during devolatilisation and char oxidation each has been discussed in some detail in the following sections (organic influence of pyrolysis and char formation in Sections 2.5 and 2.6 and inorganic matter influence in Section 2.8).

2.5.1. Hemicellulose Pyrolysis

Hemicellulose is the least thermally stable of the three major biomass components and is generally accepted to pyrolyse at the lowest temperature of between 200 and 280°C (Yang et al., 2006, Yang et al., 2007). Two distinct peaks have been observed in the decay profile, the first of which occurs between 200 and 280°C for wheat straw hemicellulose and is attributed to the decomposition of xylan side chain structures. The second, between 280 and 350°C, being ascribed to the fragmentation and depolymerisation of the polysaccharide chain (Di Blasi and Lanzetta, 1997; Peng and Wu, 2010; Shen et al., 2010).

Closer analysis of the rapid decomposition pathway of hemicellulose, which initially appears to proceed via a series of single step, reveals that, in fact, a multitude of complex degradation processes occur simultaneously, giving rise to the rapid decomposition of the polymer (Lv and Wu 2012)

Further investigation of the volatile gas species released during these thermal decomposition events using on-line gas analysis reveals that, during the first peak of mass loss mainly CO and methanol are volatilised, followed by primarily CO₂, acetic and aldehyde-type product evolution during the second degradation maximum. These findings confirm that the branched side chains of the hemicellulose polymer are most active, contributing to the first rapid mass loss peak with CO and methanol formation, followed by intensive depolymerisation of xylan units, giving rise to the second devolatilisation peak.

The reaction sequences undergone by hemicellulose units during their thermal decomposition are highly complex and include a range of competitive elimination, dehydration, bond cleavage, depolymerisation, reformation, ring scission and recombination reactions, all of which ultimately act to decompose the hemicellulose structure to form reactive intermediate products which undergo further decay to form a variety of permanent gaseous products, individual reaction pathways having been extensively investigated by Shen et al., 2010.

2.5.2. Cellulose Pyrolysis

Cellulose pyrolysis is found to occur at somewhat higher temperatures than that of hemicelluloses; decomposition occurs in the range of 315 – 400°C, with a maximum weight loss ensuing at around 355°C (Yang et al., 2006, Yang et al., 2007). The higher degree of thermal stability exhibited by cellulose can easily be explained by the linear, highly cross linked structure it adopts which gives rise to a strong, well ordered compound which is stabilised by inter and intra-chain hydrogen bonds, making it more difficult to decompose (Sullivan and Ball, 2012, Yang et al., 2007).

The thermal decomposition pathways of cellulose have been widely studied with pyrolytic techniques being employed primarily for their elucidation. These studies have

given rise to the generally accepted Broido-Shafizadeh model for cellulose devolatilisation which states that, as the cellulose polymer is heated, glycosidic bonds along the polymer chain undergo heterolytic thermolysis with the vaporisation of trapped moisture, giving rise to a reduction in the degree of polymerisation (Figure 2-13). This initiation reaction generally occurs at around 250°C (significant thermolysis being possible at lower temperatures in the presence of electron acceptors such as proton-donating acid catalysts or metallic cations) and generates a more labile polymer network known as active cellulose which can more easily undergo further thermal breakdown (Balat, 2008; Sullivan and Ball, 2012; White et al., 2011). This initiation step requires high apparent activation energy, in the region of 242.7 kJ mol⁻¹, but is accompanied by only minimal mass loss of around 3-6% (White et al., 2011). Following conformational reorganisation to form active cellulose the polymer can undergo one of two competing reactions, experiencing either volatilisation to form gaseous products or charring to produce solid carbonaceous char residues.

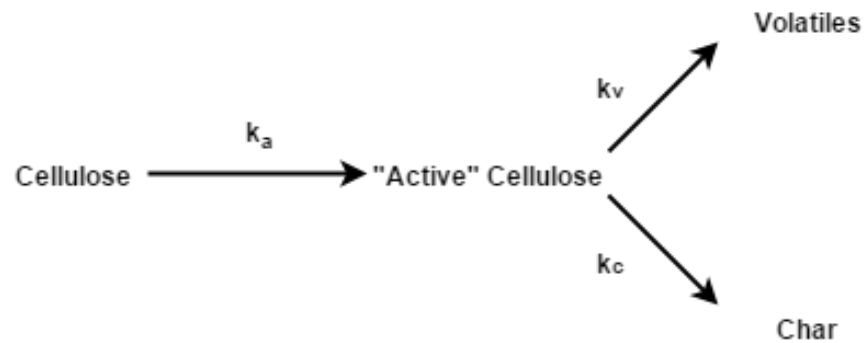


Figure 2-13 Broido-Shafizadeh Model for Cellulose Devolatilisation

(adapted from White et al., 2011)

The low molecular weight compounds formed during cellulose decomposition can then be readily oxidised to form a flaming combustion zone around the pyrolysing fuel particle. This in effect preserves the oxygen deprivation of the solid fuel, preventing oxidative combustion and maintaining pyrolytic devolatilisation (Sami et al., 2001).

2.5.3. Lignin Pyrolysis

Unlike hemicellulose and cellulose, which both undergo rapid thermal devolatilisation over a limited temperature range; lignin experiences a much less severe, continuous and gradual decomposition during pyrolysis.

The devolatilisation of lignin, although proceeding gradually over a large temperature range, has been observed to occur in three distinct stages, three discrete peaks in the mass loss profile being evident (Liu et al., 2008). The initial decomposition is characterised by the loss of water through evaporation of absorbed water below 100°C, followed by cracking of aliphatic hydroxyl groups in lateral side chains at temperatures in excess of 100°C. Some minor alteration of the lignin structure accompanies this initial decay with limited cleavage of lateral C-C bonds being evidenced by the evolution of gaseous CO₂ in minor quantities.

At around 225°C the lignin polymer enters the second devolatilisation stage which continues until the temperature reaches ~325°C, experiencing more significant pyrolytic decomposition of the fuel structure, coupled with the associated release of a range of volatile gaseous species. Large quantities of monomeric phenols are also released during this initial fuel decomposition, being due to the cleavage of main chain ether linkages within the polymer.

Melkior et al., 2012 reveal, however, that no cleavage of β -O-4 ether linkages is evidenced in the ^{13}C NMR spectrum of beech wood below 245°C, this reaction being minimal up to 300°C. The primary degradation route is instead believed to be the loss of methoxyl group side chains syringyl units.

Only at higher temperatures (300-400°C) are substituted phenols produced as the aromatic components are broken down, their chemical makeup being indicative of the characteristic composition of the original lignin structure (Asmadi et al., 2011; Liu et al., 2008; Hosoya et al., 2007).

Further increases in temperature over 400°C induce more rapid polymer degradation with maximum rates of mass loss and volatile release. During this period the gaseous product distribution switches from a predominance of large molecular phenolic volatiles towards low molecular weight species such as CO, CO₂ and a range of hydrocarbon species including methane (Asmadi et al., 2011; Liu et al., 2008).

A pyrolysis pathway for lignin, which includes the impact of solid, liquid and gaseous phase interactions, has been proposed by Asmadi and co-workers 2011 and can be seen in Figure 2-14.

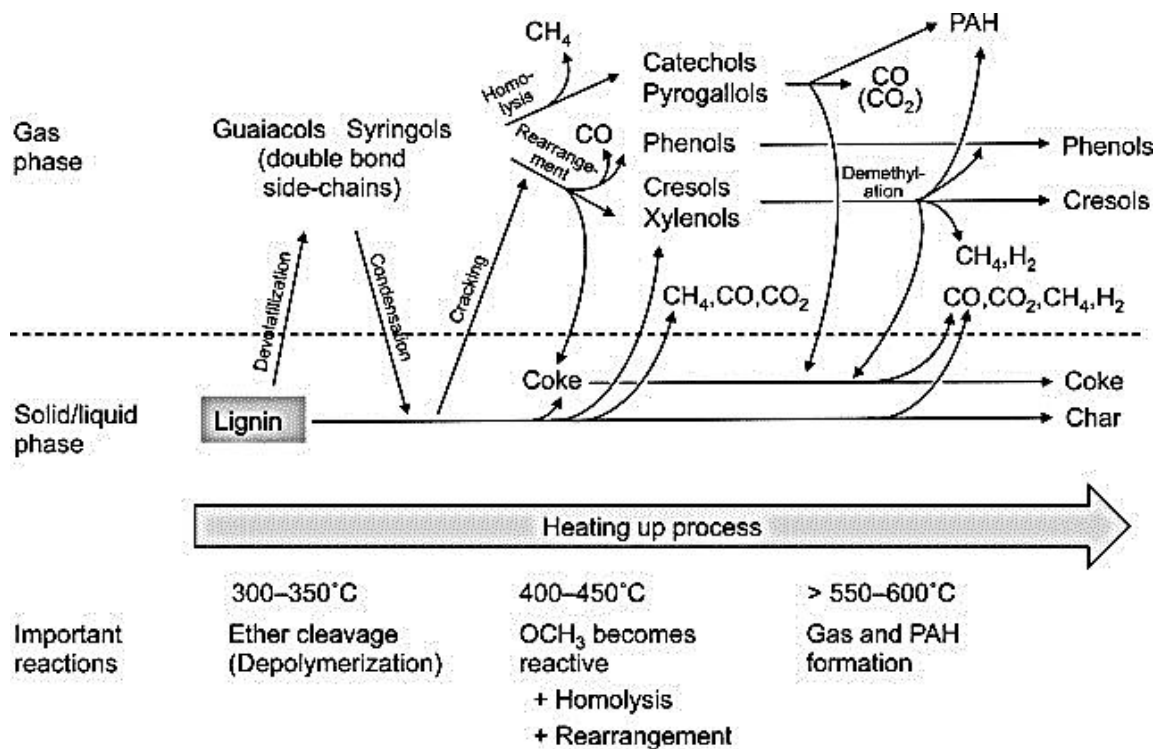


Figure 2-14: Proposed Lignin Pyrolysis Pathway (Asmadi et al., 2011)

Further investigation of gaseous yields and char produced during lignin pyrolysis (Jones et al., 2010) has revealed that the primary gaseous products formed during lignin devolatilisation represented mainly phenols and aromatic acids. These findings, coupled with the high char yield resulting from lignin pyrolysis, indicate that the major devolatilisation step occurs via dehydration reactions with some decarboxylation, decarbonylation and dehydrogenation. This decomposition leaves the aromatic polymer structure intact as a char product, with the majority of volatile products originating from the numerous lignin side groups.

¹³C Nuclear Magnetic Resonance (NMR) techniques also reveal clear depletion of lignin substructures and increasing aromatic character of the resultant char (Sharma et al., 2004) (Figure 2-15). At 600°C the char formed consisted almost entirely of aromatic carbon, all phenolic, aliphatic, methoxyl and hydroxymethyl carbons having been lost, with no organic oxygen containing substituents remaining.

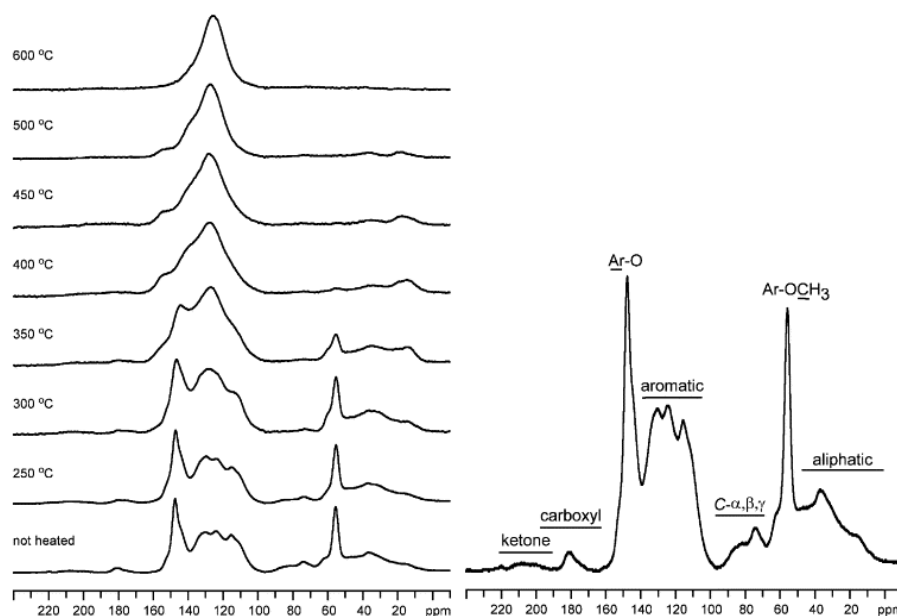


Figure 2-15 Temperature Dependence of the ^{13}C CPMAS NMR Spectra of Chars from Alkali Lignin, Prepared under Pyrolytic Conditions (Adapted from Sharma et al., 2004)

2.5.4. Summary

It is clear from the wealth of research discussed above that the individual pyrolysis behaviour of the three major biomass components is well studied. However, the majority of this research has concentrated on the chemical characterisation of gaseous pyrolysis products. Although the character of pyrolysis gases will influence the combustion processes, all volatile gases are extremely reactive during high temperature combustion and thus will ignited easily and burn extremely rapidly. Significantly less research has been conducted regarding the overall yield of volatile, the factors which determine volatile matter and char yields, and the form of remaining chars.

2.6. Biomass Char Formation and Combustion

2.6.1. Biomass Char Formation

As has been stated previously each of the cellulose, hemicellulose and lignin fractions of biomass materials undergo differing degrees of devolatilisation to produce differing residual char yields (Stefanidis et al., 2014; Yang et al., 2006). Both hemicellulose and cellulose components undergo rapid pyrolytic mass loss at relatively low temperatures with little char formation occurring, especially for cellulosic fibres. Lignin however undergoes slow, gradual devolatilisation over a wide temperature range, from ambient to 900°C producing a considerable char yield in line with its increased aromatic carbon content of around 40%. Overall, char yields obtained from pyrolysis of lignocellulosic materials has been closely linked with the lignin content of the fuel with several studies presenting linear correlations between percentage lignin composition and fixed carbon yields (Demirbas, 2003; Haykiri Acma et al., 2011; Rhen et al., 2007). The study conducted by Rhen et al., 2007 reports a strong linear correlation of char yield and the sum of klason lignin and extractives content with R^2 value of 0.91. Given that certain biomass are known to contain significant quantities of various aromatic extractive compounds, most of which are phenolic in nature, many being derivative of the phenylpropanoid structure, this increase in char yield observed as a consequence of the presence of extractive material in the biomass matrix is most likely to be due to an increase in the overall content of thermally stable aromatic structures within the biomass (Sjostrom, 1981). In addition to this, Demirbas 2003 studied the char formation from pyrolysis of 13 different biomass varieties, ranging from shells, husks and herbaceous materials to hard and softwoods in an effort to quantify the prevailing influences of the three primary pseudo-components on the yield of char obtained under slow heating pyrolysis in a thermogravimetric analyser. The findings of this investigation

revealed close non-linear relationships between the lignin content and char yields (R^2 correlation coefficients of 0.9937, 0.9871 and 0.8400 for low, high and all lignin contents respectively) but was unable to derive a single relationship to accommodate all biomass types studied.

Although the above studies clearly indicate the important role played by lignin constituents, especially thermally stable aromatic carbon compounds, in determining both the char yield and char reactivities observed for a range of lignocellulosic biomass fuels, no concerted attempt has been made to fully understand or quantify the influence that aromatic carbon content has during pyrolysis and char combustion reactions.

The structure of these lignocellulosic char products vary greatly in their physical and chemical nature due to the initial fuel composition and alterations which occur during the evolution of volatile gases from the original material during pyrolysis (Gani and Naruse, 2007).

The yield, morphology and reactivity of biomass chars are influenced primarily by the development of fluidity, fuel softening and release rate of volatiles during the devolatilisation process, this being determined by the structural composition of the original material, the quantity and variety of inorganic matter and prevailing pyrolysis conditions (Di Blasi, 2009).

Heating rates experienced during devolatilisation have been shown to have a profound impact on the formation and reactivity of biomass chars. Biagini et al., 2008 and Biagini et al., 2009, Guerrero et al., 2005, Janse et al., 1998 all report a significant increase in the oxidative reactivity of biomass chars with increasing pyrolysis heating rates. This enhanced combustion reactivity is thought to be a consequence of the more rapid

release of volatile gases from the fuel particle with higher pyrolysis heating rates which results in the production of a more porous solid structure due to the development of considerable internal overpressure within the particle and the coalescence of smaller pores. This open char structure, with a high macroporous character, is more open to the diffusion of oxygen during the combustion phase and enhances the occurrence of oxidative gasification reactions on the surface of large pores, therefore allowing for higher char burnout rates. In addition to the opening of char porosity, rapid gas release also acts at the molecular level, promoting transformation of the solid matrix with thermal scission of organic bonds to give polymer fragmentation, giving rise to an increase in the number of active sites for subsequent heterogeneous reactions between the carbonaceous char surface and the surrounding oxidative gas mixture. Coupling both the increase in char surface area and the concentration of active sites for further reaction results in a drastic increase in the char burnout reactivity (Biagini et al., 2009; Di Blasi, 2009).

A number of studies have analysed the form and reactivity of biomass chars generated under rapid heating entrained flow environments analogues to those experienced during PF devolatilisation (Biagini et al., 2008; Borrego et al., 2009; Fisher et al., 2012; Jarvis et al., 2011; McNamee et al., 2015; Pottmaier et al., 2013). Each has observed considerable alteration of the structure of the char in line with that of coal, evidencing at least some fluidity development, this being best characterised by Borrego et al., 2009 who observed the formation of cenospheric and network like biomass char structures following devolatilisation under N₂ in a drop tube furnace at 950°C. It is also reported that chars generated under higher particle heating rates (i.e. during prompt heating in entrained flow conditions) generally have greater reactivity than those generated under fixed bed, slow heating conditions due the substantial development of internal porosity (Fisher et al., 2012), however, Pottmaier et al., 2013 showed a significant decrease in

the rate of char oxidation following increases in drop tube furnace temperatures from 900 to 1300°C due to the thermal annealing of the char (these experiments in fact being conducted using the identical drop tube as utilised throughout this study).

The rapid release of volatile gases from the biomass fuel particle through hemicelluloses, cellulose and, to a limited degree, lignin decomposition acts to fundamentally alter the integral structure of the particle. Such alterations act to open up the porous structure of the char, increasing the surface area available for further oxidation and allowing easier diffusion of oxygen into the porous carbon framework. Both of these factors have a significant impact on the further combustive oxidation of the char, determining the degree of carbon burnout, time for char combustion and the final burnout temperature achieved, all of which influence the economic and environmental suitability of the fuel (Hasan Khan Tusha et al., 2012). The considerable variability in the composition of biomass feedstocks and the dependence of char conformation on this makeup gives rise to the complexity of char structures and their high degree of heterogeneity both between and within individual char particles.

Wang et al., 2012 have conducted a range of experiments to investigate the evolution of char structure during pyrolysis and subsequently assess its influence on the combustion reactivity of the resultant char. The findings of this study confirm that the activation energy of char combustion is closely correlated with the level of microstructural organisation within the char, revealing that those chars which possess less organised, highly amorphous structures are far more reactive than those with well-ordered, crystalline arrangements.

Avila et al., 2011 have attempted to assess the influence of biomass char structure on the thermal behaviour of the char during combustion with the aim of composing a characterisation system based upon the makeup of the fuel and the structure of

intermediate chars which is able to predict char burnout behaviour. This work utilised a simplified coal char classification system to characterise biomass chars as being either thin walled, thick walled or solid depending upon their morphological traits as determined by polished block oil immersion microscopy. It was found that fuels with higher lignin content experience peak mass loss of volatiles at higher temperatures than those with lower lignin; the char produced also undergoes burnout at lower rates and presents higher final burnout temperatures. These high lignin fuels also tended to produce thicker walled chars with evidence of some solid char forms, whereas low lignin, herbaceous species gave rise to thinner walled chars with minimal solid character. The thickest walled chars were shown to be the least reactive, displaying the highest burnout temperatures with thin walled chars exhibiting greatly enhanced reactivity.

Several studies have observed a two stage combustion step with two distinguishable peaks in fuel mass loss being observed during char oxidation (Darvell et al., 2010; Munir et al., 2009; Xu et al., 2012). These studies postulate that, similarly to differing devolatilisation pathways of dissimilar biological structures, the formation of different char fractions from the conversion of individual biological tissue types within the original sample has given rise to chars with differing thermal reactivities. These findings show that plant components with significantly different structural compositions form carbonaceous chars which differ considerably in their structural make up due to their differing devolatilisation characteristics, giving rise to chars with varying combustion reactivities. This suggestion is supported by the findings of Rhen et al., 2007 who discovered that stem, branch and bark tissues from Norway Spruce all produced different char yields during pyrolysis, these chars all exhibiting distinct oxidative activities depending upon the hemicelluloses, cellulose and lignin content of the parent material.

All of these studies clearly highlight the importance of original fuel composition on devolatilisation dynamics and the evolution of char materials during pyrolysis, undoubtedly acting to significantly modify the reactivity of the char. As such it is obvious that, if the combustion performance of biomass fuels is to be characterised with any degree of accuracy, a clearer understanding of the critical compositional factors determining fuel behaviour through devolatilisation, char formation and char combustion are necessary. It is clear also that the behaviour of individual biomass components, especially lignin structures, have a significant influence on all of these processes, fully understanding throughout the process is necessary.

2.6.2. Evolution of Fluidity

As has been evidenced from coal, the formation of liquid mobile transition phases during devolatilisation is able to significantly alter the morphological properties of char particles. Although the evolution of fluidity has been known to occur during the thermal treatment of biomass for some time, very little research has been conducted on the influence of biomass constituent mobility on the fundamental processes governing the devolatilisation of biomass fuels and how this might impact their overall thermochemical conversion. A recent study conducted by Dufour et al., 2012 has assessed the origin of molecular mobility within biomass during pyrolysis using in-situ high temperature ^1H NMR (known as Proton Magnetic Resonance Thermal Analysis (PMRTA)) which is able to quantify the proportion of mobile protons within the lignocellulosic samples (in this case *Miscanthus x Giganteus* – a herbaceous biomass) and their individual biopolymer constituents.

This study has observed that lignin forms a completely mobile phase above 150°C , remaining fully mobile over a large temperature window, ranging from 200 to 350°C . At temperatures below 200°C the lignin initially undergoes a glass transition phase in which

the mobility of the polymer increases prior to the commencement of pyrolytic loss of volatile matter which was seen to begin at $\sim 200^{\circ}\text{C}$. Following this glass transition the fluid fraction within the lignin was seen to increase from 150 to 225°C due to the commencement of bond cleavage within the structure evidenced by the loss of volatile mass. Between 200 and 350°C the homolytic cleavage of aryl ether bonds, primarily β -O-4 linkages, demethoxylation and re-condensation reactions act to thermally depolymerise the lignin structure and produce small lignin derived fractions with high mobility. Above 350°C the mobile fraction decreases rapidly due to the formation of solid char compounds via radical condensation reactions of lignin aromatics in the mobile phase, minimal lignin fluidity being observed between 350 and 450°C . The ultimate loss in fluidity has been attributed to the high temperature evolution of char surface functionalities with the loss of methyl moieties and consequent release of CO . The increased tendency of lignin to form a liquid intermediate phase during devolatilisation has also been observed in a number of other studies include that of Narayan and Antal, 1996.

Cellulose mobility is seen to be far lower than that of lignin (35 % mobile fraction being produced as opposed to 100% for lignin), beginning to increase only slowly at temperatures greater than 250°C and developing rapidly from 300 - 325°C . This mobile phase is thought to originate from the decomposition of active cellulose to form an intermediate liquid state mixture of disordered, amorphous carbohydrates including cellobiosane, cellotiosane and levoglucosan.

Xylan forms a 65% mobile phase between 200 and 275°C , with the development of mobility commencing after devolatilisation has begun. It is thus believed that the xylan mobile fraction does not originate from the transformation of native xylan structures

but instead from the formation of visco-elastic pyrolytic liquids within the sample particle, maximum fluidity and maximum mass loss being observed to coincide at 275°C.

Further analysis of the fluidity developments of native miscanthus, a synthetic polymer blend of similar composition and de-ashed miscanthus samples reveals that the interaction of cellulose, hemicellulose and lignin polymers alongside their further interaction with inorganic constituents during pyrolysis has a drastic impact on the evolution of molecular mobility during pyrolysis. These interactions are believed to depend highly on the structural conformation of the biomass samples with differing associations occurring between the biopolymer constituents, for instance lignin is seen to chemical bind to xylan but not cellulose in the biomass matrix, with proton donation from the cellulose being able to stabilise lignin derived radical species, thus influencing fluidity developments. Furthermore, interpolymer chemical cross-linking between polymers may allow crystalline cellulose microfibrils to strengthen the polymer network and inhibit evolution of fluidity.

Demineralised miscanthus was shown to produce a considerably greater degree of fluidity than the raw fuel which is thought to be due to the removal of alkaline inhibition of activated cellulose depolymerisation reactions (Radlein et al., 1987)

Under rapid heating, this development of biomass pseudo-component mobility alongside the rapid production of volatile matter, will dictate the ultimate form of the char produced and this will most likely be linked both to the content and fluidity development of lignin compounds and the influence of inherent mineral matter on molecular mobility.

2.7. Biomass Upgrading and Composition (Torrefaction and Hydrothermal Upgrading)

Given the importance of fuel energy density, grindability and hydrophobicity of biomass fuels for utilisation at utility scale, a number of biomass upgrading processes have been developed to improve the above characteristics for biomass fuels which show reduced energy density compared to coal, resist pulverisation (especially in milling equipment utilised for coal) and are highly hydrophilic and cannot be exposed to water without considerable physical and biological degradation.

One of the most promising and furthest developed upgrading techniques is torrefaction. Torrefaction describes a thermo-chemical pre-treatment process which is conducted under an oxygen deficient or inert atmosphere with the biomass being heated to 200-300°C. During this moderate heating the biomass dries and partially pyrolyses with the loss of moisture and various low molecular weight volatiles, decreasing the mass of the fuel whilst maintaining the majority of its energy content (Bergman et al., 2005).

Given the greater thermal reactivity of hemicellulose structures they appear to decompose in preference to other biomass components during torrefaction this acts to limit the ability of the fuel to form hydrogen bonds with water and results in the development of hydrophobicity (Bridgeman et al., 2008) whilst encouraging the evolution of light, low energy density components which produces a more energy dense product fuel.

Torrefaction helps improve handling and milling performance by increasing the brittleness of the biomass by disruption of the internal lignocellulosic structure (Bridgeman et al., 2010).

The influence of torrefaction on both devolatilisation and char oxidation behaviour has been widely studied (Arias et al., 2008; Fisher et al., 2012; Jones et al., 2012; McNamee et al., 2015) with torrefied biomass being recognised to produce significantly less volatiles during pyrolysis (due to the loss of volatile fuel components during torrefaction) and gives rise to considerably less reactive chars. Other than the differing influence of char surface area there is as yet little evidence to suggest why torrefied biomass chars are considerably less reactive than raw fuel counterparts, however. McNamee et al., 2015 have observed a reduction in the inherent char reaction rate normalised for surface area changes which suggests that, as well as developing less surface area the torrefied biomass chars are also less chemically reactive.

In addition to torrefaction, mild hydrothermal treatments such as steam explosion of biomass fibres prior to pelletisation are being utilised for the production of improved solid fuels for power production. In contrast to torrefaction, steam explosion does not rely upon the volatilisation of reactive fuel components but instead utilises low residence time steam treatment with steam temperatures in the range of 180 – 240°C and pressures of 10 – 35 bar followed explosive decompression (Lam, 2011). Both the effect of heating the biomass with saturated steam and the rapid reduction in pressure results in defiberisation of the biomass, re-ordering the lignocellulosic structure. As lignin softens during heating at temperatures between 60 and 100°C (Kaliyan and Morey, 2006; van Dam et al., 2004) it is able to migrate during the steam treatment and coat the outside of defiberised cellulose particles. This process gives the steam exploded material its characteristic “black” colouration and both enhances the binding of the material during pelletisation and conveys significant hydrophobicity (Suzuki et al., 1998; Shaw et al., 2009). These properties are advantageous in the preparation of densified fuel for power generation as the product is resistant to water adsorption during transport and storage – allowing for simplified storage arrangements either outside or

in open sided buildings and prevent degradation of the pellets through water damage and physical impacts.

2.8. Inorganic Matter and its Impact

Although it is clear that the structural composition of biomass has a major influence in its thermochemical properties, a wealth of literature has also outlined the key importance of inorganic and mineral species, especially alkali/alkaline earth metals (AAEMs) in determining combustion dynamics during devolatilisation and char conversion.

2.8.1. AAEM Influence on Devolatilisation Processes

Fuentes and associates, 2008 conducted a thorough investigation of the influence potassium, phosphorous, magnesium, iron and calcium content of short rotation willow coppice have on pyrolysis and char combustion processes. This involved the comparison of raw, hydrochloric acid washed (demineralised) and inorganic impregnated (following demineralisation) willow samples to give an understanding of the impact each inorganic species has on both devolatilisation and char combustion. Thermo-gravimetric decomposition profiles of the varying samples revealed that, following demineralisation, initial decomposition and volatile gas release from polysaccharide decomposition within the willow was shifted from 378 to 379.5°C, indicating that some of the materials removed from the willow by acid washing do exhibit catalytic effects on willow devolatilisation. Both potassium and phosphorus impregnated samples were shown to strongly catalyse the initial decomposition of the willow, lowering the temperature of the main pyrolytic decomposition peak by 28.3 and 95 °C respectively. Conversely Ca, Fe and Mg were seen to have little or no impact on the devolatilisation process.

Study of the gaseous material formed during fuel devolatilisation using on line mass-spectrometry indicates that the distribution and yield of pyrolytic compounds can be significantly altered by demineralisation and inorganic impregnation of raw biomass. This is indicative of the high dependence of primary pyrolysis mechanisms on the inorganic matter content of the fuel. A number of studies (Eom et al., 2012; Nowakowski et al., 2007) have evidenced that increased potassium content resulted in a major shift in the gaseous product distribution formed during pyrolysis of biomass, individual lignocellulosic sub-components and model compounds triggering a reduction in the yield of primary volatile gases such as levoglucosan, pyrans and furans in favour of the increased production of low molecular weight gases such as formic and acetic acids, glyoxal, hydroxyacetaldehyde and acetol (Fuentes et al., 2008). These changes are generally attributed to a fundamental alteration of the thermal decomposition mechanism, with heterolytic depolymerisation, ring fission and glucose fragmentation reactions being preferentially catalysed by potassium at the expense of competing levoglucosan formation via dehydration, rehydration, decarboxylation and decarbonylation of cellulose and hemicellulose. Similar results are report by Fuentes et al., 2008 and Fahmi et al., 2007 who observed a 900% increase in the pyrolytic levoglucosan yield from *festuca mairei* grass upon removal of inorganic minerals by water washing at elevated temperature. This study also revealed that both raw and demineralised samples produced a similar diversity of compounds during devolatilisation with only the yields of each compound being significantly altered. This preservation of the type of product species obtained indicates that both cellulose depolymerisation and fragmentary ring-scission reactions occur competitively at the same time, the dominance of one set of reactions over the over being determined by the catalytic effects of fuel alkali/alkaline earth metal content.

Nowakowski and Jones, 2008 have summarised the distribution of cellulose pyrolysis products whilst reporting increases in char yield for all biopolymers investigated. An increase was observed from 7.7% for raw cellulose to 27.7% for potassium impregnated cellulose; from 5.7% for raw levoglucosan to 20.8% for levoglucosan in the presence of added CH_3COOK and from 37% to 51% for lignin.

Nowakowski and Jones, 2008 propose that, not only is there a shift away from initial levoglucosan formation from cellulose decomposition, but the presence of potassium species also acts to promote the decomposition of what levoglucosan is produced to form lower molecular weight species which are then open to subsequent base catalysed polymerisation reactions acting to further increase the char yield.

2.8.2. AAEM Influence on Char Formation and Oxidation

With regards the composition of char formed from biomass containing appreciable AAEM contents, Wang et al., 2012 have observed that, although biomass pyrolysis would be anticipated to produce chars with a more disordered internal structure due to their low-rank (exhibiting behaviour much akin to that of a brown coal), rice straw chars are in fact only slightly less well-organised than that produced during pyrolysis of a low-volatile anthracitic coal. This drastic difference between expected and actual rice straw char structure is thought to be due to the highly elevated alkali metal content of the biomass fuel and their significant influence on devolatilisation reactions. Li et al., 2006 and Sathe et al., 1999 postulate that this is due to the role played by exchangeable cations in promoting radical bond-breaking and bond-forming reactions which occur during pyrolysis of both biomass and high alkali containing brown coals. These reactions greatly enhance ring condensation, giving rise to a more highly condensed biomass char than would otherwise be expected.

Jones et al., 2007 have postulated that a similar retention of more highly ordered biomass chars is also promoted by the presence of potassium within the fuel matrix. This acts to preserve the solid, porous structure of the char particle throughout combustion, suppressing the formation of liquid tar fractions, thus allowing for greatly enhanced char burnout rates for potassium containing biomass when compared to demineralised fuel samples whose char burnout may last for anything up to 20s as opposed to ~4s (Figure 2-16).

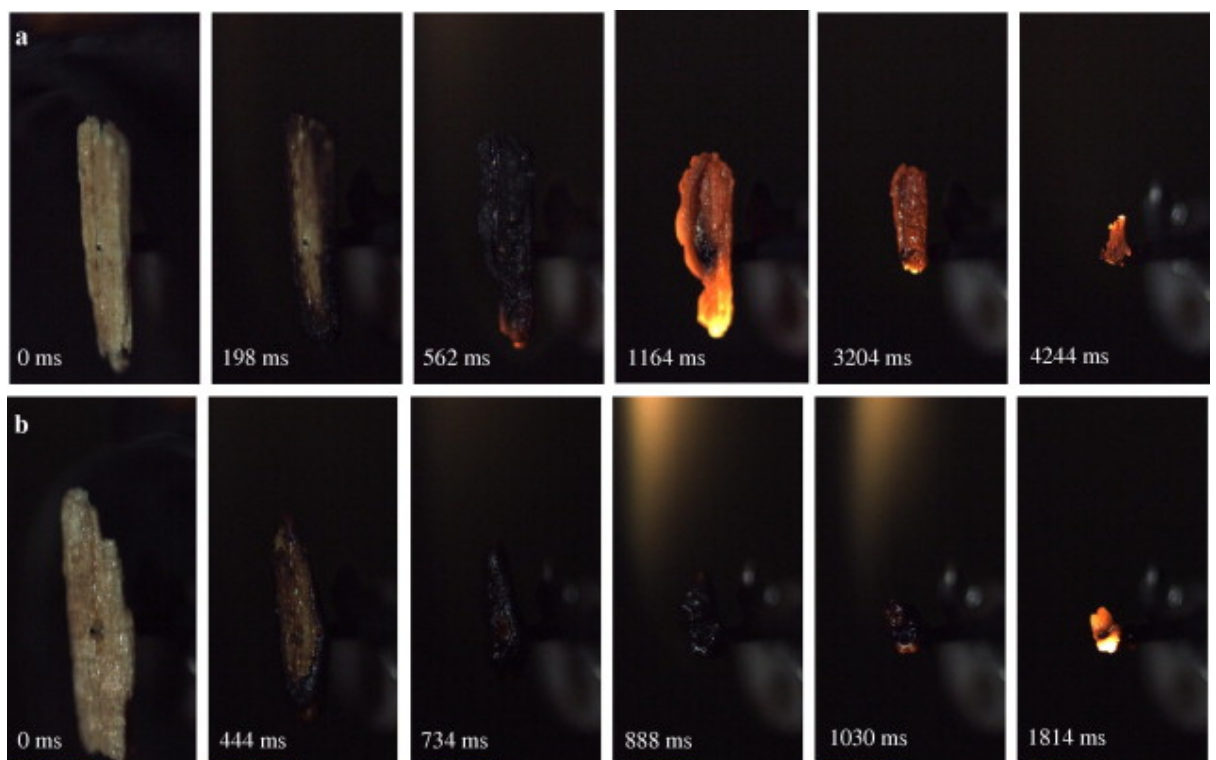


Figure 2-16 Willow Particle Combustion Profile using Meker Burner

(a) K impregnated Willow Particle (b) Demineralised Willow Particle

Jones et al., 2007

Raveendran et al., 1995 reported an increase in char surface area for five biomass species following HCl and NaOH demineralisation. This increase in surface area is thought to be due to the increase in volatile matter content and thus increased rate of

volatile matter loss from pyrolysing particles which acts both to increase pore formation and reduce volatile matter residence times in the pores; suppressing volatile matter condensation. Further to this, Downie et al., 2009 and Joseph et al., 2009 following extensive review of existing literature go so far as to conclude that biomass chars produced from woody species tend to exhibit larger surface areas, and contain higher proportions of meso and macropores compared to herbaceous chars.

Some researchers have attributed the loss of char surface area with increasing biomass mineral content to the blocking of char pores with ash following pyrolysis (Lee et al., 2010). This is especially true of biomass fuels which contain significant quantities of SiO_2 which is able to melt under high pyrolysis treatment temperatures and thus effectively fill char pore structures and reduced surface area (Pottmaier et al., 2013).

These findings are in contradiction to a wealth of research concerning the role of alkali metals during biomass and coal char formation which show that increased use of potassium, calcium and sodium based mineral additives results not only in increased char yield but also increased char surface area formation via chemical activation (Ahmadpour and Do 1997; Díaz-Teran et al., 2003; Ehrburger et al., 1986;). This has led to the wide-spread application of alkali/alkaline metal additives for activation of biomass chars for charcoal and activated carbon production.

Xu and Sheng, 2012 observed a decrease in the pyrolysis and char combustion reactivity of cornstalk biomass on inorganic leaching, with an increase in the initiation temperature for both stages being evident, after water and HCl demineralisation of the of the samples. This change in reactivity was postulated to be due entirely to the loss of catalytic inorganic species as the overall structure of the material, as revealed by X-Ray Diffraction (XRD), was seen to remain unchanged during the washing process.

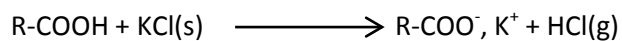
Similarly to K fuel content, Wang et al., 2006 found that a range of Na-based biomass species were able to catalyse devolatilisation, reducing onset and maximum weight loss temperatures. This study also revealed that Na catalytic effects stimulated the formation of char structures during pyrolysis, increasing the exothermic nature of these processes.

The inherent metal content of biomass not only significantly alters the decomposition of the primary structural polymers, thus influencing overall fuel volatilisation and char formation, but also has a substantial impact on the oxidation and burnout of solid carbonaceous chars. The generally accepted mechanism for metal catalysed oxidation of carbon surfaces, as described by Jones et al., 2005, involves a series of oxidation – reduction cycles whereby adsorbing oxygen molecules are able to make contact with the carbon surface of the char particle at the metal oxide (or carbonate) interface. Interaction between the metallic species and the carbon surface results in a substantial weakening of the C-C bonds of adjacent carbon atoms, effectively activating them to reaction with oxygen which leads to its easy association with the surface and subsequent release of CO gas, this being widely considered to be the rate limiting step in the gasification of char during combustion (Backreedy et al., 2003, Jones et al., 2005). Lv et al., 2010 postulate that the key factor in assessing the influence of alkali and alkaline earth metals on the pyrolysis and gasification and char combustion of biomass materials is thus the association of these species within the biomass structure and its interaction with the lignocellulosic constituent during combustion process.

2.8.3. Inorganic Constituent Dynamics and Their Impact

The degree to which inorganic species are released to the gas phase during the devolatilisation processes may have an influence on the role played by inorganic catalytic reactions on the combustion process.

The significant release of HCl gas observed during fuel devolatilisation has been attributed to the low temperature interaction of potassium chloride mineral structures with the organic biomass matrix. Björkman and Strömberg, 1997 proposed that this rapid release of HCl was brought about by ion exchange reactions occurring between the carboxylic functionalities of the fuel biopolymers and potassium chloride (KCl) minerals as outlined below:



This led to the substantial release of chlorine at temperatures between 300 and 400°C, being most extensive for highly oxidised biopolymers such as hemicellulose.

Further investigation has revealed that generally greater than 80% of the fuel chlorine content is volatilised during initial combustion stages. This is in contrast with potassium which undergoes a lesser degree of volatilisation, losing 10-40% of the initial content to the gas phase, retention in the bottom ash being far more significant (Jensen et al., 2001).

This retention of potassium in the solid matrix is due primarily to the migration of potassium to form discrete salt particle in the form of K_2CO_3 , KCl and K_2SO_4 in char particle pores and surfaces and the association of K with oxygen functionalities of the char matrix (Zolin et al., 2001). Some incorporation of potassium in the organic char structure and subsequent formation of alkali metal silicates with high thermal stability was also observed (Jensen et al., 2000; Wornat et al., 1995). All of these factors effectively act to limit the loss of potassium during the devolatilisation phase, encouraging its retention in char structures, with appreciable release of potassium being observed only during char oxidation at elevated temperatures (>900°C) (Jensen et al., 2000) with K retention continuing even to temperatures of 1613K (Zolin et al., 2001).

The retention of K throughout the pyrolysis stage is thought to be due to the high diffusional resistance of K containing compounds which are predominantly distributed throughout the pore structure of char particles coupled with the increased thermal stability of char bound K species, such as K_2CO_3 , under pyrolytic conditions.

Olsson et al. 1997 similarly observed only minimal loss of K during the initial stages of the devolatilisation phase with the vast majority of K release occurring at elevated temperatures with char conversion. The magnitude of this later potassium release was found to correlate with the chlorine content of the fuel under investigation (wheat straw). These findings were corroborated by Baxter et al. 1998 who likewise detailed a strong positive correlation between the release of K to the gas phase and the original Cl content of the fuel. It can thus be concluded that chlorine is able to act as a strong facilitator of K gasification from the char matrix and thus influences the degree to which potassium can play a role in the thermal decomposition of the fuel during combustion.

Na compounds such as Na_2O and $NaCl$ which occur as discrete phases within the biomass matrix are more easily lost than organically bound K, leading to the more significant influence of potassium catalysis on char oxidation behaviour (Long et al., 2012).

The release of catalytic inorganic materials from biomass not only determines the quantity of catalytic material left in the char structure, and thus ability to influence the char burnout of the fuel, but may also have an impact on the gaseous phase reactions of volatiles following their volatilisation from the fuel particle, determining gaseous flame characteristics and secondary charring reactions. Raveendran and Ganesh, 1998 and 1995 propose that the presence of inorganic minerals, both within the organic structure of pyrolysing material and in the gas phase following volatilisation, act to catalyse the char forming secondary reactions of volatiles both in the surrounding gas cloud and

within the fuel particles. This in turn can be seen to have an impact on the evolution of pore structure within the resulting char due to the deposition of these secondary amorphous chars on the surface of the char pore structure, thus influencing char reactivity further.

2.9. Summary of Findings

An analysis of the existing literature with regards to solid fuel combustion of both coal and biomass derived fuels has been conducted. The key findings of this literature review are summarised as follows:

- ▶ A wealth of literature regarding the differing devolatilisation and char oxidation dynamics of different coals exists and has been widely utilised to elucidate the potential of given fuels in utility scale PF boilers. This has led to the derivation of a number of coal classification systems which have been successfully used to correlate the physiochemical composition of coals, through analysis of maceral pseudo-components, with char yield, structure and reactivity. This has enabled a relatively clear understanding of the potential differences between coals when burned in PF firing plant to be gained from basic analysis of their initial composition
- ▶ The role of aromatic carbon content of coals is seen to be key in determining the behaviour of coals and their individual maceral components during both char formation and combustion reactions and has been closely correlated with conversion dynamics. Given the fact that lignocellulosic biomass fuels likewise contain both aromatic and non-aromatic carbon forms, the degree of aromaticity of these fuels will impact the combustion of biomass through devolatilisation and subsequent char oxidation. Although widely recognised this

influence is yet to be studied in detail or quantified in the context of PF combustion

- ▶ The composition of lignocellulosic biomass as to their hemicellulose, cellulose and lignin composition alongside mineral matter interactions have been widely studied, however, very little information is available which elucidates the driving forces determining overall pyrolysis yields and very few quantitative studies have been conducted to determine the role of alkali/alkaline earth metals or aromatic carbon on pyrolysis char yield or reactivity
- ▶ There is no existing classification of biomass fuels which is able to provide valid information on the behaviour of biomass fuels during combustion under PF firing conditions, where both devolatilisation and char oxidation dynamics play a role in determining the overall efficacy of the combustion process

2.10. Project Aims and Objectives

Given the clearly established importance of both the organic and inorganic structure of biomass fuels on their combustion performance, the need to fully understand potential fuel performance factors, including volatility, during pyrolysis and subsequent char reactivity prior to adoption in PF fired utility boilers there is requirement for a new performance related classification of biomass fuels. This study will concentrate on the well-established predictive correlations available for coal devolatilisation and char oxidation but applied to the classification of a range of lignocellulosic biomass materials with the aim to establish a new characterisation system which will aid in the prediction of key combustion parameters.

The individual aims of this investigation are detailed as follows:

- ▶ Determination and quantification of the impact of key compositional factors influencing volatile matter and char yields of varied biomass fuels (to include aromatic carbon and mineral matter species contents) during both slow heating fixed bed and rapid heating simulated PF entrained flow pyrolysis conditions
- ▶ The study of variations in combustion related performance factors (including devolatilisation and char reactivities) as a function of biomass composition and char characteristics with special emphasis on char oxidation in PF fired furnaces
- ▶ Investigate the relationships which describe the reactivity of high heating rate and temperature entrained flow reactor biomass chars in relation to the chemical and physical nature of the char particles and the original composition of the parent fuel
- ▶ The establishment of a new biomass classification system based upon universal, quantitative correlations able to predict critical combustion performance indicators for lignocellulosic biomass fuels including volatile matter/char yields, char structure and char combustion reactivity based upon understanding of their chemical and structural composition. Given the clear influence of both aromatic carbon and alkali/alkaline earth minerals evidenced above, this study will concentrate predominantly on the prediction of performance during pulverised fuel combustion from analyses of fuel aromaticity and mineral concentrations.

Chapter 3: Materials and Methodology

This chapter discusses the biomass fuel materials utilised and the experimental techniques used throughout the investigation of these materials in the context of the aims of the investigation. This includes fuel selection and preparation, fuel characterisation, fuel devolatilisation and char generation, char reactivity assessment and char characterisation.

3.1. Fuel Selection and Preparation

Fuel selection and preparation form a vital component of any study and has been conducted in an effort to allow a fully quantified, universal assessment of the influence of aromatic carbon and mineral matter components on the volatile matter and char yield and subsequent char reactivity of all potential lignocellulosic biomass fuels under consideration for use in PF firing utility boilers. This involved thorough selection of raw fuel materials to cover all available fuel sources (agricultural wastes, forestry products and purpose cultivated energy crop materials) and plant types (hardwood, softwood, herbaceous and waste plant material) with varying chemical, physical and mineral matter compositions. Further to this, samples were subject to a number of chemical and thermochemical conversion techniques described in the following subsections 3.1.1 – 3.1.4 to produce samples with a wider range of aromaticities and mineral contents and enable more quantitative assessment of the influence these constituents have on the combustion behaviour of lignocellulosic materials.

3.1.1 Raw Fuel Selection

Chosen raw fuel samples include gymnospermous hardwood, angiospermous softwood and herbaceous plant varieties all of which differ in their composition of the three major biopolymer components, the chemical structure of these structural compounds, aromatic carbon content and inorganic mineral matter compositions. The chosen fuels are also representative of a range of commercially available non-coal materials currently being used, or considered for use, by UK power producers including traditional forestry products, short rotation biofuels and agricultural/industrial waste products.

The biomass fuels used throughout the study and a brief description of each is given as follows:

Wheat Straw Pellets:

Straw residues that remain following the harvest of cereal and oil grains forms one of the largest potential sources of secure, commercially available lignocellulosic biomass feedstocks. In the UK nearly 12 million tonnes was produced during 2007, of which 54% was derived from wheat production (Copeland and Turley 2008). Given the global availability of straw materials they have received increasing interest as a source of bioenergy generation via combustion and gasification – this has led to the construction and continued development of a number of straw fired combustion plants both in the UK (Sleaford, Brigg and Elean power stations) and elsewhere. Straw material was of interest during this study not only due to the potential availability of the fuel but also due to its high mineral matter content which is known to give rise to increased char production and increased char combustion rates (Nowakowski et al., 2007). The fuel utilised was provided in the form of 7 mm densified pellets.

Corn Stover Pellets:

Corn stover comprises both the stalk and leaf residues produced during the harvest of maize for grain. Due to improper climatic conditions the vast majority of maize produced in the UK is utilised for animal feed and thus produces significantly less unutilised residue than that harvested for grain, however, global production of maize grain is significant with annually available quantities of corn stover in the USA being estimated as 75 million dry tonnes and being described as “a major untapped source of agriculture derived biomass” (Perlack et al., 2005). The corn stover sample utilised during this study has been densified to produce standard 7 mm pellets as preferred in large scale pellet handling systems.

Pine Woodchips:

To date, softwood pine derived fuels have formed the mainstay of most biomass fuelled power generation assets due to their widespread commercial utilisation, large scale production (traditionally for pulp and paper production, an industry currently undergoing continued recession and efficiency improvement) and established processing and supply chains. Purpose cultivated forestry, diseased and pest ridden wood and pine residues from forestry and manufacturing activities form the one of the greatest sources of non-herbaceous plant residues and consistently form an important feedstock for biomass for energy projects. In the case of most of the on-going coal to biomass conversion projects utilising PF firing systems pine wood pellets have become the chosen primary fuel due to their generally sound commercial status, wide availability and beneficial fuel characteristics (very low volume, largely benign ash content reducing ash handling and slagging/fouling propensities) (DRAX, 2015).

Olive Cake Pellets:

Pelletised residue resulting from industrial olive oil production. This includes the hard, woody olive stones and more heterogeneous fleshy tissue materials. 98% of all olive oil production comes from the Mediterranean with Spain, Italy, Greece and Turkey all contributing significant proportions of this total. This easy, relatively cheap sourcing of olive residues has made them a key source of biomass for large scale co-firing activities throughout the UK, as a supply infrastructure develops and a pelletising industry emerges these materials are likely to remain an important potential source of widely available, cheaply procured biomass fuel for power generation. Alongside their industrial relevance olive residues are also of interest due to their structural composition which is shown to include a high degree of lignin and hemicellulose with consequently reduced levels of cellulose, thus differing greatly from other biomass sources where cellulose commonly forms the primary constituent, furthermore, the alkali / alkaline earth mineral matter content is high with consequent influence on char formation, combustion and ash chemistry related reactions.

Miscanthus Pellets:

A perennial, rhizomatous herbaceous grass originating from Asia which has been widely trialled for use as both a solid biofuel for combustion and a source of digestible sugars for liquid biofuel production. Rapid growth rate, low inorganic mineral content, high biomass yield (up to ~10 t/acre) and longevity (10-15 years once established) of Miscanthus make it ideal for use as an annually harvested short rotation energy crop (Clifton-brown et al., 2004). Miscanthus' annual production cycle includes a dormant stage during which moisture travels from the stem and leaf material back into the rhizome, reducing the moisture content following harvest to typically less than 15%

making it ideal for further processing, transportation and use as a renewable fuel source.

Eucalyptus Pellets:

A fast growing evergreen hardwood species which grows readily in both tropical and temperate climates, Eucalyptus species have been widely acclaimed for their potential utilisation as a short rotation coppice energy crop (Rockwood et al., 2008). Many eucalyptus varieties are particularly well suited for this method of harvesting due to the high dry-matter yield per hectare, rapid regrowth rate - facilitating frequent cropping, easily employable harvesting techniques and high energy content of the material. Eucalyptus wood lignin content has also been found to be amongst the highest of any woody biomass material, ranging from 25-35% (Vassilev et al., 2010), this gives rise to an increase in the aromatic carbon content of the fuel.

Mixed Softwood Pellets:

With the popularity of low ash softwood pellets for power generation applications commercially available mixed softwood pellets imported from the east coast of the United States were sourced to act as a control fuel to gauge the relative performance of differing fuels against those being proposed for use in coal to biomass converted plant.

Alongside the use of varied biomass fuels a selection of raw coals have been studied in order to highlight differences between biomass and coal fuels and to benchmark the potential effects of variation within the biomass types studied.

El Cerrejon:

El Cerrejon is a Columbian high volatile bituminous coal sourced from the North of Columbia and is one of the largest open cast coal mines in the world covering 170,000

acres in total. El Cerrejon is commercially important given the relatively large export quantities (32.03 million tonnes in 2011); of which 58% is exported for consumption in European coal fired power plants.

Kellingley Coal:

Following the closure of Thoresby deep mine in 2015 Kellingley became the last remaining deep mine operating in the UK under UK Coal. Kellingley coal is a bituminous coal and is characterised by relatively high volatile matter and liptinite content.

Kellingley is predominantly utilised by local pulverised coal fired plants of Ferrybridge, DRAX and Eggborough with production of 1.5 million tonnes in 2008.

Thoresby:

The Thoresby deep mine was the last remaining deep mine in operation in Nottinghamshire, UK (a traditional coal producing county) until its closure in 2015. The mine produced around 1 million tones of coal per year in the final years of its life all of which was consumed in the local pulverised coal plants of EDF Cottam and West Burton. Thoresby coal is typified by lower volatile mater and liptinite content than Kellingley coal and is typically less reactive both during devolatilisation and char combustion reactions for this reason.

3.1.2 Chemical Delignification

Although the selected biomass do possess a relatively wide range of aromatic carbon and mineral matter contents, in order to fully quantify the influence of lignin derived aromatic carbon structural components it was desirable to generate samples containing a wider range of aromatic components through chemical delignification of raw samples.

This will further enable analysis of combustion dynamics of residues which may arise from the production of liquid biofuels. The necessity of developing a sustainable

alternative to the petroleum-based industry for fuel and chemicals has led to acceleration in the progression of bio-refinery processes used to treat biologically derived materials. These techniques traditionally include enzymatic fractionation, steam explosion, chemical hydrolysis using hot water, ammonia fibre explosion, acid hydrolysis (either dilute or concentrated) and organosolv processes (Mosier et al., 2005).

Of these approaches the use of strong acids has been most widely utilised in industry to achieve the separation of cellulose fibres from lignin and hemicellulose biopolymers. The treatment of biomass with strong acids such as, sulphuric and hydrochloric acids, hydrolyses the holocellulose components of the parent material, breaking down the cell wall structure and releasing monomeric sugars to the hydrolysate. This leaves lignin as an insoluble residue which can be easily separated by filtration. Although these techniques do offer a flexible, cheap and convenient route to biomass fractionation, extensive alteration of the chemical structure of isolated fractions can result from the chemical reactions occurring between the substrate and acid reagents and any lignin separated may be heavily contaminated with process impurities such as non-hydrolysed sugars, feedstock minerals and other chemical reagents. As such, acidic fractionation was discounted as a route to sample delignification due to the fact that any lignified material collected would be unrepresentative of the parent fuel due to the considerable alteration of chemical structure brought about by acid treatment.

An alternative to the use of destructive, harsh acid pre-treatment for the separation of biomass constituents can be found in the utilisation of organosolv processes. Originally developed by General Electric in the 1970's for the production of clean turbine generator biofuels and subsequently adopted as a pulping technique in the pulp and paper industry (Ruiz et al., 2011) organosolv methods involve the treatment of lignocellulosic biomass with an organic solvent, alcohols or organic acids being widely

used, at elevated temperatures. This results in the extraction of lignin from the biomass matrix following the thermochemical breakdown of inter-polymer bonding within the lignin-cellulose-complex (Harmsen et al., 2010). Lignin is separated from the pre-treated mixture by washing with aqueous ethanol followed by precipitation of organosolv lignin using water, centrifugation and air drying. The holocellulose present within the feedstock is left as a solid residue, being easily isolated by filtration and thorough washing. The treatment method employed during this study follows that of Pan et al. (2006) giving isolation of pure, solid lignin and partially delignified biomass so as to keep degradation of the native biopolymer structures to a minimum (Pan et al., 2008). This method has been shown to produce a relatively unaltered lignin product closely representative of that found within the original biomass. Organosolv lignins exhibits high molecular weight, low polydispersity and high aromatic character and are free of any significant holocellulose (cellulose + hemicellulose) contamination (Villaverde et al., 2009), all of which indicates their relative similarity to native lignin structures as found within the original plant material.

Firstly, dry biomass samples of known mass, ground to below 2 mm, were placed in a Parr pressure reactor vessel alongside 65% aqueous ethanol solution (8:1 liquid:solid loading). The resultant mixture was acidified to 1% using 2 M sulfuric acid solution before being heated in the closed pressure vessel to 180°C at 3 °C/min with constant stirring at 120 rpm. The vapour pressure of ethanol at this temperature results in a pressure within the vessel of just under 20 bar. Elevated temperature, pressure and mixing is maintained for 1 hour before cooling the reactor contents to room temperature using internal water cooling loops. Following this extraction process the resultant mixture is filtered, solid holocellulose rich material being washed thoroughly with 60°C 65% aqueous ethanol. The solution and washings collected are combined and lignin solids are precipitated out of solution with the addition of 3x the volume of

deionised water. Solid lignin is then isolated from the resultant suspension by centrifugation at 4000 rpm for 20 minutes before drying at 60°C for 24 hours (See Figure 3-1 for a process flow).

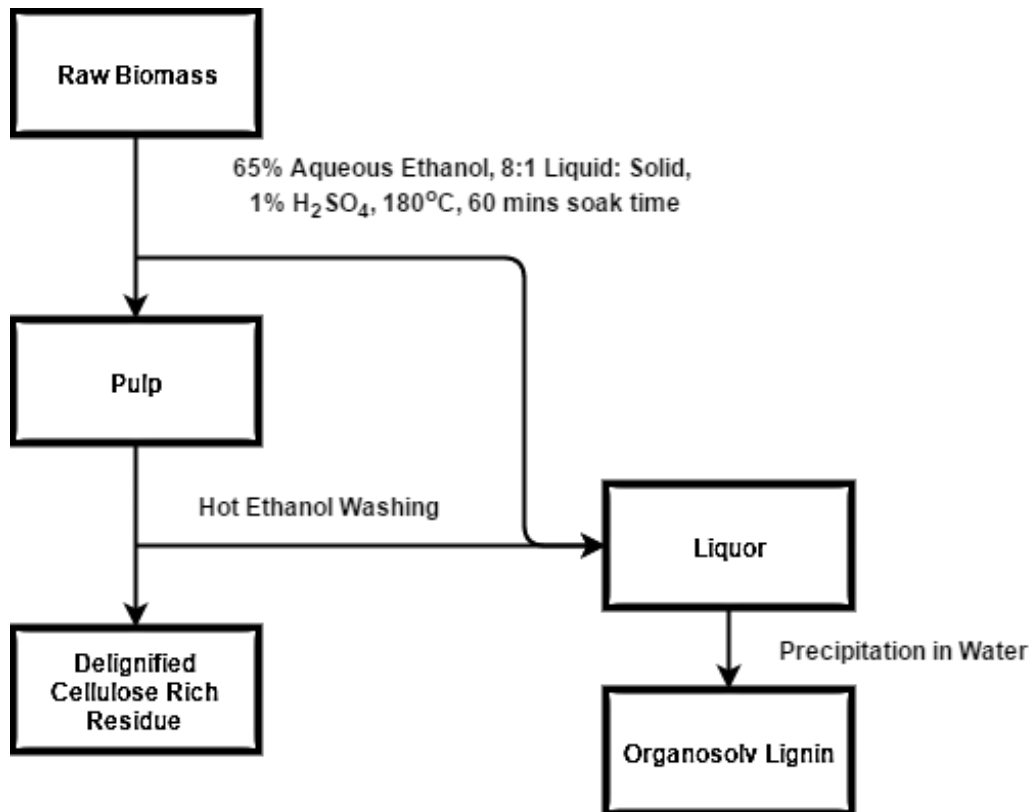


Figure 3-1 Organosolv Process Flow (adapted from Brosse et al., 2009)

By allowing the effective isolation of constituents which closely resemble those found within the natural material the physical and thermochemical properties of these components can be analysed reliably and their influence on the overall combustion characteristics of the parent fuel can be determined accurately.

3.1.3 Demineralisation

Some of those parent fuels utilised and their delignified analogues were found to contain significant quantities of varying mineral species, especially alkali / alkaline earth metals, which are known to significantly influence the combustion behaviour of biomass

and fossil fuels through both devolatilisation and char combustion processes. In order to further understand this influence and quantify its impact on combustion properties, namely char formation and burnout, samples were chemically demineralised using a modified HCl washing technique to remove ion-exchangeable mineral species.

In order to moderate the acidic degradation usually observed during HCl demineralisation a low concentration (1 M) HCl solution was utilised over minimum soak times (60 minutes). 10 g of milled (<2 mm) biomass was placed in 150 ml HCl. The mixture was heated to 60°C and kept at this temperature with constant stirring for 1 hour. Washings were then removed by filtration and the solid demineralised product was washed repeatedly with deionised water until washings were seen to be Cl free by silver nitrate.

3.1.4 Torrefaction

For the purposes of this study sample torrefaction was carried out using an Elite Thermal Systems horizontal tube furnace with internal quartz work tube of 61 mm diameter. The sample was weighed accurately onto a ceramic sample boat which was placed centrally within the furnace work tube. The closed work tube was connected to a nitrogen gas supply and exhaust gas condenser, nitrogen being introduced into the work tube at a flow of 5 Lmin⁻¹ in order to maintain an inert environment and prevent sample combustion. The gas flow was established 10 minutes prior to heating in order to purge the reaction vessel completely of air. The furnace was then heated at 20 °Cmin⁻¹ to the desired temperature (240, 260 and 280°C being used). The sample was maintained at this temperature for 60 minutes prior to cooling and collection.

Of the raw biomass samples selected wheat straw pellets, corn stover pellets, pine woodchips, and mixed softwood pellets were utilised for torrefaction at the three temperatures outlined above. Study of the char formation and combustion behaviour of

torrefied samples generated will not only enable assessment of biomass derived fuels with a wider range of aromatic carbon contents but will also facilitate analysis of any differing behaviours of native aromatic structures when compared with those derived through aromatisation of aliphatic structures produced during torrefaction.

3.1.5. Milling and Sizing

Prior to characterisation and charring of the selected samples and their delignified, demineralised and torrefied analogues the samples were milled to the appropriate particle sizes using a laboratory bench-top planetary ball mill (Retch PM 100 ball mill). The pulveriser utilises 8 stainless steel grinding balls that are held inside the grinding bowl.

100 cm³ of the desired sample is placed into the grinding bowl containing the eight balls, both of which are of stainless steel construction. The total weight of the bowl + balls + sample + lid is measured and the bowl is loaded into the PM100, the corresponding counterbalance weight being set and the lid clamp secured. On commencement of operation the grinding bowl is rotated at a speed of 250 revolutions per minute for 4 minutes. Following pulverisation the samples generated were sieved to the desired size fraction using steel sieve screens with inter wire spacing of 500, 250 and 125 microns giving the desired size fraction of and 125 – 250 µm. The sieves were mounted in ascending size order on a Retsch AS 200 sieve shaker with the sample placed on the uppermost sieve. The shaker was then operated for 15 minutes with fuel particles being allowed to fall through each sieve depending upon their respective size.

Of the size fractions generated only those of 125 – 250 microns were utilised for the generation of char. This is due to restrictions in the utilisable size range that could be accommodated within the charring equipment utilised (namely the drop tube furnace).

It must be noted that significant differences in particle aspect ratios were observed following pulverisation depending upon the physical structure and breakage mechanisms of differing fuels. Samples which exhibited a highly fibrous nature, especially pine woodchips, tended to produce a long, thin needle like particle on milling – whereas pelletised fuels tended to produce more compressed, spherical particles. Of all the fuels analysed olive cake was seen to produce the most homogenous, spherical sample following pulverisation. These observed differences in particle shape and aspect ratio will give rise to differences in the size of particles separated during milling. Those fuels which produce needle like structures with a small and large aspect are more likely to exhibit larger sizes for any given particle size range than those of more spherical character with the smaller aspect of the needle allowing transition through the sieve.

3.2. Fuel Characterisation

In order to assess the influence of chemical and structural composition of the selected fuels on char formation and combustion dynamics a thorough assessment of the organic and inorganic chemical make-up of the fuels was conducted. All characterisations were conducted with biomass samples in the size range of 125 – 250 µm, identical to those utilised in combustion and char generation experiments. Fuel characterisation results were accepted only once reproducibility of a triplicate analysis was obtained within 5% for elemental analysis and ¹³C NMR spectral determination and 10% for mineral matter quantifications.

3.2.1. Elemental Analysis

Elemental or ultimate analysis is used to quantifying the wt% carbon (C), hydrogen (H), oxygen (O), nitrogen (N) and sulfur (S) content of the sample material. This analysis was conducted using ultimate analysis techniques which rely on the combustion of the fuel

sample in the presence of oxygen to produce a range of combustion gases which typically include CO₂, H₂O, SO₂, SO₃, NO₂, NO and N₂ (SO₃ and nitrogen oxides being subsequently reduced to SO₂ and N₂ respectively). These gases are then passed through an absorption column which delays the transition of each gas depending upon its characteristics, releasing each sequentially for detection by a Thermal Conductivity Detector which is able to determine the wt% of each element against the original weight of the sample and a stored standard calibration sample curve.

Analysis of the bulk chemical composition of the biomass fuels allows for basic analysis of the overall bulk chemical composition of each sample, their C/H and C/O content ratios which can be utilised as an indicator of total fuel reactivity and the structural composition of the fuels as to their aromatic and aliphatic organic carbon content (McKendry, 2002).

A flash EA 1112 elemental analyser was used to carry out the elemental analysis. Samples were precisely weighed to be approximately 2.5 mg and placed within individual tin foil capsules which were compressed into a spherical shape, taking care to ensure that all air contained within the capsule is expelled without loss of any of the sample material.

Empty capsules are utilised as a blank to correct the quantification of sample contents for a non-zero baseline reading. A capsule containing an accurately determined quantity of 2,5-(Bis(5-tert-butyl-2-benzo-oxazol-2-yl) thiophene (BBOT) (~1.5 mg) was utilised as a standard of known chemical composition (C=72.52; H=6.09; N=6.51; O=7.43; S=7.44) against which the determination of unknown sample composition was made. Further BBOT capsules were utilised following the testing of three unknowns to ensure that the determination of chemical concentrations remains close to that of the actual standard and to give a quantitative indication of the variance in results obtained.

The standard is used as a reference check, it produces known standard peaks and the sample peaks are then calibrated against these. Once all capsules are prepared they are inserted into the auto sampler. A leak test is performed to ensure that there are no gas leaks with the EA equipment at the commencement of testing. The EA auto-sampler then injects each capsule into the combustion chamber individually where the sample is combusted completely in an oxygen atmosphere. The combustion product gasses are transported to the chromatographic column where separation and quantification of the relative combustion products is conducted which allows for a determination of the concentration of individual elements within the sample. The data is processed using Eager 300 software, which is able to provide accurate quantification of carbon, hydrogen, nitrogen and sulfur content of the sample following peak integration with oxygen content being determined by difference.

3.2.2. Mineral Matter Quantification

Given its relative importance during devolatilisation, char formation and combustion processes it is necessary to quantify the presence of inorganic species in the raw fuel with AAEMs being of most interest.

ICP-MS (inductively coupled plasma mass spectrophotometry) is an analytical technique used to detect the trace metal composition in a sample. The biomass samples must be in solution for the ICP-MS analysis and are thus digested using nitric acid. The method for digestion of the samples involved weighing out the samples into a conical flask, 20 ±2 mg of ash being used for each run, measured to the nearest 0.1 mg. In a fume cupboard 10 ml of concentrated nitric acid was added to the flasks. The biomass samples were then subject to microwave digestion for 50 minutes using an Anton Parr Multiwave 3000 microwave. 10 ml of milli-Q water was pipetted into each flask, and they were left to cool down (while still in the fume cupboard). After the samples had

cooled, they were filtered (under gravity using filter paper and funnel) into 50 ml volumetric flasks whilst adding the rinsings. The solutions were then diluted by 100 times such that the mineral matter content of the solutions were within the limit of detection of the ICP-MS apparatus.

Multi-element analysis of diluted solutions was undertaken by ICP-MS (Thermo-Fisher Scientific iCAP-Q). The instrument employs collision-cell technology with kinetic energy discrimination to remove polyatomic interferences; helium was the collision cell gas utilised. Samples were introduced from an autosampler (Cetac ASX-520) incorporating an ASXpress™ rapid uptake module through a PEEK nebulizer (Burgener Mira Mist).

A range of external multi-element calibration standards (Claritas-PPT grade CLMS-2 from SPEX Certiprep Inc., Metuchen, NJ, USA) included As, Cd, Cu, Fe, Mn, Pb, Se and Zn, in the range 0 – 100 µg L⁻¹ (0, 20, 40, 100 µg L⁻¹). A bespoke external multi-element calibration solution (PlasmaCAL, SCP Science, France) was used to create Ca, Mg, Na and K standards in the range 0-30 mg L⁻¹. Phosphorus calibration utilized an in-house KH₂PO₄ solution standard (10 mg L⁻¹ P). Sample processing was undertaken using Qtegra™ software (Thermo-Fisher Scientific) utilizing external cross-calibration between pulse-counting and analogue detector modes when required.

3.2.3. Aromaticity by Solid State CP-MAS¹³C NMR

Solid state cross-polarization-magic angle spinning (CP-MAS) ¹³C nuclear magnetic resonance (NMR) has become a powerful tool for determining the chemical structure of a range of complex organic substances which includes a number of solid fuels such as coals of varying rank (including lignite) and lignocellulosic biomass fuels.

Solid State ¹³C CP-MAS NMR is able to provide significant information regarding the chemical environment in which carbon atoms are situated within an organic structure.

For any given ^{13}C atom within an organic matrix differing radio frequencies require the application of a unique magnetic field in order to bring it into a resonance condition (with spin alignment alternating from one spin state to another). The magnitude of this magnetic field is dependent upon the chemical environment surrounding the atoms of interest and the magnetic field strength needed to induce resonance is a reliable indicator of the chemical environment in the molecule within which the atom resides.

During NMR spectroscopy the spatial proximity or chemical bonding between atoms can result in considerable, orientation dependent interaction of nuclear spins. In solution state NMR these interactions are broadly averaged due to the Brownian motion adopted by the liquid, however, during solid state NMR spectroscopy the limited mobility afforded individual chemical constituents within the solid matrix often results in a dramatic increase in anisotropic interactions between nuclei which can result in considerable line broadening which will influence the reliability of solid state spectra. In order to avoid these interactions and enhance the resolution of solid state NMR spectra a technique known as Magic Angle Spinning (MAS) is applied to mimic the averaging of process in solution state NMR. By selecting the angle of the applied magnetic field such that it corresponds to the zero point of the spatial portion of the Hamiltonian equation (this being known as the Magic Angle of 54.74°) and spinning the sample in this frame at a requisite frequency the chemical shift anisotropy can be averaged to the point that it can effectively be neglected. As such line broadening effects of anisotropic interactions are dramatically reduced and the resolution of solid state NMR spectra is greatly improved.

Given the relatively low abundance of ^{13}C atoms within an organic chemical structure it is beneficial to utilise methods which are able to effectively amplify the signal generated from the ^{13}C nuclei when compared to direct excitation and allow faster repetition rate.

This is achieved using a technique known as Cross Polarisation (CP). CP enables the transferral of polarisation from more abundant nuclei to less abundant nuclei of interest (in this case from ^1H spins to ^{13}C spins), enhancing the signal to noise ratio considerably.

Since abundant spins are strongly dipolar coupled they are subject to large changes in the magnetic field due to motion, this results in a rapid spin lattice relaxation in more abundant nuclei. By setting the power of the magnetic field on each channel (^1H and ^{13}C) such that the radio frequency for excitation is roughly equal efficient polarisation transfer from more abundant to less abundant nuclei is achieved and thus the recycle delay is no longer dependent upon the time taken for slowly relaxing dilute nuclei to relax, rather, it is dependent upon the more rapidly relaxing protons. Utilisation of cross polarisation from ^1H to ^{13}C spins dramatically increases the number of signal acquisitions which can be achieved within a period of time and thus increases the ability to complete ^{13}C NMR acquisitions with adequate signal to noise ratio so as to be useful.

^{13}C NMR spectra were acquired using a Bruker Avance 200 spectrometer. A 7mm zirconia rotor was filled with sample and compressed to limit any movement of the sample during analysis. The rotor was placed within the NMR probe and allowed to spin at ~ 5000 rpm using compressed air for five minutes prior to each signal acquisition in order to stabilise the sample packing and improve the field homogenization. Chemical shifts, given in parts per million (ppm), were referred to the resonance signal of tetramethylsilane (TMS). A proton frequency of 200 MHz and ^{13}C frequency of 50 MHz were utilised throughout with magic angle spinning speed of 5 kHz, ^1H radio field strength of 4.7 Tesla, cross polarisation contact time of 1 ms, a 1.5 second recycle delay time and 50 Hz line broadening factor were applied throughout the acquisitions. Where considerable peak overlap occurs ACD labs peak deconvolution software has been utilised to provide quantification of the individual peak integrals.

¹³C CP-MAS spectra of solid fuels provide signals relating directly to the varied organic structures present with the fuel including aromatic carbon, monlignol, hemicellulose and cellulose.

Determination of the mol% aromaticity was conducted using well demonstrated peak determinations as employed by Melkior et al., 2012 – aromatic carbon peak determinations being as shown in Table 3-1.

Peak Chemical Shift (ppm)	Structural Assignment
152.6	Lignin: S-3(e), S-5(e)
148–147	Lignins: S-3(ne), S-5(ne), G-3(ne, e), G-4(ne, e)
138-138.5	Lignins: S-1(e), S-4(e), G-1(e)
134–133	Lignins: S-1(ne), S-4(ne), G-1(ne)
121	Lignin: G-6
114–106	Lignins: G-5, G-6, S-2, S-6

Table 3-1 ¹³C NMR Aromatic Carbon Peak Assignments

S: carbon in syringyl units, G: carbon in guaiacyl units,

ne: in non-etherified arylglycerol β-aryl ethers, e: in etherified arylglycerol β-aryl ethers.

The sum of all aromatic peak integrals was utilised to calculate the aromaticity mol% of the samples, the aromatic carbon content wt% daf being calculated using this aromaticity measure and the carbon content of the fuel as shown in Equation 3.1.

Equation 3.1

$$\text{Aromatic Carbon wt\% daf} = \text{Carbon Content wt\% daf} \times \left(\frac{\text{Aromaticity mol\%}}{100} \right)$$

3.3. Char Generation and Combustion Analysis

A number of experimental procedures have been utilised to assess the combustion performance of differing biomass feedstocks, investigate their volatile matter content under differing thermal conversion conditions and generate char samples for further study of char combustion dynamics. The methods used during this study of devolatilisation and char combustion are described in the following sub sections.

3.3.1. Thermogravimetric Analysis (TGA)

Thermogravimetric analysis is a commonly utilised technique used to study the transformation of substances under varying thermal histories and gaseous atmospheric conditions which are controlled directly. TGA has been widely used in the study of solid and liquid fuels for some time and has to some extent replaced the relevant standard procedures including traditional proximate analysis due to the relative ease of equipment operation, the ability to accurately monitor individual weight losses with varying temperature alterations (in the case of proximate analysis this includes moisture, volatile matter and fixed carbon components), rapidity of measurement and the increased data resolution available.

3.3.1.1. TGA Slow Pyrolysis Char Preparation

All samples have been subjected to slow heating rate pyrolysis in the TGA in order to determine accurate char yields under a highly controlled thermal environment. Sample masses less than 10 mg of size fraction 125-250 μm were subject to pyrolysis using the following procedure:

Sweep gas: nitrogen, 100 ml/min

Heating from ambient to 100°C at 30 °Cmin⁻¹

Isothermal at 100°C for 15 mins to allow drying

Heating from 100°C to 700°C at 50 °Cmin⁻¹

Isothermal at 700°C for 30 mins to ensure complete devolatilisation

Heating from 700 to 850°C at 50 °Cmin⁻¹

Oxidative Environment (100 ml/min air)

Isothermal at 850°C for 30 mins to ensure complete combustion of all char generated

Following this the content of the fuel with regards moisture, volatile matter char and ash were determined, a typical TGA slow heating char generation profile being shown in Figure 3-2.

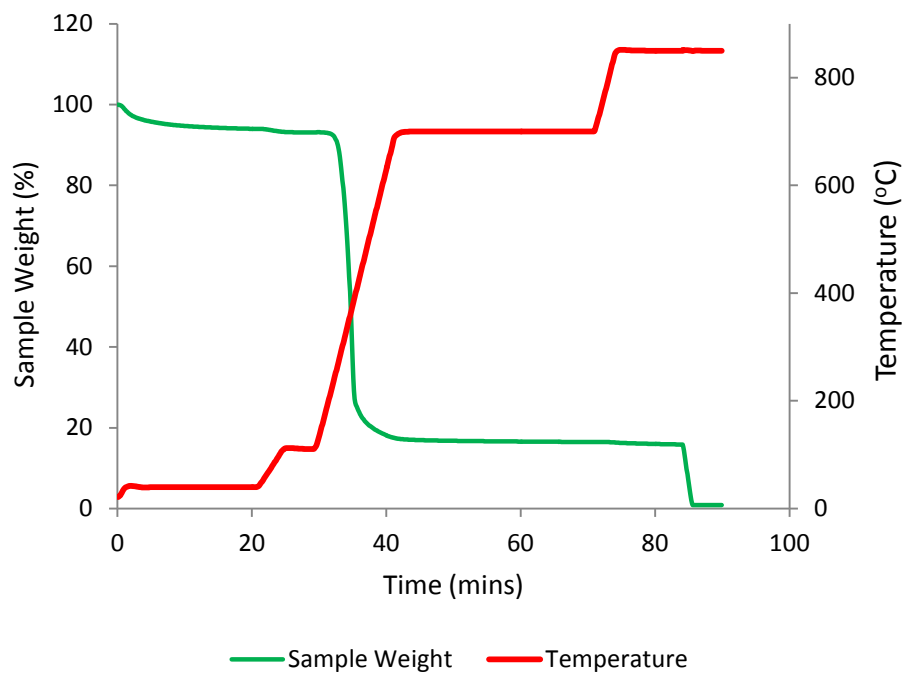


Figure 3-2 Typical Slow Heating TGA Char Generation Experiment Profile

(Raw Eucalyptus Pellets)

3.3.1.2. Non-isothermal Combustion Profiling

In order to characterise the combustion behaviour of the individual fuels and determine if the samples produced through demineralisation and delignification practices do show differing devolatilisation and char combustion dynamics prior to drop tube furnace testing each was subjected to non-isothermal combustion in the TGA. This process involved heating a sample of the fuel under oxidative conditions at a fixed heating rate (following drying) of $2.5\text{ }^{\circ}\text{Cmin}^{-1}$ from 110 to 800°C . During this heating process the fuel samples undergo a series of combustion decomposition reactions, beginning with devolatilisation followed by char combustion. For each of these processes there is an associated peak in the rate of mass loss of the sample which corresponds to the sample temperature at which the most intense reactions occur within each conversion processes. The temperature at which these mass loss peaks occur can be used to give an indication of the reactivity of the fuel with respect both devolatilisation and char combustion, the lower the temperature indicating higher reactivity – the relative magnitude and importance of individual reactions in the overall thermochemical breakdown of the sample is also indicated by the profile and peak rate of mass loss for each devolatilisation and char combustion.

This has been achieved by plotting the derivative of mass loss with regard to time ($\%\text{min}^{-1}$) against the recorded temperature of the sample. In order to minimise lag effect between the gas and sample temperatures and ensure that all processes are separated in temperature to the required degree a relatively low heating rate of $2.5\text{ }^{\circ}\text{Cmin}^{-1}$ has been utilised to generate these profiles.

3.3.2. HTF Char Generation

Given the softening nature of lignin which undergoes a glass transition at temperature significantly under 180°C it proved impractical to utilise isolated lignin fractions in the

entrained flow drop tube furnace. In order to assess the behaviour of pure lignin compounds during char formation whilst producing appreciable char for further analysis a horizontal tube furnace (HTF), identical to that used for the torrefaction of raw biomass fuels, has been utilised to generate slow heating rate chars using a range of demineralised samples and their isolated lignins (in this case demineralised raw, demineralised delignified and isolated lignins of pine woodchip and corns stover pellet fuels have been studied).

The procedure utilised was identical to that of torrefaction experiments using a heating rate of $20\text{ }^{\circ}\text{Cmin}^{-1}$, however, in the case of char generation the final temperature was increased to 700°C and the hold time at this temperature reduced to 30 minutes. Chars were allowed to cool completely in an inert environment prior to analysis; the mass of char generated being accurately determined on weighing of the samples boat and converted to a daf basis following TGA analysis.

The reactivity and surface area of HTF chars were analysed in the same manner as rapid heating DTF chars, analysis procedures being detailed in Section 3.4.

3.3.3. Entrained Flow Drop Tube Furnace (DTF)

An entrained flow drop tube furnace system has been utilised to provide a method whereby reasonable quantities of char can be produced for further analysis under conditions that mimic those experienced by fuel particles upon entering a pulverised fuel combustion boiler or entrained flow gasification reactor. This entails simulation of very high heating rates in the order of between 10^4 and $10^5\text{ }^{\circ}\text{C/second}$ and low oxygen content of the surrounding gases (between 0 and 10% - in the case of experiments reported here pyrolysis was conducted with 0% oxygen and re-firing char combustion with 5%) as experienced by fuel particles during their first few hundreds of milliseconds within the furnace or reactor.

A schematic representation of the DTF can be seen in Figure 3-3. It can be seen that the DTF comprises a number of primary components which can be summarised as:

- Gas supply system
- Heating system consisting of a pre-heater, main heater and trim heater
- Water cooled fuel feeder and collection probes
- Vacuum system, char collection and gas filtration

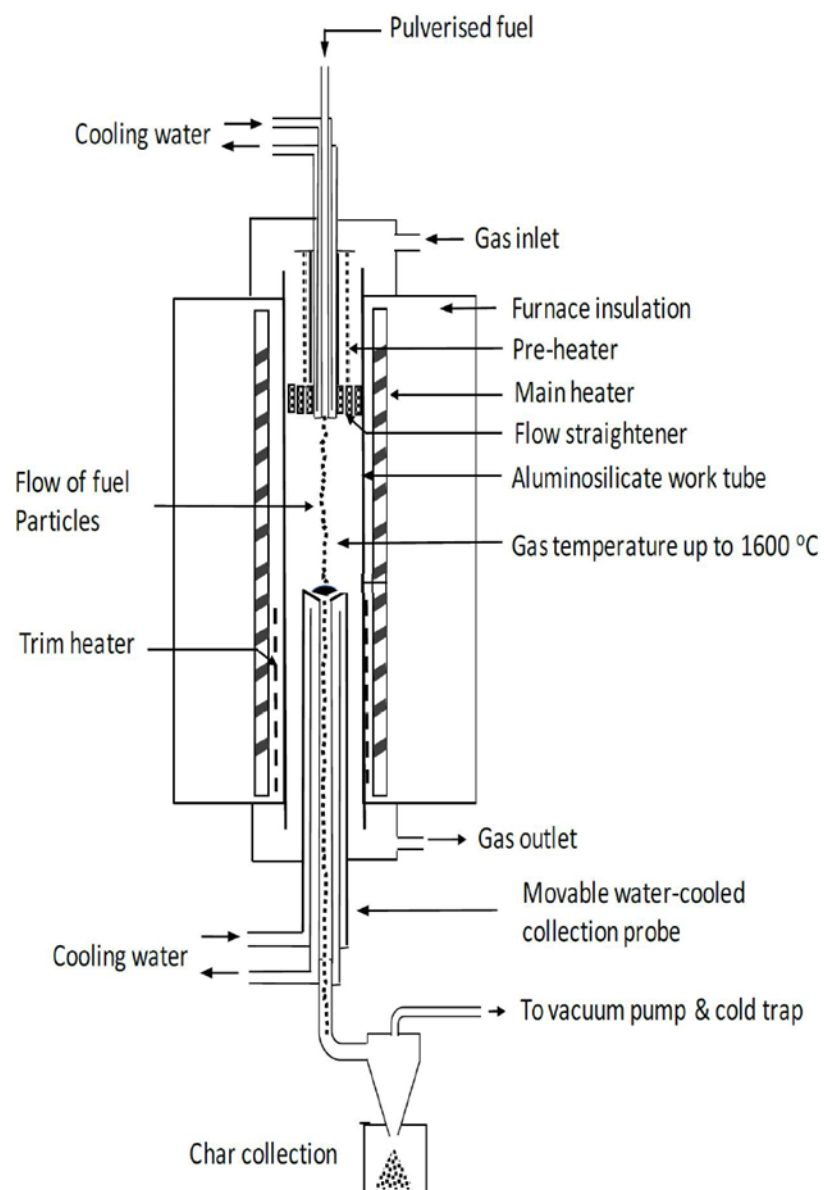


Figure 3-3 Drop Tube Furnace Schematic

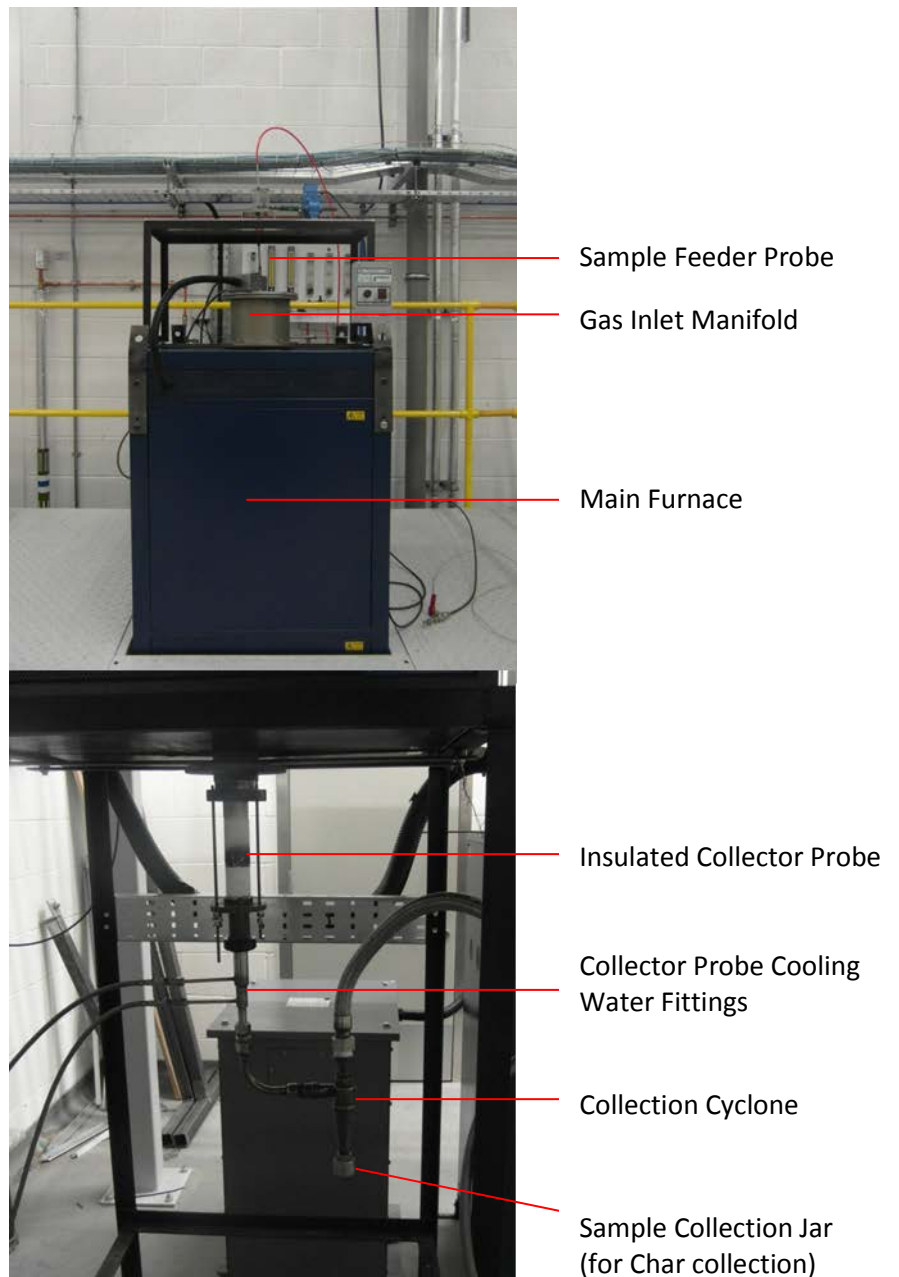


Figure 3-4 Drop Tube Furnace

3.3.3.1. Gas Supply System

The gases supplied to the DTF are strictly controlled using calibrated flow metering equipment. The furnace can be fed using a number of gas lines to achieve the desired gaseous devolatilisation/combustion atmosphere within the main work tube. In the case of this investigation the areas of most interest were the quantification of volatile matter yields obtained during high heating rate and final temperature conditions similar to

those experienced in utility scale entrained flow thermochemical conversion infrastructure (including PF fired combustion boilers and entrained flow gasifiers) and the reactivity of subsequent chars formed during the devolatilisation process. As such an inert gaseous atmosphere was chosen for operation of the DTF to limit the oxygen content of the atmosphere as far as possible and reduce the occurrence of combustion reactions. A sufficient flow of N₂ gas was maintained through the gas inlet to ensure that in-leakage of air was minimised whilst maintaining the desired flow rate and residence time of fuel particles within the work tube. Incoming gas was passed through a flow straightening device mounted at the gas inlet to the furnace zone, this device acts to minimise any turbulence within the flow of incoming gas and thus control the motion of particles through the DTF to near laminar conditions, this being necessary to ensure that consistent particle residence times are maintained.

Differing fuel particle residence times are provided by altering both gas flow rates and modulating the separation distance between collector and feeder probes using specially designed collection probe suspension rods. It is assumed that flow within the furnace is entirely laminar and that the gas velocity at any point in the tube is a function of its radial position. As such a laminar flow velocity profile can be applied (Farrow, 2013; Le Manquais, 2011) as shown in equation 3-2.

Equation 3.2

$$\frac{v_r}{v} = 1 - \frac{r^2}{R^2}$$

Where v_r is the gas velocity at a radius r from the centreline of the work tube and v is the average velocity of the gas flow across the entire tube radius R .

In the centre of the work tube where $r = 0$ and $v_r = v$ the following expression can be used.

Equation 3.3

$$v = \frac{1}{2}v_0$$

Thus the particle velocity at the centreline, v_0 , can be expressed as.

Equation 3.4

$$v_0 = \frac{L}{2t}$$

Where t is the particle residence time within the furnace and L is the distance separating feeder probe outlet and collector probe inlet. This velocity is related to the volumetric flow rate of the furnace gas, Q , and the cross sectional area of the tube by the following expressions.

Equation 3.5

$$v_0 = \frac{Q}{A} = \frac{Q}{\pi R^2}$$

Combining equations 3-4 and 3-5 the following expression is derived.

Equations 3.6

$$t = \frac{L\pi R^2}{2Q}$$

Equation 3.7

$$Q_2 = \frac{Q_1 T_2}{T_1}$$

The required collector probe separation distance and gas feed flow rate required to achieve differing furnace particle residence times with a furnace temperature of 1300°C

(used for preparation of char samples) and 1100°C (used for char re-firing) are shown in Table 3-2.

Furnace Residence Time	Collection Probe Separation Distance (cm)	Furnace Temperature (°C)	Required Gas Flow Rate (L/min)
50 ms	11	1100	28.1
		1300	24.6
100 ms	15	1100	19.2
		1300	16.7
200 ms	22	1100	14.1
		1300	12.3
400 ms	45	1100	14.4
		1300	12.5
600 ms	65	1100	12.1
		1300	11.0

Table 3-2 DTF Gas Flow Rate and Collection Probe Separation Distance to Achieve Desired Furnace Residence Time as 1100 and 1300°C Furnace Temperatures

3.3.3.2. Heating System

Three separate heaters are utilised to maintain the desired temperature set-point across the length of the reactor tube. The upper or pre-heater acts to heat the incoming gas stream to the desired temperature so as to avoid excessive cooling of the upper drop tube and thus ensure that particles experience immediate heating upon injection into the furnace, thus providing the desired residence time of fuel particles within a gaseous environment at the correct temperature. The main heater is used to set the bulk temperature across the work tube – providing the bulk of the heating duty of the furnace. The lower or trim heater ensures that the bottom of the furnace remains close to the designated temperature, controlling the cooling of the furnace which arises from the presence of the water cooled collection probe.

Previous work conducted using a near identical DTF (Barranco Melendez, 2001) (from which the DTF used in this study was designed) recorded the gas temperature profile along the centreline of the furnace work tube as a function of the distance from the feeder probe at furnace temperature of 1300 °C and residence time of 200, 400 and 600 ms (Figure 3-5).

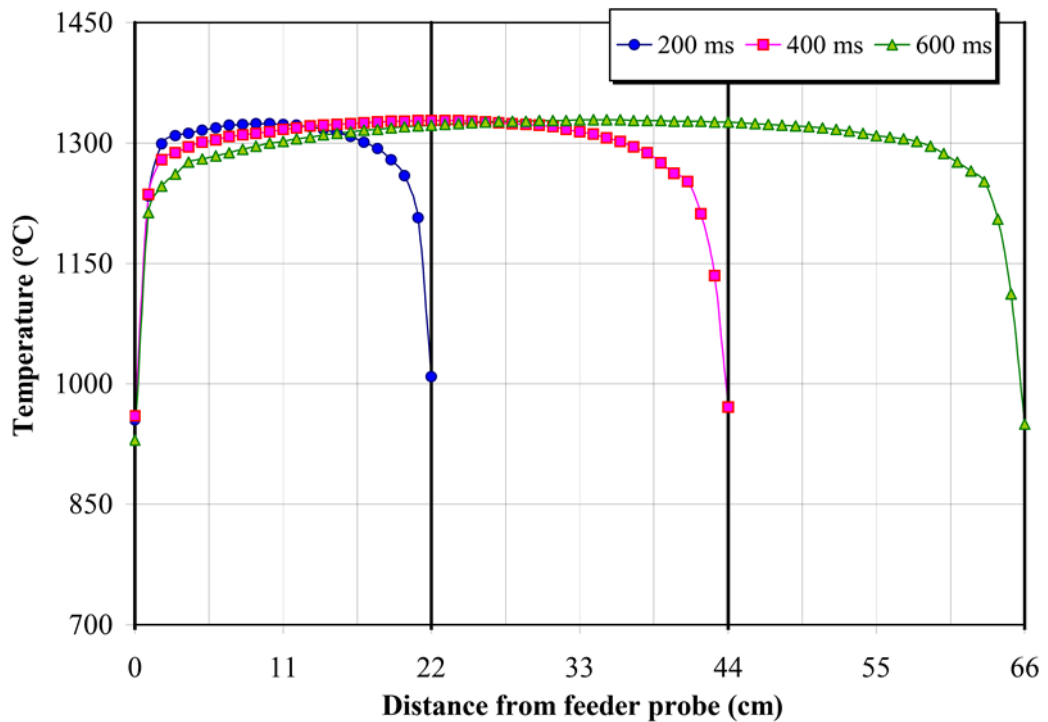


Figure 3-5 DTF Temperature Profiles

As can be seen, there are rapid temperature gradients as gas leaves and enters the water cooled feeder and collector probes. Further to this, the collector probe position does not appear to alter the temperature profile significantly, with the desired temperature being achieved across the majority of the furnace residence time.

3.3.3.3. Water Cooled Feeder and Collector Probes

Fuel feeding into and char collection from the drop tube is conducted using water cooled probes of Inconel steel construction inserted into the top and bottom of the

furnace respectively. Although the feeder probe is fixed in place the insertion distance of the collector probe is altered to provide the desired residence time of fuel particles within the furnace.

3.3.4. DTF Char Generation

Chars were generated from biomass and coal samples utilising the DTF to simulate the rapid heating rate, high temperature and oxygen deficient conditions experience by fuels on introduction to commercial PF fired boiler systems. This was achieved by manually feeding ~4-5 grams of each sample, sieved to size fraction of 125-250 μm , through the feeder probe into the furnace over a period of 15-30 minutes depending upon the flow characteristics of the fuel in question. Following the completion of sample feeding the collection pot was retained in place in order to ensure complete cooling of the sample to temperature below the ignition point of the char such that when opened to atmospheric oxygen rich condition no combustion was allowed to occur. This was done whilst stopping both the nitrogen gas flow into the furnace and the exhaust gas flow from the furnace.

For the purposes of this investigation all DTF devolatilisation experiments were conducted using a gas temperature of 1300°C, this being deemed high enough to provide valid information regarding the devolatilisation behaviour of the chosen fuels under conditions similar to those experienced in pulverised fuel fired systems without considerably increasing the temperatures encountered in the lower portions of the fuel feeding probe, which, given the high reactivity of the biomass being utilised was shown to cause premature devolatilisation and release of tars which significantly hampered the feeding process.

Residence time for all DTF char generation runs were maintained at the maximum residence of 600 ms in order to give a quantification of the total achievable volatile matter and char yields at the chosen DTF temperature conditions.

Steel char sample collectors were weighed using a precision weighing balance before prior to (empty) and following collection (full) of the char sample. From these measurements an accurate figure for the mass of char collected was derived by difference.

Volatile matter and char yields obtained during entrained flow devolatilisation of solid fuels are commonly conducted using what is known as the ash tracer method. The poor collection efficiencies realised using entrained flow furnace apparatus would result in gross over estimate of volatile matter mass losses when based solely on the mass yield of char obtained, especially when utilising greater residence times with increased separation of feeder and collector probes. In order to accommodate this discrepancy in collection efficiency and volatile matter yield the ash content in the char collected as a proportion of the ash within the feed material is utilised in the ash tracer method as a marker for the determination of the actual mass loss of the fuel during devolatilisation, this is done using Equation 3.8.

Equation 3.8

$$VM_{DTF} = \frac{10^4 \times (Ash_{char} - Ash_{fuel})}{Ash_{char} \times (100 - Ash_{fuel})} \text{ (wt\% daf)}$$

Where VM_{DTF} is the volatile matter content wt% daf, Ash_{fuel} is the ash content wt% db of the fuel being introduced to the drop tube and Ash_{char} is the as ash content of the char collected wt% db.

Although this determination of volatile matter yield is accurate for coal devolatilisation where the active mineral matter content is fairly small and the total ash content relatively high, it is not able to provide accurate determination of biomass pyrolysis yield due to the generally low ash content of the fuel and the higher lability of AAEMs to volatilisation under high heating rate (Farrow et al., 2015). In order to determine an accurate volatile yield an artificial ash, silica tracer has been used to augment the ash content of the feed biomass and provide greater thermal stability of the ash. This has involved the doping of fuels samples with 10 wt% oven dried silica of the same particle size of the fuels (125 – 250 μm) which has been calcined at 900°C, thoroughly mixed with the biomass sample before being fed into the DTF.

The volatile matter content evolved in the drop tube is then calculated using Equation 3.9.

Equation 3.9

$$VM_{DTF} = \frac{10^4 \times (Ash_{char} - Ash_{fuel+Si})}{Ash_{char} \times (100 - Ash_{fuel+Si})} \text{ (wt\% daf)}$$

Where $Ash_{fuel+Si}$ is the total non-combustible content of the fuel and silica mixture wt% db and Ash_{char} is the ash content of the char generated using this mixture.

3.3.5. DTF Char Re-firing

Chars of selected biomass fuels generated in the DTF were re-fired in the DTF to simulate high temperature combustion of the char in boiler like conditions. These experiments involved reintroducing DTF chars to the furnace at a temperature of 1100°C and a gas atmosphere consisting of 5 volume% O₂ in N₂. These conditions were selected both to give slightly delayed burnout of the char particles by reducing temperature and oxygen availability, enabling analysis of any differences experienced in the combustive conversion process between the chars and to simulate conditions

experience by char particles traveling through the boiler where temperatures are reduced on leaving the high temperature burner combustion zone and oxygen availability increases with introduction of burner secondary/tertiary and overfire air (typical economiser exit flue gas oxygen content of PF fired coal boilers being maintained at levels of 2-4 volume% depending on the reactivity of the fuel being utilised and selected in order to reduce heat loss in the flue gas and to simultaneously minimise CO, unburned char and NO_x emissions). This makes 5% O₂ a relatively realistic char combustion environment as the bulk of char oxidation will occur in the overfire air zone prior to reaching the upper furnace where platen superheater heat absorption reduce temperature dramatically and slow char combustion reactions considerably.

Re-firing was conducted at residence times of 50, 100, 200, 400 and 600 ms to provide insight into the char combustion process as it proceeds from low to high conversion.

The char conversion % was calculated using the traditional ash tracer method commonly utilised for the measurement of solid fuel conversion through devolatilisation and char combustion in entrained flow reactors (Borrego et al., 2009, Shuangning et al., 2006, Simone et al., 2009). This method utilises the level of ash collected as a proportion of the ash introduced in the initial sample acts as a marker for the determination of the collection efficiency of the equipment, knowing which allows a valid calculation of the mass conversion using equation 3.2 with Ash_{fuel} being replaced by the ash content of the char prior to re-firing and Ash_{char} being that of the re-burned fuel following combustion.

It is assumed when using this method to quantify conversion factors that no significant further volatilisation of ash components is undergone during the combustion re-firing process. This would appear reasonable given the reduction in furnace temperatures utilised in comparison with DTF devolatilisation char preparation runs which were conducted at 1300°C as opposed to the 1100°C utilised for char re-firing.

Chars collected following re-firing in the DTF at differing residence times was conducted similarly to that of chars produced through devolatilisation, the procedures for which are described in Section 3.4. below.

3.4. Char Characterisation

3.4.1. Char Reactivity

In order to study the relative reactivity of the chars generated using the HTF and DTF isothermal char combustion was conducted for all chars across a range of temperatures, the results of which allow the kinetic parameters of conversion to be calculated (including the first order rate constant k , activation energy E_a , and pre-exponential function A).

During this process the chars under investigation were combusted at four predetermined temperatures of 375, 400, 425 and 450°C. This was achieved by heating the sample of limited mass (5-10 mg) in the TGA under an inert gas (nitrogen) atmosphere to the desired char burnout temperature before introducing air to the reactor and allowing combustion of the sample to proceed. By doing this a characteristic char burnout profile is produced which shows the progress of mass loss of the char as it is converted during combustion. The degree of mass loss throughout the process can be characterised using a relative fractional weight conversion factor, α which has been calculated using equation 3.10.

Equation 3.10

$$\alpha = \frac{m_o - m_t}{m_o - m_f}$$

Where α is the fraction weight conversion factor ranging from 0 for no conversion to 1 for full conversion, m_o is the total initial mass of the char sample prior to combustion, m_t is the mass of char remaining at time t and m_f is the final mass following full conversion of combustible fractions within the char sample (i.e. the ash content)

α is used to trace the combustion of the char regardless of the quantity of char utilised or its ash content and thus provides a valid comparison of char reactivities between fuels with varying char yields.

The conversion rate is then given by:

Equation 3.11

$$\frac{\delta\alpha}{\delta t} = k_a(1 - \alpha)$$

Where α is the fraction weight conversion factor, t is time and k is the first order rate constant.

Integration of equation 3.11 subject to the initial condition whereby $\alpha = 0$ at $t = 0$ gives:

Equation 3.12

$$-\ln(1 - \alpha) = k_a t$$

The apparent first order rate constant k_a is then determined graphically by the gradient of a straight line plot of $-\ln(1 - \alpha)$ vs. time with respect to the partial pressure of oxygen. Subsequently, kinetic parameters of activation energy (E_a), and pre-exponential function are derived from the gradient and intercept of a straight line plot of $\ln k_a$ vs. $1/T$ (T being the isothermal combustion temperature) formed from each isothermal char combustion temperature using the Arrhenius rate equation as follows:

Equation 3.13

$$\ln k_a = \ln A - \frac{E_a}{RT}$$

Where R is the gas constant (8.314 JK⁻¹mol⁻¹).

As such, by conducting isothermal combustion of the char samples produced at a range of combustion temperatures the activation energy and pre-exponential function can be accurately determined.

Further to this, the time taken to reach 90% char conversion (t₉₀ in minutes) at an isothermal combustion temperature of 450°C has been used as a convenient indication of the char reactivity for each sample, those chars with more rapid conversion and thus lower values of t₉₀ having higher char reactivity.

It is desirable when assessing the relative reactivity of fuel chars to minimise the influence of pore and bulk diffusion during isothermal combustion, as such experiments should be conducted under conditions whereby char oxidation proceeds in a kinetically controlled regime where the rate of reaction between the char and oxygen is far lower than both pore and bulk diffusion phenomenon (i.e. combustion regime I). In order to achieve this the temperature at which isothermal combustion is conducted must be sufficiently low. In order to determine the temperature range to be utilised the most reactive char species generated (in this case that of raw corn stover pellets) has been subjected to isothermal char conversion over a number of temperatures ranging from 375 and 675°C and an Arrhenius plot has been generated using the results as shown in Figure 3-6.

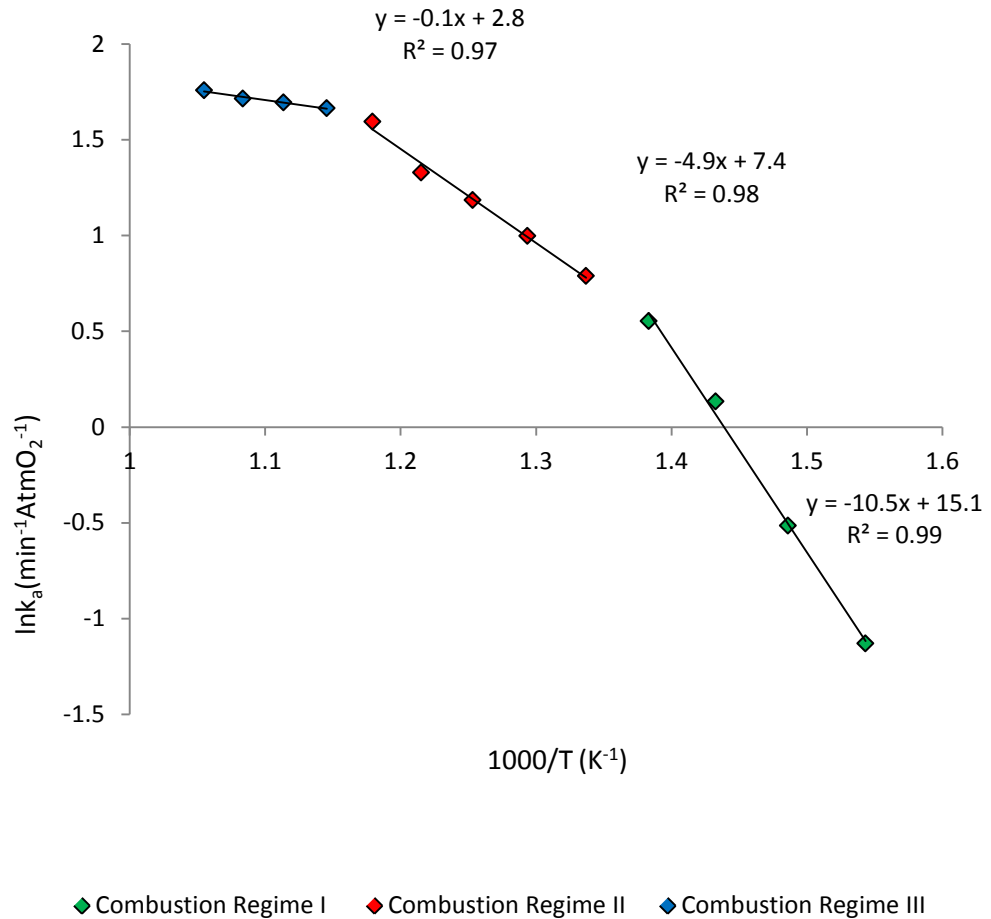


Figure 3-6 Arrhenius Plot for Corn Stover DTF Char under Varying Combustion Regime

As can be observed chemical control appears to have been achieved during isothermal combustion between 375 and 450°C providing valid quantifications of the chemical reactivity parameters of the char, increasing the temperature to 500 – 600°C shifts the reaction into regime II whereby both pore diffusion and chemical reactivity limit the global rate of char conversion, resulting in a quantification of the activation energy $\sim 1/2$ of that observed under chemical control. Moving to even higher temperatures results in the increased importance of bulk diffusion as the reaction of char and oxygen increases dramatically such that all reactions take place at the outer surface of the char particle with instantaneous consumption of oxygen, char conversion rates being dictated primarily by the rate of oxygen diffusion through the particle boundary layer to the char

surface giving little dependence of rate constant on temperature and reducing the observed activation energy dramatically.

Given the above observations isothermal char combustion temperatures of 375, 400, 425 and 450°C have been utilised throughout.

Where desirable the apparent first order rate constant has been normalised for surface area of the char to produce an inherent rate constant.

3.4.2. BET Surface Area Analysis

In order to assess the importance of total char surface area in determining the combustion reactivity of the DTF and HTF chars generated the surface area of each char (generated in the absence of silica doping) was measured using the Brunauer–Emmett–Teller (BET) surface area quantification method.

There is continued conjecture among the scientific community as to role played by char micro and macro pore structures in influencing the rate of char oxidation (Arias et al., 2007; Feng and Bhatia, 2003) and thus the most pertinent analytical methodologies for determination of active char surface area during combustion. However, a number of studies of char combustion dynamics have proposed the improved efficacy of N₂ adsorption BET surface area over that of CO₂ adsorption for correlation with combustion reactivity due to the unavailability of very small micropores to oxidising media during combustion reactions and the observed dormancy of this mode of pore during char burnout.

These determinations were conducted using Micrometrics ASAP® 2420 Accelerated Surface Area and Porosimetry apparatus. The analysis was carried out under nitrogen gas at -196°C, nitrogen is absorbed by the porous structure of the char samples at a number of relative partial pressures, the volume of nitrogen adsorbed at each pressure

being measured. The partial pressure is then reduced systematically to facilitate the desorption of adsorbed gas molecules, the volume of desorbed gas is also measured throughout. From these measurements an adsorption and desorption isotherm can be plotted as shown in Figure 3-7 for adsorption.

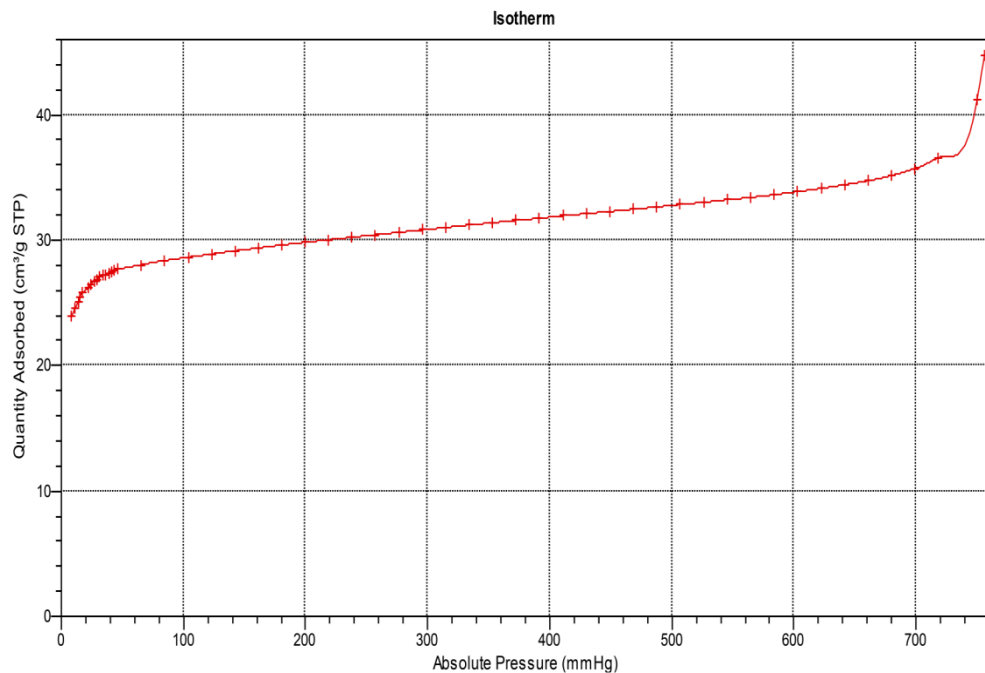


Figure 3-7 Adsorption Isotherm for BET Surface Area Analysis

Due to the highly variable ash content of the chars generated and their re-fired analogues a direct quantification of surface area was not sufficient to provide insight into the varying of surface area of the char alone, as such all of the BET surface area measurements quoted have been corrected to an ash free basis. This was achieved by assuming that the pore surface area of ash components can be neglected and following a determination of the surface area of silica tracer additives which were subtracted from the overall BET surface area determination (all silica surface areas were less than $25 \text{ m}^2\text{g}^{-1}$). This may result in an overestimation of char pore surface areas but does provide more consistent determination of char pore surface areas.

3.4.3. Char Morphology Assessment by Optical Microscopy

Char morphology refers to the size, dimensions, internal macroporosity and optical anisotropy of the chars. Study of the morphological characteristics can provide a valuable insight into the factors determining the rate of char combustion and the processes undergone by the fuel during the charring process which can have a significant influence on subsequent char conversion dynamics.

Char morphology has been assessed using optical oil immersion microscopy. Chars prepared using the DTF were mounted in epoxy resin blocks which were hardened and polished to provide a cross sectional image through char particles and reveal their internal porosity. Blocks were viewed using an Orthoplan polarising light microscope connected to a computer to enable image saving. An automated point counter was used to count the char structure type with a total of 200 points being identified per sample. The movement of the imager between each recorded point is automated and the distance moved each time is constant.

An abridged char characterisation system has been utilised to classify individual chars during manual point counting. Chars were identified according to the classification system currently used by the International Committee for Coal and Organic Petrology as outline in Lester et al., 2010 and are as follows:

- Tenuisphere: Thin walled single char particle with little internal structure
- Tenuinetwork: Thin walled char with considerable internal network structure
- Crassisphere: Thick walled single char particle with little internal structure
- Crassinetwork: Thick walled char with considerable internal network structure
- Mixed Dense: Solid char particle showing little internal porosity development

Given the differing nature of biomass chars the char counts have been converted to be classed as thin walled, thick walled or solid as per the method of Avila et al., 2011.

Where structures have been identified that largely retain the physical structure of the parent biological material these have been included within the solid classification due to their thick walled, condensed structure – these chars are thought to derived from non-softening components of the biomass material which are unable to swell and develop any considerable structure as known to occur during coal pyrolysis.

The total % of each char type observed has been recorded and is compared with total porosity measures as obtained using BET surface area analysis.

Chapter 4: Basic Fuel Characterisation

4.1. Elemental Analysis (C, H, N, O)

Quantification elemental composition of all samples utilised as determined by flash elemental analysis are shown in Table 4-1 with associated atomic O:C and H:C ratios being presented in Table 4-2 and in the form of a Van Krevellen diagram in Figure 4-1.

All raw biomass have similar bulk chemical compositions with carbon content in the range 45-49 wt% daf, H content of 5.1-6.1 wt% daf and O content of 42.3-48.4. Biomass nitrogen content, key in determining NO_x generating potential during combustion processes is highly variable across biomass utilised and ranges from almost nil to 2 wt% daf, this variability follows deviations in biomass protein content which serves as the major source of N in lignocellulosic materials (Sjostrom, 2013) to the extent that protein content can easily be determined using pre-established nitrogen factors (Hames et al., 2008).

Although raw biomass bulk compositions are relatively similar such that they occupy a relatively well defined region of the Van Krevellen diagram shown in Figure 4-1 they do differ significantly in their structural constitution, mineral matter composition and thermochemical behaviour (as evidence in Chapters 6 and 7) fuel modification through the chosen delignification, demineralisation and torrefaction pre-treatments impact both chemical and structural compositions and thus influence thermochemical conversion dynamics during combustion processes. As such detailed appraisal of the effect these treatments have on fuel characteristics is required and detailed in the following sections.

Sample	C (wt% Daf)	H (wt% Daf)	N (wt% Daf)	O* (wt% Daf)
Wheat Straw Pellets	45.5	5.1	1.3	48.2
Delignified Wheat Straw	40.9	5.5	0.5	53.1
Wheat Straw Lignin	54	5.8	2.6	37.6
Corn Stover Pellets	45	5.5	2	47.5
Delignified Corn Stover	44.2	5.6	0.7	49.5
Corn Stover Lignin	63.1	6.5	4.5	25.8
Pine Woodchips	48.2	6.3	<0.1	45.6
Delignified Pine Woodchips	49.3	6.4	<0.1	44.4
Pine Lignin	65	6.3	<0.1	28.7
Olive Cake Pellets	48.6	5.8	1.5	44.2
Delignified Olive Cake	48.6	5.9	0.8	44.7
Olive Cake Lignin	65.3	7.1	3.4	24.3
Miscanthus Pellets	45.9	5.9	0.4	47.7
Delignified Miscanthus	44.1	6.1	0.2	49.5
Miscanthus Lignin	65	6	0.9	28.2
Eucalyptus Pellets	45.5	6.1	<0.1	48.4
Delignified Eucalyptus	45.3	6.1	<0.1	48.6
Eucalyptus Lignin	66.5	6	<0.1	27.4
Mixed Softwood Pellets	49	5.8	1.5	43.8
Delignified Mixed Softwood	49.7	5.8	0.6	44
Mixed Softwood Lignin	66.9	7.3	1.8	24
Torrefied Wheat Straw 240°C	49.6	4.7	1.2	44.5
Torrefied Wheat Straw 260°C	53.1	4.4	1.2	41.2
Torrefied Wheat Straw 280°C	60.4	4.2	1.3	34.1
Torrefied Corn Stover 240°C	50.3	5.2	1.9	42.7
Torrefied Corn Stover 260°C	57.6	4.9	1.9	35.6
Torrefied Corn Stover 280° C	62.3	4.5	1.9	31.4
Torrefied Pine 240°C	53.3	5.9	<0.1	40.8
Torrefied Pine 260°C	56.8	5.7	<0.1	37.5
Torrefied Pine 280°C	62.4	5.3	<0.1	32.3
Torrefied Mixed Softwood 240°C	52.5	5.6	1.4	40.5
Torrefied Mixed Softwood 260°C	54.7	5.5	1.2	38.6
Torrefied Mixed Softwood 280°C	60.6	5.1	1.5	32.7
Steam Explosion Mixed Woods	50.3	5.9	<0.1	43.8
Demineralised Wheat Straw Pellets	43.1	5.6	0.9	50.4
Demineralised Delignified Wheat Straw	41.1	5.7	0.4	52.8
Demineralise Corn Stover Pellets	46.1	5.5	1.8	46.6
Demineralised Delignified Corn Stover	45.0	5.6	0.6	48.9
Demineralised Pine Woodchips	48.7	6.1	<0.1	45.2
Demineralised Delignified Pine Woodchips	50.4	6.5	<0.1	43.1
Demineralised Miscanthus Pellets	46.9	6.1	<0.1	47.1
Demineralised Delignified Miscanthus	45.6	6.1	<0.1	48.3
Demineralised Eucalyptus Pellets	47.5	6	<0.1	46.4
Demineralised Delignified Eucalyptus	45.1	6	<0.1	48.9
Demineralised Mixed Softwood Pellets	49.1	5.8	1.4	43.7
Demineralised Delignified Mixed Softwood	49.6	5.8	0.5	44.1
Demineralised Steam Explosion Mixed Wood	50.5	5.9	<0.1	43.6
El Cerrejon Coal	72.8	6.2	1.3	19.6
Kellingley Coal	85.2	6.1	2.3	5.5
Thoresby Coal	84.7	4.92	2.0	7.8

* O content calculated by difference

Table 4-1 Sample Organic Elemental Composition

In order to assess any significant differences in the organic chemical composition of the biomass and the influences of fuel pre-treatment techniques including delignification, demineralisation and torrefaction the atomic H:C ratio and O:C ratio have been determined (Table 4-2).

Sample	Atomic O:C Ratio	Atomic H:C ratio
Wheat Straw Pellets	0.79	1.35
Delignified Wheat Straw	0.97	1.61
Wheat Straw Lignin	0.52	1.29
Corn Stover Pellets	0.79	1.47
Delignified Corn Stover	0.84	1.52
Corn Stover Lignin	0.31	1.24
Pine Woodchips	0.71	1.57
Delignified Pine Woodchips	0.68	1.56
Pine Lignin	0.33	1.16
Olive Cake Pellets	0.68	1.43
Delignified Olive Cake	0.69	1.46
Olive Cake Lignin	0.28	1.30
Miscanthus Pellets	0.78	1.54
Delignified Miscanthus	0.84	1.66
Miscanthus Lignin	0.33	1.11
Eucalyptus Pellets	0.80	1.61
Delignified Eucalyptus	0.80	1.62
Eucalyptus Lignin	0.31	1.08
Mixed Softwood Pellets	0.67	1.42
Delignified Mixed Softwood	0.66	1.40
Mixed Softwood Lignin	0.27	1.31
Torrefied Wheat Straw 240°C	0.67	1.14
Torrefied Wheat Straw 260°C	0.58	0.99
Torrefied Wheat Straw 280°C	0.42	0.83
Torrefied Corn Stover 240°C	0.64	1.24
Torrefied Corn Stover 260°C	0.46	1.02
Torrefied Corn Stover 280°C	0.38	0.87
Torrefied Pine 240°C	0.57	1.33
Torrefied Pine 260°C	0.50	1.20
Torrefied Pine 280°C	0.39	1.02
Torrefied Mixed Softwood 240°C	0.58	1.28
Torrefied Mixed Softwood 260°C	0.53	1.21
Torrefied Mixed Softwood 280°C	0.40	1.01
Steam Explosion Mixed Woods	0.65	1.41
Demineralised Wheat Straw Pellets	0.88	1.56
Demineralised Delignified Wheat Straw	0.96	1.66
Demineralise Corn Stover Pellets	0.76	1.43
Demineralised Delignified Corn Stover	0.82	1.49
Demineralised Pine Woodchips	0.70	1.50
Demineralised Delignified Pine Woodchips	0.64	1.55
Demineralised Miscanthus Pellets	0.75	1.56
Demineralised Delignified Miscanthus	0.79	1.61
Demineralised Eucalyptus Pellets	0.73	1.52
Demineralised Delignified Eucalyptus	0.81	1.60
Demineralised Mixed Softwood Pellets	0.67	1.42
Demineralised Delignified Mixed Softwood	0.67	1.40
Demineralised Steam Explosion Mixed Wood	0.65	1.40
El Cerrejon Coal	0.20	1.02
Kellingley Coal	0.05	0.86
Thoresby Coal	0.07	0.70

Table 4-2 Atomic O:C and H:C Ratios

Plotting these figure on a Van Krevellen diagram of atomic H:C vs. atomic O:C ratios provides useful information of the chemical characteristics of the fuels (Figure 4-1).

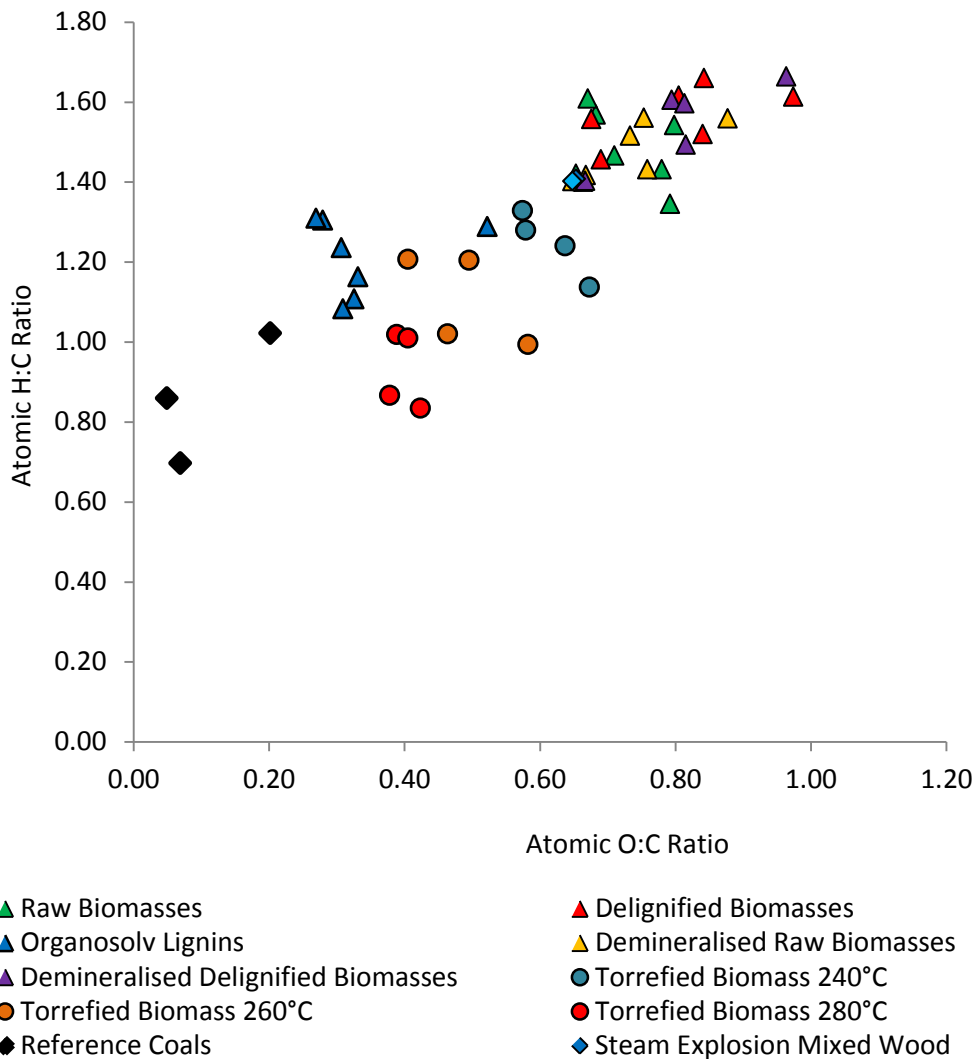


Figure 4-1 Van Krevellen Diagram (Atomic H:C vs. O:C Ratios)

4.1.1. Impact of Organosolv Delignification on Elemental Composition

Partial delignification through organosolv pulping techniques does result in alteration of the organic composition of lignocellulosic material in a number of ways. Firstly the removal of lignin which, due to its aromatic nature, is relatively high in carbon will result in a decrease in the total carbon content of the sample whilst the simultaneous acid

hydrolysis of hemicellulose and removal of free sugars and extractive material may also influence bulk chemical compositions.

It can be seen that the removal of lignin during organosolv delignification results in marked decreases in the carbon content of herbaceous biomass such as wheat straw, corn stover and Miscanthus. The carbon content of herbaceous organosolv residues are lower than raw fuels by between 0.8 and 4.6 wt% daf. This is accompanied by an increase in the oxygen and hydrogen contents of the fuels varying between 1.8 and 5 wt% daf and 0.1 and 0.4 wt% daf respectively. These decreases in carbon and increases in oxygen and hydrogen content are most likely due to the substantial removal of aromatic carbon structures present within the lignin fraction during organosolv processing. These lignin compounds are rich in conjugated aromatic ring structures and thus contain higher levels of carbon and lower oxygen and hydrogen contents than either cellulose or hemicellulose constituents, this being evidenced in the organic chemical composition of the organosolv lignins generated (C wt% ranging between 54 and 66.9 wt% daf). It can further be seen in Figure 4-1 that lignins isolated during organosolv pulping are preferentially depleted in oxygen rather than hydrogen, this results in the greater losses of oxygen when compared to hydrogen during delignification.

These influences are far less obvious in the case of woody biomass including pine woodchips, eucalyptus pellets and mixed softwood pellets, all of which exhibited an increase in the carbon content of organosolv residues compared to the raw fuel. It is clear from these results that the alteration of the lignocellulosic matrix during organosolv pulping differs depending on the nature of raw material being utilised. There are a number of potential explanations for this observation, the most likely being that

the hydrolysis of hemicellulose and removal of free sugars results in an increase in the carbonaceous character through loss of material with relatively low carbon content.

These alterations in chemical composition are shown in the Van Krevelen diagram Figure 4-1 where delignified herbaceous samples can be seen to occupy positions further to the upper right hand regions of the plot and are characterised by higher O:C and H:C ratios. The points for these samples also lie on the same, relatively straight line relationship between O:C and H:C atomic ratio which typifies simultaneous changes in C, O and H content for all biomass and lignitic coal varieties.

SEM image analysis has been conducted for both raw and delignified wheat straw and pine samples in order to give an insight into the differing structural reordering of the feedstocks undergone by herbaceous and woody biomass respectively as shown in Figures 4-2 – 4-5.

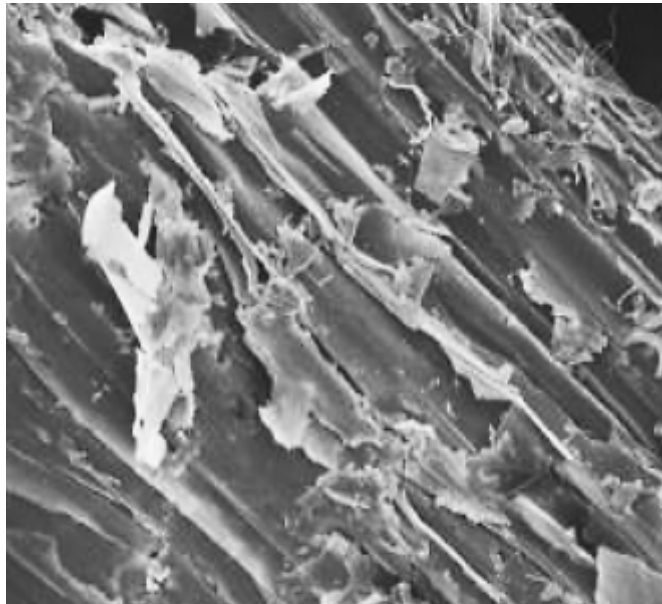


Figure 4-2 Raw Wheat Straw Pellet SEM Image

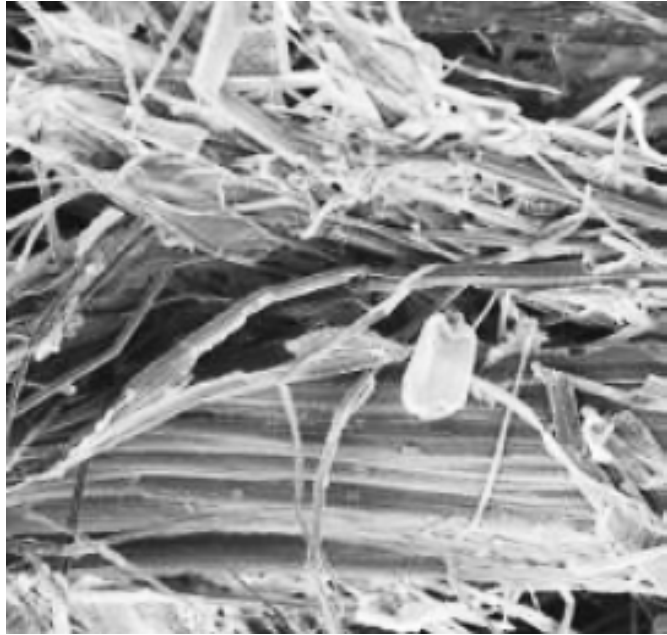


Figure 4-3 Delignified Wheat Straw Pellet SEM Image

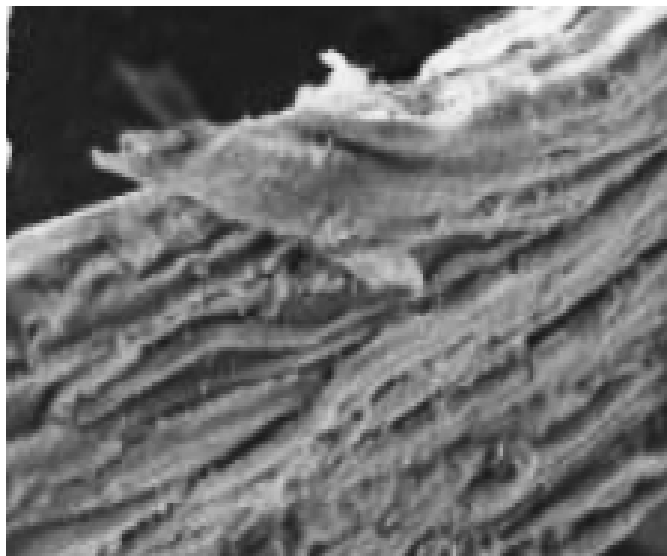


Figure 4-4 Raw Pine Woodchip SEM Image

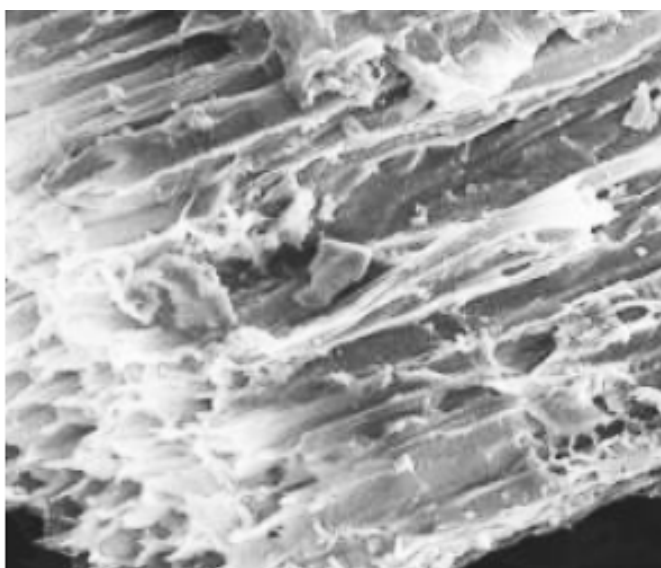


Figure 4-5 Delignified Pine Woodchip SEM Image
10 μm

SEM imaging reveals that both wheat straw and pine samples undergo considerable physical alteration during organosolv delignification. For wheat straw pellets this appears to involve considerable defiberisation of the plant structure to produce a disordered arrangement of cellulosic fibres. Pine woodchips similarly undergo an opening of the cellulosic plant structure with removal of the lignin coating and depletion of hemicellulose and extractive material, the conversion of pine structures appears to be considerably less severe than in the case of straw pellets with no significant evidence of defiberisation being observed. These observations are confirmed by the considerable loss of carbon content for wheat straw pellets following lignin removal and consequent increases in H:C and O:C atomic ratios which are far less evident for woody feedstocks such as pine woodchips. This further indicates the lability of herbaceous biomass to chemical and physical degradation when compared to woody fuels which may influence subsequent thermochemical reactivity.

4.1.2. Impact of Acid Demineralisation on Elemental Composition

HCl washing demineralisation has a varied influence on bulk chemical composition; however, changes in organic elemental composition are consistently small in

comparison to delignification processes. In common with delignification alterations the modification of woody feedstocks (with the exception of raw eucalyptus pellets) were comparatively small compared to herbaceous fuels, woody biomass undergoing only very slight change in carbon content ($\pm 0.1 - 0.2\%$) coupled with comparably slight alteration of H, O and N content.

4.1.3. Impact of Torrefaction on Elemental Composition

The volatilisation of reactive biomass constituents, largely comprising hemicellulose, during torrefaction gives rise to the preferential loss of components relatively low in carbon and high in hydrogen and oxygen content. This gives rise to increases in the carbon content of the torrefied sample with reductions in hydrogen and oxygen content. These influences increase with increasing severity of torrefaction, carbon increases become more severe with increases in torrefaction temperature and loss of more thermally stable biomass components. Plotting carbon content with raw fuel composition existing at ambient temperature of $\sim 25^{\circ}\text{C}$ gives an appreciation of the increasing concentration of carbon as shown in Figure 4-6. Accumulation of carbon in the torrefied fuel appears to accelerate considerably following treatment at temperatures above 240°C . This is due to the individual degradation behaviour of biomass pseudo-components which are known to undergo pyrolysis across a narrow range of characteristic temperatures. Peak mass loss for hemicellulose occurs between 200 and 350°C via a multi-step process which gives rise to a double peak in the mass loss profile (Lv and Wu 2012; Shen et al., 2010). As the torrefaction temperature is increased the first loss of volatiles and concentration of carbon in the torrefied product occurs with the loss of reactive hemicellulose side chains, more intensive hemicellulose volatilisation occurring as the temperature increases and promotes more widespread decomposition of the xylan core structure.

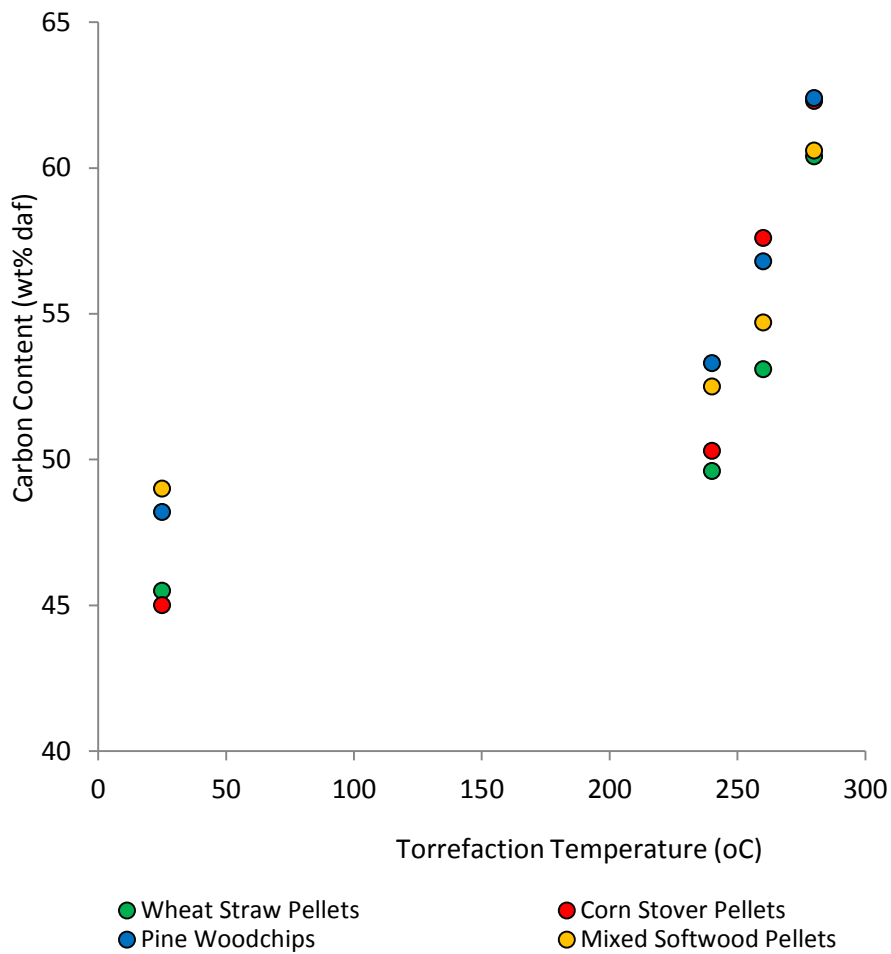


Figure 4-6 Carbon Content vs. Torrefaction Temperature

It can be seen in Figure 4-1 that the torrefaction of biomass also results in a preferential depletion in hydrogen over oxygen causing the relationship of H:C and O:C ratios to shift away from that exhibited by raw biomass materials and lignitic fuels. This effect has been observed previously (Van de Stelt et al., 2011) whereby hydrogen appears to be the most labile of the elemental constituents during mild pyrolytic torrefaction. Given that the oxygen content of a fuel is instrumental in determining its reactivity during both devolatilisation and char oxidation reactions the significant loss of oxygen containing substituents during torrefaction, especially at higher temperature is likely to have an impact on thermochemical decomposition behaviour. Fuel bound oxygen is known to disrupt the ordered nature of the fuels carbon matrix increasing devolatilisation reactivity and volatile matter yields (Jenkins et al., 1998).

4.2. Ash Content and Speciation

Sample	Na (wt% db)	K (wt% db)	Mg (wt% db)	Ca (wt% db)	Al (wt% db)	Total Ash Content (wt% db)*
Wheat Straw Pellets	0.01	1.36	0.13	0.52	0.04	8.57
Delignified Wheat Straw	0.01	0.58	0.08	0.77	0.04	9.72
Wheat Straw Lignin	<0.01	0.01	<0.01	<0.01	<0.01	0.39
Corn Stover Pellets	0.01	1.92	0.35	0.6	0.05	7.14
Delignified Corn Stover	0.01	0.56	0.34	0.31	0.06	10.10
Corn Stover Lignin	0.01	0.2	0.02	0.01	<0.01	0.62
Pine Woodchips	<0.01	0.09	0.02	0.12	0.02	1.81
Delignified Pine Woodchips	0.01	0.04	0.01	0.14	0.02	3.21
Pine Lignin	<0.01	0.01	<0.01	<0.01	<0.01	0.36
Olive Cake Pellets	0.06	2.52	0.25	0.67	0.07	5.98
Delignified Olive Cake	0.01	1.1	0.37	1.77	0.17	10.50
Olive Cake Lignin	0.01	0.12	0.01	<0.01	<0.01	1.60
Miscanthus Pellets	0.03	0.06	0.03	0.21	0.02	1.49
Delignified Miscanthus	0.02	0.05	0.02	0.28	<0.01	1.16
Miscanthus Lignin	<0.01	0	<0.01	0.02	<0.01	0.38
Eucalyptus Pellets	0.01	0.05	0.02	0.09	0.02	0.88
Delignified Eucalyptus	<0.01	0.01	<0.01	0.19	0.03	0.47
Eucalyptus Lignin	<0.01	0.01	<0.01	<0.01	<0.01	0.29
Mixed Softwood Pellets	0.02	0.44	0.04	0.12	0.01	1.51
Delignified Mixed Softwood	0.01	0.17	0.01	0.27	<0.01	5.10
Mixed Softwood Lignin	<0.01	0.01	<0.01	<0.01	<0.01	0.74
Torrefied Wheat Straw 240°C	0.01	1.33	0.13	0.56	0.03	8.62
Torrefied Wheat Straw 260°C	0.01	1.36	0.13	0.58	0.03	9.21
Torrefied Wheat Straw 280°C	0.01	1.45	0.13	0.83	0.02	9.30
Torrefied Corn Stover 240°C	0.01	1.52	0.31	0.46	0.05	8.77
Torrefied Corn Stover 260°C	0.01	1.72	0.33	0.45	0.05	8.66
Torrefied Corn Stover 280° C	0.01	1.62	0.32	0.48	0.05	9.24
Torrefied Pine 240°C	<0.01	0.08	0.02	0.11	0.02	1.99
Torrefied Pine 260°C	<0.01	0.07	0.02	0.07	0.01	2.11
Torrefied Pine 280°C	<0.01	0.06	0.01	0.06	0.01	2.16
Torrefied Mixed Softwood 240°C	0.01	0.27	0.03	0.07	0.01	1.63
Torrefied Mixed Softwood 260°C	0.01	0.32	0.02	0.09	0.01	1.75
Torrefied Mixed Softwood 280°C	<0.01	0.43	0.03	0.1	<0.01	1.86
Steam Exploded Mixed Wood	<0.01	0.1	0.03	0.24	0.01	1.21
Demineralised Wheat Straw Pellets	<0.01	0.01	<0.01	<0.01	0.01	7.67
Demineralised Delignified Wheat Straw	<0.01	0.01	<0.01	<0.01	0.02	10.16
Demineralise Corn Stover Pellets	<0.01	0.01	<0.01	<0.01	<0.01	7.37
Demineralised Delignified Corn Stover	<0.01	0.01	<0.01	0.01	0.01	10.03
Demineralised Pine Woodchips	<0.01	0.01	<0.01	<0.01	<0.01	1.89
Demineralised Delignified Pine Woodchips	<0.01	0.01	<0.01	<0.01	<0.01	3.42
Demineralised Miscanthus Pellets	0.03	<0.01	<0.01	0.01	<0.01	1.29
Demineralised Delignified Miscanthus	0.02	0.01	<0.01	0.01	<0.01	1.11
Demineralised Eucalyptus Pellets	<0.01	<0.01	<0.01	0.01	0.01	0.99
Demineralised Delignified Eucalyptus	<0.01	<0.01	0.01	0.01	0.03	1.15
Demineralised Mixed Softwood Pellets	<0.01	<0.01	<0.01	0.01	<0.01	1.59
Demineralised Delignified Mixed Softwood	<0.01	<0.01	<0.01	0.01	<0.01	4.88
Demineralised Steam Exploded Mixed Wood	<0.01	0.01	<0.01	0.07	<0.01	0.58

*As determined upon complete combustion in the TGA

Table 4-3 Abridged Total Ash and Inorganic Elemental Composition

A clear distinction can be drawn between herbaceous and agricultural residue species and clean wood derived fuels in terms of total ash content and mineral speciation in raw fuels. Wheat straw, corn stover and olive cake pellets all contain levels of total ash greater than 5 wt% db (with wheat straw containing the maximum of 8.6 wt% db) which is in line with the greater absorption of inorganic minerals during their short growing season (Koppejan and Van Loo, 2012). All other raw fuels contain less than 2 wt% ash on a dry basis. Miscanthus is unique as being a fast growing herbaceous biomass feedstock with relatively low levels of ash (1.49 wt% db), making it of interest for use as a fuel in combustion infrastructure due to the reduced burden of ash related operating issues such as slagging and fouling of heat exchange surfaces.

4.2.1. Impact of Organosolv Delignification on Inorganic Chemical Composition

The removal of lignin alongside some hemicellulose, free sugars and extractive material during organosolv delignification does influence both the total ash quantity and the speciation of ion exchangeable mineral components.

With the exception of miscanthus and eucalyptus pellet samples all other biomass experience an increase in the ash content of the solid delignified product following delignification (increases ranging from 1.15 to 4.52 wt% db for wheat straw and olive cake pellets respectively). Increases in ash content of delignified samples is due primarily to the removal of very low ash contain lignin structures and extractive material and the preferential concentration of inorganics in the remaining solid delignified residue. Although the bulk ash content increases, in general ion exchangeable species are lost due to the intensive alcohol and water washing procedures utilised. This results in the reduction of K content for all fuels following lignin separation, Ca however appears to be concentrated within the cellulosic residue produced most likely as a result

of the differing distributions of alkali metals within the biomass structure, their solubility and their differing lability to removal during the organosolv washing procedures employed.

4.2.2. Impact of Acid Demineralisation on Inorganic Chemical

Composition

Demineralisation using dilute HCl and deionised water appears to have a mixed influence on the total ash content of the samples depending upon the ash speciation and degree of alteration of the organic chemical structure of the fuel. The change in total ash content upon demineralisation was less than 1% all cases which is indicative of the minimal total loss of organic components during demineralisation.

The influence of demineralisation procedures upon ion-exchangeable alkali/alkaline earth metal species is more marked and gives rise to a consistent depletion in K, Ca, Mg and Na contents to the point that most are either at or below the lower limit of reliable detection using the instrumentation available (all values that were below 0.01 wt% db were seen to produce considerable variation in repeat determinations and have thus been reported above as being <0.01 wt% db for this reason).

It can be concluded that any results obtained during conversion of demineralised fuels are consistent with behaviours in the absence of any significant contribution of inorganic mineral interactions.

4.2.3. Impact of Torrefaction on Inorganic Chemical Composition

The torrefaction of the chosen fuels does result in a concentration of incombustible ash in the torrefied material due to the loss of organic constituents during torrefaction. AAEM species, especially K and Ca are also concentrated within the torrefied fuel to some degree.

4.3. Aromatic Carbon Content by ¹³C NMR Spectroscopy

The quantifications of aromaticity conducted using SS CPMAS ¹³C NMR of the fuels and calculated aromatic carbon contents (wt% daf) are shown in Table 4-4.

Sample	Aromaticity (mol %)	Aromatic Carbon (wt% Daf)
Wheat Straw Pellets	16.4	7.5
Delignified Wheat Straw	12.6	5.2
Wheat Straw Lignin	63.7	34.4
Corn Stover Pellets	20.5	9.2
Delignified Corn Stover	7.7	3.4
Corn Stover Lignin	44.7	28.2
Pine Woodchips	28.3	13.6
Delignified Pine Woodchips	18.2	9.0
Pine Lignin	55.2	35.9
Olive Cake Pellets	20.6	10
Delignified Olive Cake	10.7	5.2
Olive Cake Lignin	44.6	29.1
Miscanthus Pellets	25.2	11.6
Delignified Miscanthus	11.8	5.2
Miscanthus Lignin	52.4	34.0
Eucalyptus Pellets	32.9	15.0
Delignified Eucalyptus	13.1	6.0
Eucalyptus Lignin	55.8	37.1
Mixed Softwood Pellets	15.5	7.6
Delignified Mixed Softwood	12.5	6.2
Mixed Softwood Lignin	48	32.1
Torrefied Wheat Straw 240°C	30.1	14.9
Torrefied Wheat Straw 260°C	35	18.6
Torrefied Wheat Straw 280°C	47.9	28.9
Torrefied Corn Stover 240°C	32.3	16.2
Torrefied Corn Stover 260°C	41.6	24.0
Torrefied Corn Stover 280°C	53	32.0
Torrefied Pine 240°C	35.9	19.1
Torrefied Pine 260°C	45.6	25.9
Torrefied Pine 280°C	61.4	38.3
Torrefied Mixed Softwood 240°C	29.9	15.7
Torrefied Mixed Softwood 260°C	35.2	19.2
Torrefied Mixed Softwood 280°C	48.1	29.2
Steam Explosion Mixed Woods	34.3	17.3
Demineralised Wheat Straw Pellets	31.09	12.8
Demineralised Delignified Wheat Straw	20.35	8.8
Demineralise Corn Stover Pellets	20.3	9.4
Demineralised Delignified Corn Stover	9.7	4.4
Demineralised Pine Woodchips	28.1	13.7
Demineralised Delignified Pine Woodchips	17.5	8.8
Demineralised Miscanthus Pellets	25.9	12.1
Demineralised Delignified Miscanthus	13	5.9
Demineralised Eucalyptus Pellets	27.2	12.9
Demineralised Delignified Eucalyptus	15.9	7.2
Demineralised Mixed Softwood Pellets	15.5	7.6
Demineralised Delignified Mixed Softwood	13	6.4
Demineralised Steam Explosion Mixed Wood	37.3	18.8

Table 4-4 Biomass Aromaticity and Aromatic Carbon Content

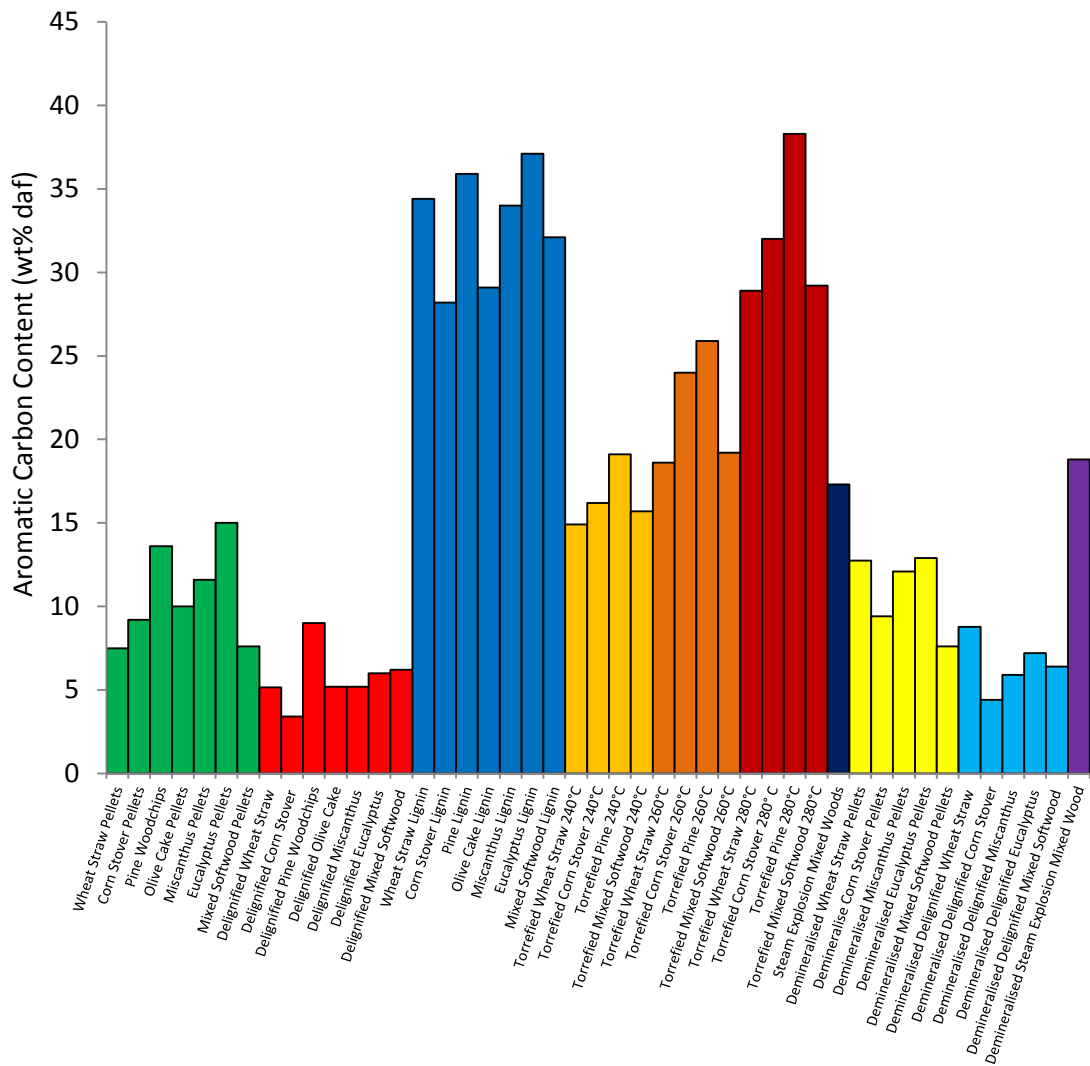


Figure 4-7 Column Plot of Aromatic Carbon Content

It is evident on assessment of Figure 4-7 that the varied sample groups can be characterised by differing aromatic carbon contents. Delignified samples have the lowest aromatic character, with raw samples being significantly higher in aromaticity and lignins containing the highest aromatic carbon content. The aromatic carbon character of torrefied fuels increases with increasing torrefaction severity and loss of reactive non-aromatic carbon structures. Demineralisation practices do alter the

aromatic carbon content of the fuels; however, these alterations are maintained at a relatively modest level and still enable study of the impact of varied aromaticities on char generation and oxidation processes in the absence of any significant mineral interactions.

4.3.1. Impact of Organosolv Delignification on Aromatic Carbon

Content

As anticipated the partial removal of the lignin component of the fuels does result in an appreciable decrease in the aromatic content of all fuels ranging from 1.4 to 9% (representing a decrease of between 20 and 63% in the aromatic content of the original fuel).

4.3.2. Impact of Acid Demineralisation on Aromatic Carbon Content

With the exception of eucalyptus pellets, acid demineralisation causes an increase in the aromatic carbon content of the sample, alterations being minimal except for that of wheat straw samples which are seen to increase in aromatic carbon wt% daf of 5.25 and 3.62 wt% daf for raw and delignified samples respectively. A wide range of aromatic carbon contents of 4.4 – 18.8 wt% daf are still available for analysis within the demineralised fuels and this is comparable to the range exhibited by non-demineralised raw and delignified samples of 3.4 – 17.3 wt% daf.

Organosolv lignins and olive cake samples have not been subject to demineralisation in this study due to the considerable degradation which occurs during the acid treatment of these samples which was observed to largely destroy non-aromatic components and considerably alter the chemical structure of the aromatic carbon compounds which remain rendering them entirely unrepresentative of lignocellulosic constituents found in nature.

4.3.3. Impact of Torrefaction on Aromatic Carbon Content

The preferential volatilisation of reactive aliphatic components of hemicellulose and lignin associated with mild pyrolytic torrefaction clearly results in an increase in the aromatic carbon content of the torrefied materials which increases with increasing torrefaction temperature and increased loss of saccharide material. These observations fit well with those of Melkior et al., 2012 who similarly utilised ^{13}C NMR for the assessment of aromatisation of torrefied biomass under varying torrefaction temperatures. Increase in aromatic carbon over the raw fuel following torrefaction at 280°C were between 21.4 and 24.7 wt% daf. It was believed that this increase was greater than that expected purely from the preferential depletion of non-aromatic carbon structures and as such a detailed analysis of the torrefaction yields obtained has been conducted in Chapter 5.

4.4. Summary

All of the chosen fuels have been fully characterised as to bulk chemical composition, inorganic mineral matter concentrations and aromatic carbon content alongside their delignified, demineralised and torrefied analogues and isolated lignin components. Overall the pre-treatments utilised appear to provide a suitable range of samples to enable study of the influence of aromatic carbon content, alkali/alkaline earth mineral activity and varying physiochemical characteristics on the pyrolytic devolatilisation behaviour, the nature of char formations generated and subsequent char oxidation reactivity for a range of lignocellulosic fuels. The following conclusions have been drawn from the basic fuel characterisation work described:

- ▶ All fuel samples are well characterised using the Van Krevelen method of plotting atomic H:C vs. O:C ratios to gain fuller understanding of fuel organic composition
- ▶ Organosolv pulping is able to provide significant delignification of the parent biomass fuels which results in a comparable decrease in the aromatic carbon content. These pre-treatments also influence the mineral matter composition of the fuels and this must be considered during analysis of thermochemical conversion behaviours.
- ▶ Although HCl acid washing demineralisation processes do influence the organic chemical composition of treated fuels they do provide very high ion exchangeable mineral matter removal efficiencies and reduce active AAEM contents to very low levels. Any alteration of the organic chemical composition is relatively modest and aromatic carbon contents are retained across a range which are closely comparable to those of the non-demineralised samples allowing valid assessment of the influence of aromatic carbon content in the absence of significant mineral matter influences
- ▶ Biomass torrefaction using a range of torrefaction temperatures does provide a means of producing samples with increased aromatic carbon character and increased structural condensation. The torrefaction process also appears to result in the preferential loss of oxygen rich fuel components which will influence its pyrolysis and char combustion properties.

Chapter 5: Biomass Sample Preparation Methods

This chapter describes the influence of the chosen fuel preparation techniques on the chemical and physical composition of the fuels and their derived analogues. This includes a detailed quantification of the mass balance of aromatic carbon through the organosolv delignification process as measured using ^{13}C NMR techniques – a first of a kind balance of organic structures through this form of chemical biomass fractionation.

5.1. Organosolv Delignification

Given the recent interest in fractionation of lignocellulosic biomass for the production of green chemicals and fuels, organosolv delignification has gained wide interest as a simple, mild and economically attractive method of de-fiberising biomass materials whilst removing a high percentage of the lignin content of the feedstock by solubilisation to leave a cellulose rich, open structured residue which can be more readily converted to valuable renewable fuels.

Given this interest, continued efforts have been made to make valid determinations of the mass and energy balances of the organosolv process through computer aided modelling, bench and pilot scale investigations. Given the relative importance of lignin removal efficiencies and the potential application of lignin derived chemicals in green chemistry these quantification of mass balance have often focused on the accounting of lignin molecules throughout the fractionation treatment to give an overview of separation dynamics. The determination of lignin contents of differing process fractions, which include a largely delignified, cellulose rich solid residue, a precipitated solid lignin and a large volume of solvent washings, is undertaken using a number of determination techniques which are not necessarily complementary in accurate determination of process balances (Benner et al., 1990).

Given these drawbacks and the necessity to fully understand the fuel pre-treatment process utilised throughout this investigation a detailed accounting of organic component fractionation during the ethanol organosolv process has been conducted independently from the preparation of samples for investigation of combustion behaviour (samples prepared for aromatic carbon balances presented in this section were prepared prior to mass delignification of all fuel samples for further combustion analysis). Special emphasis has been placed on the utilisation of combined chemical analysis and aromaticity quantification using ^{13}C NMR to fully appreciate the transformation of aromatic and aliphatic biomass components during fractionation.

5.1.1. Aromatic Carbon Balances of Organosolv Fractionation Using ^{13}C NMR

The mass of original and resultant fractions was accurately recorded through the fractionation of both pine woodchip and straw pellet feedstocks to enable a quantification of relevant pseudo-component mass balances during organosolv fractionation. In this case the liquor produced from the processes (as shown in Figure 3-1) was evaporated to dryness to account for the loss of solid mass in the solvent solution (shown as liquor solids below). The total mass balance of the process is shown in Figures 5.1 and 5.2 for pine and wheat straw fractionation respectively.

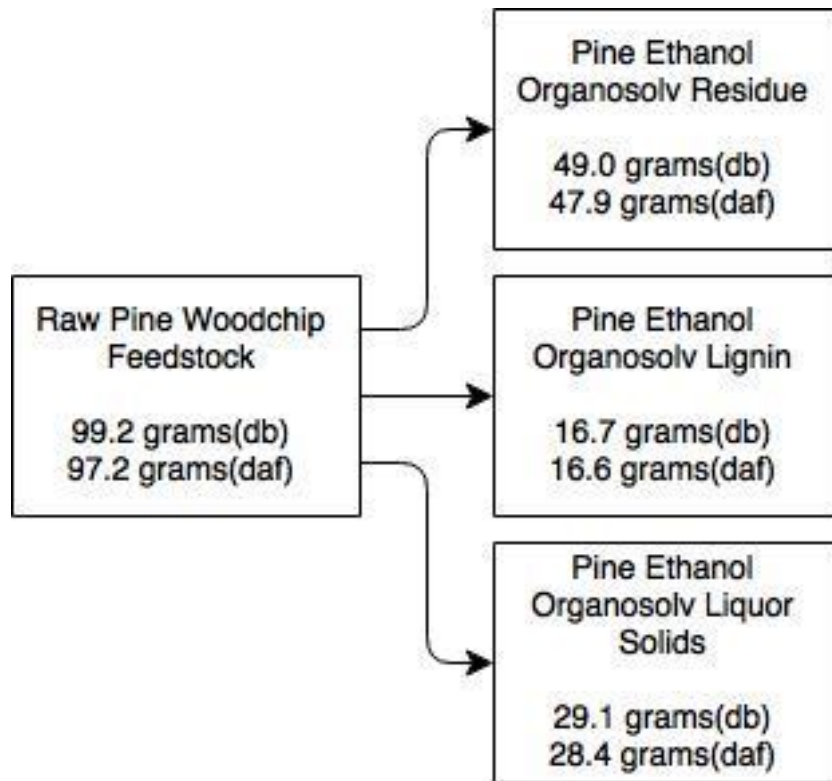


Figure 5-1 Pine Ethanol Organosolv Mass Fractionation

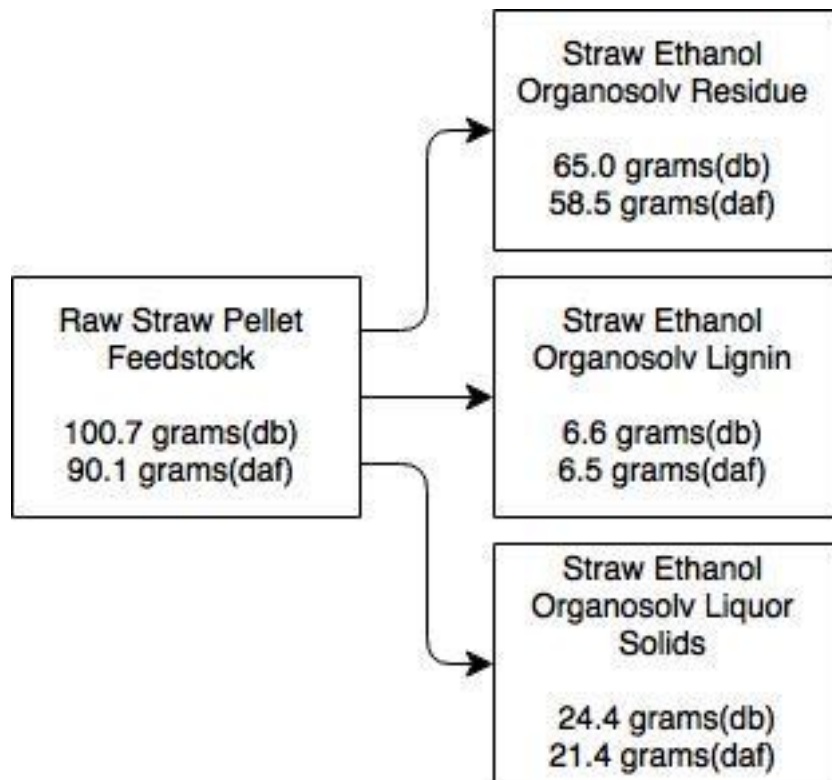


Figure 5-2 Wheat Straw Ethanol Organosolv Mass Fractionation

In order to further understand the fractionation dynamics each fraction was characterised as to their elemental as well as their structural aromaticity using ^{13}C NMR – results being summarised in and Tables 5-1, 5-2 and Figures 5-1 and 5-2 with corresponding ^{13}C NMR Spectra being presented in Figures 5-3 and 5-4.

Fraction	Mass % (daf)			
	N	C	H	O
Raw Pine	<0.01	46.68 (0.18)	6.16 (0.07)	47.16 (0.32)
Pine Residue	<0.01	45.40 (0.73)	6.10 (0.03)	48.49 (0.74)
Pine Lignin	<0.01	61.67 (0.88)	5.74 (0.05)	32.59 (0.91)
Pine Liquor Solids	<0.01	46.48 (0.09)	6.41 (0.07)	47.11 (0.65)
Raw Straw	1.28 (0.05)	45.49 (0.28)	5.05 (0.07)	48.18 (0.44)
Straw Residue	0.45 (0.03)	40.90 (0.08)	5.52 (0.10)	53.13 (0.47)
Straw Lignin	2.60 (0.12)	54.00 (0.54)	5.83 (0.14)	37.57 (0.63)
Straw Liquor Solids	1.49 (0.08)	39.02 (0.15)	5.97 (0.08)	53.52 (0.35)

**Values in parenthesis refer to standard deviations as determined using triplicate analyses*

Table 5-1 Organic Elemental Composition of Organosolv Fractions

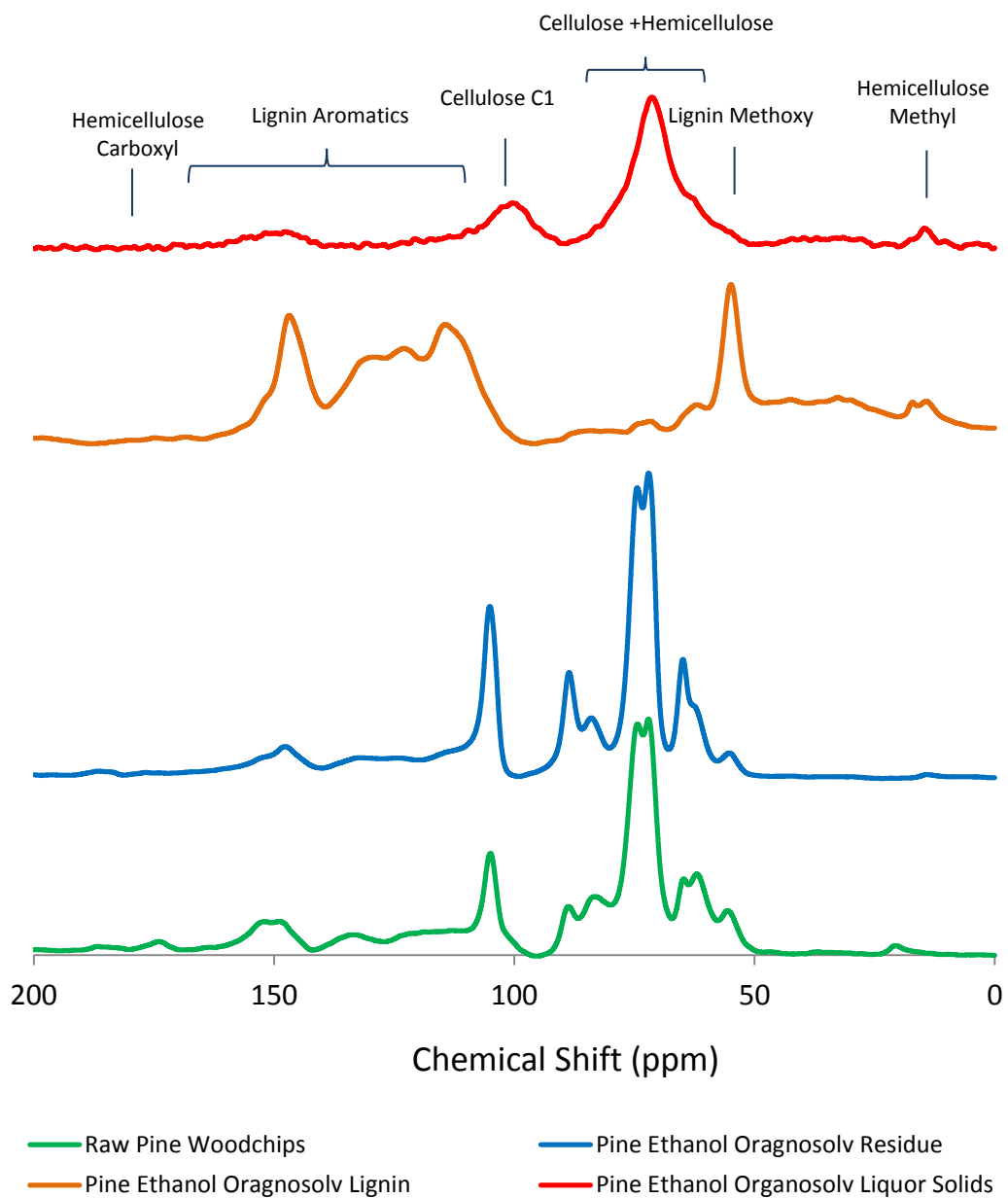


Figure 5-3 ^{13}C SS CPMAS NMR Spectra of Pine Ethanol Organosolv Fractions

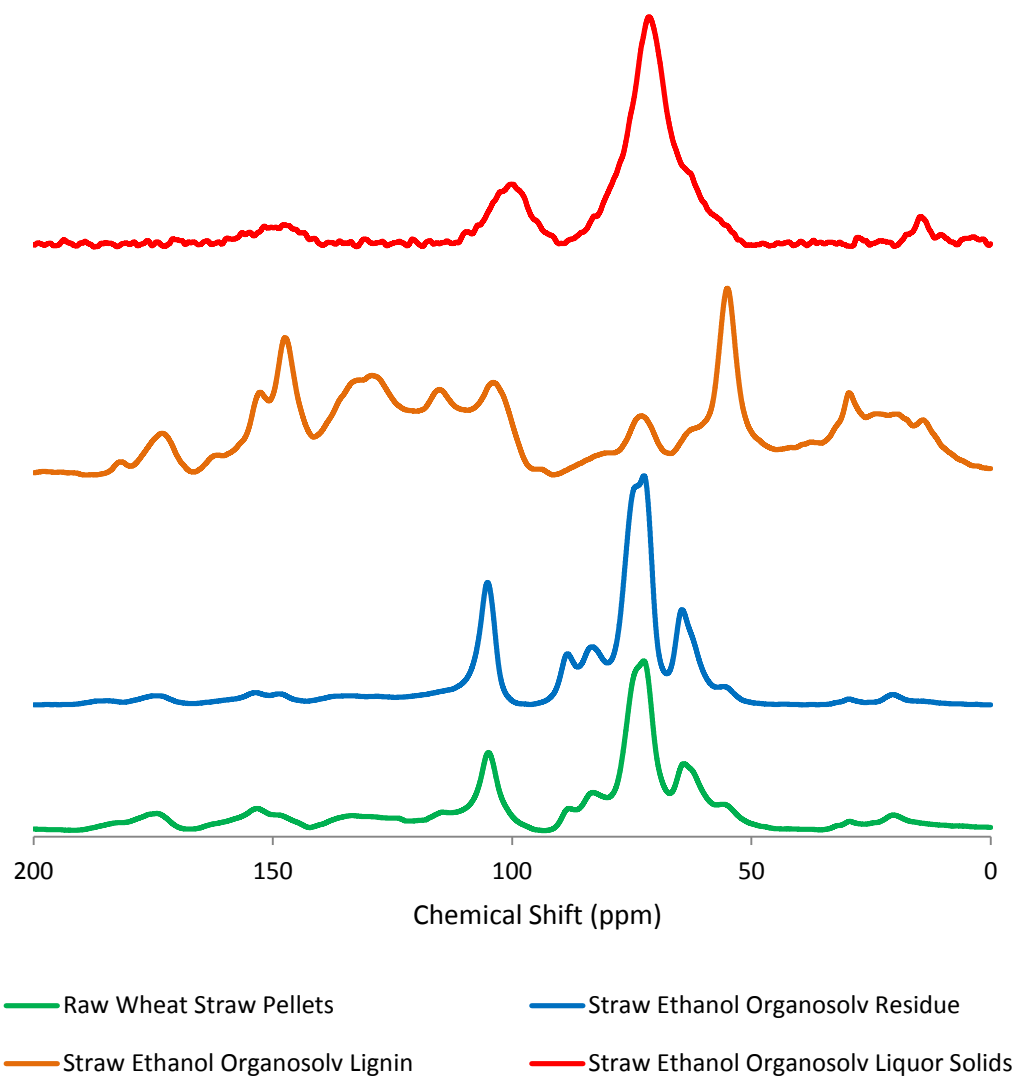


Figure 5-4 ^{13}C SS CPMAS NMR Spectra of Wheat Straw Ethanol Organosolv Fractions

Aromaticity of each fraction was then determined through integration of the relevant peaks within the NMR spectra (shown in Figures 5-3 and 5-4) as described in Chapter 3, from which a mass of aromatic carbon for each fraction was calculated and a mass balance derived. The result of total organic matter, carbon and aromatic carbon mass balances for both pine and wheat straw fractionations are shown in Table 5-2 below.

Fraction	Mass (g db)	Mol % Aromatic Carbon	Total Organic Matter (g daf)	Total Carbon (g daf)	Total Aromatic Carbon (g daf)	% Original Aromatic Carbon
Raw Pine Woodchips	99.2	22.6	97.2	45.4	10.3	100
Pine Ethanol Organosolv Residue (Delignified)	49.0	18.8	47.9	21.8	3.7	35.3
Pine Ethanol Organosolv Lignin	16.7	54.6	16.6	10.2	5.4	52.5
Pine Ethanol Organosolv Liquor Solids	29.1	6.0	28.4	13.2	0.8	7.7
<u>Total Mass Balance (%)</u>	<u>95.6</u>		<u>95.6</u>	<u>99.6</u>	<u>95.5</u>	
Raw Wheat Straw Pellets	100.7	15.2	90.1	37.8	5.7	100
Straw Ethanol Organosolv Residue (Delignified)	65.0	12.6	58.5	23.9	3	52.6
Straw Ethanol Organosolv Lignin	6.6	53.1	6.5	3.5	1.9	32.6
Straw Ethanol Organosolv Liquor Solids	24.4	7.2	21.4	8.3	0.6	10.5
<u>Total Mass Balance (%)</u>	<u>95.3</u>		<u>95.9</u>	<u>94.5</u>	<u>95.8</u>	

Table 5-2 Ethanol Organosolv Total, Carbon and Aromatic Carbon Mass Balances

As can be observed above consistently high accounting of mass flows during ethanol organosolv processes can be achieved with ¹³C NMR allowing the fate of aromatic carbon structures to be determined accurately with aromatic carbon accounting; total accounting of 95.3 and 95.8% of aromatic carbon are achieved for pine and wheat straw feedstocks respectively. It is also evident from the above balances that, although considerable delignification of biomass is achievable with wt% aromatic carbon content being reduced from 10.4 to 7.6% for pine and 6.3 to 5.1% for wheat straw, ethanol organosolv residues isolated during this initial study continued to contain a considerable quantity of aromatic carbon. On study of the existing literature it became evident that

this was likely due to the application of strict residue washing procedures using hot aqueous ethanol solvent immediately following the extraction process which is known to play a significant role in the prevention of lignin re-deposition on the fibrous residue surface following solubilisation (Garlock et al., 2011; Selig et al., 2007). As such all further organosolv fractionations were conducted with increased hot ethanol washing procedures.

The above balances are the first reported mass balance of streams produced using organosolv pulping techniques using ^{13}C NMR techniques. Most lignin balances involve the quantification of klason lignin determinations to trace the original lignin content of the biomass material through the fractionation process. The ability of the ^{13}C NMR aromatic carbon quantifications to accurately account for the fate of aromatic structures during organosolv delignification also confirms the capability of ^{13}C NMR techniques to provide accurate quantification of aromatic carbon content of a range of lignocellulosic samples, including those containing both high levels of aromatic carbon such as ethanol organosolv lignins and low levels in delignified samples.

In addition to the chemical changes occurring during organosolv fractionation the biomass samples also undergo physical defiberisation during the pulping process which is evidence in a general reduction in the particle size alongside shape and colour alterations.

5.2. Torrefaction

In order to understand the influence of torrefaction on the fuel properties of a range of biomass fuels pine woodchips, mixed softwood pellets, wheat straw pellets and corn stover pellets have been subjected to torrefaction as described in Chapter 3. An

overview of the respective mass yields obtained during torrefaction with differing reactor temperatures are shown below in Table 5-3.

Sample	Torrefaction Temperature (°C)	Mass Yield of Torrefied Material (wt% daf)	Mass Loss Between Torrefaction Conditions (wt% daf)
Pine Woodchips	Raw	100	
	240	81.6	18.4
	260	74.9	6.7
	280	67.8	7.1
Wheat Straw Pellets	Raw	100	
	240	74.2	25.9
	260	68.3	5.9
	280	46.2	22.1
Corn Stover Pellets	Raw	100	
	240	76.8	23.2
	260	58.2	18.6
	280	42.8	15.4
Mixed Softwood Pellets	Raw	100	
	240	80.2	19.8
	260	72.0	8.2
	280	61.3	10.7

Table 5-3 Torrefaction Mass Yields

As observed and fully anticipated, the mass yield of torrefied material decreased with increased torrefaction temperature given the increased severity of the thermal treatment which gives rise to more widespread decomposition of lignocellulosic material and thus greater mass loss during torrefaction. An assessment of the mass loss differences between the differing torrefaction temperatures utilised as shown above reveals that the highest difference in mass loss during torrefaction is experienced in the transition between the raw sample and that torrefied at 240°C (ranging from 18.4 and 25.85 wt% loss). This shows that even modest heating of the biomass to 240°C consistently gives rise to relatively high mass losses due to the decomposition of the most labile fractions of the lignocellulosic matrix which includes the most reactive components of hemicellulose structures present. Increasing the torrefaction temperature further enable the breakdown of more thermally stable components within the fuel and provide increased mass loss of the sample.

A plot of the difference in mass loss between each torrefaction condition (Figure 5-5) shows clearly that the mass loss in transition from raw fuel to that torrefied at 240°C is consistently higher than those for transition from torrefaction at 240 to 260°C and 260 to 280°C. All samples with the exception of corn stover pellets show a minimum in the mass loss differences between torrefaction at 240 and 260°C followed by an increase in the mass loss difference from 260 to 280°C. It is believed that this minima occurs because torrefaction at 240°C is able to produce significant decomposition of both reactive hemicellulose structures and labile aliphatic lignin side groups which gives rise to the high mass losses observed, further heating to 260°C is able only to induce more complete destruction of the hemicellulose content without inducing any significant decomposition in the more thermally stable cellulose fibres. The increase in mass loss induced in moving from torrefaction temperatures of 260 to 280°C is most likely a consequence of the initial reaction of cellulose components alongside the recalcitrant core xylan chains of hemicellulose known to decompose at higher temperatures than labile hemicellulose or lignin side groups.

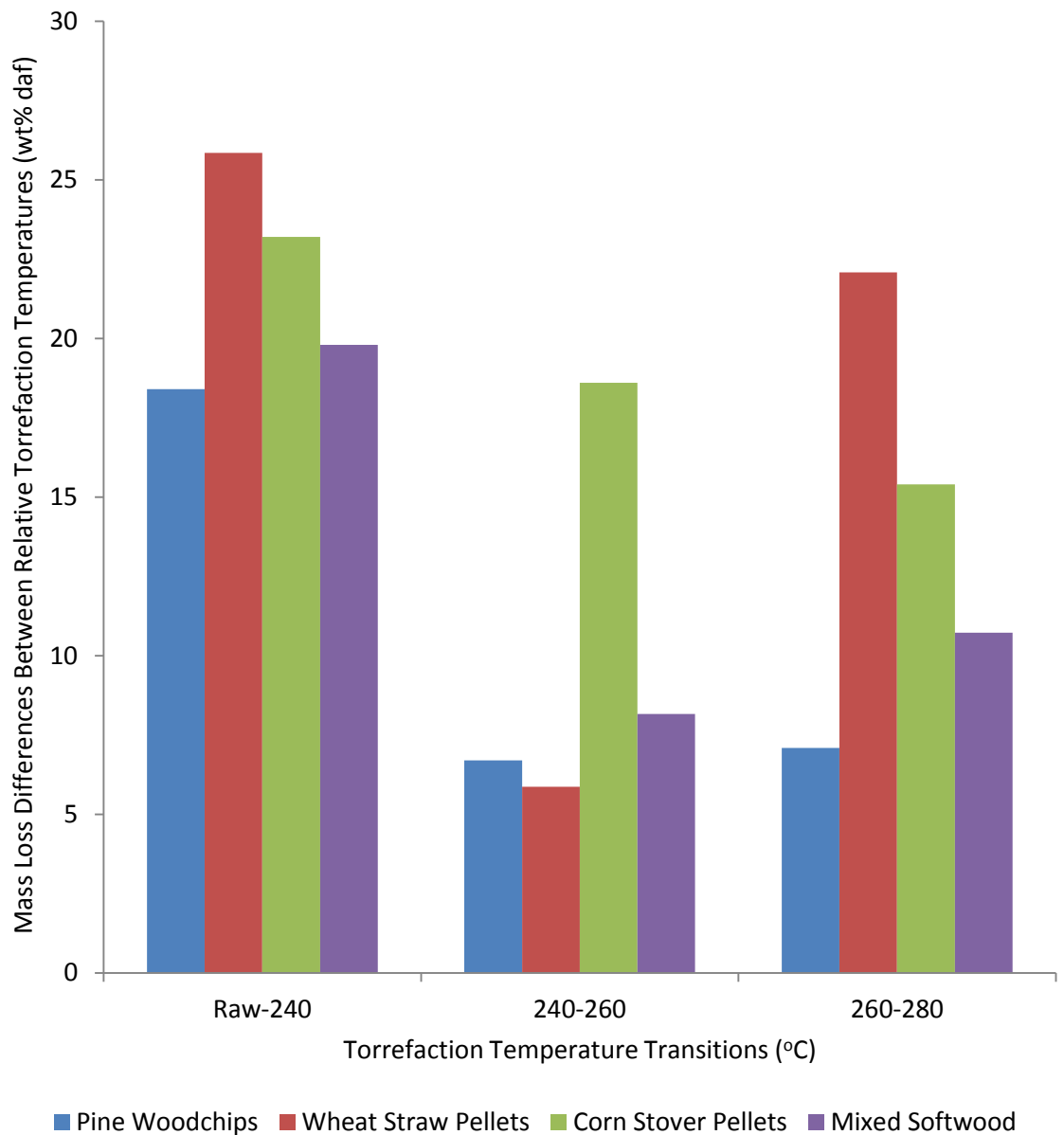


Figure 5-5 Torrefaction Temperature Mass loss Differences

Although the above is true of pine woodchips, wheat straw pellets and mixed softwood pellets; corn stover pellets show a more linear, decreasing trend in the differences in mass loss with increasing torrefaction temperature. This is accompanied by most dramatic total mass reductions during torrefaction. There are a number of potential reasons for this, the first being the appreciable quantity of alkali and alkaline earth mineral species present within the corn stover pellets. These metals are known to have

a dramatic influence upon the temperature at which each of the lignocellulosic pseudo-components decompose during pyrolysis reactions and may have considerably altered the mass loss behaviour of the corn stover pellets. Wheat straw pellets also contain appreciable K and Ca contents but show no linearity in mass loss. This theory is supported by the fact that the difference in mass loss for each fuel between torrefaction at 240 and 260°C correlates with the wt% K+Ca content, the higher the content of these alkali/alkaline earth metal the higher the mass loss difference between torrefaction at 240 and 260°C in the order corn stover > wheat straw > mixed softwood ≈ pine woodchips. Herbaceous biomass such as wheat straw and corn stover are also known to contain increased levels of hemicellulose in comparison to the woody species utilised and this too may have contributed to the relative mass loss profiles observed during torrefaction.

In order to characterise the effect of torrefaction on the structural composition of the biomass fuels and most importantly the content of aromatic carbon ¹³C NMR was conducted to provide a quantification of aromatic carbon content and an analysis of the selective decomposition of aliphatic holocellulosic components during the torrefaction process, stacked ¹³C NMR spectra for each fuel torrefied being presented in Figures 5-6 to 5-9.

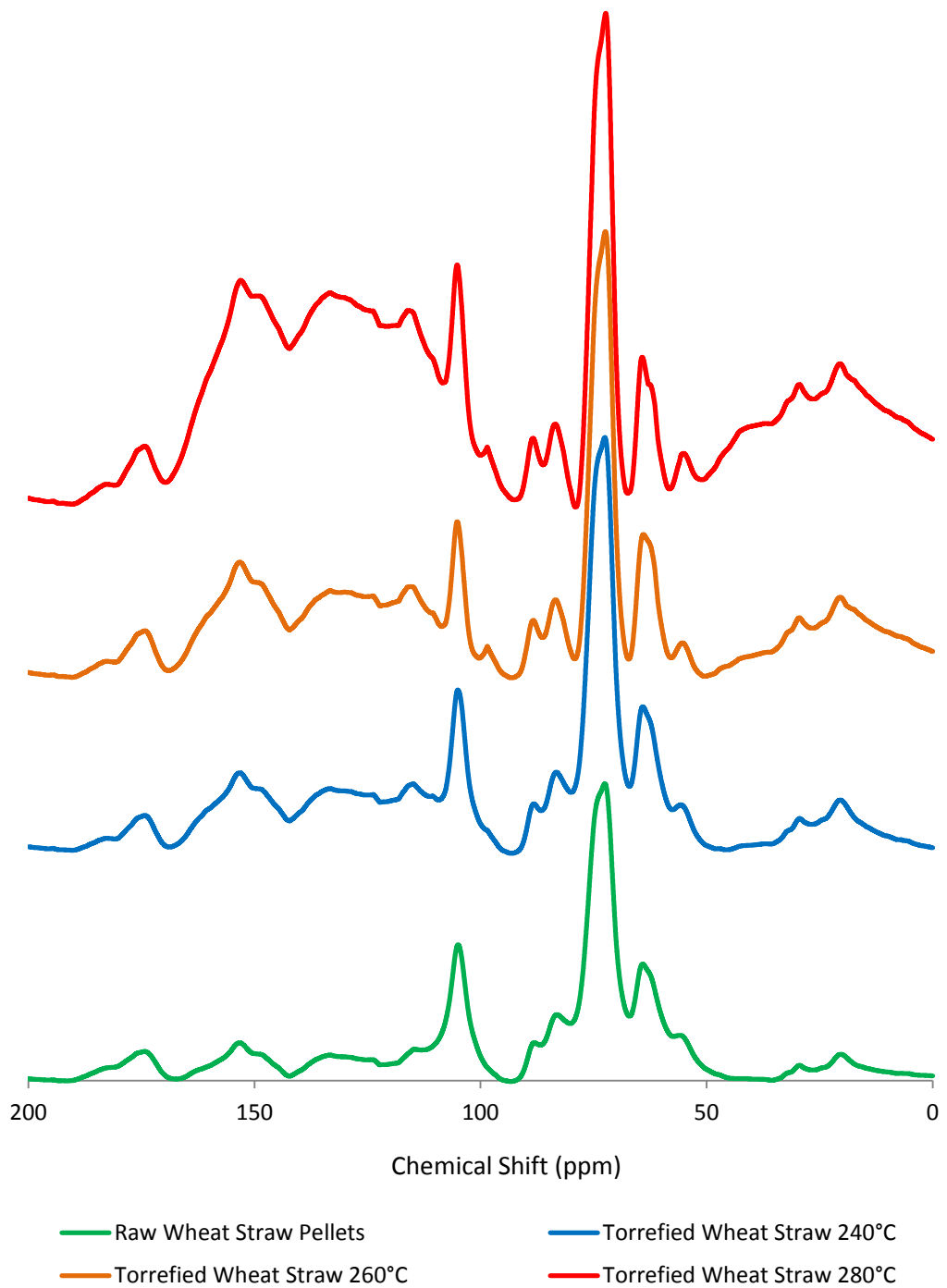


Figure 5-6 ¹³C NMR Spectra of Raw and Torrefied Wheat Straw Pellets

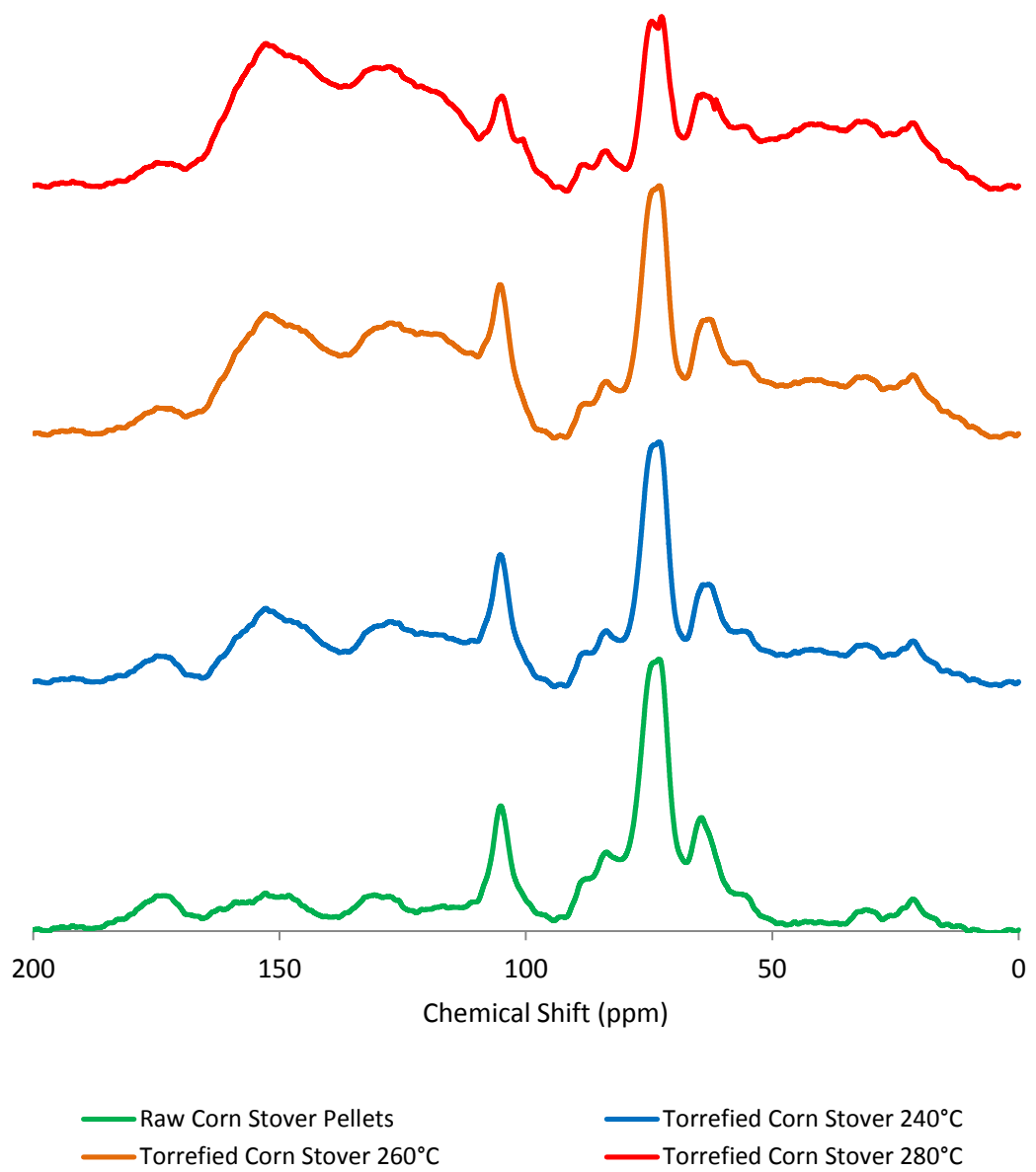


Figure 5-7 ¹³C NMR Spectra of Raw and Corn Stover Pellets

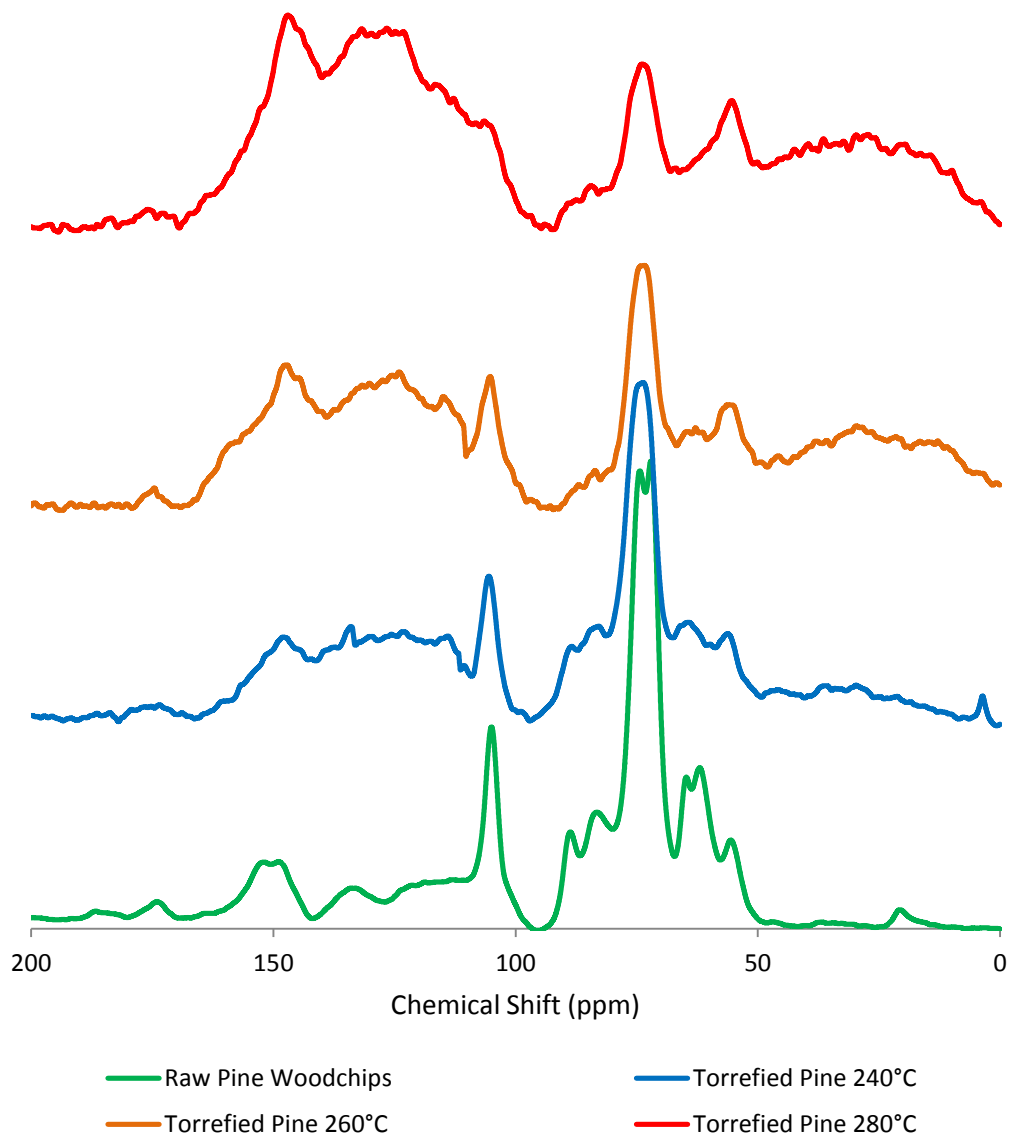


Figure 5-8 ^{13}C NMR Spectra of Raw and Torrefied Pine Woodchips

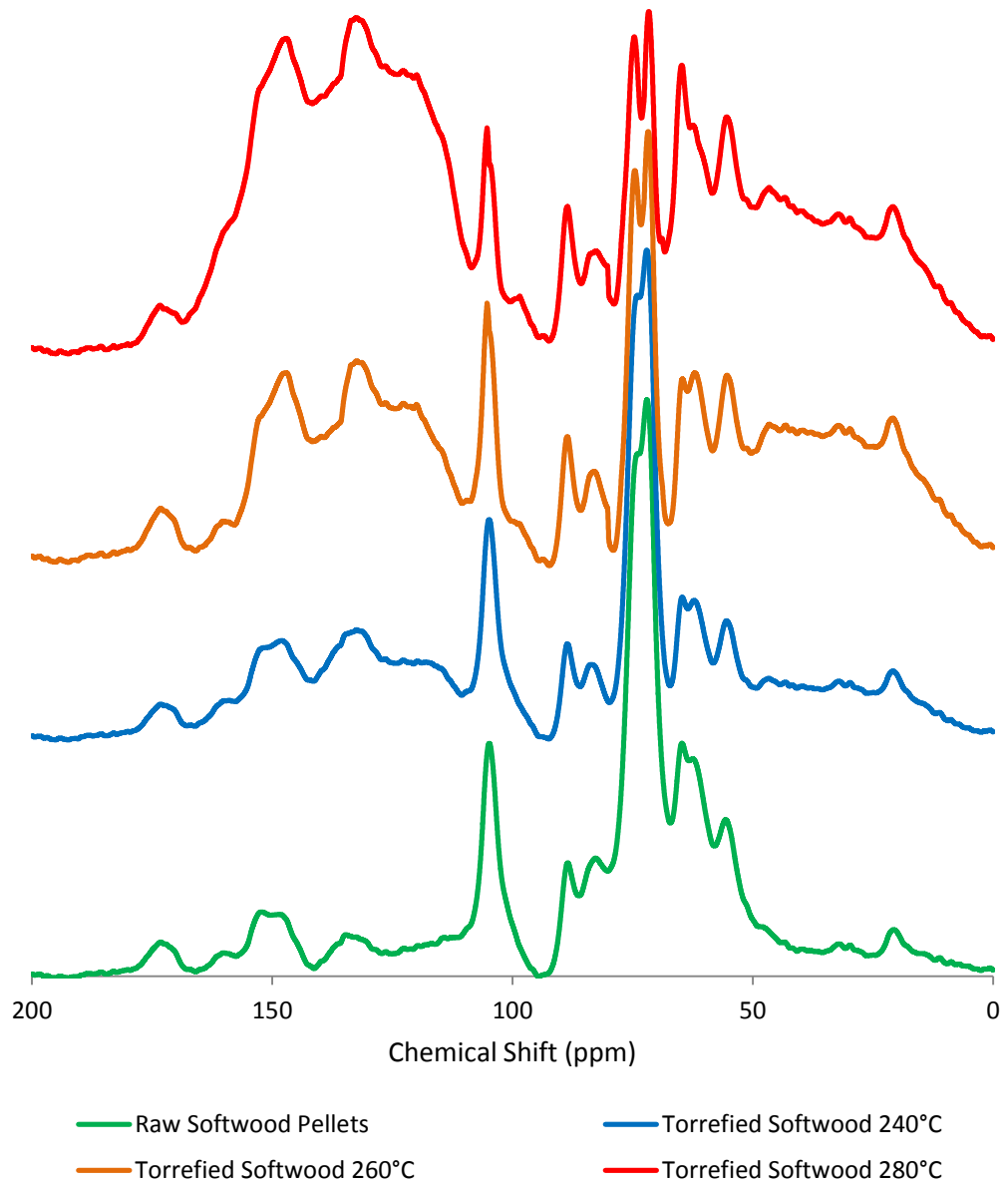


Figure 5-9 ¹³C NMR Spectra of Raw and Torrefied Mixed Softwood Pellets

A consistent pattern of conversion can be seen for all fuels undergoing torrefaction in the ^{13}C NMR spectra whereby the aromatic carbon portion of the spectra (106-170 ppm) is considerably increased with increasing torrefaction temperature. This is coupled with a decrease in the peaks corresponding to the carbohydrate content of the fuels (mostly cellulose) which occur in the chemical shift region of 60-100 ppm. These peaks become less distinguished with increasing torrefaction temperature severity, they lose their distinction and instead become merged to form a broad, undistinguished peak region at 0 – 90 ppm which corresponds to a large number of heterogeneous aliphatic carbon structures formed due to the occurrence of ring scission reactions involving the thermal decomposition of saccharidal ring structure of hemicelluloses and cellulose to form a range of aliphatic compounds.

The assignments reported above and transformation observed throughout the torrefaction process are consistent with previously published torrefaction studies utilising ^{13}C NMR (Hill et al., 2013; Melkior et al., 2012; Park et al., 2013).

Given the dramatic increases observed in aromatic carbon peaks through torrefaction, the proportion of aromatic carbon increasing with increasing torrefaction temperature, a mass balance of aromatic carbon was conducted using the aromaticity as derived using the above ^{13}C NMR spectra, the carbon content of the fuels and the torrefaction mass yields as shown in equation 5.1.

Equation 5.1

$$\% \text{ AC Mass Balance} = \frac{\left(\frac{\text{AC wt}\%}{100} \times \text{Torrefaction Mass Yield wt}\%\right)}{\text{Raw Biomass AC wt}\%} \text{ wt}\% \text{ daf}$$

Where AC wt% is the wt% daf aromatic carbon in the sample.

A table of the relative aromatic carbon contents and the total mass of aromatic carbon present within each sample is shown in Table 5-4 below.

Sample	Torrefaction Temperature	Aromatic Carbon (wt% daf)	Total Mass of Aromatic Carbon (grams)	Aromatic Carbon Mass Balance (% of original)
Pine Woodchips	Raw	13.6	13.6	100.0
	240	19.1	15.6	114.6
	260	25.9	19.4	142.6
	280	38.3	26.0	190.9
Wheat Straw Pellets	Raw	7.5	7.5	100.0
	240	14.9	11.0	147.3
	260	18.6	12.7	169.3
	280	28.9	13.4	178.0
Corn Stover Pellets	Raw	9.2	9.2	100.0
	240	16.2	12.4	135.2
	260	24	14.0	151.8
	280	32	13.7	148.9
Mixed Softwood	Raw	7.6	7.6	100.0
	240	15.7	12.6	165.7
	260	19.2	13.8	182.0
	280	29.2	17.9	235.5

Table 5-4 Aromatic Carbon Balances of Torrefaction Processes

Table 5-4 shows that the aromatic carbon content of torrefied samples increases considerably with increasing torrefaction temperature for all fuels studied. Furthermore, this increase in the aromatic content of the torrefied fuels goes beyond that anticipated due to the preferential loss of less thermally stable, non-aromatic components such that the total mass of aromatic carbon structures as quantified using ¹³C NMR is higher in all torrefied samples than that of the parent fuel, the total aromatic carbon mass increasing with increasing torrefaction temperature. The total mass of aromatic carbon was seen to increase to between 150 and 235% of the original aromatic carbon mass in the parent sample at torrefaction temperatures of 280°C regardless of the considerable mass loss occurring at this temperature. This indicates that considerable aromatisation of polysaccharidal material is occurring during the

torrefaction process to produce new aromatic carbon structures within the torrefied fuels. Although these aromatisation reactions which are thought to proceed via polycondensation have been observed in the case of cellulose pyrolysis (Agrawal, 1988; Russell et al., 1984; Wang et al., 2014; Wooten et al., 2004) their influence in torrefaction reactions and the subsequent dynamics of utilisation of torrefied material as a fuel have not yet been explored.

A plot of the aromatic carbon mass balance figure as % of original aromatic carbon against the mass loss occurring during torrefaction for each torrefaction temperature is shown in Figure 5-10.

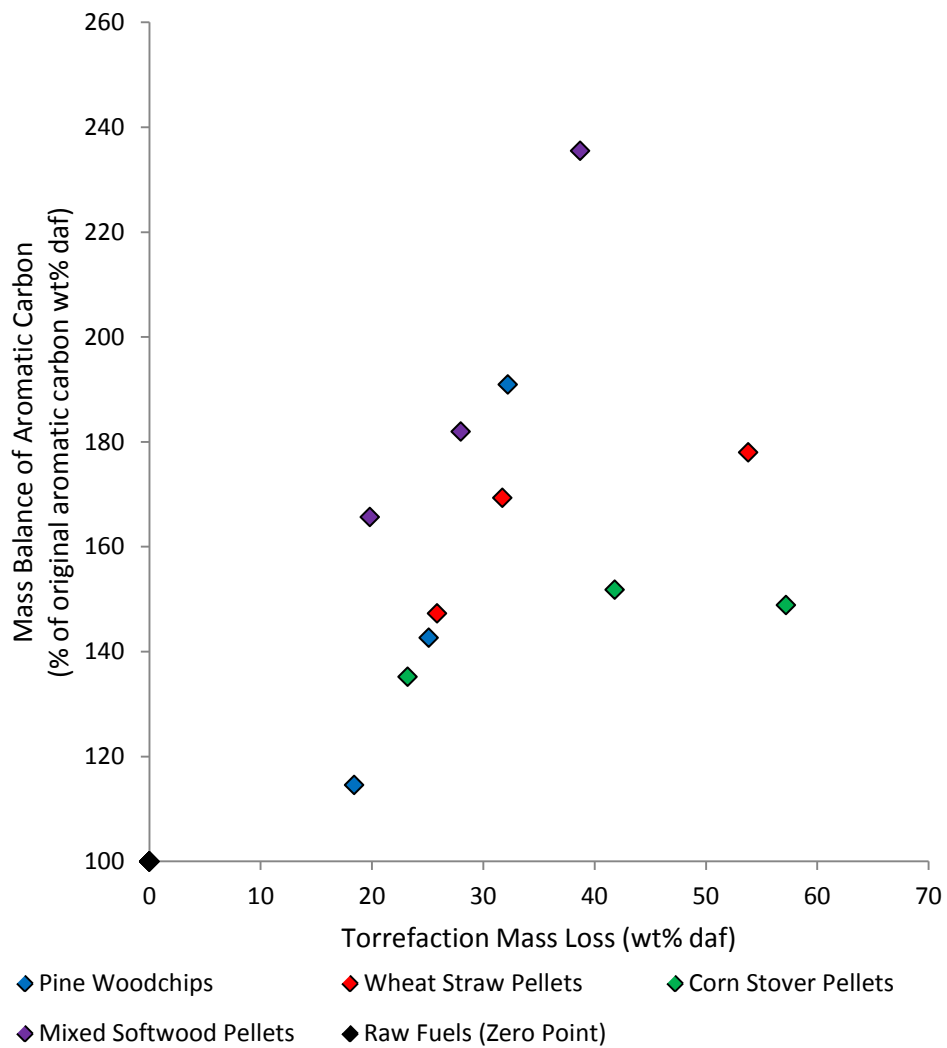


Figure 5-10 Aromatic Carbon Mass Balance vs. Torrefaction Mass Loss

A distinct increasing trend of aromatic carbon content with increasing torrefaction mass loss can be seen for all fuels. The aromatisation of woody biomass during torrefaction appears to commence with the initial mass loss of the fuel and proceeds with increase torrefaction severity. The increase in total aromatic carbon proceeds relatively linearly with loss of organic mass, the trend for both mixed softwoods and pine showing continually increasing aromatisation of torrefied fuels with increasing torrefaction temperature. Both herbaceous species also undergo linear increases in aromatic carbon availability in line with mass losses on initial heating (significant increases in total aromatic carbon mass being evidenced for both wheat straw and corn stover following torrefaction at 240°C). The increasing trend of aromatic carbon mass is less severe than for woody fuels with final aromatic carbon structures containing 150-175% of the initial aromatic carbon mass present in the raw fuel following loss of 54-57% of the daf mass of the sample. In comparison, woody fuels achieved an increase in total aromatic carbon mass between 190 and 235% of the starting mass follow the loss of only ~32-39 % daf fuel mass. In fact the increasing levels of aromatisation in torrefied herbaceous material appears to level off after 260°C especially for corn stover pellets, increasing torrefaction temperature having limited impact on increased total aromatic carbon mass after this point.

This shows that significant differences exist in both the aromatisation and organic material decomposition of woody and non-woody fuels during torrefaction which is likely due both to variations in the nature of the organic lignocellulosic matrix and the content and speciation of mineral matter compositions, which were high in AAEM mineral species in both of the herbaceous biomass tested in this case.

SEM analysis has been conducted for raw and torrefied mixed softwood pellets in order to assess the impact on torrefaction severity upon the physical nature of the fuel (Figure

5-11). On assessment of evolution of fuel structure with torrefaction degree a consistent condensation of the structure can be observed with increasing torrefaction temperature to the point that following torrefaction 280°C a fused structure appears to have been adopted which indicates some significant plasticisation of the lignocellulosic matrix has occurred. Samples torrefied at 240°C seem to take on a more disorganised, spalled outer surface, this is accompanied by some mass loss and appears to mark the commencement of hemicellulose decomposition which disrupts the physical structure of the hemicellulose rich components surrounding cellulose microfibrils. The hemicellulosic matrix surrounding the fibrous cellulose structures appears to disintegrate more completely with increasing torrefaction severity which mirrors its loss in mass, this gives rise to a smoother, more uniform appearance of the torrefied fuel as observed following torrefaction at 260 and 280°C.

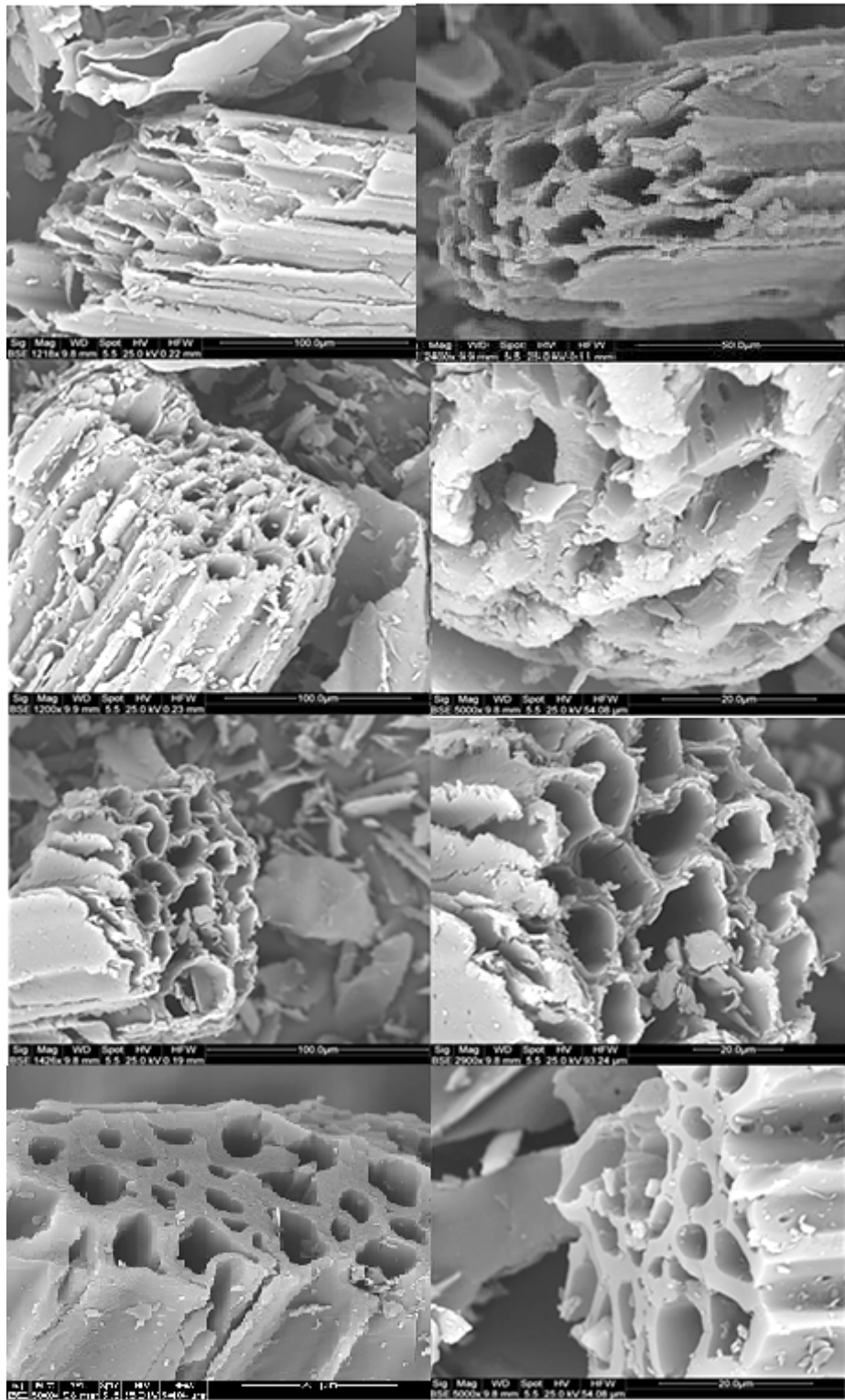


*Figure 5-11 SEM Images of Raw and Torrefied Mixed Softwood
 (From top to bottom: Raw; Torrefied 240; Torrefied 260; Torrefied 280)*

5.3. HCl Washing and Partial Demineralisation

As has been explained in Chapter 3 the demineralisation process utilised throughout this study has been significantly modified such that the HCl concentrations utilised have been lowered from in some cases as high as 5 molar to 1 molar concentration. This reduction in the concentration of HCl was adopted in order to avoid any significant degradation in the chemical structure of the primary lignocellulosic which would consequently influence their behaviour during devolatilisation and combustion trials. Initial demineralisation studies were conducted using 5 molar HCl as the primary washing medium, however considerable decolouration, de-fiberisation and loss of organic matter were observed, following which more dilute acid concentrations and reduced retention times were adopted in order to minimise any significant alteration of the core organic structure of the samples. Although both the soak times and acid concentration were reduced following initial demineralisation trial results the temperature maintained during the acid washing process was retained at 60°C throughout, any lowering of the temperature significantly reducing the efficiency of mineral removal without considerably influencing the impact on organic structure degradation.

It has been seen that the acid/water washing method utilised was able to significantly reduce the abundance of ion exchangeable mineral species in the biomass samples such that concentrations of all prevalent alkali/alkaline earth minerals (Na, K, Mg and Ca) being reduced to below 0.07 wt%, with the majority being below the limit of reliable quantification for the apparatus utilised (this being represented as <0.01). The effectiveness of these mineral extraction procedures are in line with those presented in the literature which generally utilise far higher acid concentrations. As such it can be concluded that combined washing procedures using dilute (1 molar) HCl and deionised

water are able to achieve comparable removal efficiencies of the ion exchangeable species of interest (in this alkali and alkaline earth metals) for the study of combustion behaviour.

5.4. Summary

- ▶ Accurate, complete balances of aromatic carbon content through organosolv pulping processes have been achieved using quantitative ^{13}C NMR techniques which confirm their ability to provide precise, reliable quantification of aromatic carbon contents of a range of biomass materials
- ▶ The influence of the torrefaction process at varying temperature severities on the mass yield and structural alteration of a number of biomass fuels has been investigated. ^{13}C NMR techniques have proved useful in determining the individual decomposition mechanisms occurring during torrefaction of these fuels and have shown through quantitative calculation of aromatic carbon content that considerable aromatisation of aliphatic and polysaccharidal material which gives rise to increasing aromatic character of torrefied fuels with increased torrefaction temperature. Coupling this significant aromatisation with the loss of hemicellulose structures and alteration of the physical nature of the fuel as evidence using SEM image analysis there is likely to be significant alteration of the thermochemical behaviour of torrefied fuels during both devolatilisation and char oxidation reactions occurring during the combustion process, both of which will be studied in detail in the following chapters
- ▶ The applicability of the demineralisation practices adopted throughout the study have been confirmed and their influence on both inorganic and organic phase compositions of the biomass materials utilised have been assessed. It has been shown that combined dilute HCl and deionised water washing procedures

are able to reduce the abundance of alkali/alkaline earth metals to appreciably low levels such that their influence upon combustion reactions is limited whilst minimising the influence of acid degradation on the organic structure of the biomasses, resulting in only minor concentration of total incombustible ash in the demineralised material.

Chapter 6: Predication of Pyrolysis Char Yields

6.1. TGA Slow Heating Pyrolysis Char Yield

As has been described in Chapter 3 all samples have been subject to pyrolysis under slow heating rate conditions ($50\text{ }^{\circ}\text{Cmin}^{-1}$) using a thermogravimetric analyser. Table 6-1 shows the char yields obtained under slow heating on a dry ash free basis.

Sample	Slow Heating Char Yield (daf)
Wheat Straw Pellets	18.87
Delignified Wheat Straw	14.40
Wheat Straw Lignin	34.60
Corn Stover Pellets	19.50
Delignified Corn Stover	11.10
Corn Stover Lignin	33.70
Pine Woodchips	15.18
Delignified Pine Woodchips	10.80
Pine Lignin	37.90
Olive Cake Pellets	20.08
Delignified Olive Cake	15.00
Olive Cake Lignin	32.40
Miscanthus Pellets	18.40
Delignified Miscanthus	8.70
Miscanthus Lignin	34.20
Eucalyptus Pellets	16.73
Delignified Eucalyptus	7.00
Eucalyptus Lignin	37.10
Mixed Softwood Pellets	15.14
Delignified Mixed Softwood	15.60
Mixed Softwood Lignin	32.30
Torrefied Wheat Straw 240°C	26.60
Torrefied Wheat Straw 260°C	28.90
Torrefied Wheat Straw 280°C	35.91
Torrefied Corn Stover 240°C	27.80
Torrefied Corn Stover 260°C	32.63
Torrefied Corn Stover 280°C	41.32
Torrefied Pine 240°C	19.01
Torrefied Pine 260°C	24.37
Torrefied Pine 280°C	37.83
Torrefied Mixed Softwood 240°C	24.70
Torrefied Mixed Softwood 260°C	30.26
Torrefied Mixed Softwood 280°C	37.73
Steam Explosion Mixed Woods	24.24
Demineralised Wheat Straw Pellets	13.97
Demineralised Delignified Wheat Straw	9.00
Demineralise Corn Stover Pellets	9.60
Demineralised Delignified Corn Stover	4.98
Demineralised Pine Woodchips	12.10
Demineralised Delignified Pine Woodchips	5.67
Demineralised Miscanthus Pellets	14.50
Demineralised Delignified Miscanthus	9.40
Demineralised Eucalyptus Pellets	12.67
Demineralised Delignified Eucalyptus	8.30
Demineralised Mixed Softwood Pellets	7.50
Demineralised Delignified Mixed Softwood	6.57
Demineralised Steam Explosion Mixed Wood	20.98

Table 6-1 Char Yields under TGA Slow Heating Pyrolysis

In order to evaluate any correlations existing between chemical and physical composition and slow heating char yield plots of char yield (wt% daf) vs. K+Ca content (wt% db), H:C atomic ratio, O:C atomic ratio and aromatic carbon content (wt% daf) are presented in Figures 6-1 – 6-4.

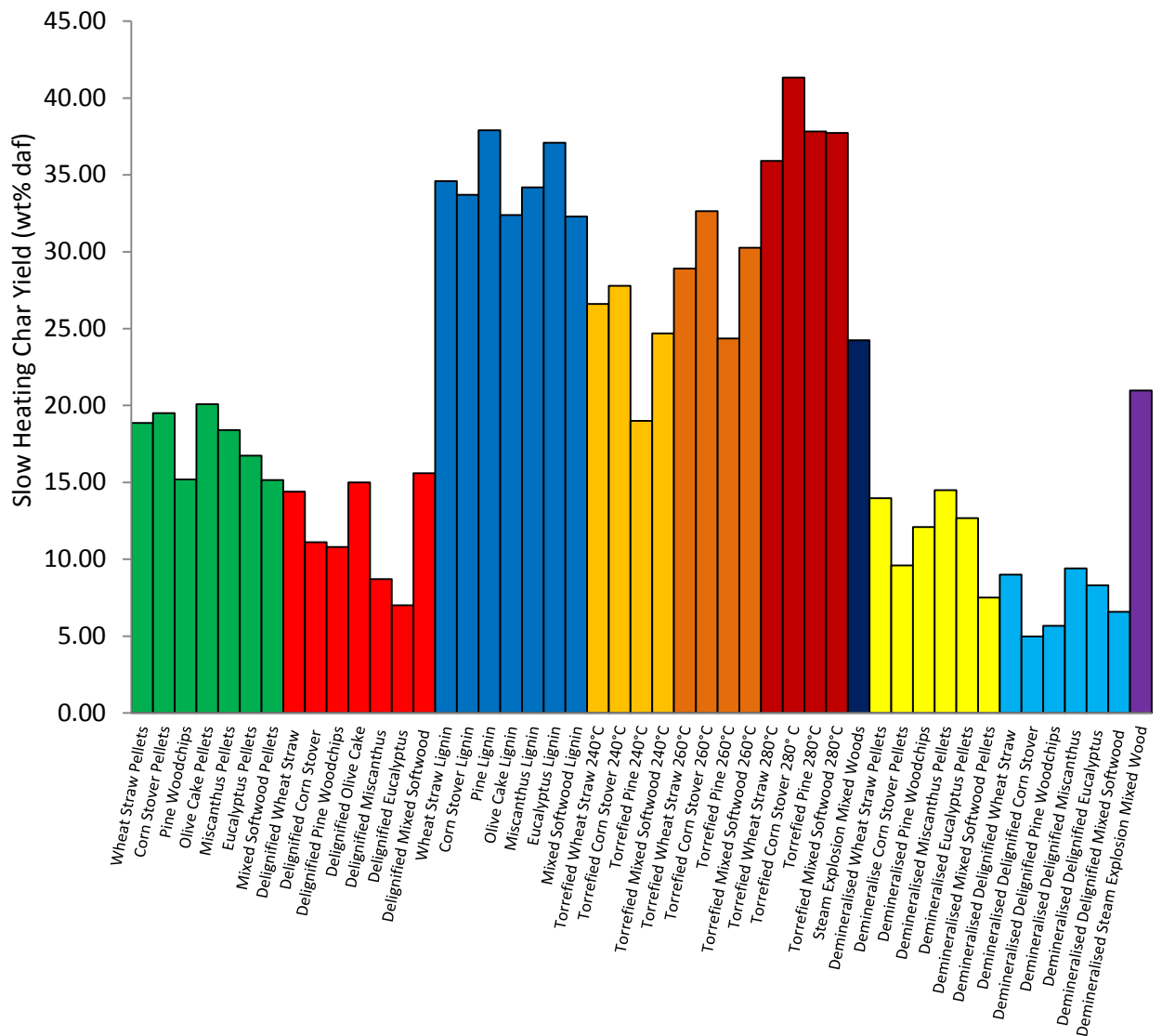


Figure 6-1 Column Plot of Slow Heating Pyrolysis Char Yields

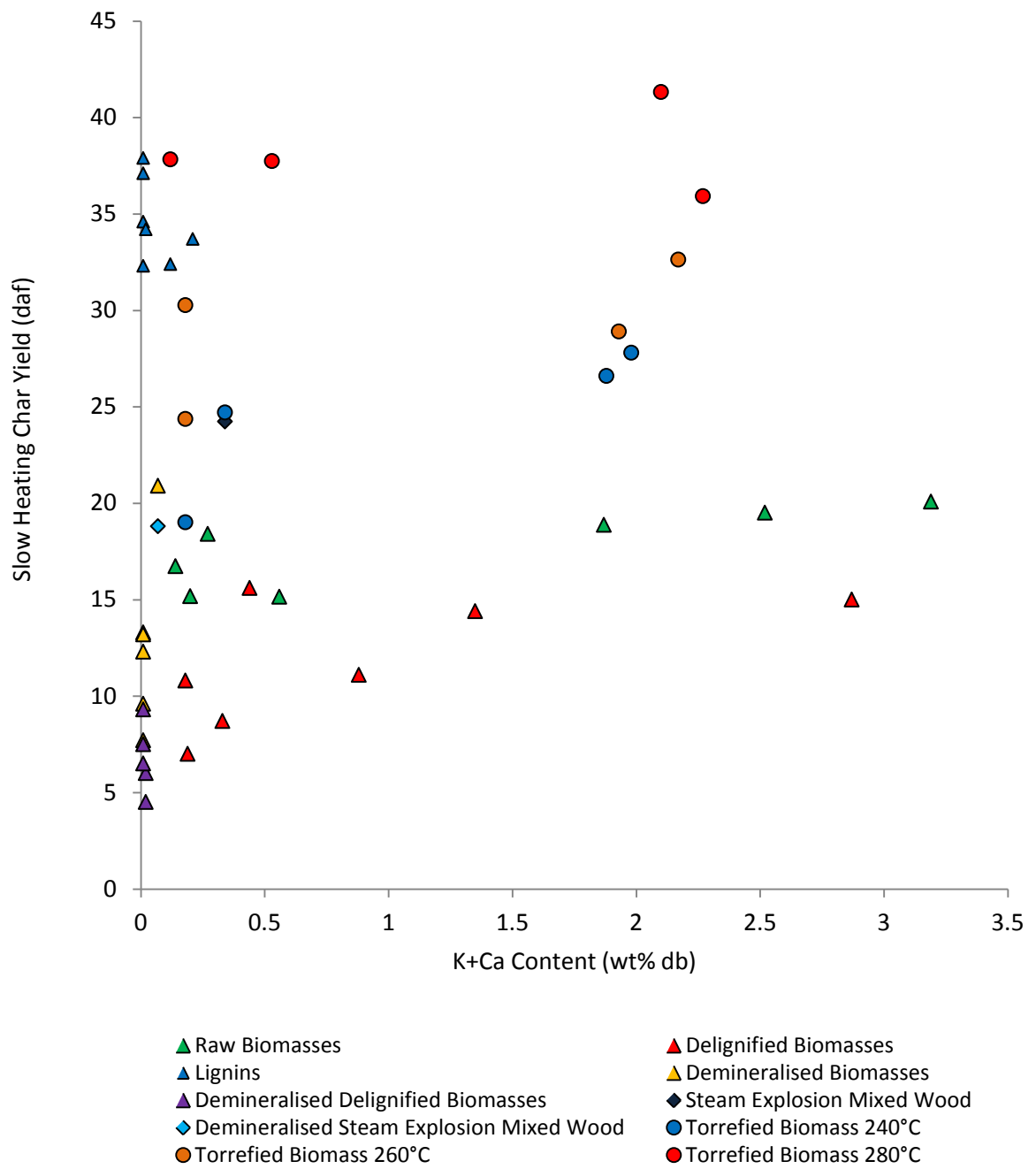


Figure 6-2 Slow Heating Pyrolysis Char Yield vs. K+Ca Content

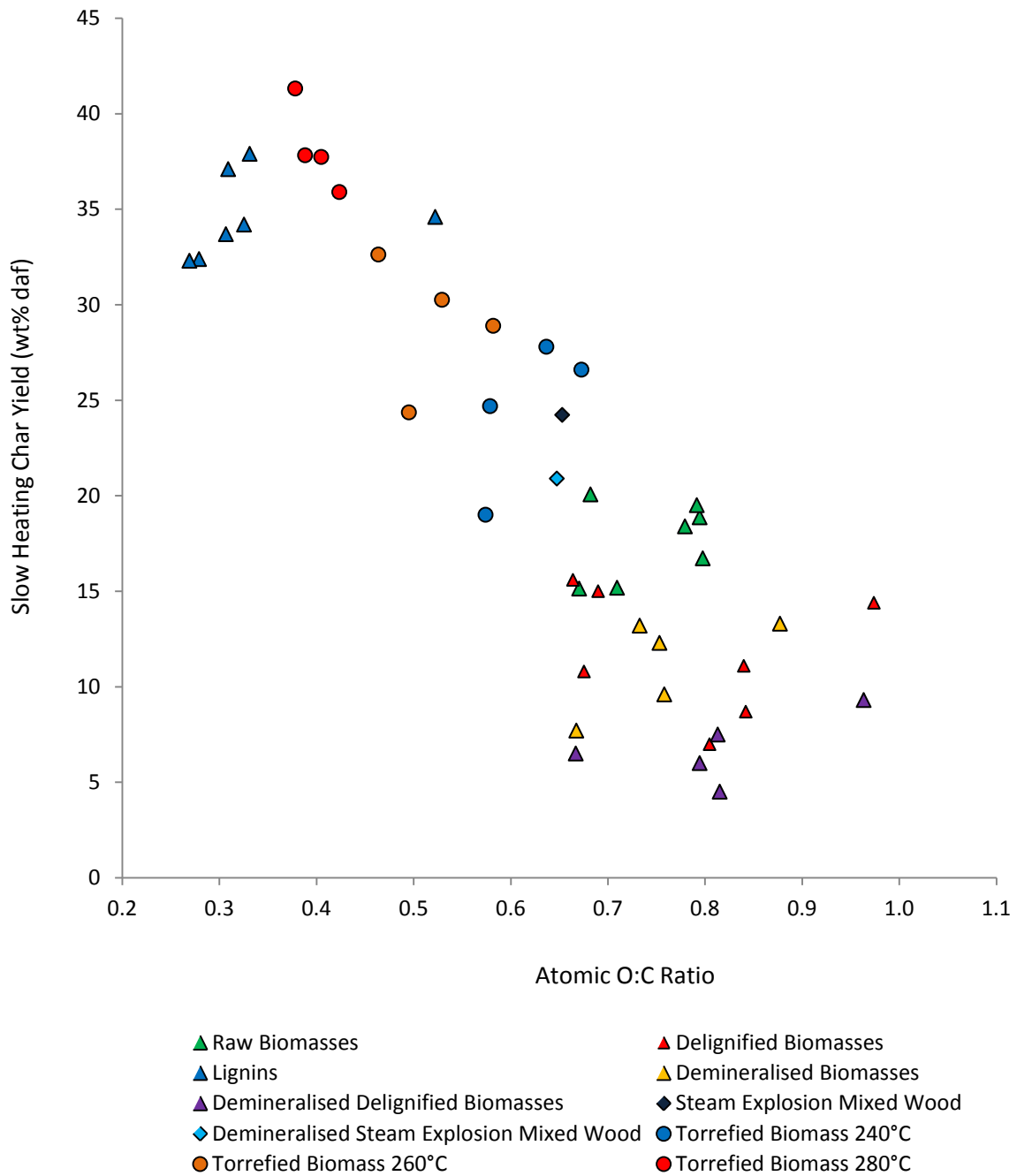


Figure 6-3 Slow Heating Pyrolysis Char Yield vs. Atomic O:C Ratio

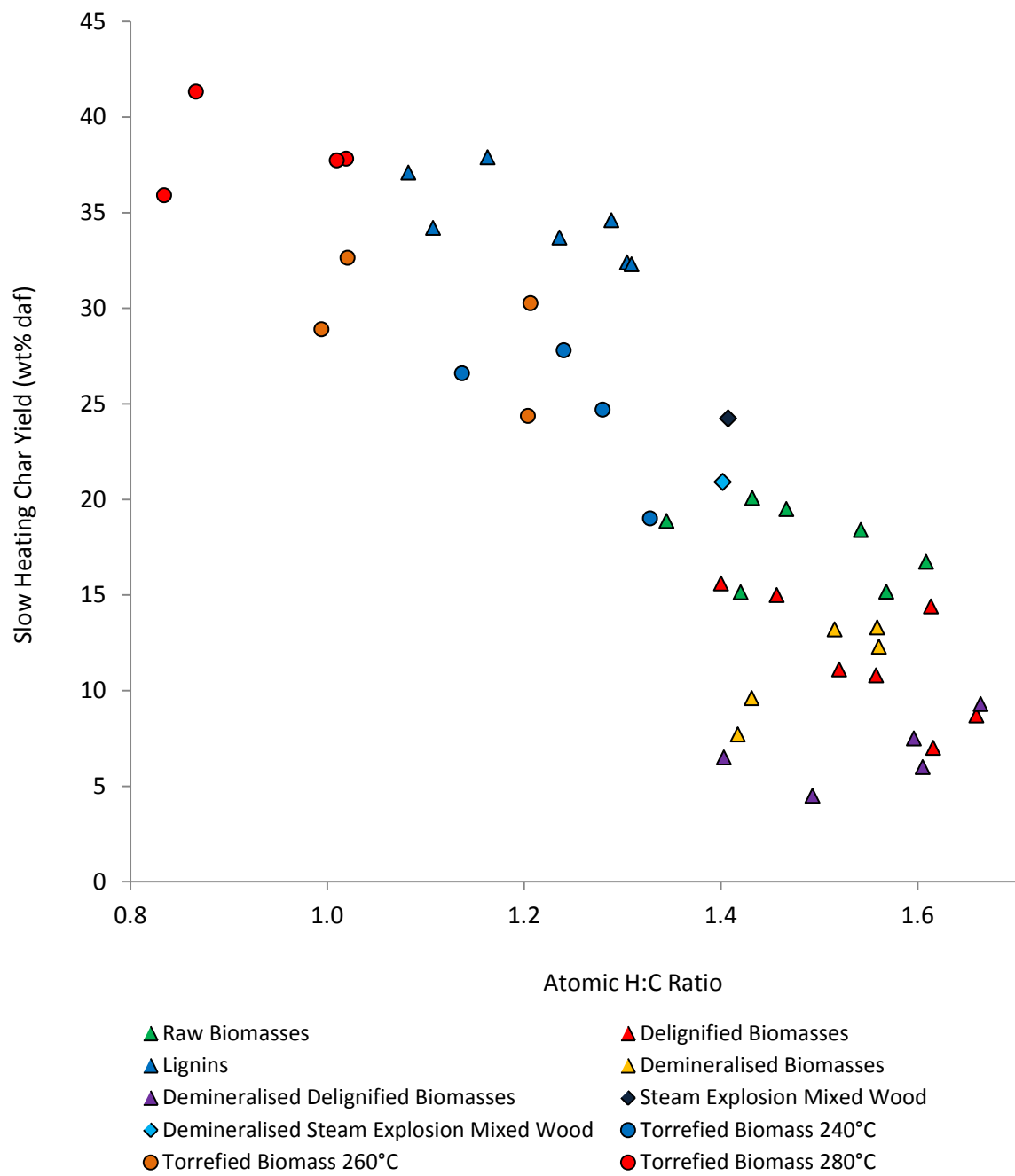


Figure 6-4 Slow Heating Pyrolysis Char Yield vs. Atomic H:C Ratio

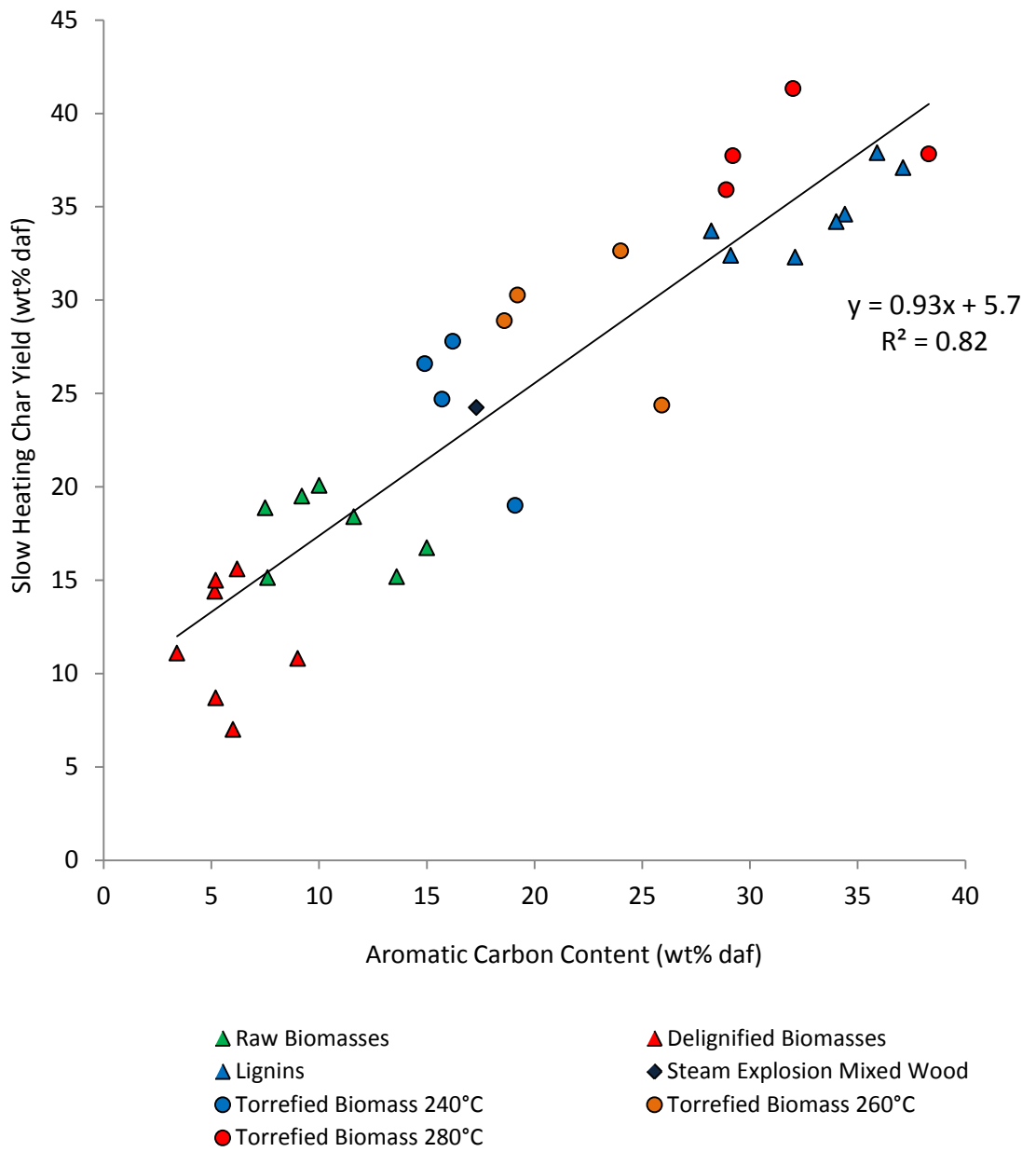


Figure 6-5 Slow Heating Pyrolysis Char Yield vs. Aromatic Carbon Content for all Non-Demineralised Biomasses

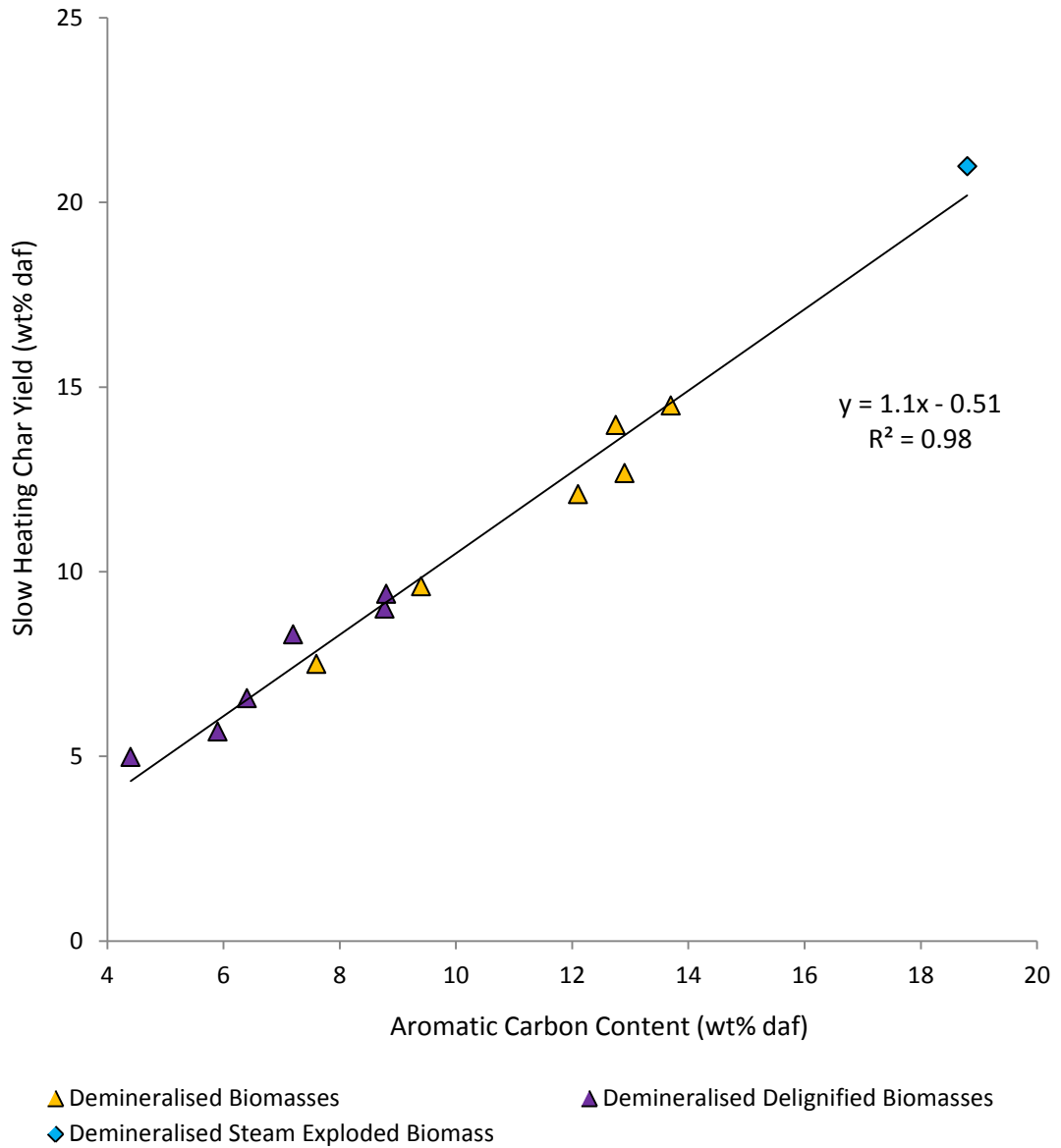


Figure 6-6 Slow Heating Char Yield vs. Aromatic Carbon Content for all Demineralised Biomasses

A general increase in slow pyrolysis char yield can be observed within each group of fuels tested in Figure 6-1 with increasing content of K+Ca mineral components. This increase is thought to be due to the enhancement of cross linking char formation reactions brought about by participation of alkali/alkaline earth metal carboxylic acid salts. Although the trend is noticeable the increases in char yield are less significant than anticipated given the generally accepted role played by AAEMs in increasing biomass pyrolysis char yields considerably. The reduction in the observed severity of AAEM enhanced char formation is thought to be due to the negatively correlated relationship existing between aromatic carbon content and AAEM concentration as evidenced by Fahmi et al., 2007 who observed an association relating lignin and total metal content of a range of biomass fuels. This relationship gives rise to reduced levels of thermally stable aromatic carbon structures present within those biomasses, typically herbaceous species, which contain considerable quantities of these minerals (namely corn stover, olive cake and wheat straw pellets whose aromatic carbon contents range between 7.5 and 10 wt%).

All data points to the extreme left hand side of Figure 5-1 are associated with very low mineral matter content fuels, being predominantly those which have undergone ash removal during processing either through organosolv delignification or HCl partial demineralisation. Although the influence of AAEM metal concentration on char yield have largely been removed there continues to be significant variation in the char yield obtained. Char yields for demineralised biomass fuels and demineralised delignified analogues fall in the range of 7.7 – 13.3% wt% daf and 6.5 – 9.3 wt% daf respectively. This variability in the absence of mineral matter influences is thought to be due to the varying lignin content of the varying samples following organosolv delignification. Lignin samples, which likewise contain very low AAEM contents following isolation exhibit char yields of 32 – 38 wt% daf due to their enhanced aromatic carbon content.

Plotting the observed char yield figures against both atomic O:C and H:C ratios provides insight into the influence of both elemental chemical composition and the degree of structural condensation of the fuel on char yield (see Figures 5-2 and 5-3). As expected the char yield appears to decrease with increasing O:C and H:C ratios as the level of sample aromaticity declines. Although this is true there is considerable scatter of the results at any given characteristic ratio due to mineral matter influences and heterogeneity of the fuels. The results obtained for char yield vs. atomic O:C ratio appear to be more orderly than those for H:C ratios with the char yield for individual sample groups being more clearly defined due to the considerable overlap in H:C ratios between different samples groups. Neither relationship appears to be linear in nature for all samples with most significant deviations being observed for high H:C and O:C ratio fuels which have been acid demineralised (demineralised biomass and demineralised delignified biomass) which exhibit lower char yields than anticipated by linear correlation with atomic ratios. This is again most likely due to the removal of mineral species which influence pyrolytic char yield.

Plotting slow heating char yield for all non-demineralised samples directly against aromatic carbon wt% daf as determined using ^{13}C NMR and elemental composition (Figure 5-5) provides a closer linear relationship with clearly defined char yields for individual sample groups. This clearly indicates the important role played by thermally stable aromatic carbon constituents; however, considerable scatter still exists within the relationship which precludes the accurate determination of char yield from aromatic carbon content directly (R^2 of 0.82 being achieved). It is postulated that the observed scatter is due to differing contents and speciation of mineral species active in encouragement of char formation reactions. As such a corresponding plot of slow heating char yield vs. aromatic carbon wt% has been produced using only those samples having undergone partial demineralisation via HCl and deionised water washing

procedures (Figure 5-6). A strong linear correlation of aromatic carbon and slow heating pyrolysis char contents can be seen with R^2 correlation coefficient of 0.98 (far in excess of that for non-demineralised samples) following removal of active mineral species (especially AAEMs). Although the relationship derived here appears to be close to 1:1 (1.0:1.1) with a given mass of aromatic carbon giving rise to a corresponding quantity of char during pyrolysis this is unlikely to be the case given the well documented evidence which indicates that both cellulose and hemicellulose structures undergo aromatisation during charring reactions to give rise to an appreciable quantity of char following pyrolysis (Wooten et al., 2004; Raveendran et al., 1995). Nevertheless, the observed correlation of char yield and aromatic carbon character clearly demonstrates the importance of biomass aromaticity (and thus lignin content) on char formation in the absence of mineral interactions.

This finding also supports a number of studies which indicate that mineral enhanced charring of biomass components during pyrolysis reactions mostly acts within the polysaccharidal component of the biomass (DeGroot and Shafizadeh, 1984) being especially active in hemicellulose char formation reactions due to the prevalence of glucuronic acids.

Having established the underlying influence of aromatic carbon content on biomass char yields and assuming that this relationship holds across all non-demineralised samples a theoretical value for additional char yield due to the action of mineral matter components can be derived by subtracting the char yield assumed to be formed from the aromatic carbon component (in this case taken as 1 gram of char per gram of aromatic carbon assuming no pyrolytic conversion of aromatic structures under the current slow heating regime) from the total experimentally observed char yield for the sample. It is not in this case possible to merely subtract the char yield of demineralised

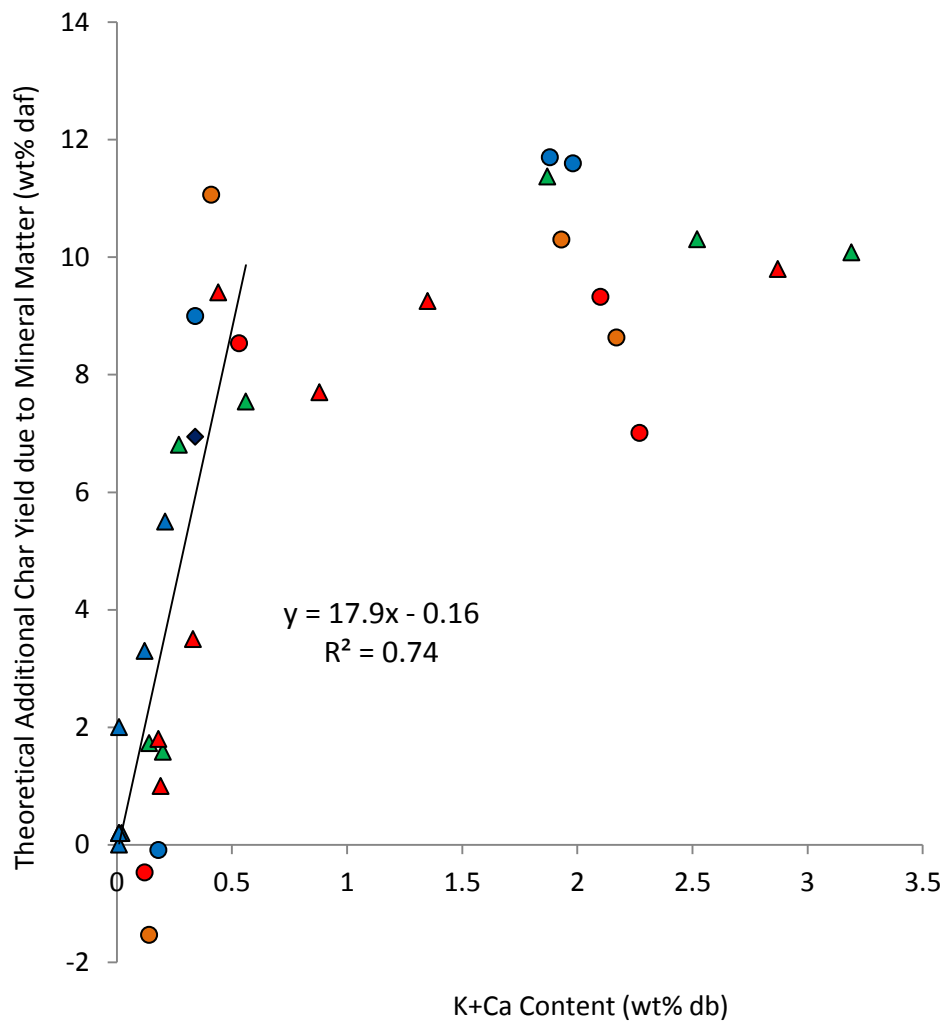
samples from those of non-demineralised analogues due to the modification of organic chemical structure which accompanies the removal of mineral matter during acid washing, which has been shown to commonly remove a portion of the holocellulosic content of the samples (especially herbaceous biomasses) due to the severity of the HCl washing process (See Chapter 4).

As has been observed previously in Chapter 4, the most abundant alkali/alkaline earth minerals observed across the range of biomass utilised were K and Ca, with contents of up to 2.52 and 1.77 wt% db respectively. This is in contrast to Na and Mg whose measured content were below 0.06 and 0.37 wt% db only. Given this reduced abundance and the close relationship between Mg, K and Ca contents K and Ca were selected as the key components for further investigation.

A table and plot of theoretical additional char yield vs. K+Ca content can be seen in Table 6-3 and Figure 6-7 in which a rapid, relatively linear initial increase in the additional char yield is observed with increasing K+Ca concentrations. This trend continues until ~0.6 wt% K+Ca is reached, after which there is a broad plateau and increased spread in the calculated additional char yield. Although considerable variation in the additional char yield is seen above 0.6 wt% db K+Ca content; the average enhancement of charring corresponds to an additional char yield of 9.76 wt% daf. The levelling off of the influence of increasing AAEM content on char yield is thought to be due either to the limiting of charring reactions at low metal concentration or due to the varying dispersion of alkali metals in the fuel. It is possible that at low (in this case <0.6 wt% db) K+Ca concentrations, charring of non-aromatic components is limited by the lack of inorganic alkali and alkaline earth metals available. Beyond 0.6 wt% K+Ca charring reactions of aliphatic carbons are no longer constrained by the availability of these metals and are most likely limited by the number of active sites able to

accommodate the action of mineral species. Once all active sites within the biomass matrix become saturated due to the sufficient availability of K and Ca (above 0.6 wt%), any addition of these elements has a minimal additional effect on the char yield.

Conversely the reduction in AAEM enhanced charring at higher metal loadings may be due to the variation in their dispersion with increasing concentration. At low AAEM contents the metals are more likely dispersed fairly widely within the fuel in intimate contact with the organic, combustible components of the fuel. As the metal concentration increases the size of mineral clusters are likely to increase and thus limit their dispersion within the fuel, negatively influencing the observed activity of the metals unable to make effective contact with the organic fuel components during pyrolysis. Good dispersion of active metal species either intrinsic to fuel or added as a catalytic additive has been shown to enhance their influence during pyrolysis significantly (Sutton et al., 2001), however, knowledge of the direct influence of alkali metal dispersion on biomass char yields is limited.



- ▲ Raw Biomasses
- Torrefied Biomass 240°C
- ◆ Steam Exploded Mixed Wood
- ▲ Delignified Biomasses
- Torrefied Biomass 260°C
- ▲ Lignins
- Torrefied Biomass 280°C

Figure 6-7 Theoretical Additional Char Yield under Slow Heating vs. K+Ca Content for Non-demineralised Biomass

Sample	Theoretical Additional Slow Heating Char Yield (wt% daf)
Wheat Straw Pellets	11.4
Delignified Wheat Straw	9.3
Corn Stover Pellets	10.3
Delignified Corn Stover	7.7
Pine Woodchips	1.6
Delignified Pine Woodchips	1.8
Olive Cake Pellets	10.1
Delignified Olive Cake	9.8
Miscanthus Pellets	6.8
Delignified Miscanthus	3.5
Eucalyptus Pellets	1.7
Delignified Eucalyptus	1.0
Mixed Softwood Pellets	7.5
Delignified Mixed Softwood	9.4
Torrefied Wheat Straw 240°C	11.7
Torrefied Wheat Straw 260°C	10.3
Torrefied Wheat Straw 280°C	7.0
Torrefied Corn Stover 240°C	11.6
Torrefied Corn Stover 260°C	8.6
Torrefied Corn Stover 280°C	9.3
Torrefied Pine 240°C	-0.1
Torrefied Pine 260°C	-1.5
Torrefied Pine 280°C	-0.5
Torrefied Mixed Softwood 240°C	9.0
Torrefied Mixed Softwood 260°C	11.1
Torrefied Mixed Softwood 280°C	8.5
Steam Explosion Mixed Woods	6.9

Table 6-3 Theoretical Slow Heating Additional Char Yield due to Mineral Matter Influence

These findings support previous work (Agblevor et al., 1995) which has observed similar activity for a range of grass species during fluidised bed pyrolysis whereby initial increases in char yield with increasing K+Ca content are rapid and relatively linear, any further addition of these minerals above a certain level (in this case being ~2% K+Ca db) has little further impact on the char yield. The differences in the relation of AAEM content and char yield between this study and the results presented here are likely due to the nature of the heating regimes employed – the study in question utilised prompt heating in a fluidised bed at 700°C whereas the results presented above use only slow heating (50 °Cmin⁻¹), the pyrolysis conditions and results of this study are thus more closely represented by prompt, rapid heating pyrolysis experiments conducted in the entrained flow DTF and discussed in detail later in this chapter. Similar results are also

reported by Fahmi et al., 2007 in a study of the char formation of range of both washed and unwashed grass species which revealed a similar, rapidly increasing trend in char yield with increasing K+Na content at low concentrations with a subsequent plateau in this increase following a certain concentration point. Although the point of plateau in this study was somewhat lower than that observed in the work presented (being just below 0.5 wt%) the influence of Ca content on the char forming reactions was neglected in favour of that for Na, as previously iterated, Na has been largely ignored in this study due to its relatively low abundance in the bulk of the fuel analysed.

A decrease in the char yield enhancement due to AAEM induced reactions can be observed for high AAEM containing torrefied fuels with increases in the torrefaction temperature utilised. This may again be due to the fact that mineral enhanced charring is primarily thought to act via active sites associated with saccharidal material, especially hemicellulose glucuronic acid sites. As torrefaction temperature is increased greater portions of the hemicellulose structure is lost as volatile gaseous species, leaving fewer potential sites for the action of AAEM in encouraging char formation via cross linking reactions and producing a decrease in the additional char yield observed. Although it is clear in the torrefied fuels utilised here that sufficient active sites remain available to produce considerable additional charring by AAEM participation (the minimum theoretical additional char yield for samples with K+Ca contents greater than 0.6 wt% db being 7 wt% daf for wheat straw pellets torrefied at 280°C) more severe torrefaction or carbonisation of biomass may further reduce the availability of hemicellulose active sites for the action of AAEMs and thus render the chosen characterisation of char yield less effective.

Using the relation of additional char yield as a function of increasing K+Ca content defined above for the purposes of a simplified empirical calculation of the biomass char

yield it is assumed that above 0.6 wt% db K+Ca content a fixed additional char yield of 9.76 wt% daf can be applied as a quantification of the influence of enhanced char yield due to AAEM content. Below 0.6 wt% db K+Ca a linear correlation of additional char yield vs. K+Ca content is assumed alongside the assumption of equal char and aromatic carbon contents allowing a least squares regression to be conducted to select a value for the factor describing the relationship of K+Ca content with additional char yield such that the sum of the squared differences between calculated and observed char yield is minimised. Completing this process gives rise to the following empirical relationship for prediction of slow heating char yield given quantification of aromatic carbon and K+Ca contents:

Equation 6.1

$$SHCY = (1 \times \textit{Aromatic Carbon}) + (16.1 \times (K + Ca))$$

Where SHCY is the char yield obtained in wt% daf under slow heating in the TGA and below 0.6 wt% db K+Ca content, Aromatic Carbon is the aromatic carbon wt% daf and K+Ca is the wt% db of K+Ca content.

A corresponding relationship can be utilised which describes the relationship between volatile matter yield and aliphatic carbon, K+Ca content and volatile matter yield.

Equation 6.2

$$RHVM \textit{Yield} = (1 \times \textit{Aliphatic Carbon}) - (16.1 \times (K + Ca))$$

A plot of the calculated char yield against the observed char yield under TGA slow heating can be seen in Figure 6-8.

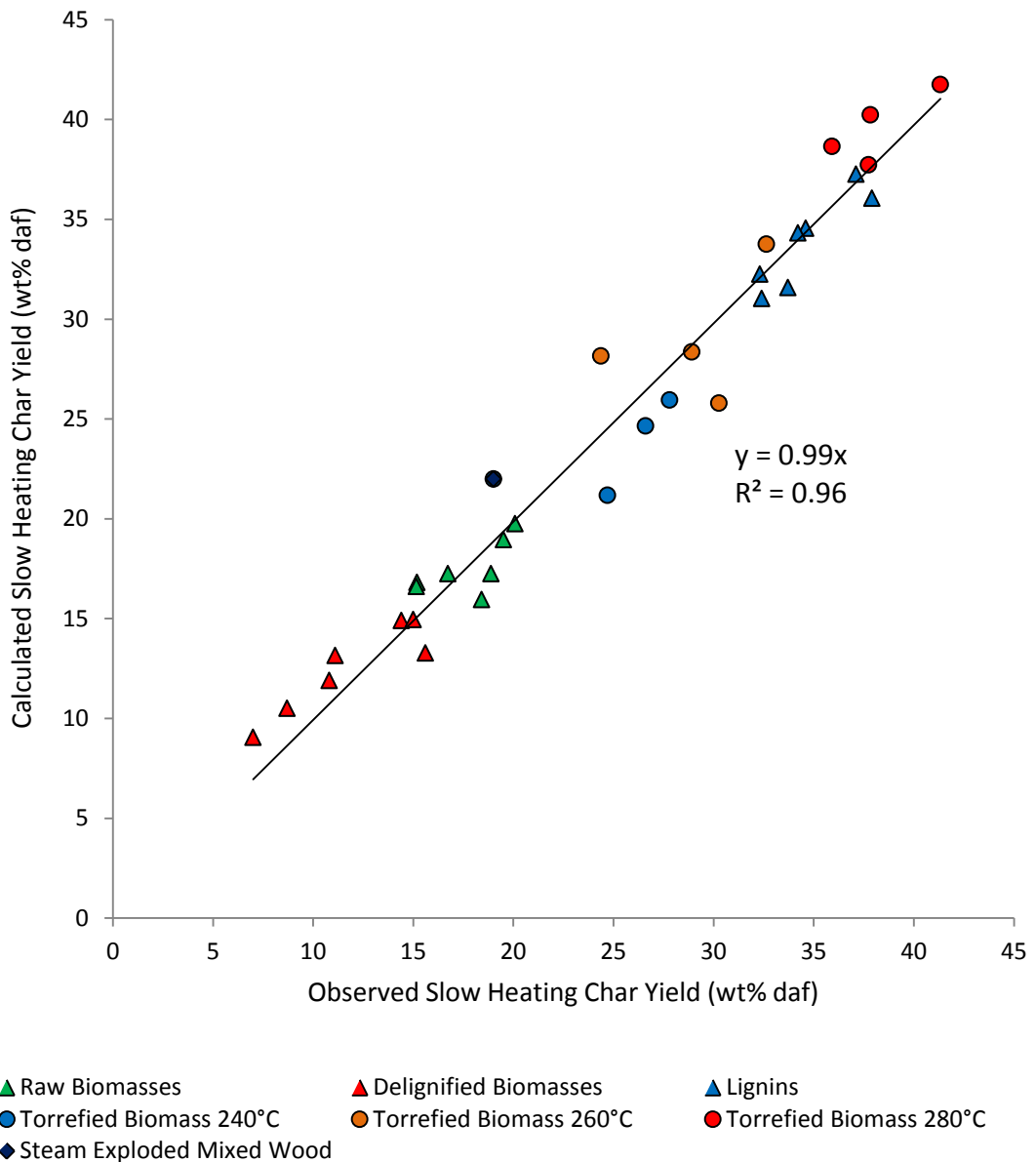


Figure 6-8 Calculated vs. Observed Slow Heating Pyrolysis Char Yield

As can be seen the correlation between calculated and observed slow heating char yields is far closer than that achievable using elemental ratio correlations, all predicted char yields falling within +5 and -4 wt% daf of the experimentally determined char yield as shown in Figure 6-9. The error of prediction as presented here appears to show no bias across the range of experimentally observed char yields and is thus equally valid for the variety of samples utilised throughout. This equates to average relative error in determination of 7.9% with a standard deviation in errors of 7%.

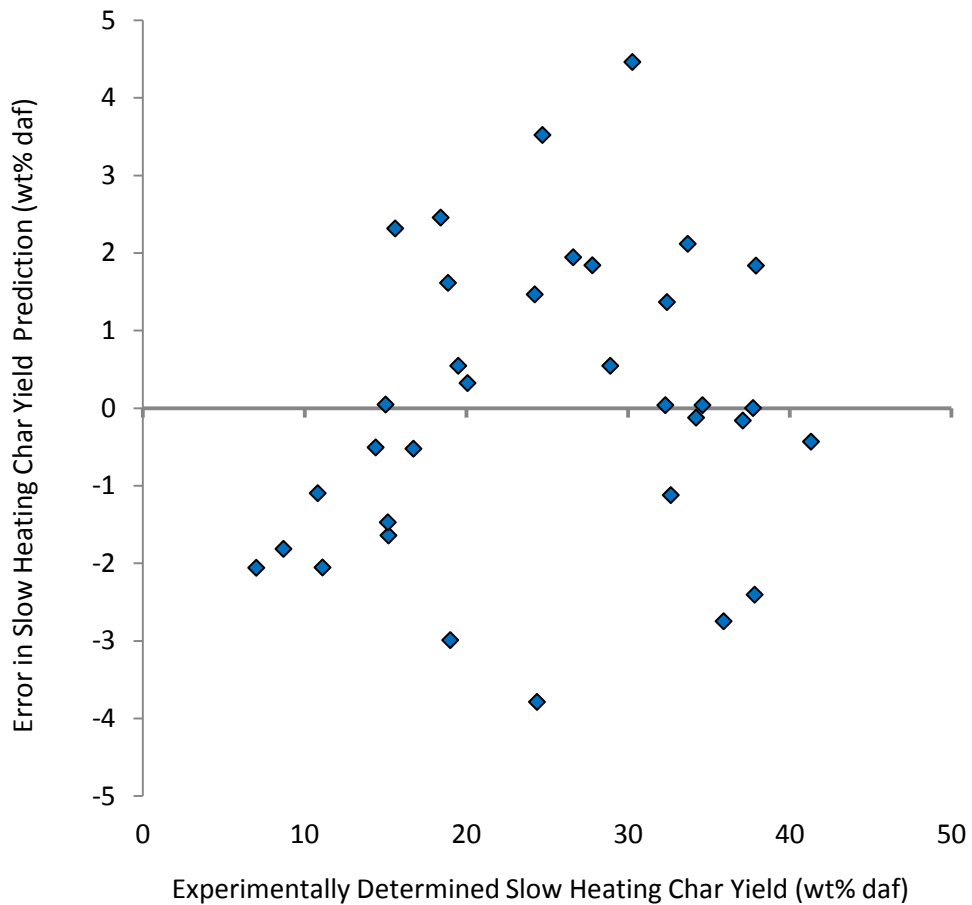


Figure 6-9 Error of Prediction for Slow Heating Pyrolysis Char Yield Calculation

6.2. DTF Rapid Heating Pyrolysis Char Yield

A similar programme of works to that conducted using TGA slow heating pyrolysis has been completed using the entrained flow drop tube furnace in an effort to assess the influence of aromatic carbon and inorganic mineral matter on char yields under conditions which mimic those experienced during very rapid heating fuel devolatilisation under pulverised fuel combustion applications.

Table 6-4 shows the DTF char yield on a dry ash free basis for all samples which is depicted as a column plot in Figure 6-10. All of the DTF char yields are considerably

lower than their TGA counterparts, this being due partly to the far higher heating rates experienced during prompt heating entrained flow pyrolysis and partly due to the higher final temperatures reached in the DTF (1300 as opposed to 850°C).

A similar trend can be observed as that recorded for slow heating pyrolysis whereby delignified and demineralised fuels producing lower char yields than raw samples, torrefaction acting to increase char yield significantly, volatile matter decreasing in line with the torrefaction temperatures employed. For raw samples the rapid heating volatile matter yields are all in excess of 90% with a maximum yield of 93.8 wt% daf being achieved for mixed softwood pellets (char yields varying in the range 6.2 – 9.9 wt% daf). Following demineralisation the char yields for non-delignified biomass are reduced to between 4.3 and 7.1 wt%. Delignified samples exhibit char yields in the range 3.9 – 6.6 wt% which is lowered further to 2 – 4.8 wt% upon demineralisation.

Trends of rapid heating char yield as a function of altering O: C and H: C ratio are presented in Figures 6-10 and 6-11.

Sample	Rapid Heating Char Yield (wt% daf)
Wheat Straw Pellets	9.7
Delignified Wheat Straw	6.6
Corn Stover Pellets	9.1
Delignified Corn Stover	4.0
Pine Woodchips	7.9
Delignified Pine Woodchips	5.6
Miscanthus Pellets	8.0
Delignified Miscanthus	4.0
Eucalyptus Pellets	9.9
Delignified Eucalyptus	3.9
Mixed Softwood Pellets	6.2
Delignified Mixed Softwood	4.5
Torrefied Wheat Straw 240°C	13.1
Torrefied Wheat Straw 260°C	15.0
Torrefied Wheat Straw 280°C	20.7
Torrefied Corn Stover 240°C	14.6
Torrefied Corn Stover 260°C	20.1
Torrefied Corn Stover 280° C	23.6
Torrefied Pine 240°C	10.8
Torrefied Pine 260°C	15.5
Torrefied Pine 280°C	22.5
Torrefied Mixed Softwood 240°C	9.2
Torrefied Mixed Softwood 260°C	12.9
Torrefied Mixed Softwood 280°C	17.2
Steam Explosion Mixed Woods	10.6
Demineralised Wheat Straw Pellets	6.3
Demineralised Delignified Wheat Straw	4.0
Demineralise Corn Stover Pellets	4.7
Demineralised Delignified Corn Stover	2.0
Demineralised Pine Woodchips	6.5
Demineralised Delignified Pine Woodchips	2.5
Demineralised Miscanthus Pellets	7.1
Demineralised Delignified Miscanthus	4.8
Demineralised Eucalyptus Pellets	4.3
Demineralised Delignified Eucalyptus	3.2
Demineralised Mixed Softwood Pellets	10.9
Demineralised Delignified Mixed Softwood	6.8
Demineralised Steam Explosion Mixed Wood	4.7

Table 6-4 Char Yields under DTF Rapid Heating Pyrolysis

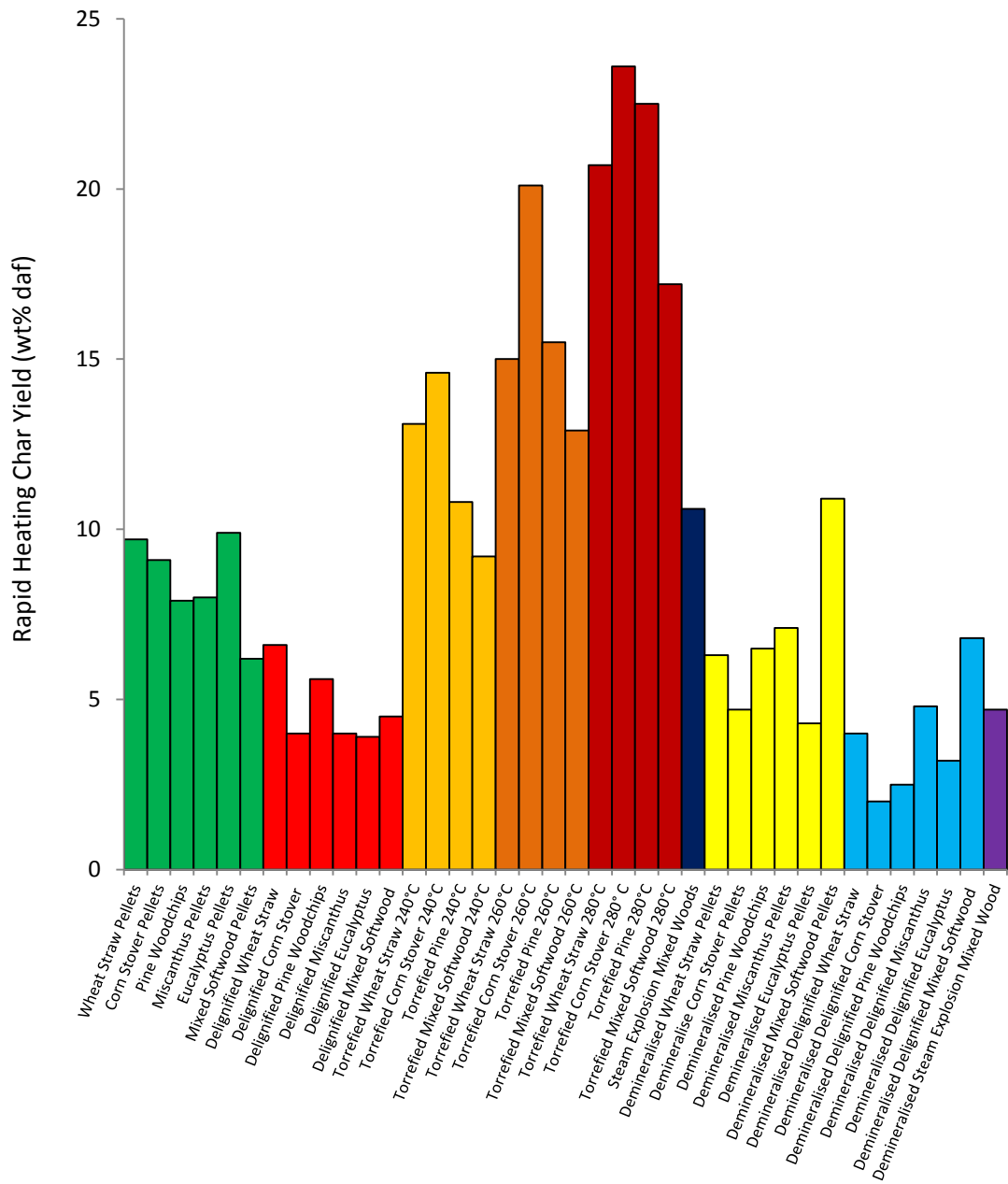


Figure 6-10 Column Plot of DTF Rapid Heating Pyrolysis Char Yields

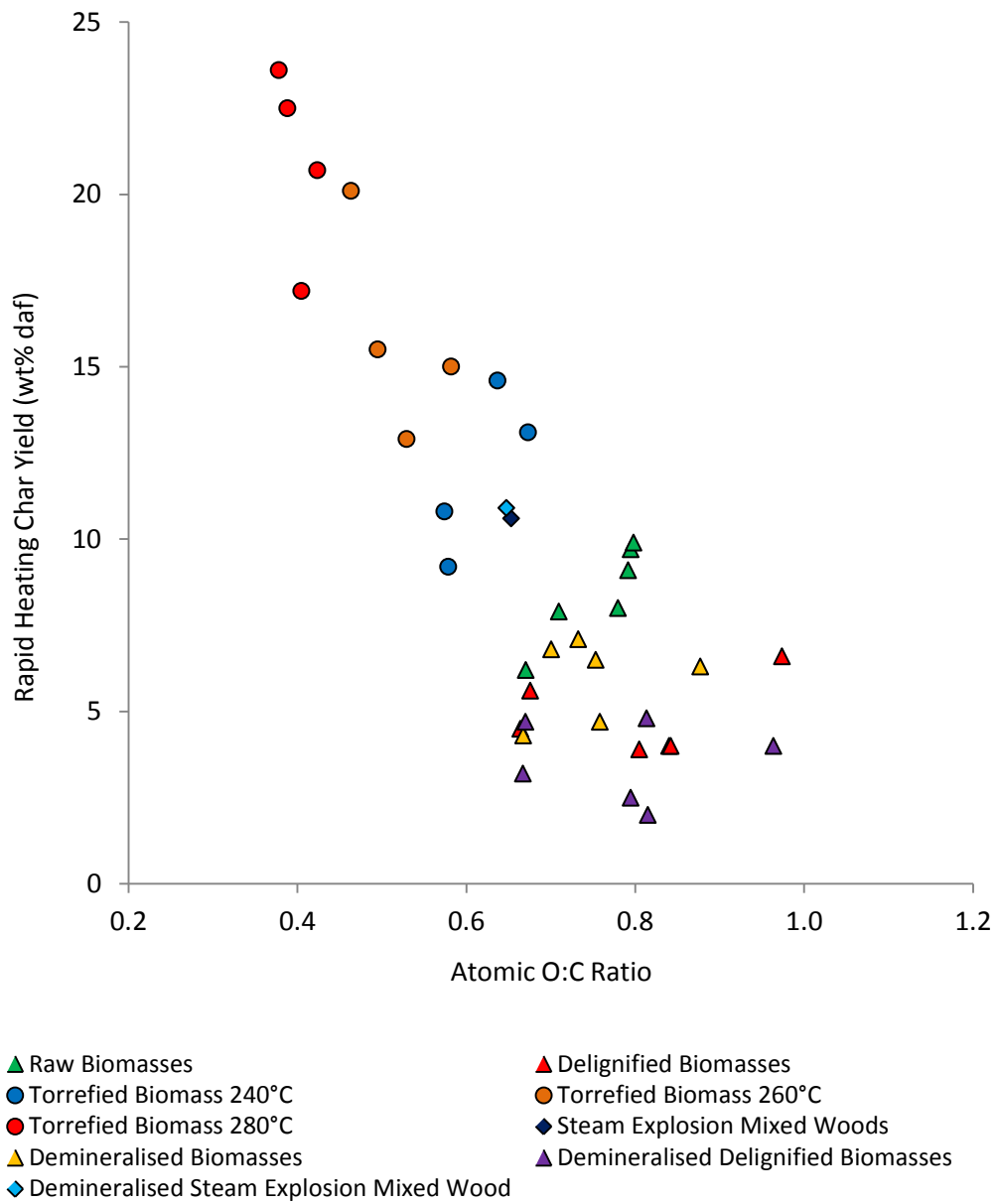


Figure 6-11 Rapid Heating Pyrolysis Char Yield vs. Atomic O:C Ratio

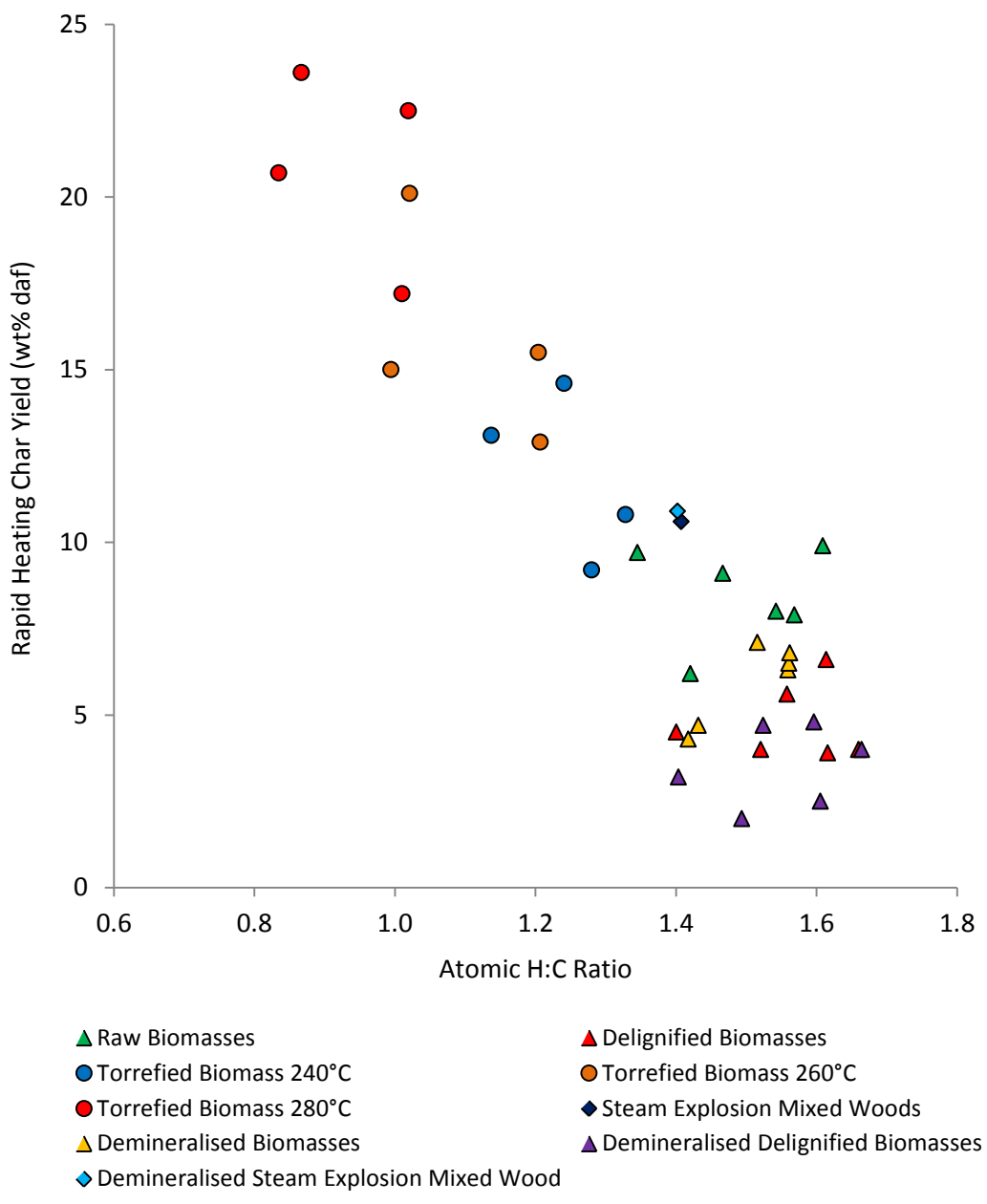


Figure 6-12 Rapid Heating Pyrolysis Char Yield vs. Atomic H:C Ratio

Similar trends are observed during rapid heating as were seen with slow heating TGA experiments with increasing carbon and decreasing H and O content leading to increases in char formation. Biomass sample groups again appear to more distinctly categorised using O:C ratio than H:C, showing considerably less scatter in the correlation. The scatter in the relation between atomic ratios and char yield appears to reduce as the carbon character increases, being much more defined for torrefied fuels than for raw and delignified samples and their demineralised analogues. However, neither correlation is thought to be consistent enough to provide the level of accuracy required in the prediction of char yield, especially for raw biomass samples which show the most significant deviation of rapid heating char yield at any given O:C or H:C ratio.

As such DTF char yields have been plotted against the aromatic carbon wt% of the samples in Figure 6-13. Although, as with the slow heating case, there is a well-defined, positive linear trend of char yield as a function of increased aromatic carbon content, considerable scatter remains in the straight line plot which provides an R^2 correlation coefficient of 0.88. This being said, the scatter in the relation of char yield and aromatic carbon for rapid heating pyrolysis is considerably reduced when compared with the slow heating case which results in an appreciable improvement in the R^2 value from 0.82. It was postulated that the reduced activity of AAEM species in promoting char cross linking reactions under rapid heating, the rapid loss of both organic and inorganic volatiles and the greater overall volatile matter yield may be the cause of the reduction in deviation from correlation of char yield with aromatic carbon content.

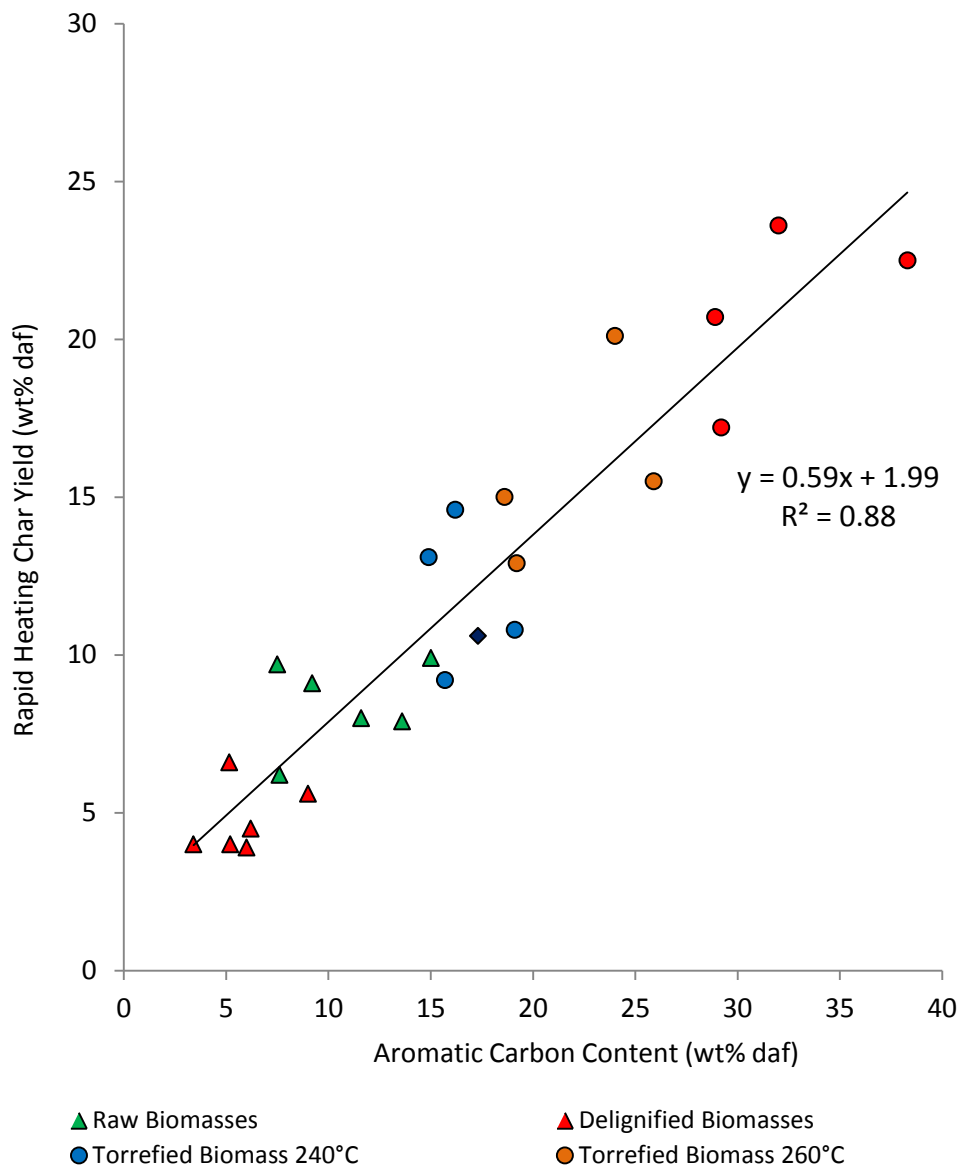


Figure 6-13 Rapid Heating Pyrolysis Char Yield vs. Aromatic Carbon Content for all Non-Demineralised Biomass

In order to consider the underlying influence of aromatic carbon on char yields, a plot of char wt% vs. aromatic carbon wt% for demineralised biomass only is presented in Figure 6-14. Again a close linear correlation ($R^2 = 0.95$) is observed with an increase in aromatic carbon wt% giving rise to a comparable rise in char yields. In contrast to TGA slow pyrolysis, the direct relationship between aromatic carbon and char content no longer holds, 1 wt% aromatic carbon giving rise to 0.58 wt% char following pyrolysis under DTF conditions. This reduction in the char yield for any given aromatic carbon wt% is again due to the severity of the rapid heating pyrolysis environment employed which is not only able to volatilise labile holocellulosic compounds and aliphatic lignin side-chains but is also able to give rise to decomposition of the thermally stable aromatic lignin core structure. This underlying formation of char due to the thermally resistant nature of aromatic components can be assumed to act similarly for all biomass samples studied as following the linear expression expressed in Figure 6-14. This allows for the definition of any increase in the char yield above this linear relationship as being the result of enhanced charring of aliphatic biomass components due to the influence of alkali and alkaline earth metal species present within the biomass. Plotting this additional char yield against the wt% K+Ca gives an indication of the magnitude of this enhancement in char production with alterations in inorganic mineral concentrations (Figure 6-15).

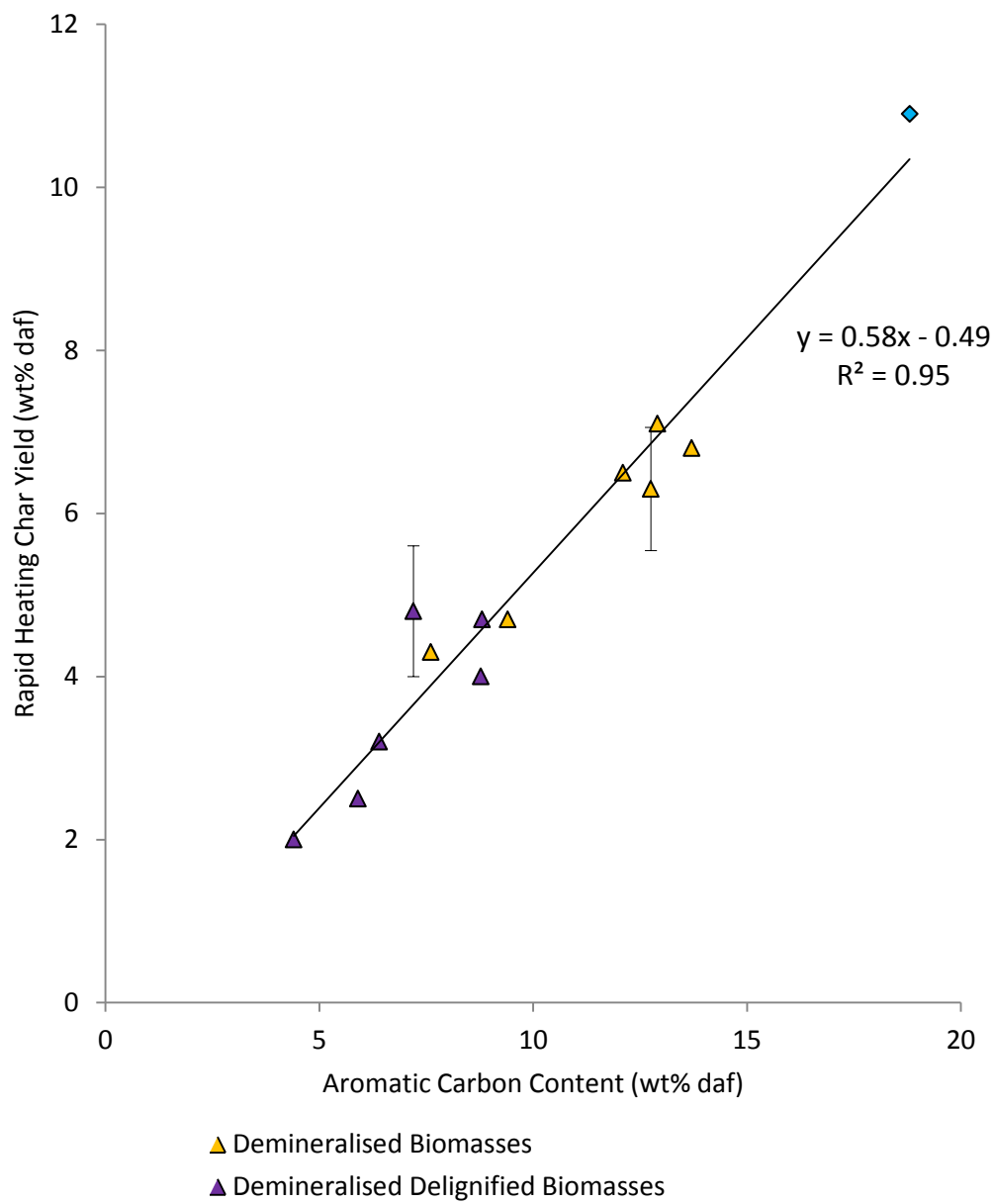


Figure 6-14 Rapid Heating Char Yield vs. Aromatic Carbon Content for all Demineralised Biomass

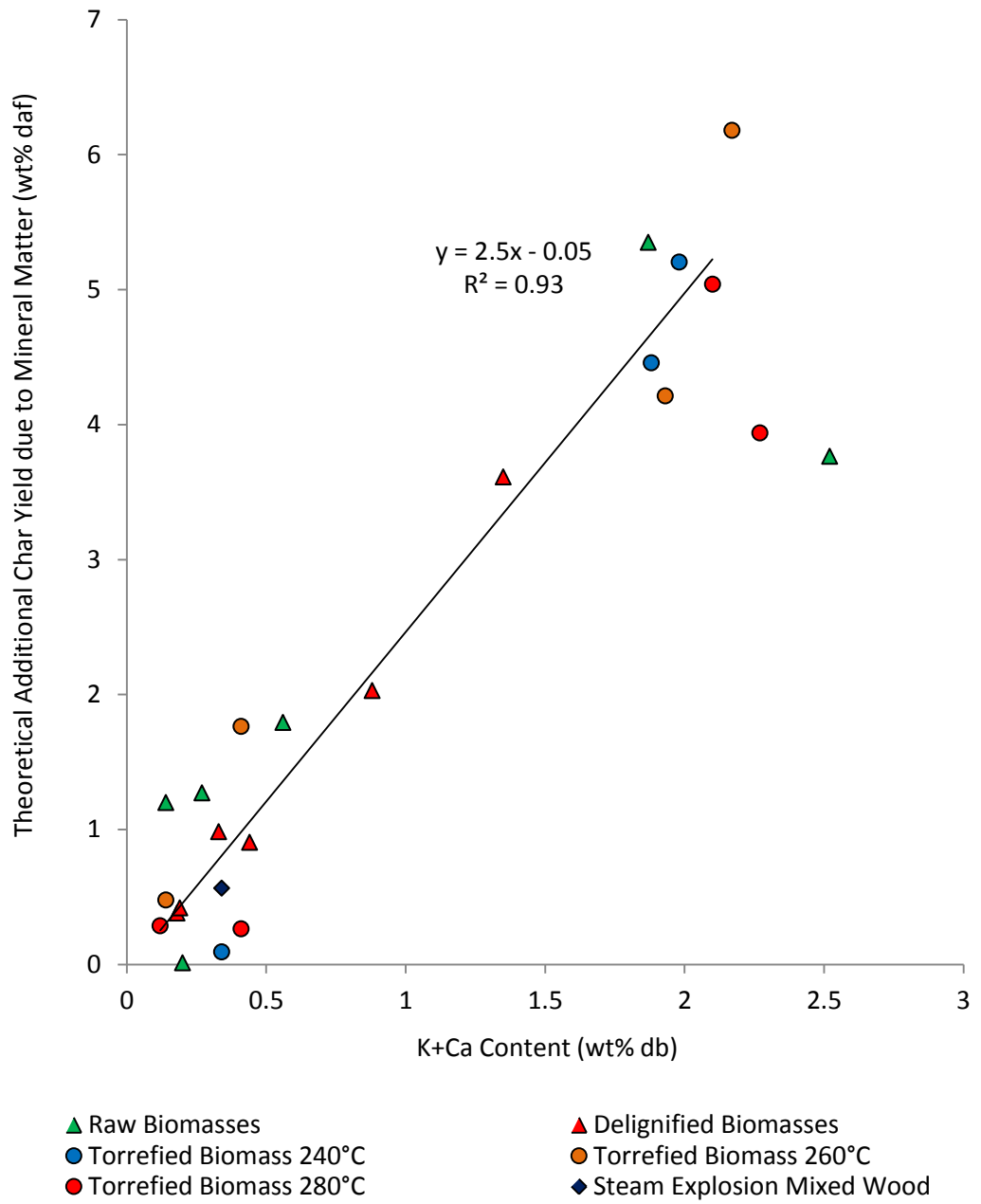


Figure 6-15 Theoretical Additional Char Yield under Rapid Heating vs. K+Ca Content for Non-demineralised Biomass

A similar trend as to that seen under slow pyrolysis TGA is seen with a rapid initial increase in additional char yield with increasing K+Ca content followed by a plateau with no further augmentation of char yield with increased mineral content beyond a certain value. Under rapid heating however, this increase is not as marked as in the slow heating case and the plateau does not appear until much higher mineral contents (~2 wt% K+Ca as opposed to ~0.6 wt% db). Furthermore, the maximum achievable additional char yield due to mineral influence is lower than observed under slow heating (~5% as opposed to ~10%). The upper boundary of this relationship appears to occur at the highest K+Ca contents tested in this study, as such there is potential for the increasing char yield enhancement with increased AAEM content to continue beyond the levels of K+Ca tested in this investigation, as such biomass of higher mineral matter content may exhibit additional char yields above those catered for in the empirical correlations proposed here. It is thought likely that the differing volatilisation of metal species under rapid heating conditions causes this observable difference between behaviour under rapid and slow heating pyrolysis. There are indications that the relationship of K+Ca content and theoretical additional char yield does plateau beyond 2 wt% K+Ca, however this is based predominantly on the behaviour of torrefied wheat straw and corn stover fuels which are undergoing preferential loss of hemicellulose components known to accommodate the action of AAEM in enhancing char yields (Agblevor et al., 1995).

Although there are differences between slow and rapid heating cases, an empirical relationship for char yield can still be derived by least squares regression assuming an underlying, fixed relationship between aromatic carbon and char wt% and by applying a linear increase in the additional char yield due to the influence of mineral matter to a certain concentration (2 wt% db K+Ca) above which a fixed average additional char content (4.77 wt% daf) can be applied (Equation 6.3):

Equation 6.3

$$RHCY = (0.58 \times \text{Aromatic Carbon}) + (2.43 \times (K + Ca))$$

Where RHCY is the char yield obtained in wt% daf under rapid heating in the DTF below 2 wt% db K+Ca content, Aromatic Carbon is the aromatic carbon wt% daf and K+Ca is the wt% db of K+Ca content.

A corresponding relationship exists correlating the biomass aliphatic carbon and mineral matter content with volatile matter yields as outlined in Equation 6-4 below:

Equation 6-4

$$RHVM \text{ Yield} = (0.42 \times \text{Aliphatic Carbon}) - (2.43 \times (K + Ca))$$

Where RHCY is the volatile matter yield obtained in wt% daf under rapid heating in the DTF below 2 wt% db K+Ca content and Aliphatic carbon is the wt% daf of all non-aromatic carbon.

Plotting predicted rapid heating char yields vs. those experimental derived as shown in figure 6-16 shows the very close correlation of calculated and observed results with R² correlation coefficient of 0.99.

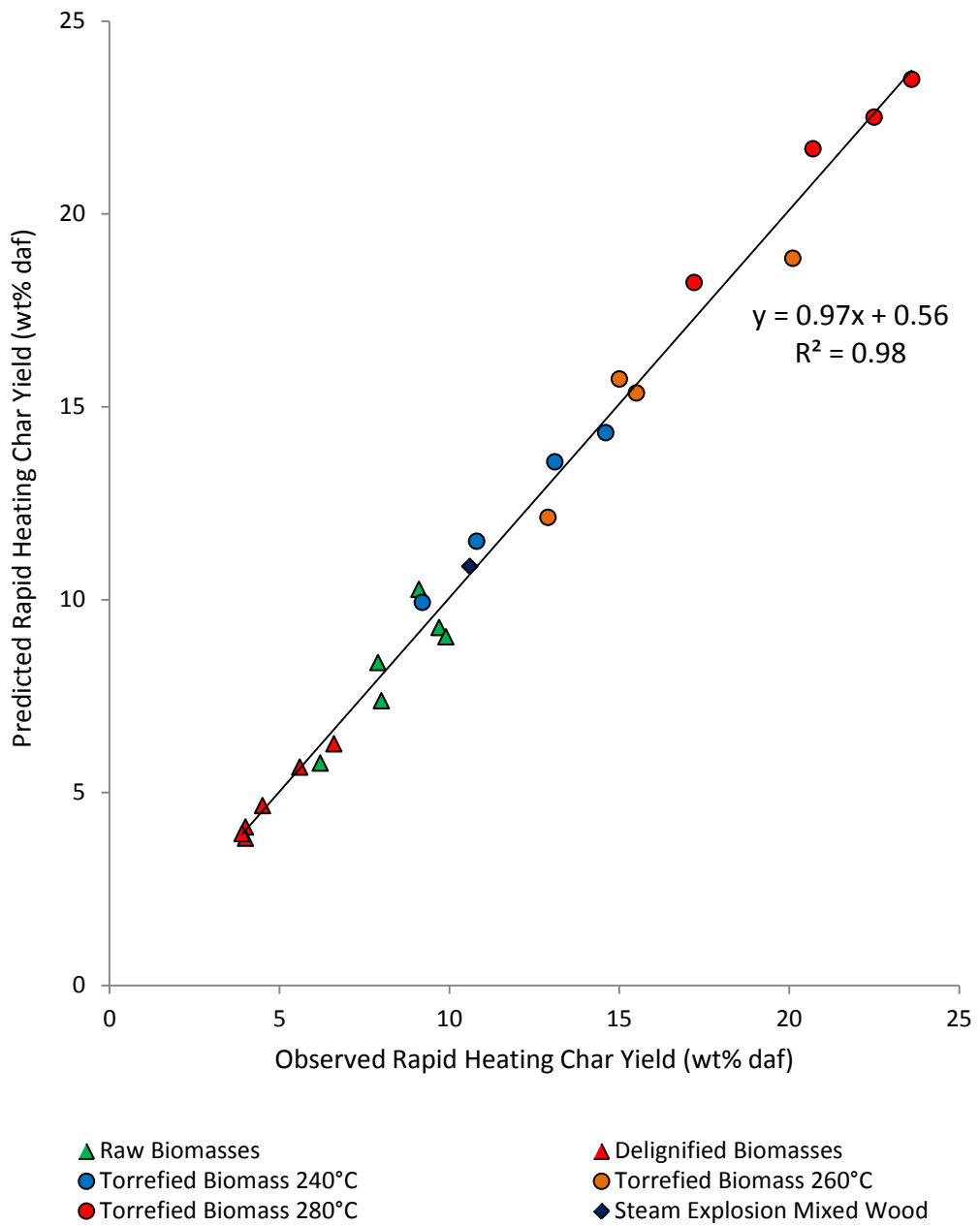


Figure 6-16 Calculated vs. Observed Rapid Heating Pyrolysis Char Yield

It is thought that the superiority of the empirically derived formula for prediction of rapid heating over slow heating char yield is due to a number of factors including the very high volatile matter yields achieved in the DTF and the reduced activity of mineral matter charring enhancements under prompt heating entrained flow pyrolysis conditions.

A plot of the errors in char yields determined utilising Equation 6-4 are plotted against the experimentally determined char yield in Figure 6-17 below. The average % error in the predictions is 8.4% with a standard deviation in errors of 8.6%.

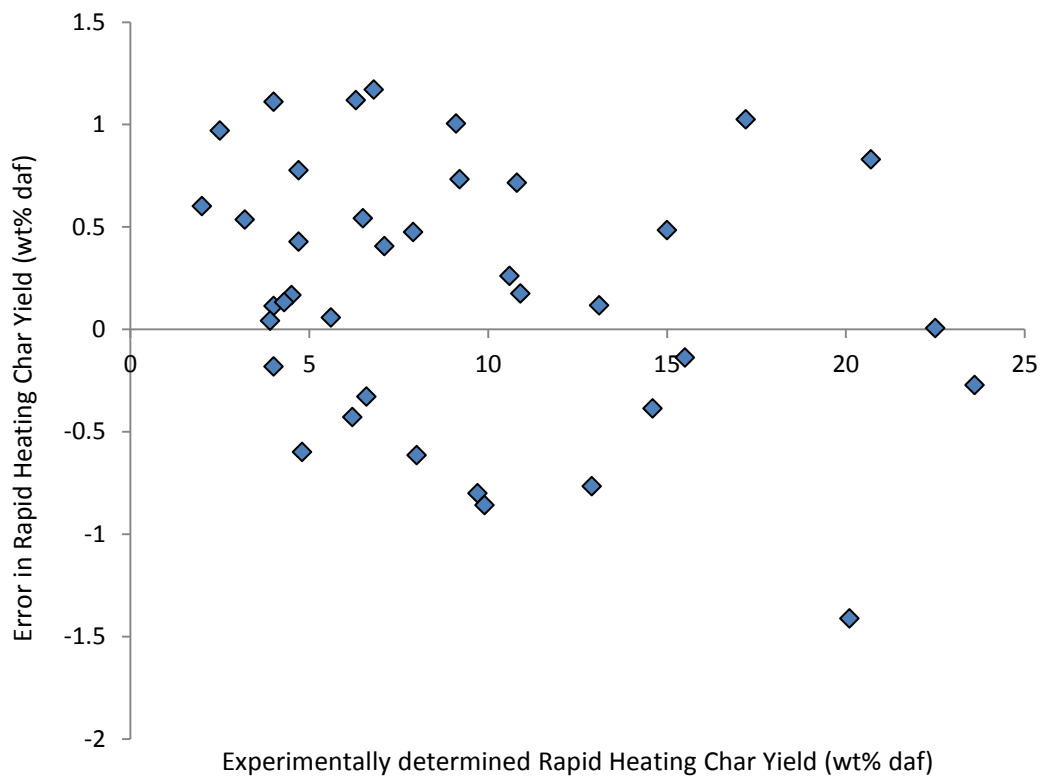


Figure 6-17 Error of Prediction for Rapid Heating Pyrolysis Char Yield Calculation

6.3. Summary

A method for the correlation of aromatic carbon and K+Ca content of biomass fuels with char yield has been derived for both slow heating TGA and entrained flow rapid heating DTF pyrolysis

- ▶ Close linear relationships between pyrolytic char yields and aromatic carbon wt% of HCl acid washed biomass samples have been observed under both slow and fast pyrolysis conditions.
- ▶ The study on the influence of mineral matter on char yields has enabled the combined concentration of K and Ca, the most abundant metals to quantify the increase in char yield obtained over the range 0.01 to 3.19 wt% db in the samples investigated.
- ▶ Combining the relationships for the influence of aromatic carbon wt% and the K+Ca contents on char yields has allowed for the derivation of empirical relationships able to predict char yields for both slow and fast pyrolysis as follows:

- Slow Pyrolysis

$$CY = (1 \times \text{Aromatic Carbon wt\%}) + (15.91 \times \text{Sum K+Ca wt\%})$$

This is applicable in the range 0 to 0.6 wt% K+Ca (Db) above which a fixed average additional char content of 9.76 wt% (daf) can be applied.

- Fast Pyrolysis

$$CY = (0.58 \times \text{Aromatic Carbon wt\%}) + (2.43 \times \text{Sum K+Ca wt\%})$$

This is applicable in the range 0 to 2 wt% db K+Ca above which a fixed average additional char content of 4.77 wt% (daf) can be applied.

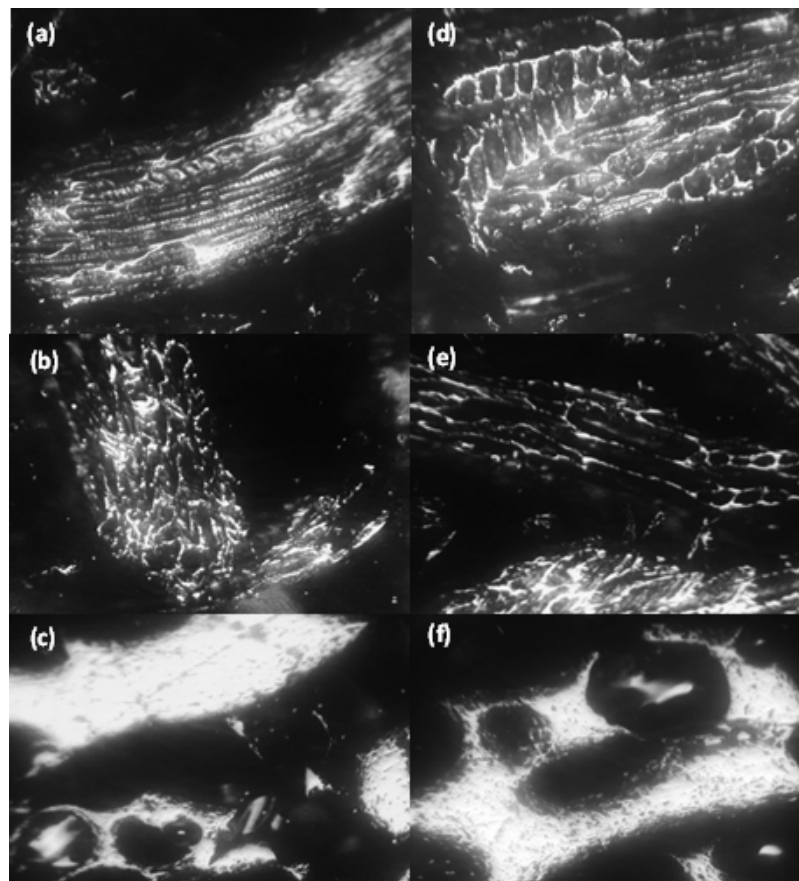
Where, in both cases, CY is the wt% char yield (daf), aromatic carbon is the wt% aromatic carbon (daf) and Sum K+Ca is the summed wt% of K+Ca (db).

- ▶ Char yields calculated using the empirical expressions derived correlate closely with experimentally determined values with R^2 of 0.96 and 0.99 for slow and fast pyrolysis conditions, respectively. It is anticipated that similar relationships can be derived and will hold for intermediate heating pyrolysis regimes between the two extremes investigated here.
- ▶ These relationships prove that accurate determination of pyrolytic yields are possible given an understanding of the chemical, structural and inorganic mineral composition of any lignocellulosic biomass feedstock and evidence the importance of aromaticity and mineral matter influences on char forming reactions. It is hoped that these relationships may prove useful in the more targeted the selection and utilisation of a wider range of these feedstocks in thermochemical conversion processes and improve the understanding of variation in process parameters required to provide efficient use of valued fuel stocks.

Chapter 7: Char Characterisation

7.1. HTF Char Morphology and Surface Area

The morphology of chars generated in the HTF using demineralised pine woodchip and corn stover fractions have been studied using optical oil immersion microscopy to assess the nature of chars generated under slow heating conditions. From this a comparison can be made between the chars derived from isolated lignins, delignified fuels and untreated fuels. Images are shown in Figure 7-1.



50 μm

Figure 7-1 HTF Char Morphology

(a) Demineralised Raw Pine Woodchips (b) Demineralised Delignified Pine (c) Pine Organosolv Lignin
(d) Demineralised Corn Stover (e) Demineralised Delignified Corn Stover (f) Corn Stover Organosolv Lignin

Demineralised raw and delignified samples for both pine and corn stover produce chars which largely retain the biological structure which characterises the raw material under HTF slow heating pyrolysis. These chars show clear cell wall forms with delignification appearing to thin the char walls through reduction in char forming aromatic carbon. Lignin HTF chars are in complete contrast to those of the other fractions and exhibit a highly fused, glassy structure with very few large macropore forms where accumulation of volatile matter has occurred during pyrolysis. The lack of external surface and extreme reduction in internal porosity of pure lignin chars is in line with the fact that lignins have been shown to undergo complete softening during pyrolysis (Dufour et al., 2012), the liquid phase formed allows the escape of volatile without considerable alteration of the structure of the particle thus limiting the formation of pores on solidification of the char. Low levels of porosity will reduce total surface area and active sight proliferation which will likely result in much reduced char combustion rates. The BET surface areas of HTF generated chars has been conducted, results corrected for ash content being shown in Table 7-1.

Sample	BET Surface Area (m²g⁻¹)
Demineralised Pine Woodchips	78.8
Demineralised Delignified Pine	97.9
Pine Lignin	17.5
Delignified Corn Stover Pellets	105.6
Demineralised Delignified Corn Stover	130.9
Corn Stover Lignin	29.9

Table 7-1 BET Surface Area of HTF Chars

The differences between the HTF chars observed under oil immersion microscopy are evident in quantification of the BET surface area. The surface area of demineralised delignified fuels is consistently greater than that of the associated demineralised parent

fuel. This can be explained on analysis of the measured surface area for lignin HTF chars which exhibit very low surface areas, each less than $30 \text{ m}^2\text{g}^{-1}$. This indicates that the softening of lignin causes the condensation of the fuel particle during pyrolysis, escape of volatiles having little influence on the porosity of the char under slow heating pyrolysis. The higher levels of lignin in raw samples not only suppresses the volatile matter content due to increased presence of thermally stable aromatic carbon but also encourages the formation of intermediate liquid phases during pyrolysis which aids in the release of volatile bubbles and thus reduces porosity development.

7.2. DTF Char Morphology and BET Surface Area

As anticipated the morphological nature of the biomass char samples generated in the entrained flow DTF varied considerably both between individual biomass fuels and between raw biomass samples and their delignified and demineralised analogues, all of which were unlike chars typically observed following entrained flow coal pyrolysis.

A table of manual point counting results of char structures is shown in Table 7-2. As has been mentioned in Chapter 3 the biomass chars obtained did not generally exhibit char morphotypes which were directly comparable to those consistently described for entrained flow, high heating rate char derived from coal and as such an abridged classification of chars has been utilised to characterise them as being of either thin walled, thick walled or solid.

It is observed that for most of the chars produced, apart from some high ash containing raw biomass, a considerable degree of softening appears to have occurred during high heating rate devolatilisation which has encouraged the formation of cenospheric type char structures with varying degrees of wall thickness and porosity. These results mirror those of recent research (Tolvanen et al., 2013) which suggests the formation of mobile

intermediate phases (liquid softening) from some of the lignocellulosic components encourages the transformation of biomass particle shape during rapid heating pyrolysis to consistently form more spherical structures. Where considerable alteration of the fuel has been observed following pyrolysis in this study chars predominantly take the form of rounded spheres or noded configurations with either a network inner wall or bubble type structure similar to those found with coal. The major differences between coal and biomass char forms can be seen on comparison of Kellingley coal chars as shown in Figure 7-2 and those of biomass fuels in Figures 7-2 – 7-8, all scales shown are of 50 μm . The principle differences being the generally reduced wall thickness of biomass chars where cenospheres have been able to develop, and the increased proliferation of smaller pores within the char walls. It is thought that the even distribution of smaller, isolated pores in the biomass chars is most likely due to the fact that considerable portions of the biomass fuels, namely the cellulosic components, do not cultivate significant levels of mobility on pyrolysis and thus effectively limit the passage of volatile bubbles formed within the pyrolysing particle, restricting their evolution from the particle and preventing coalescence. As such a multitude of smaller bubbles form within the biomass particle, effectively trapped where generated.

As anticipated, due to the relatively high char yield obtained, Kellingley coal chars exhibit considerably thicker walls than those of corresponding biomass chars which exhibit far higher loss of volatile mass during conversion. In addition to this the pores within the coal char walls are relatively large in comparison to those of biomass, this being thought to be due to the differing thermoplastic properties of the fuels. Coal particles are known to undergo significant plasticisation during pyrolysis to form an elastic metaplast (van Krevelen et al., 1956; Solomon et al., 1992), with the viscosity and pore structure of this metaplast governing the rate of volatile gas mass transport and their evolution from the devolatilising particle (Gavalas, 1982). The formation of a

mobile fluid phase is able to block the original pore structure of the coal causing some of the gaseous volatile matter being formed to be held within the metaplast which leads to the formation of bubbles within the devolatilising particle (Smith, 2013). As the proliferation of bubbles increases the volatile gases formed are able to diffuse directly into them instead of escaping the particles outer surface. This leads to the growth of internal bubbles, resulting in the continued expansion and coalescence of existing bubble structures, causing the entire coal particle to swell (Yu et al., 2007). It is likely that the bubble coalescence and growth phenomenon observed during coal devolatilisation give rise to the formation of larger, more discrete bubbles as observed for Kellingley coal DTF chars.

Both raw corn stover and wheat straw pellet fuels produce chars which closely mirror their original botanical form under rapid heating, exhibiting some of the initial cellular structure with limited evidence of plasticisation, significant structural alteration only being observed on pyrolysis of demineralised and delignified samples. Both of these raw fuel samples have high AAEM mineral contents which act to suppress the formation of mobile liquid phases and instead promote radical bond breaking and formation reactions which result in generation of more highly condensed char structures (Jones et al., 2007; Li et al., 2006; Sathe et al., 1999; Wang et al., 2012). These observations are in line with those of Borrego et al., 2009 who reported the retention of biological cell structure of high AAEM containing rice husk char particles on pyrolysis in an entrained flow drop tube furnace at 950°C under an N₂ atmosphere and Jones et al., 2007 who observed similar retention of solid structure following doping of low ash eucalyptus with 1% K. Ion exchangeable ash species removal via delignification and demineralisation methods results in a noticeable change in char formation characteristics whereby the particles appear to have undergone significantly more plasticisation during devolatilisation with evident particle swelling to produce a large proportion of large,

cenospheric structures with high degrees of porosity. This is especially noticeable for wheat straw and corn stover fuels which exhibit relatively high AAEM content and thus produce chars retaining much of the physical biological character prior to demineralisation.

Evaluation of these observations in light of the fact that lignin components have been shown to produce by far the greatest fluid character during pyrolysis, that demineralisation can greatly improve the development of fluid character (Dufour et al., 2012) and that AAEM enhanced charring is shown to act almost solely on non-aromatic biomass components suggests that for those biomass containing high levels of active inorganic mineral species the charring of non-fluid polysaccharidal material is significant. As the softening of this material is relatively low and is reduced further by the presence of these select mineral species the char formed appears not to have undergone any significant fluidity development and is thus characterised by the original form of the plant material. Low mineral matter biomass, whose char yield has been closely linked with the original aromatic carbon content of the fuel (see Chapter 6), undergo char forming reactions predominantly through retention and condensation of existing lignin derived aromatic components, known to develop a high degree of fluid character during pyrolysis and thus produce chars which exhibit significant transformation in line with those observed for high softening coals.

This hypothesis is supported by the observed differences between demineralised raw and demineralised delignified fuels, those of reduced lignin content appearing to form thinner walled, lacier chars. This is thought to be due to the decrease in aromatic carbon content brought about by delignification, upon which these demineralised fuels largely rely as a source of char, which thus increases the quantity of volatiles produced, reducing the thickness of char walls as a result.

The study of an individual char particle which appears to contain portions of char which exhibit both the original biological structure of the lignocellulosic matrix and a highly softened, spherical nature may provide some evidence as to the reaction mechanisms occurring during rapid heating entrained flow pyrolysis (see Figure 7-13). As can be seen in this figure the upper portion of the char particle has retained some of the order of the parent material with pore and cell wall structures associated with the original lignocellulosic matrix being evident, albeit with much reduced wall thicknesses due to the substantial loss of organic mass. However, the lower portion of the char has developed a spherical nature with greatly enlarged central cavity. Evaluation of the interface between these two portions reveals a thick walled boundary with limited porosity development which appears to be frozen in the melt stage with development of a large pore on the outer surface of the particle but limited swelling on the interior which retains its cellular structure.

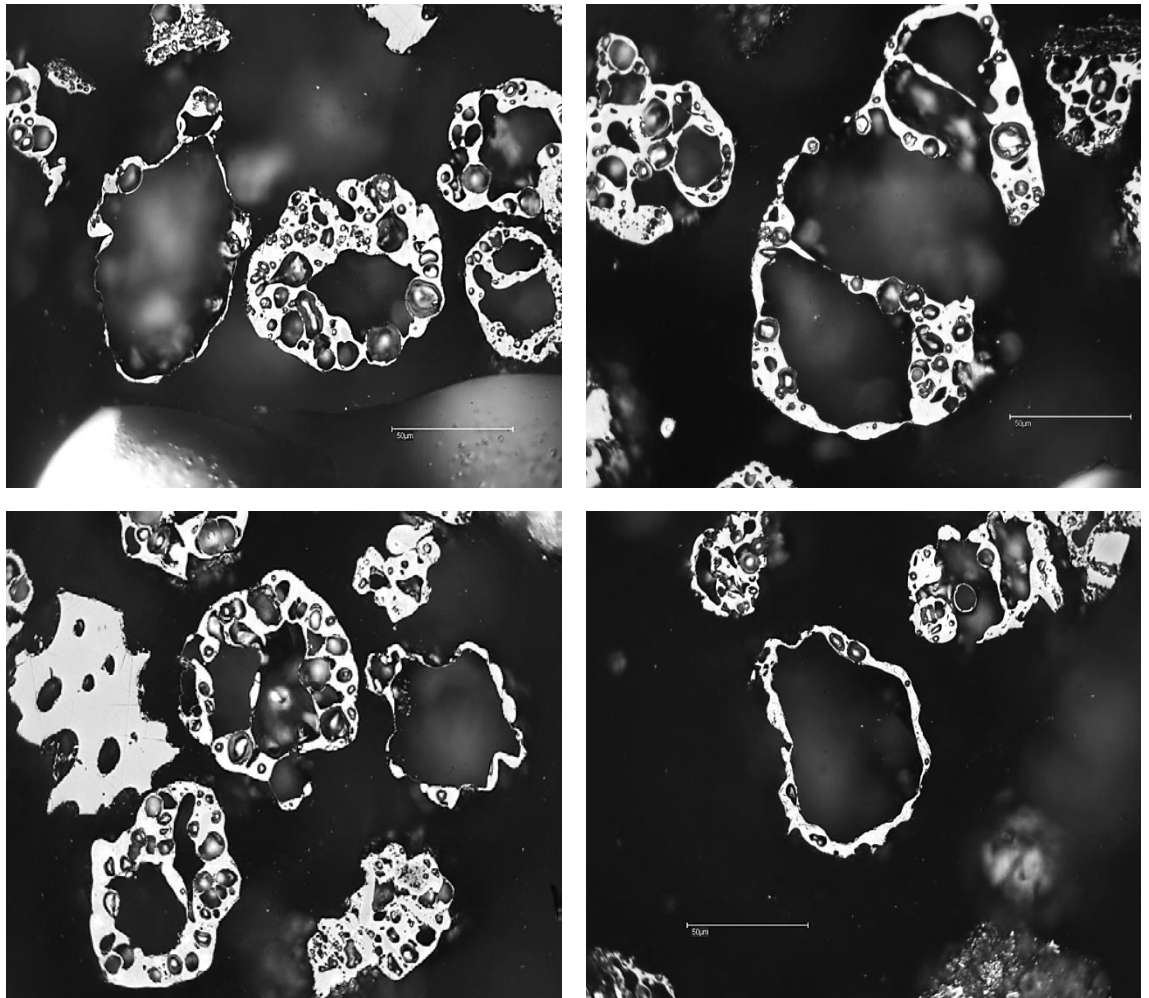


Figure 7-2 Kellingley Coal DTF Char Morphology 1300°C 600 ms (50-75 μm)

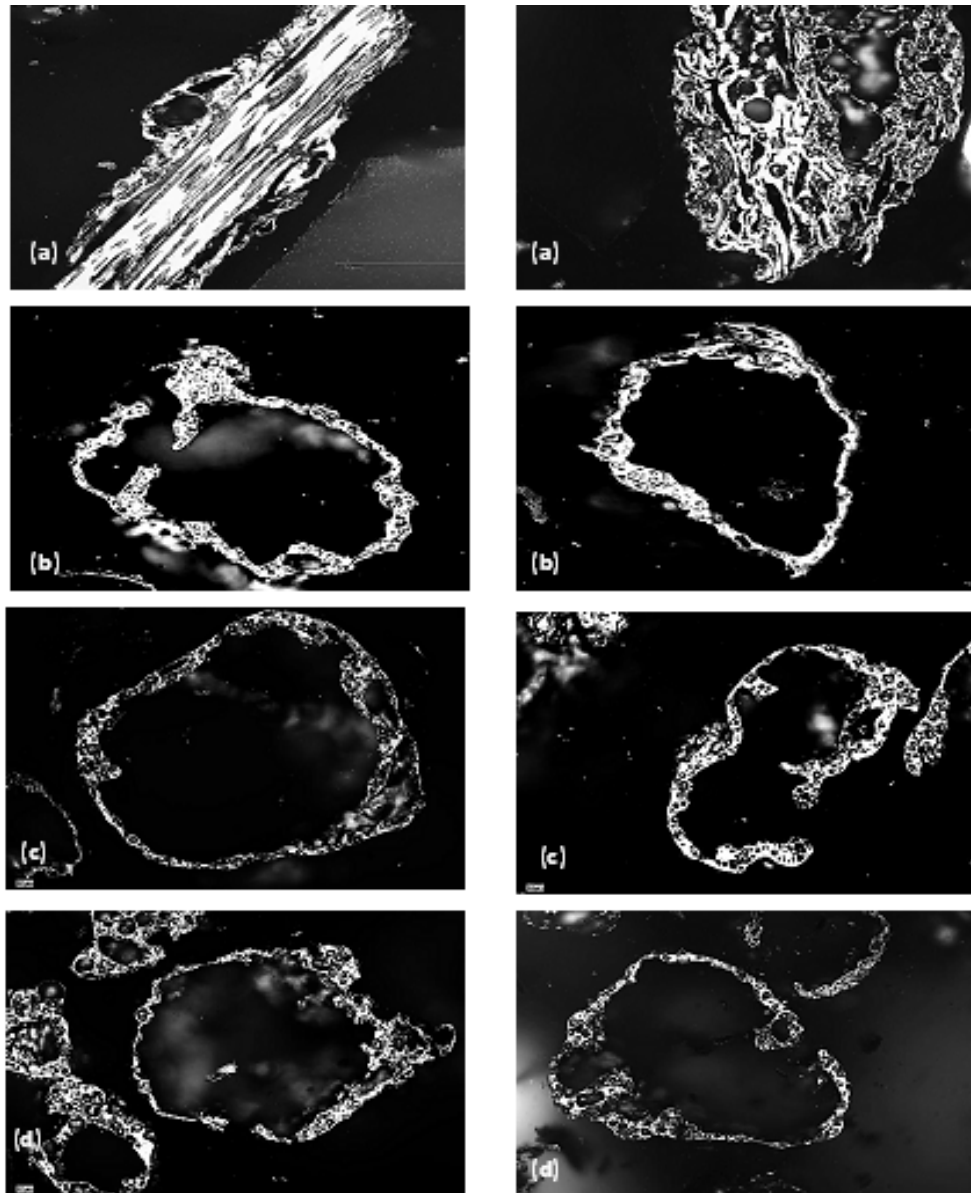


Figure 7-3 Wheat Straw Pellet Fraction DTF Char Morphologies

(a) Raw Wheat Straw Pellets (b) Demineralised Wheat Straw Pellets

(c) Delignified Wheat Straw Pellets (d) Demineralised Delignified Wheat Straw Pellets

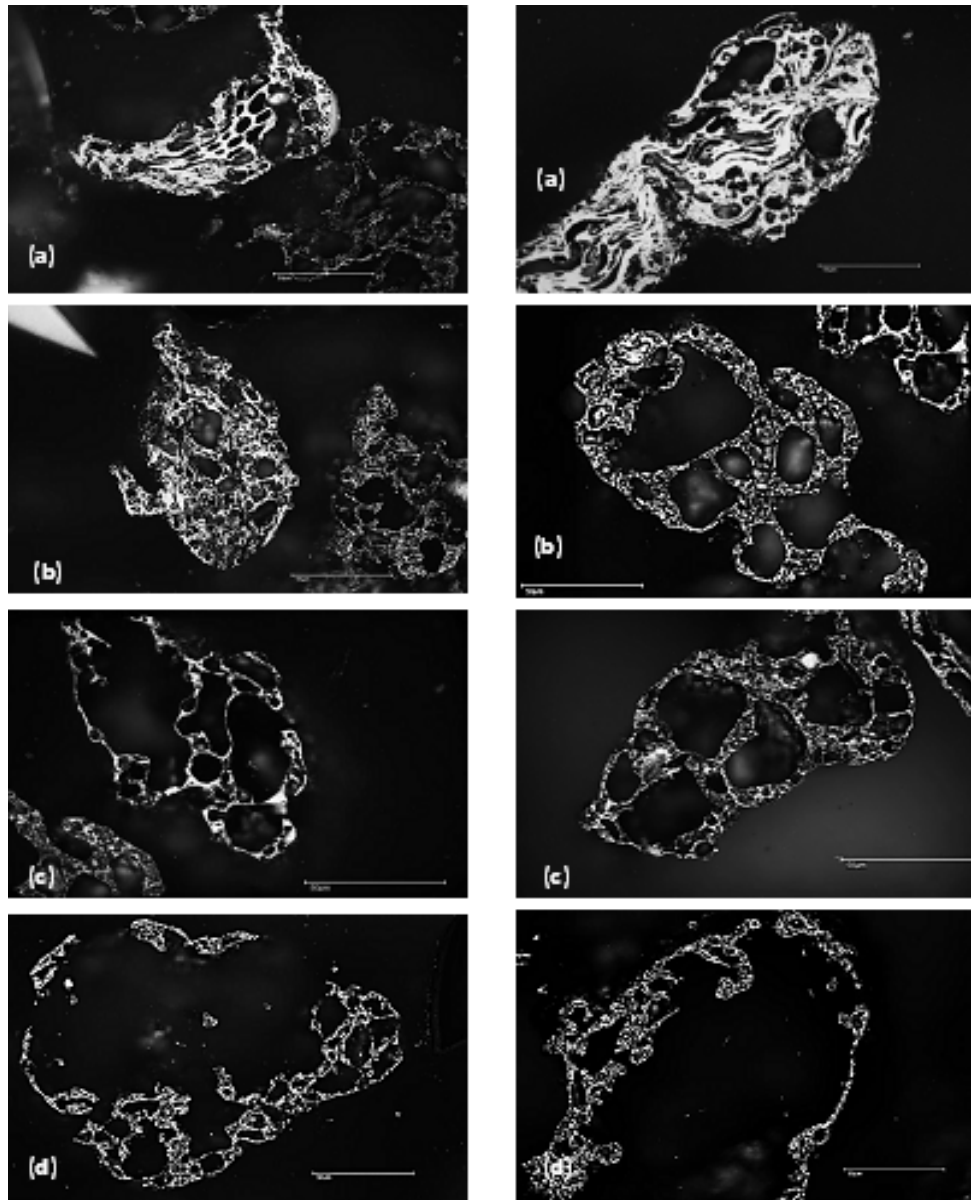


Figure 7-4 Corn Stover Pellet Fraction DTF Char Morphologies

(a) Raw Corn Stover Pellets (b) Demineralised Corn Stover Pellets

(c) Delignified Corn Stover Pellets (d) Demineralised Delignified Corn Stover Pellets

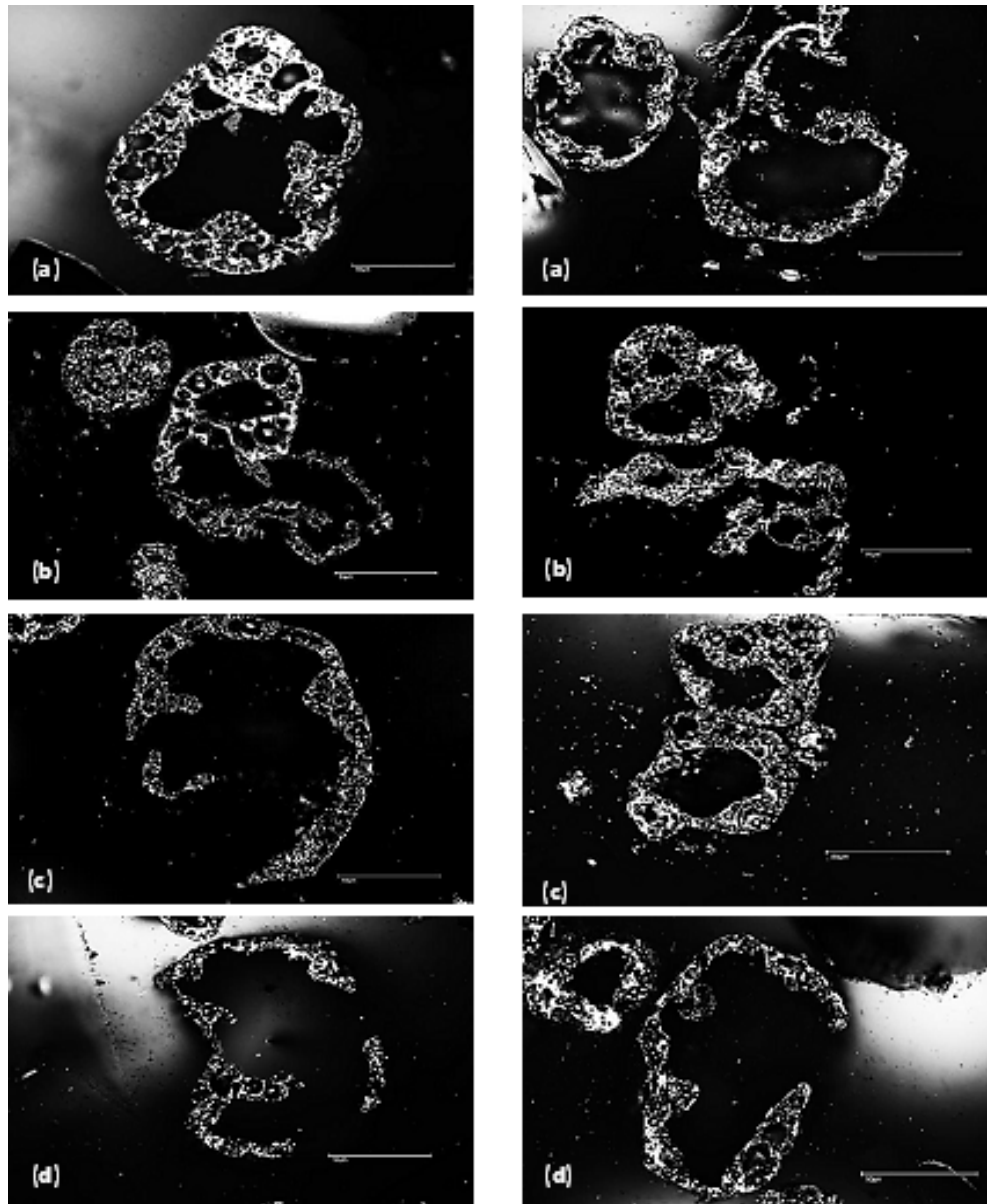


Figure 7-5 Pine Woodchip Fraction DTF Char Morphologies

(a) Raw Pine Woodchips (b) Demineralised Pine Woodchips

(c) Delignified Pine Woodchips (d) Demineralised Delignified Pine Woodchips

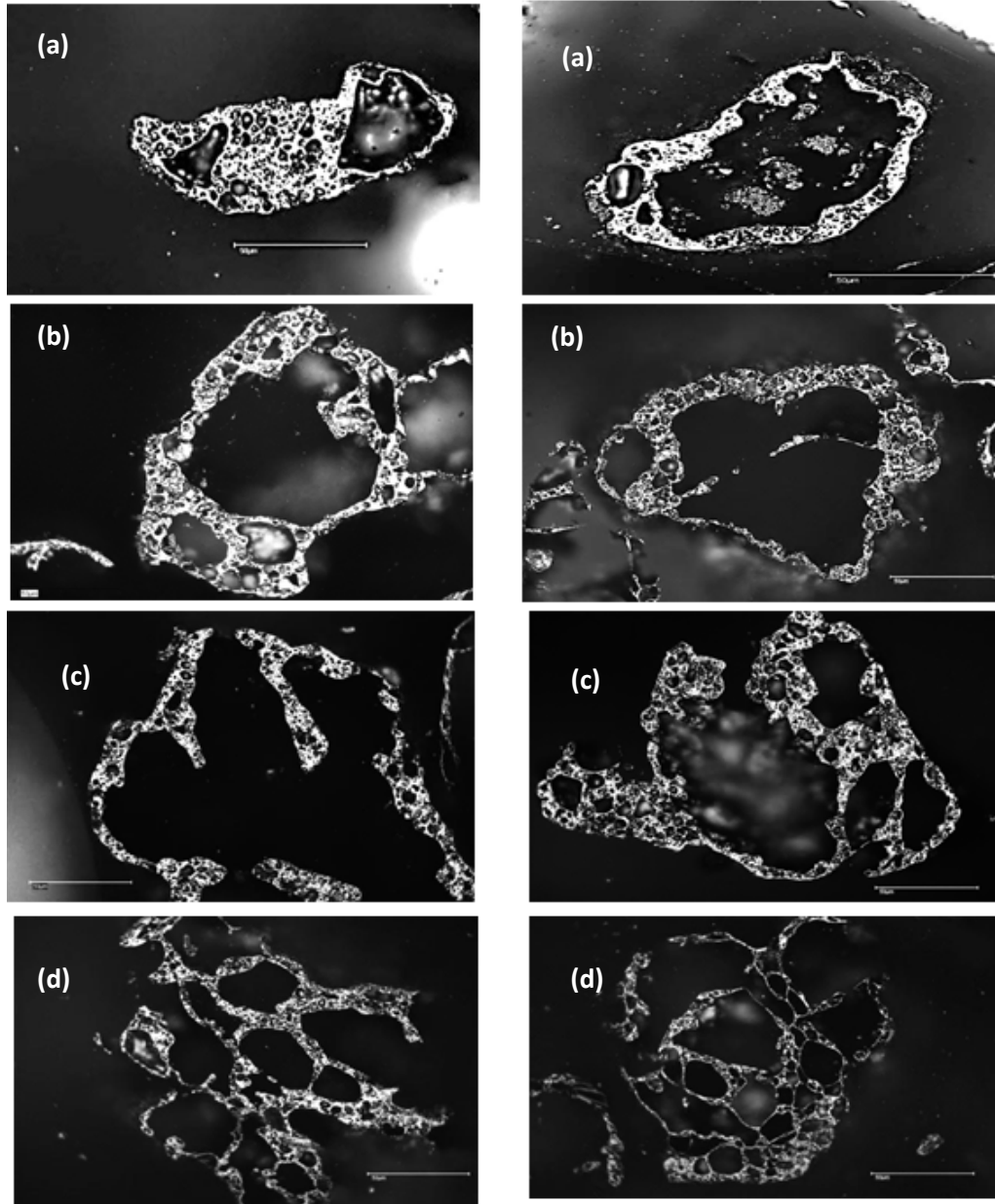
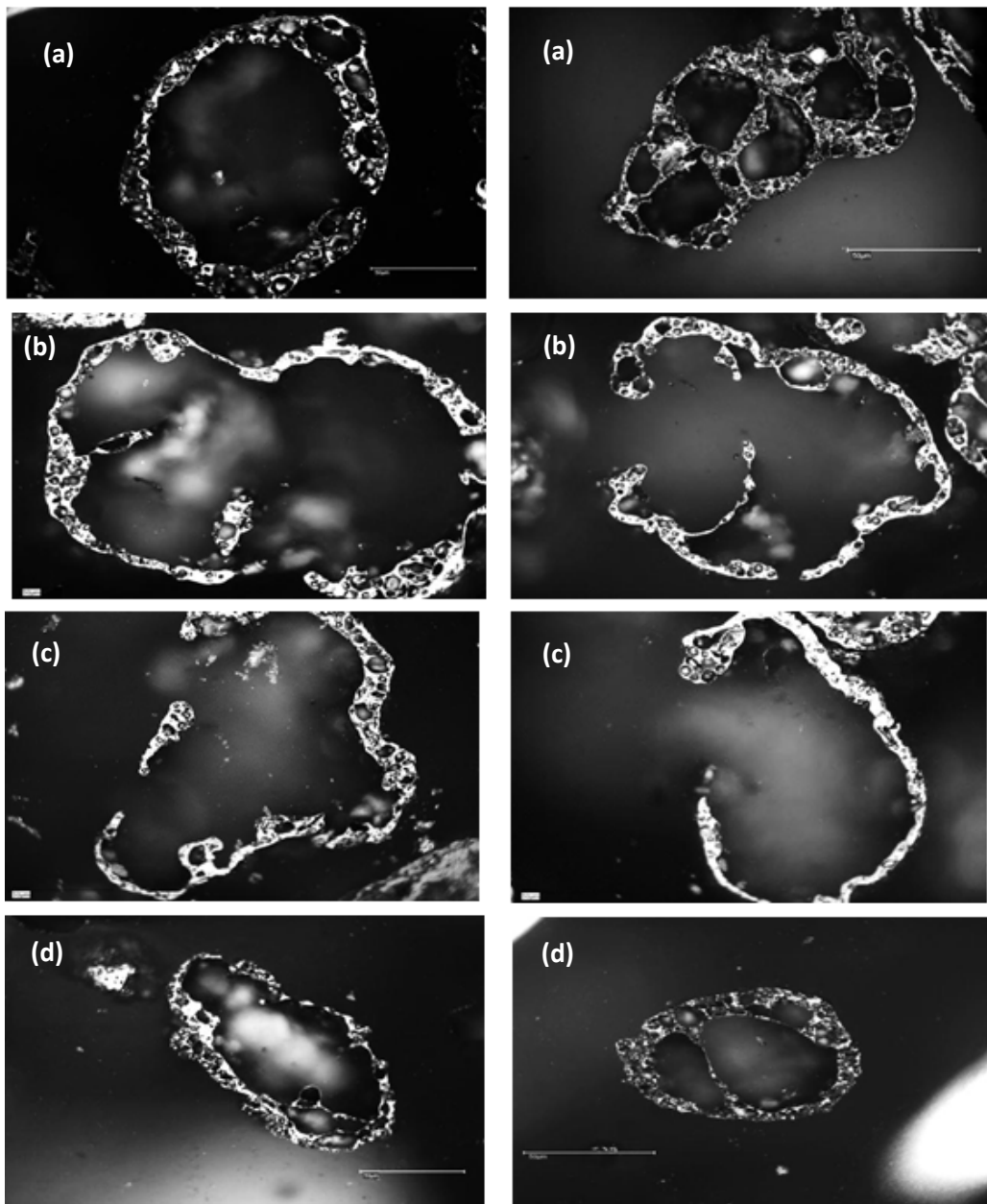


Figure 7-6 Eucalyptus Pellet Fraction DTF Char Morphologies

(a) Raw Eucalyptus Pellets (b) Demineralised Eucalyptus Pellets

(c) Delignified Eucalyptus Pellets (d) Demineralised Delignified Eucalyptus Pellets



*Figure 7-7 Miscanthus Pellet Fraction DTF Char Morphologies
(a) Raw Miscanthus Pellets (b) Demineralised Miscanthus Pellets
(c) Delignified Miscanthus Pellets (d) Demineralised Delignified Miscanthus Pellets*

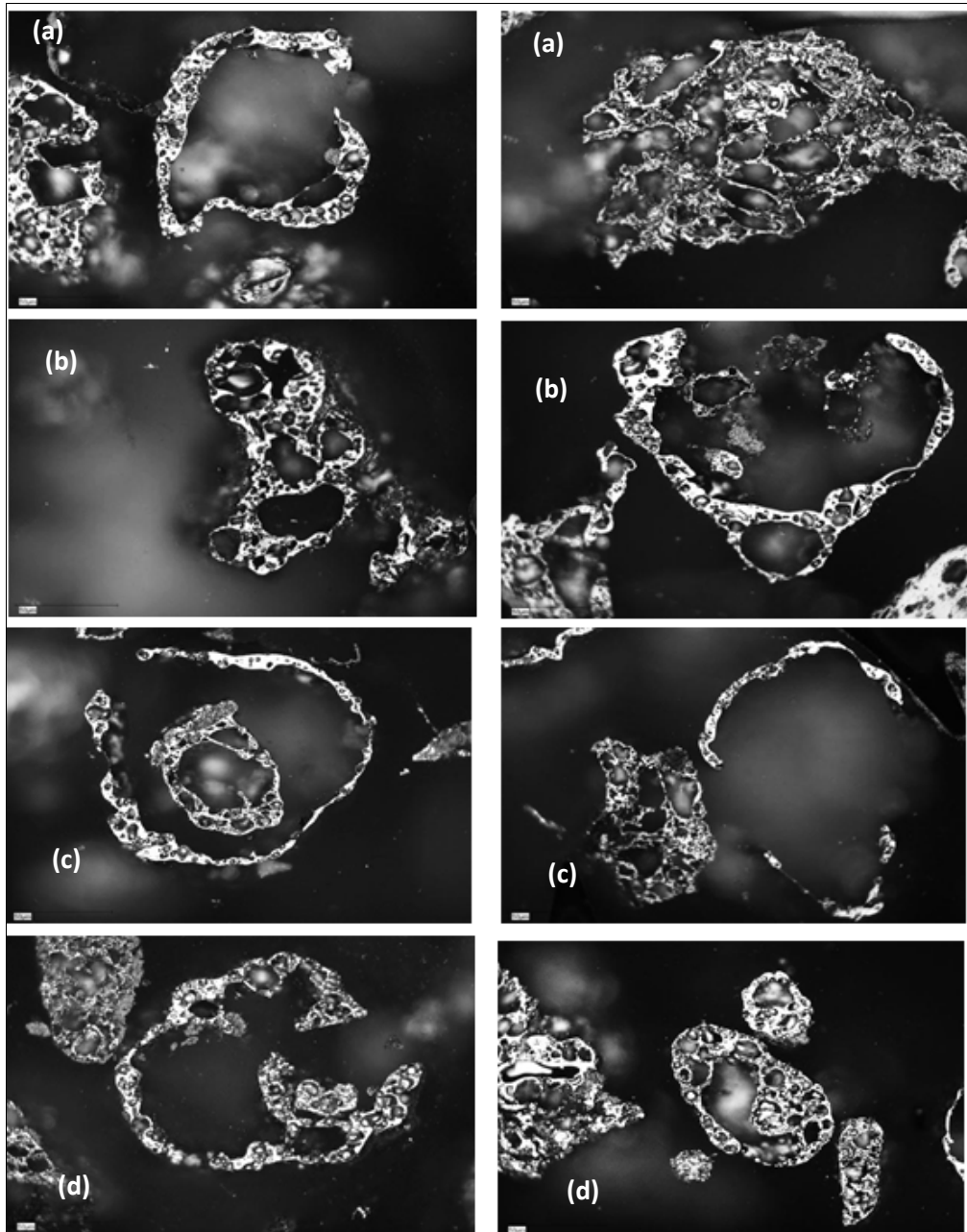


*Figure 7-8 Mixed Softwood Pellet Fraction DTF Char Morphologies
(a) Raw Miscanthus Pellets (b) Demineralised Miscanthus Pellets
(c) Delignified Miscanthus Pellets (d) Demineralised Delignified Miscanthus Pellets*

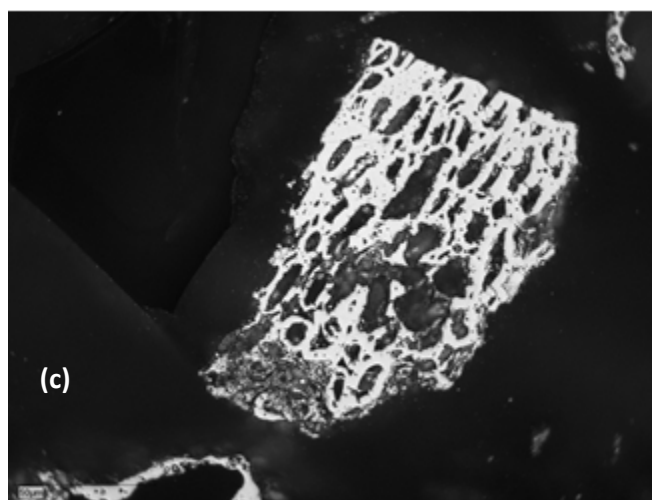
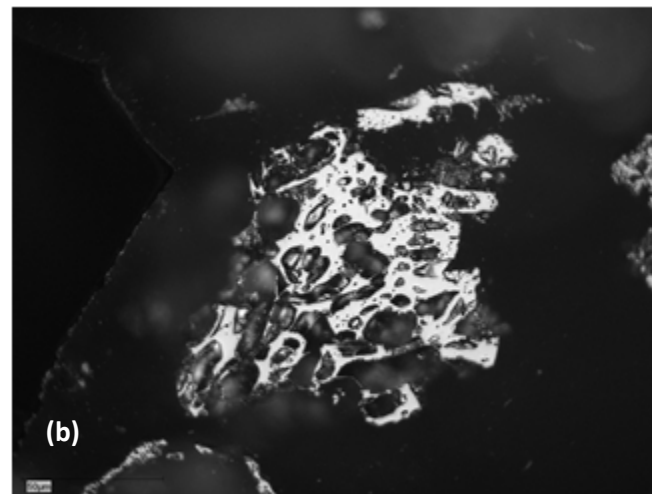
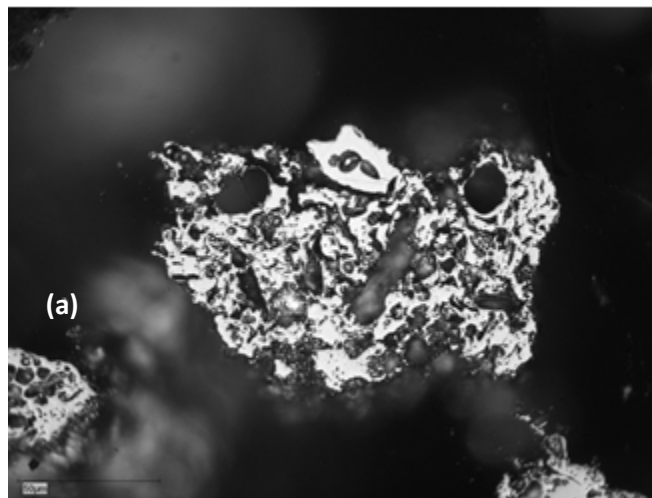


Figure 7-9 Torrefied Wheat Straw Pellets (a) 240°C (b) 260°C (c) 280°C

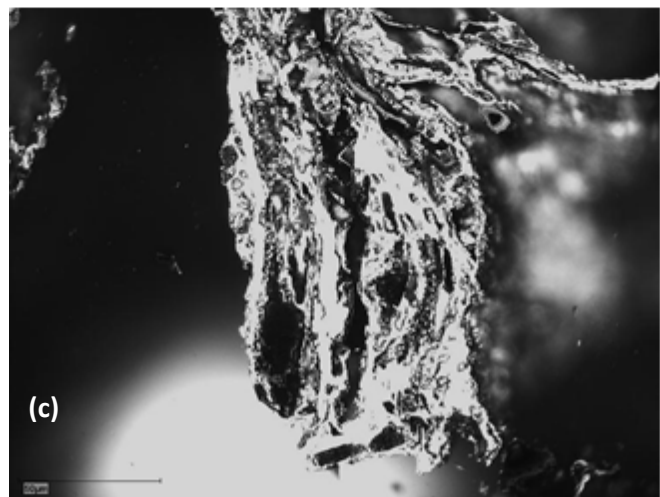
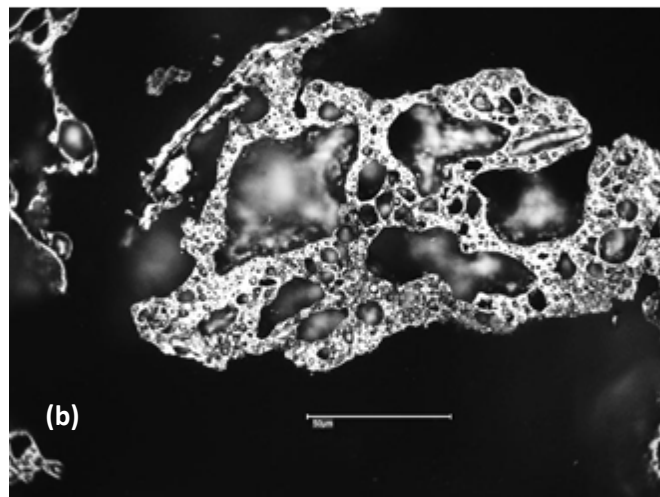
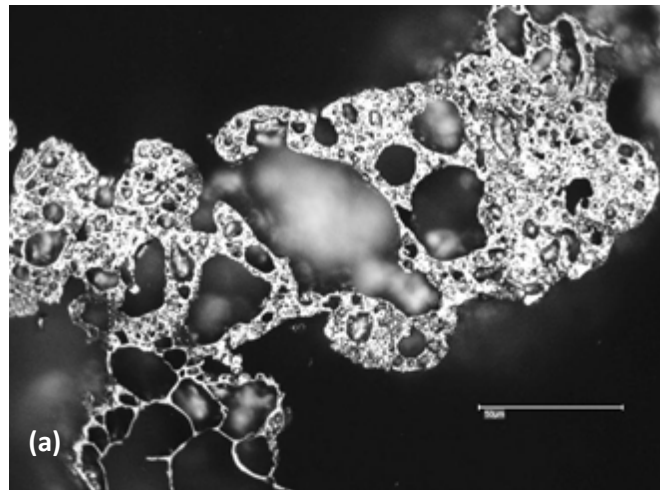


Figure 7-10 Torrefied corn Stover Pellets (a) 240°C (b) 260°C (c)280°C

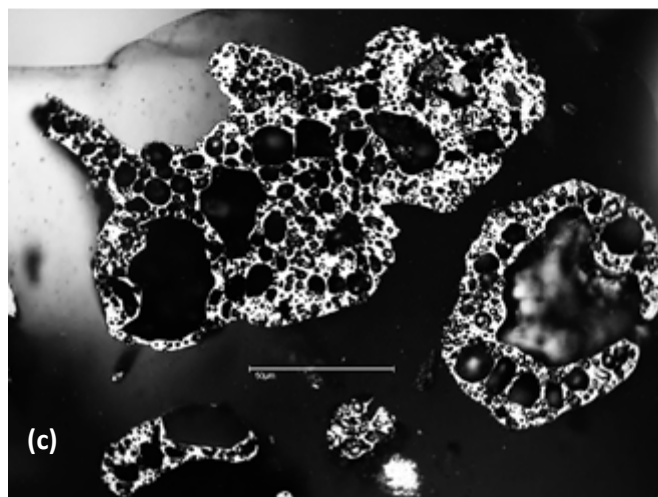
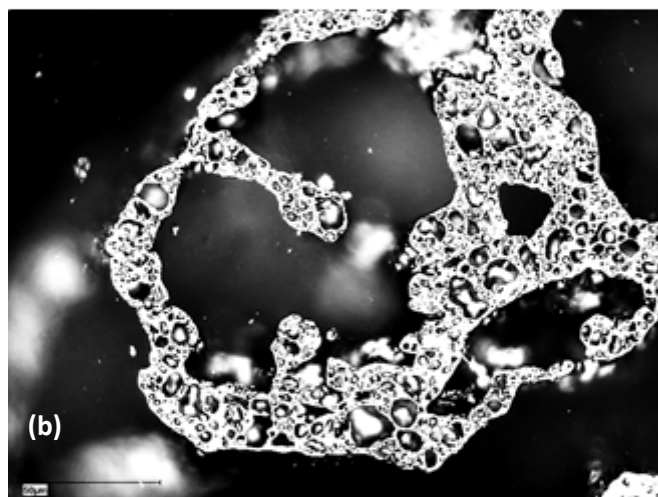
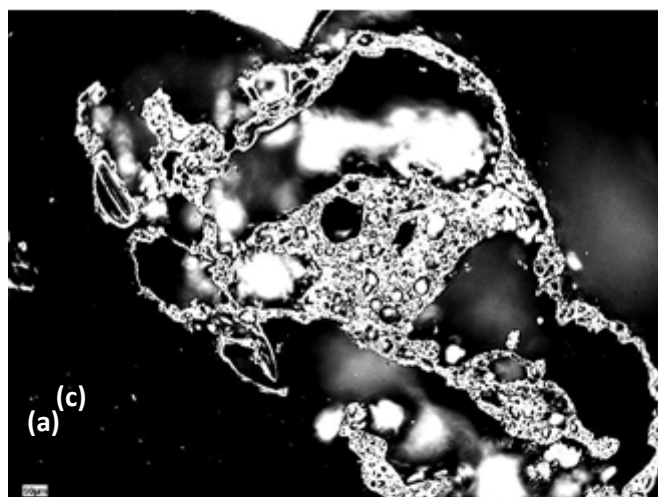


Figure 7-11 Torrefied Mixed Softwood Pellets (a) 240°C (b)260°C (c)280°C

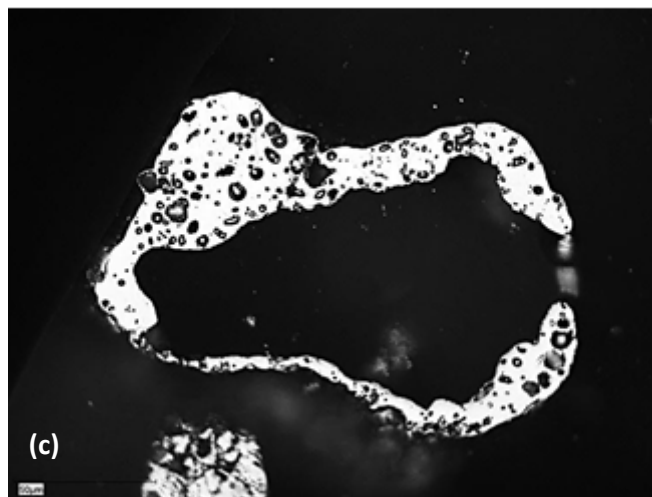
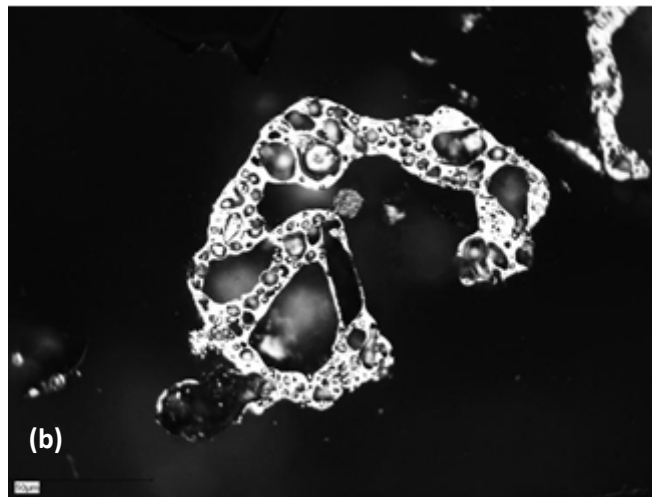
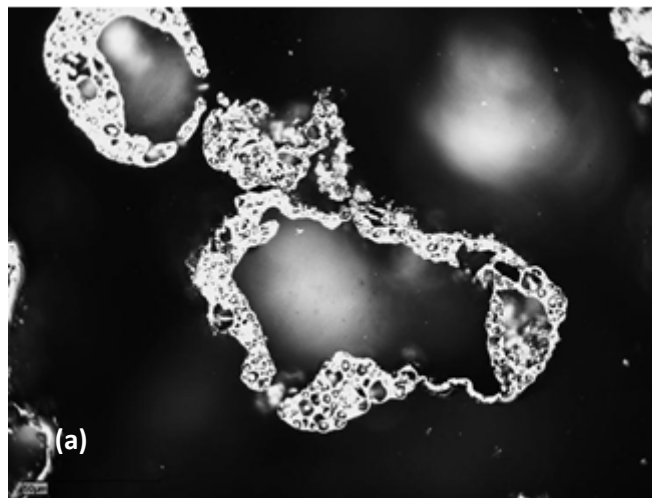
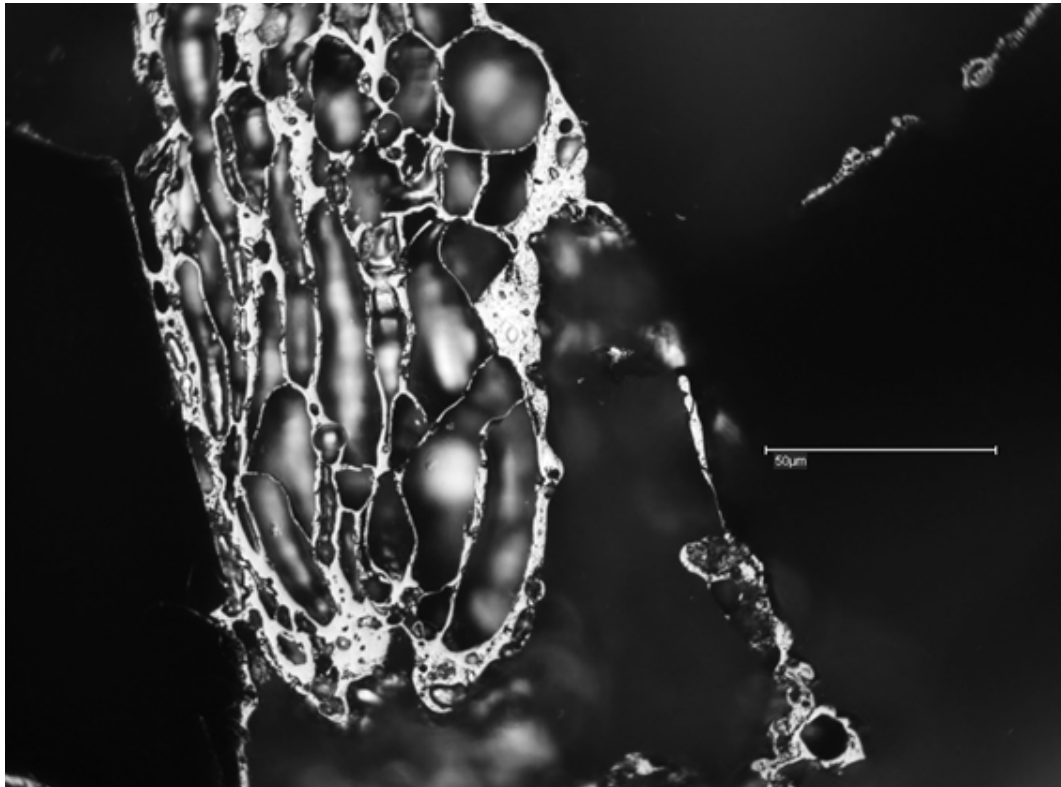


Figure 7-12 Torrefied Pine Char Morphology (a) 240°C (b)260°C (c)280°C



*Figure 7-13 Partially Swollen Char Retaining Part Cell Structure
(Raw Miscanthus Pellet DTF Char)*

Figures 7-9 to 7-11 show the influence of torrefaction on the char morphology of the biomass chars. As can be seen the thickness of the char walls and the solid nature of the char both increase significantly with torrefaction degree. This is primarily due to the higher char yield obtained for torrefied biomass which leaves a higher percentage of the fuel as char and also limits the formation of volatile matter bubbles within the pyrolysing particle, thus suppressing the development of internal char porosity. The influence of the factors discussed above on the manual char characterisation and BET surface areas are outlined in Tables 7-2 and 7-3.

Sample	Thin Walled (%)	Thick Walled (%)	Solid (%)
Wheat Straw Pellets	19.5	28.5	52.0
Delignified Wheat Straw	41.5	48.0	10.5
Corn Stover Pellets	8.0	33.0	59.0
Delignified Corn Stover	67.5	27.0	5.5.0
Pine Woodchips	32.5	56.0	11.5
Delignified Pine Woodchips	44.5	47.0	8.5
Miscanthus Pellets	22.0	42.0	36.0
Delignified Miscanthus	48.0	40.0	12.0
Eucalyptus Pellets	46.0	47.5	6.5
Delignified Eucalyptus	60.0	36.0	4.0
Mixed Softwood Pellets	39.0	42.0	19.0
Delignified Mixed Softwood	67.5	27.0	5.5
Torrefied Wheat Straw 240°C	9.5	23.5	67.0
Torrefied Wheat Straw 260°C	5.5	22.5	72.0
Torrefied Wheat Straw 280°C	4.0	21.5	74.5
Torrefied Corn Stover 240°C	6.5	32.5	61.0
Torrefied Corn Stover 260°C	2.0	26.5	71.5
Torrefied Corn Stover 280° C	1.5	21.5	77.0
Torrefied Pine 240°C	21.5	66.5	12.0
Torrefied Pine 260°C	12.0	72.0	16.0
Torrefied Pine 280°C	2.5	74.0	23.5
Torrefied Mixed Softwood 240°C	31.0	53.0	16.0
Torrefied Mixed Softwood 260°C	18.5	64.0	17.5
Torrefied Mixed Softwood 280°C	11.0	71.0	18.0
Demineralised Wheat Straw Pellets	13.5	67.0	19.5
Demineralised Delignified Wheat Straw	62.0	26.5	11.5
Demineralise Corn Stover Pellets	24.5	39.5	36.0
Demineralised Delignified Corn Stover	88.0	7.5	4.5
Demineralised Pine Woodchips	38.0	49.5	12.5
Demineralised Delignified Pine Woodchips	52.5	38.0	9.5
Demineralised Miscanthus Pellets	37.5	48.0	14.5
Demineralised Delignified Miscanthus	45.5	42.5	12.0
Demineralised Eucalyptus Pellets	41.5	52.0	6.5
Demineralised Delignified Eucalyptus	66.5	28.5	5.0
Demineralised Mixed Softwood Pellets	50.5	33.5	16.0
Demineralised Delignified Mixed Softwood	72.0	24.0	4.0
Kellingley Coal	23.0	53.0	24.0

Table 7-2 Manual Point Counting Char Morphotype Classification

Sample	BET Surface Area (m ² g ⁻¹)
Wheat Straw Pellets	97.0
Delignified Wheat Straw	141.4
Corn Stover Pellets	112.3
Delignified Corn Stover	167.7
Pine Woodchips	184.9
Delignified Pine Woodchips	187.8
Miscanthus Pellets	194.4
Delignified Miscanthus	199.6
Eucalyptus Pellets	138.6
Delignified Eucalyptus	207.9
Mixed Softwood Pellets	138.9
Delignified Mixed Softwood	151.8
Torrefied Wheat Straw 240°C	119.0
Torrefied Wheat Straw 260°C	110.0
Torrefied Wheat Straw 280°C	93.0
Torrefied Corn Stover 240°C	98.4
Torrefied Corn Stover 260°C	83.2
Torrefied Corn Stover 280° C	65.9
Torrefied Pine 240°C	143.7
Torrefied Pine 260°C	122.3
Torrefied Pine 280°C	113.5
Torrefied Mixed Softwood 240°C	112.6
Torrefied Mixed Softwood 260°C	92.3
Torrefied Mixed Softwood 280°C	76.9
Steam Explosion Mixed Woods	122.6
Demineralised Wheat Straw Pellets	173.8
Demineralised Delignified Wheat Straw	206.3
Demineralise Corn Stover Pellets	233.6
Demineralised Delignified Corn Stover	298.5
Demineralised Pine Woodchips	205.4
Demineralised Delignified Pine Woodchips	238.7
Demineralised Miscanthus Pellets	219.3
Demineralised Delignified Miscanthus	249.9
Demineralised Eucalyptus Pellets	193.4
Demineralised Delignified Eucalyptus	205.5
Demineralised Mixed Softwood Pellets	210.4
Demineralised Delignified Mixed Softwood	244.7
Demineralised Steam Explosion Mixed Wood	147.8

Table 7-3 DTF Char BET Surface Area

Both the manual char point counting and BET surface area results confirm the qualitative analysis of the influence of demineralisation and delignification processes on DTF chars whereby the number of thin walled chars increases with decreases in aromatic carbon and AAEM species at the expense of thick walled and solid chars leading to significant increases in the char BET surface area. A plot of surface area

against the measured quantity of thin wall chars is shown in Figure 7-14, showing strong positive correlation of available surface area with decreasing char wall thickness.



Figure 7-14 DTF Char BET Surface Area vs. % Thin Walled Chars

Given the hypothesis that decrease in char reactivity are driven primarily by increases in aromatic carbon and AAEM content the surface has been plotted against K+Ca content of the fuel and aromatic carbon content for non-demineralised and demineralised samples in Figure 7-15 and 7-16 respectively.

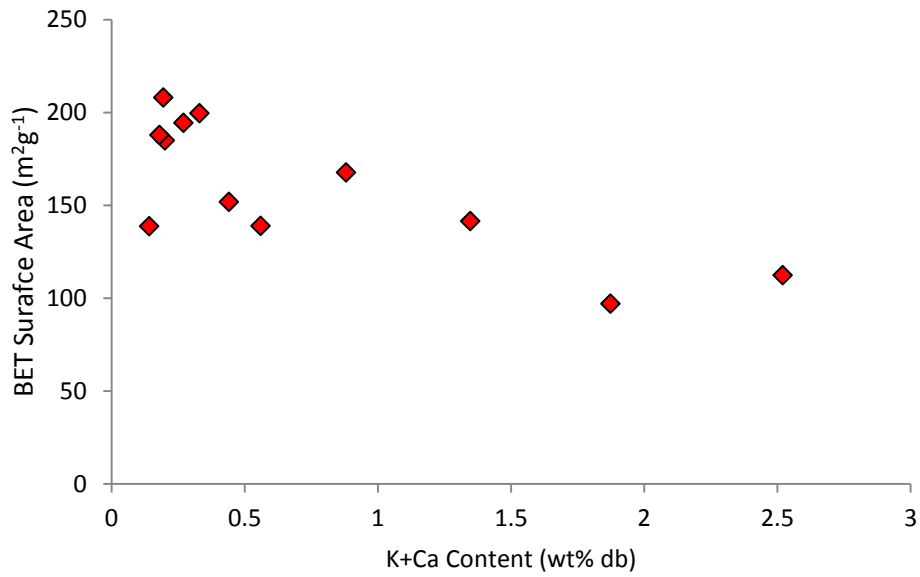


Figure 7-15 DTF Char BET Surface Area vs. K+Ca Content for Non-demineralised Fuels

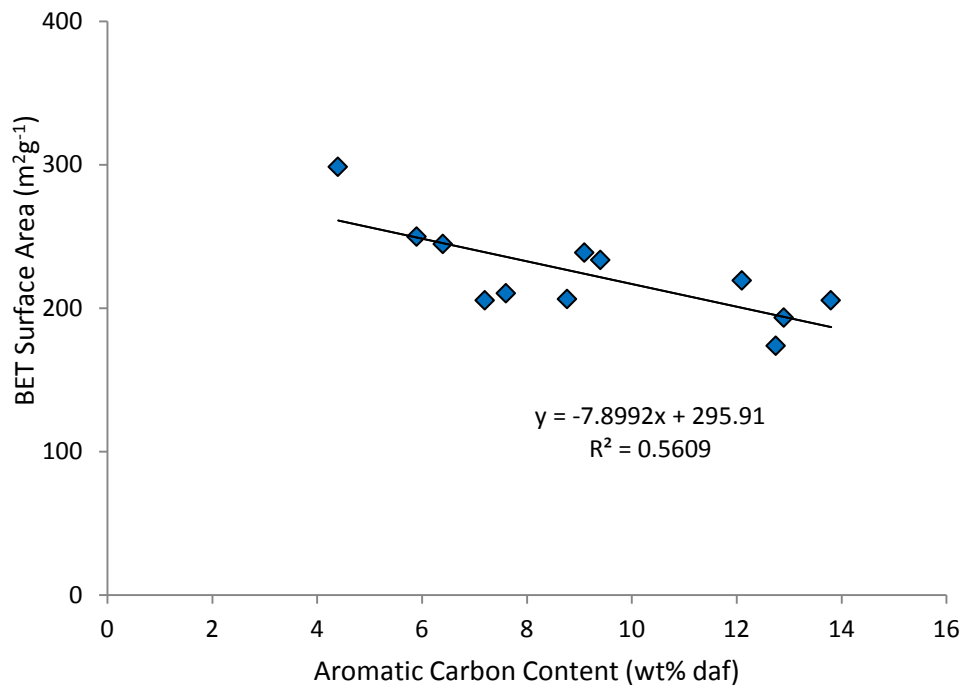


Figure 7-16 DTF Char BET Surface Area vs. Aromatic Carbon Content for Demineralised Fuels

Char surface area correlates closely with aromatic carbon content in the absence of AAEM mineral interaction, increasing K+Ca content of the fuels acting to suppress the development of char porosity and thus limiting surface area generation during pyrolysis.

These close relations do offer the potential to quantify high heating rate char surface areas given a quantification of aromatic carbon and alkali/alkaline earth mineral content of raw fuels.

If the straight line equation expressed in figure 7-16 is used to calculate the surface area of non-demineralised char anticipated on an ash free basis from quantification of their aromatic carbon content then a theoretical reduction in surface area due to the action of mineral matter alone can be derived by subtracting the calculated surface area from the observed value. These figures are shown in Table 7-4 and Figure 7-17.

Sample	Observed BET Surface Area (m ² g ⁻¹)	Calculated BET Surface Area (m ² g ⁻¹)	Observed - Calculated BET Surface Area (m ² g ⁻¹)
Wheat Straw Pellets	97.0	235.8	-138.77
Delignified Wheat Straw	141.4	254.3	-112.93
Corn Stover Pellets	112.3	222.3	-110.05
Delignified Corn Stover	167.7	268.2	-100.45
Pine Woodchips	184.9	187.6	-2.70
Delignified Pine Woodchips	187.8	223.9	-36.13
Miscanthus Pellets	194.4	203.4	-8.99
Delignified Miscanthus	199.6	253.9	-54.34
Eucalyptus Pellets	138.6	176.5	-37.95
Delignified Eucalyptus	207.9	247.6	-39.72
Mixed Softwood Pellets	138.9	235.0	-96.08
Delignified Mixed Softwood	151.8	246.0	-94.24

Table 7-4 Observed and Calculated DTF Char BET Surface Area

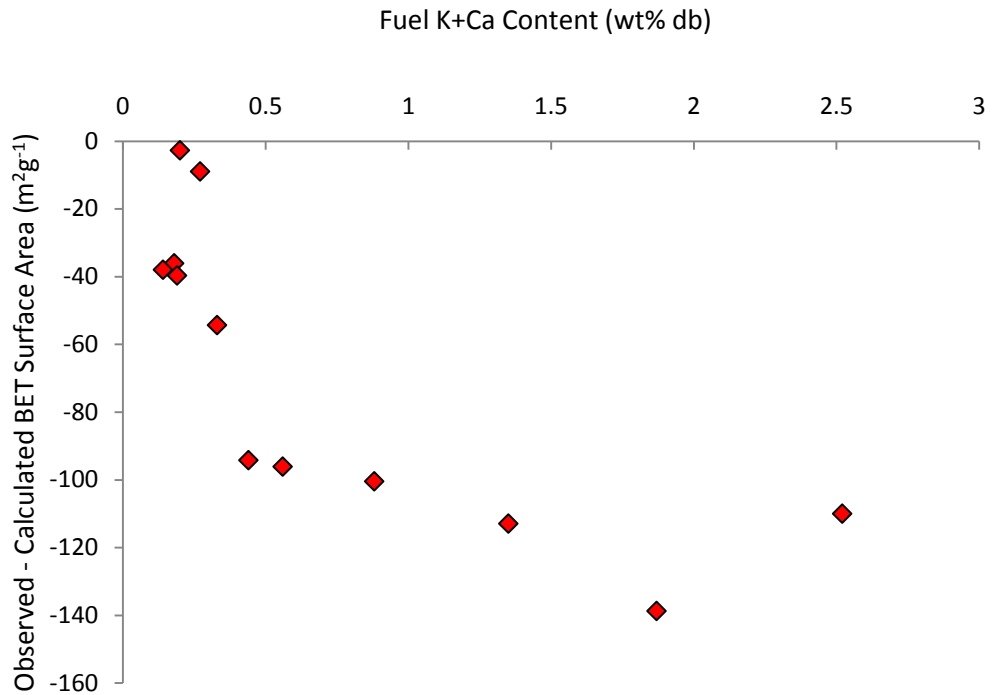


Figure 7-17 DTF Char BET Surface Area Suppression vs. Fuel K+Ca Content

It can be observed that the suppression of surface area is not consistent with increasing K+Ca content, instead being observed to act in a similar manner to that observed for the mineral enhancement of char yield with initial rapid increases in the level of surface area suppression, this increase levelling off at higher AAEM contents. This finding supports the hypothesis that mineral suppression of fluidity development during pyrolysis is linked to its enhancing role of char forming reactions by encouraging bond cleavage and reformation put forward by a number of investigators (Jones et al., 2007; Li et al., 2006; Sathe et al., 1999; Wang et al., 2012). The results presented here are also in line with those reported by De Groot and Shafizadeh, 1984 who postulated that increased char surface area following demineralisation was due principally to the increased formation of mobile phases during pyrolysis which encourages “bubbling” and pore formation. This is evidenced by char morphology images discussed above.

Given that a wealth of literature has shown the ability of alkali/alkaline metal additives to increase biomass char surface areas following pyrolysis some argue that this observable decrease in char surface area with increasing mineral content is due to the blocking of pore surface by molten ash deposits (Lee et al., 2010; Pottmaier et al., 2013). SiO₂ content of the ash has been identified as one of the primary contributors to char pore blockage, although SiO₂ was not measured during this study it is likely that those fuels which contain increased level of total ash and alkali/alkaline minerals will contain significantly more SiO₂ than low ash species and thus may contribute significantly to the observed reduction in char surface area for higher mineral biomass.

The inclusion of torrefied biomass DTF chars in a plot of surface area vs. aromatic carbon as shown in Figure 7-18 indicates that the relation linking these factors for torrefied fuels is not consistent with that reported for non-demineralised samples only. Rather, the BET surface area of torrefied biomass DTF chars follows a consistently shallower relationship with aromatic carbon content regardless of the mineral matter concentration of the torrefied sample. It can thus be concluded that the AAEM influences observed in the suppression of non-demineralised biomass DTF char surface area is not observed for torrefied fuels. This reduction in surface area suppression by AAEMs for torrefied fuels is most likely due to the transformation processes undergone by both organic and inorganic biomass components during torrefaction and may be caused by the overall reduction in polysaccharide derived material.

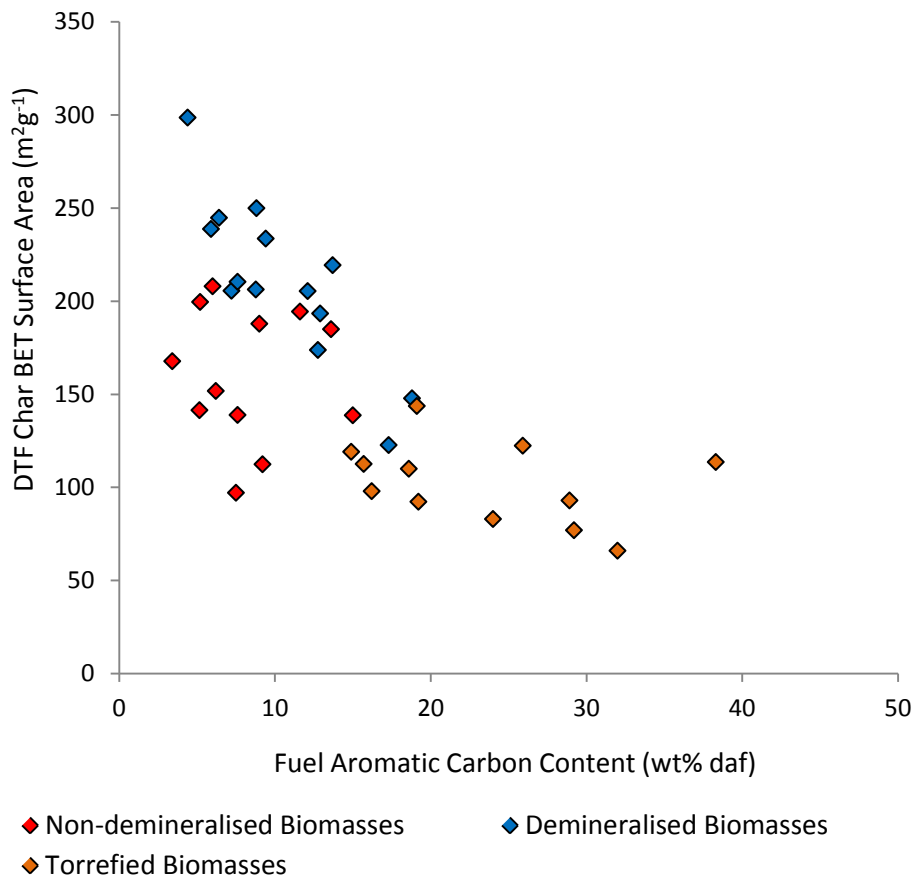


Figure 7-18 DTF Char BET Surface Area vs. Fuel Aromatic Carbon for All Samples

7.3. Summary

Chars generated from raw fuels alongside their demineralised, delignified and isolated lignin analogues under slow and rapid heating regimes have been studied using image analysis and BET surface area determinations to assess the form of the char with regards to its physical characteristics and their influence upon the available surface area of the chars which can be instrumental in determining combustive reactivity.

The findings of this study are summarised as:

- ▶ The form of demineralised raw delignified chars produced under slow heating pyrolysis appear to largely retain their biological structure with obvious cellular

forms present within the char. Little or no fluidity development is observed and no volatile induced porosity can be seen. This is not the case of isolated lignin chars which appear to experience complete softening and fluid intermediate formation to generate solely fused, glassy and solid char forms with few macropores being produced. This is evidenced in the BET surface area analyses of the chars, whereby demineralisation of raw and delignified fuels generates substantial surface area, lignin chars exhibiting very low surface area, similar to those commonly observed for raw fuels

- ▶ Conversely, chars generated under rapid heating DTF pyrolysis generally do exhibit some degree of fluidity development with considerable evolution of macroporosity. In exception to this, high AAEM containing fuels are seen to retain their botanical structure even under the severe environments experienced in the DTF. Following demineralisation all biomass chars showed evidence of having passed through a melt stage during pyrolysis which encouraged the formation of large internal cavities, thinning the walls of the char and enhancing the creation of numerous pores within the char's walls which may be exposed during combustion to enhance surface area with increased conversion of the char.
- ▶ The % of thin walled chars determined via manual point counting has been positively correlated with the BET surface area of the char, confirming the importance of char form in determining the available surface area open to oxygen attack during combustion reactions
- ▶ BET surface area has also been negatively correlated with the aromatic carbon content of demineralised fuels which clearly indicates that the presence of aromatic structures are able to suppress surface area development even when distributed within the lignocellulosic matrix. This is also true of torrefied fuels,

increasing torrefaction temperature resulting in decreases in the BET surface area with increasing aromaticity; however, the slope of this relationship is much shallower than that observed for non-demineralised samples alone. This result is indicative of a reduction in the role of both aromatic carbon and AAEMs in suppressing char surface area development during rapid heating pyrolysis of torrefied materials and may either infer that aromatic structures generated during torrefaction are able to produce chars with a higher degree of surface area or that the overriding dynamic relating BET surface area and aromatic carbon content is non-linear but in fact lies closer to the logarithmic whereby the influence of fuel aromaticity in determining BET surface area decreases with increasing aromatic carbon content.

- ▶ The contribution of AAEM K+Ca content on char surface area suppression has been calculated and is seen to follow a similar trend to that observed for mineral enhanced char yields whereby there are initial, strong increases in the suppression of surface area formation with increasing K+Ca content which level off at higher levels of mineral matter concentration (this occurring at ~2 wt% K+Ca db). This is in similarity to the observed enhancement of char yield with increases in K+Ca content under rapid heating and lends support to a number of studies which propose that alkali driven char yield enhancements also produce more condensed, lower surface area chars. It is hypothesised here that much of this reduction in char surface is linked to the organic source material of the char (either aromatic or polysaccharidal) and their varying mobile phase developments during pyrolysis. These findings are in contrast to those of a number of studies which evidence the role of alkali metal activating agents in generating chars with significantly greater surface area and this contradiction has been discussed.

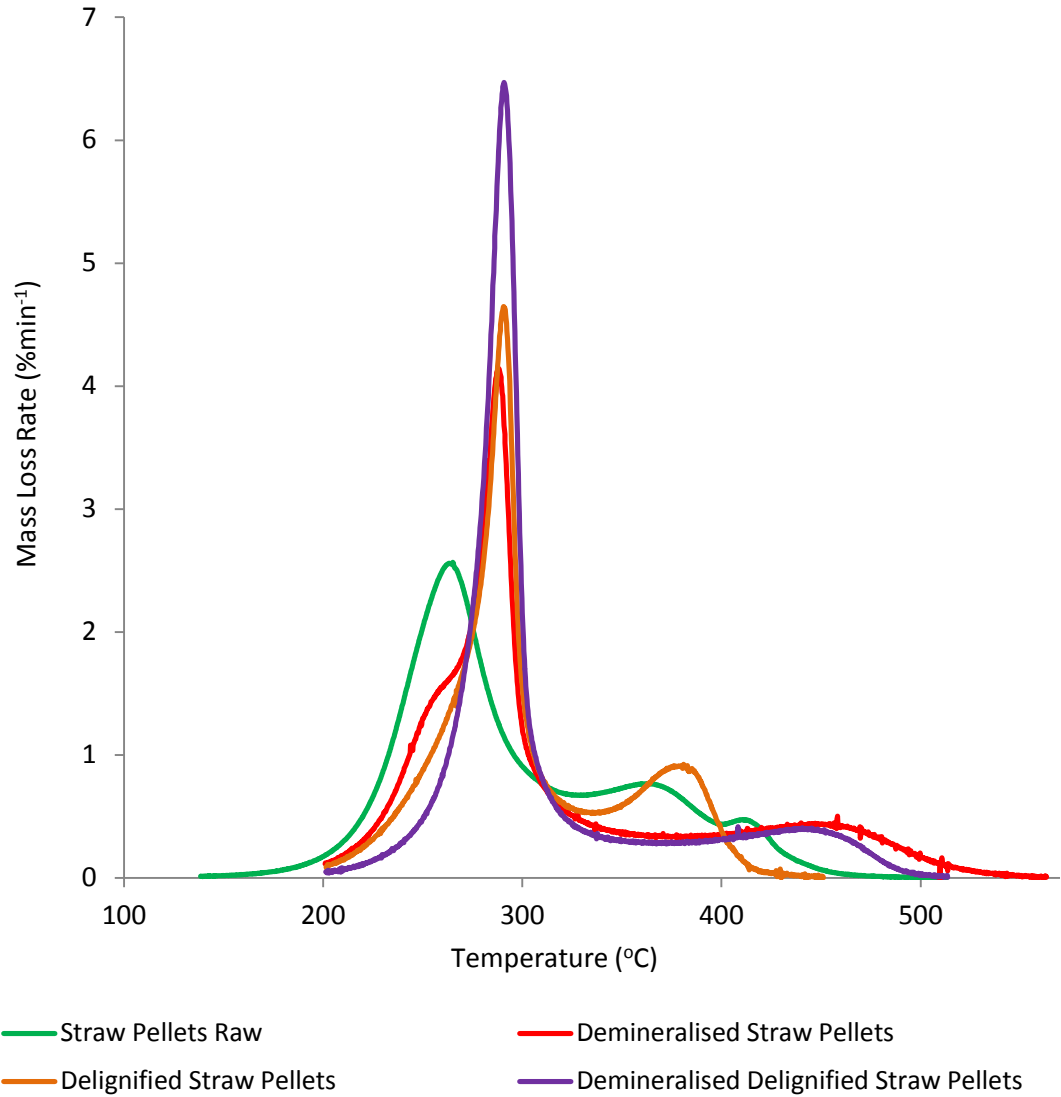
Chapter 8: Combustion Behaviour and Char Reactivity

This chapter evaluates the reactivity of the fuels under investigation using a number of analytical techniques. The rates of combustion reactions under non-isothermal slow heating and isothermal reactivity of chars produced using both slow heating and rapid heating entrained flow pyrolysis are investigated. Differences in the reactivity of fuels following delignification, demineralisation and torrefaction processes are assessed in an effort to gauge the importance of individual fuel compositional parameters in determining the reactivity of the fuels, especially during char oxidation and correlate observed char reactivities with the nature of the chars generated and thus the original composition of the parent fuel.

8.1. Non-Isothermal Combustion TGA

Non-isothermal combustion profiles of the differing fuels have been obtained as a rapid means of initially screening trends in char reactivity. This has been achieved using a TGA with heating rate of $2.5\text{ }^{\circ}\text{Cmin}^{-1}$ as discussed in Chapter 3. The derivative mass loss profiles have been analysed so as to give an appreciation of the temperatures at which peak devolatilisation and char combustion reaction rates occur and assess if extraction of mineral matter and removal of lignin appreciably alter fuel combustion dynamics.

Non-isothermal combustion profiles are shown in Figures 8-1 – 8-8.



Sample	Devolatilisation Peak		Char Conversion Peak	
	Temperature (°C)	Deriv. Weight (%min ⁻¹)	Temperature (°C)	Deriv. Weight (%min ⁻¹)
Raw Wheat Straw Pellets	265.1	2.57	363.1	0.77
Delignified Wheat Straw	290.6	4.65	380.9	0.94
Demineralised Wheat Straw	288.1	4.15	458.2	0.50
Demineralised Delignified Wheat Straw	290.9	6.47	440.6	0.41

Figure 8-1 Wheat Straw Pellet Fraction Non-isothermal Combustion Profiles

The combustion profiles of wheat straw fractions reveal considerable differences in both the devolatilisation and char conversion processes undergone by the respective fuel fractions. Raw wheat straw appears to undergo a relatively broad zone of volatile matter loss between 200 and 300°C with a corresponding peak mass loss occurring at 265.1°C with a rate of 2.57 %min⁻¹. This is followed by a double peak in the char combustion profile with two separate peaks in the combustion rate occurring at 363.1 and 410.6°C respectively. It has been postulated that double peaks in the mass loss rate during biomass char combustion can be attributable to the presence of two distinct char structures formed from the fuel during devolatilisation, this is usually assumed in cases where the composition of the fuel is known to contain several distinct phases (Kastanki and Vamvuka, 2006), such as waste products containing two differing components of the same plant material (i.e. pith and pulp, fruiting body and husk etc.). Although this is logical it does not appear to explain the observed double peak for raw wheat straw pellets which, upon grinding appear to produce a relatively homogeneous fuel with little distinction between any individual sub-components. One potential explanation for this difference in char reactivity is the mal-distribution of mineral components within the raw fuel which may lead to the generation of char particles containing both high and low AAEM contents. Those particles containing appreciable AAEM concentrations will not only produce enhanced char yields of reduced surface area (as demonstrated in Chapters 6 and 7) but those chars which retain higher mineral content are likely to undergo more rapid, catalysed char oxidation processes at lower temperatures than those with reduced mineral contents. This may result in the observation of a double char conversion peak within the non-isothermal combustion profile due to the sequential conversion of char fractions, alkali rich chars undergoing more rapid conversion than those of alkali poor counterparts. This phenomenon may also explain the lack of a double char combustion peak following sample delignification and

demineralisation pre-treatments which remove and redistribute large quantities of ion exchangeable metal species including AAEMs.

Partial demineralisation of the sample alters the thermochemical decomposition pathway significantly; the devolatilisation mass loss peak becomes considerably more distinct over a temperature range of 220 to 320°C. The peak temperature and mass loss rate during devolatilisation are increased considerably to 288°C and 4.15 %min⁻¹ respectively. This increase in peak mass loss is attributable to the increase in temperature at which peak pyrolysis rates occur. An obvious shoulder to the devolatilisation peak is observed at ~250°C which is known to correspond with the decomposition of hemicellulose structures present within the fuel which, given their highly branched nature more easily undergo devolatilisation reactions at reduced temperatures (Yang et al., 2006). The presence of a hemicellulose decomposition peak within the volatile mass loss profile of demineralised wheat straw confirms the viability of the dilute HCl washing procedure utilised throughout the study by verifying that no considerable destruction of hemicellulose structures present within the native lignocellulosic matrix is experienced during mineral extraction. The char combustion peak in the demineralised wheat straw profile is located at a significantly higher temperature of 458.2°C than that of the raw sample and is considerably less intense, with a peak mass loss rate of 0.5 %min⁻¹. These factors clearly indicate a decrease in both the char yield produced following devolatilisation (as indicated in Chapter 6) and char reactivity with the removal of inorganic mineral components.

The mass loss profile of partially delignified wheat straw pellets shows a higher peak mass loss rate of 4.65 %min⁻¹. This increase in the rate of devolatilisation when compared with demineralised wheat straw, temperatures being almost identical (288 and 290°C respectively) is most likely attributable to the removal of a significant

proportion of the thermally stable aromatic lignin components from the parent material and the partial demineralisation which occurs during organosolv fractionation of the parent biomass. By removing aromatic carbon structures the remaining organic matrix is dominated by cellulose fibres which are known to undergo strong, localised devolatilisation reactions over a fairly narrow range of temperatures as exhibited in the above profiles for all samples which have undergone partial delignification by ethanol organosolv fractionation. It is also observed that the hemicellulose shoulder of the devolatilisation profile which is present for partially demineralised wheat straw is removed following organosolv delignification; this is likely due to the loss of hemicellulose components through the considerable hydrolysis reactions known to occur during acid catalysed organosolv pulping processes (Pan et al., 2006). The char combustion rate peak for organosolv delignified wheat straw is located at a temperature of 380.9°C, this being 8°C higher than that of raw wheat straw due to the considerable loss of alkali and alkaline earth mineral species. The peak rate of char conversion is however greater than that observed for the raw sample at 4.65 %min⁻¹ – the increase in char conversion severity may be due to the differences in non-catalysed reactivity of raw and delignified wheat straw which is evidenced by the obvious higher reactivity of demineralised delignified wheat straw pellets over demineralised wheat straw pellets with peak char conversion rates occurring at 440.6°C as opposed to 458.2°C. Coupling this increase in reactivity of the organic char matrix following delignification with the still appreciable AAEM content of delignified wheat straw samples (K+Ca content of 1.35 wt% db) gives rise to a more intense, localised char oxidation peak in the profile.

The combustion profile of corn stover pellets show some commonality with those of wheat straw; the lowest temperature peak devolatilisation rate is achieved by the raw fuel, delignification and demineralisation act to increase the temperature at which peak mass loss rates occur by $\sim 30\text{-}40^\circ\text{C}$.

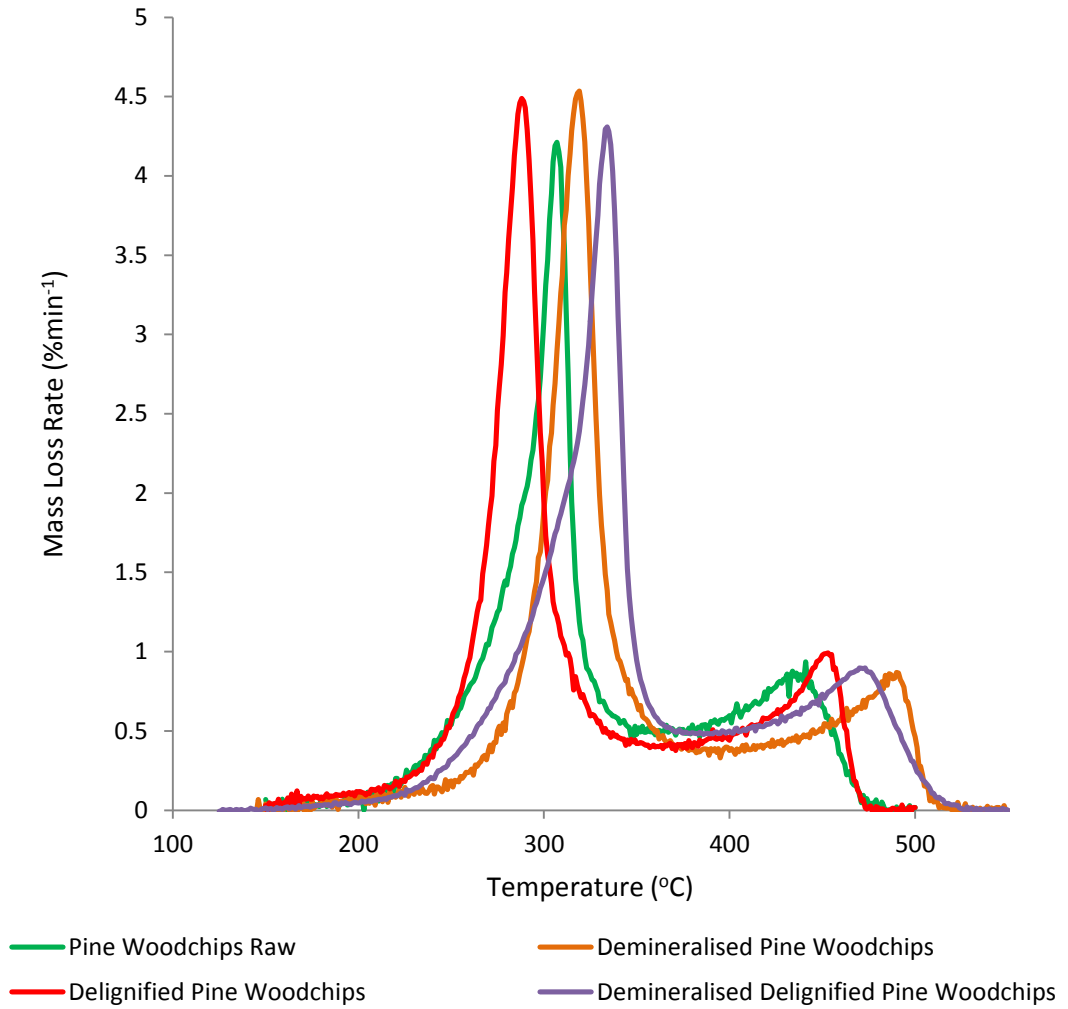
The pyrolysis profile of raw corn stover shows no evidence of a hemicellulose shoulder; instead a steady mass loss appears to occur from $\sim 150^\circ\text{C}$, the most rapid pyrolysis occurs over a relatively large temperature range of $210 - 230^\circ\text{C}$, which is very similar to that observed for wheat straw. The distribution of volatile combustion mass losses for both wheat straw and corn stover over a relatively wide temperature window is once again most likely due to the distribution of AAEM minerals, which are highly concentrated in wheat straw and corn stover, within the organic framework of the fuel. Those portions of the fuel which are rich in AAEMs will undergo catalysed volatilisation; lowering the temperature at which they experience most severe losses in mass. Given the fact that these minerals are not homogeneously distributed results in a large range of localised AAEM concentration within the fuel, thus the characteristic temperature at which devolatilisation occurs is wide ranging, producing an elongated profile of volatile mass loss. In addition to this the overlapping decomposition of hemicellulose, cellulose and lignin within the raw fuel may produce a similar effect.

The mass loss peaks become significantly more defined following demineralisation and delignification, appearing to occur over a reduced temperature window following removal of the majority of active mineral species. This observed increase in peak mass loss is due to the increased temperature at which most rapid volatile mass loss occurs.

The peak mass loss rate of of delignified fuel is greater than that associated with non-delignified analogues primarily due to the higher volatile matter yields obtained from these fuels. Although the removal of mineral matter does shift the temperature at

which maximum char oxidation rates occur for both raw and delignified fuels the char combustion peak for delignified corn stover occurs at lower temperature than the raw fuel. It is thought that this reduction in char combustion temperature is due to the combined effects of removal of thermally stable lignin components, increasing the volatile matter yield and rate of volatile release, enhancing char porosity development, and the fact that delignified corn stover appears to retain an appreciable quantity of AAEMs.

It can again be observed that peak char combustion rates occur at lower temperatures for demineralised delignified corn stover samples as opposed to the demineralised raw fuel, this being indicative of an increase in the char reactivity following the removal of lignin derived aromatic carbon in the absence of significant mineral catalysis, being most likely driven by alteration of the char surface area.

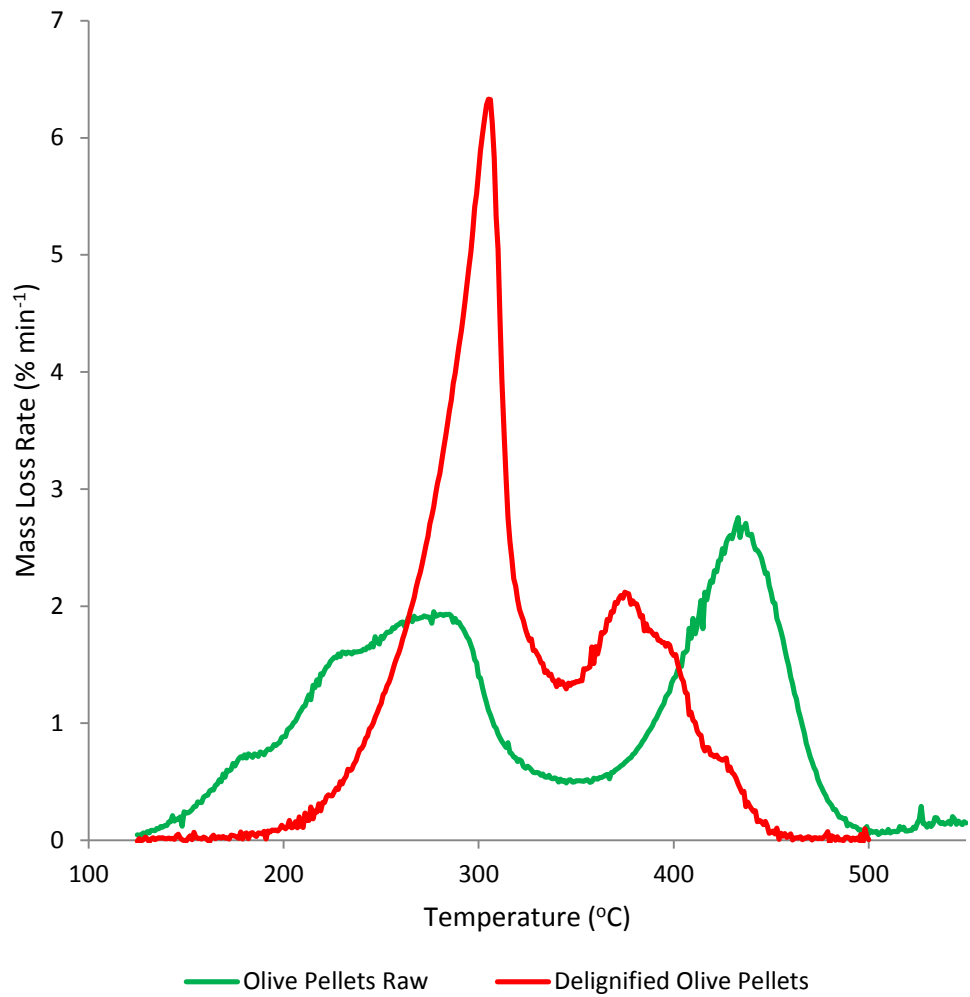


Sample	Devolatilisation Peak		Char Conversion Peak	
	Temperature (°C)	Deriv. Weight (%min ⁻¹)	Temperature (°C)	Deriv. Weight (%min ⁻¹)
Raw Pine Woodchips	307.2	4.20	441.6	0.94
Delignified Pine	288.5	4.49	453.4	0.99
Demineralised Pine	319.7	4.54	490.8	0.87
Demineralised Delignified Pine	334.6	4.31	473.8	0.90

Figure 8-3 Pine Woodchip Fraction Non-isothermal Combustion Profiles

The combustion profiles of pine woodchip fractions are considerably more consistent than those of either wheat straw or corn stover, this being most likely due to the considerably lower active mineral matter content of pine wood in comparison to these fuels. Delignification in this case acts to lower the temperature associated with peak volatile mass losses, this may be indicative of somewhat greater lability of delignified pine to pyrolysis over the raw fuel or the activity of minerals removed during the delignification process.

Demineralisation again increases the characteristic temperatures of peak devolatilisation and char oxidation for both raw and delignified pine, demineralised delignified woodchip char oxidation occurring at lower temperature than demineralised raw fuel, this being attributable to the theorised lower reactivity of char derived from more aromatic rich fuels.

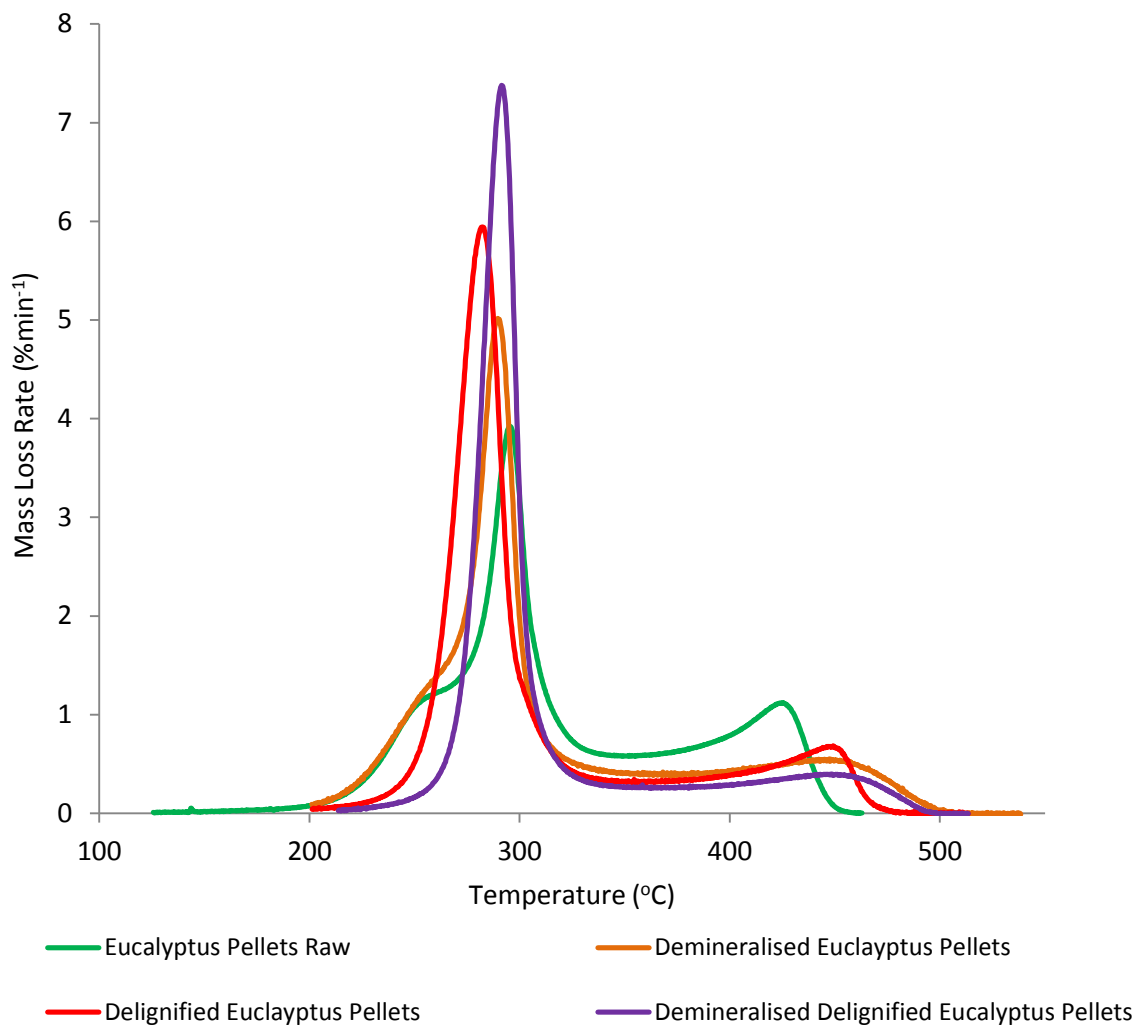


Sample	Devolatilisation Peak		Char Conversion Peak	
	Temperature (°C)	Deriv. Weight (%min ⁻¹)	Temperature (°C)	Deriv. Weight (%min ⁻¹)
Raw Olive Cake Pellets	285.4	1.93	437.6	2.71
Delignified Olive Cake Pellets	305.1	6.33	375.9	2.12

Figure 8-4 Olive Cake Pellet Fraction Non-isothermal Combustion Profiles

The combustion profiles of raw and delignified olive cake pellets are unique amongst the fuels sampled with peak rates of conversion for raw olive being achieved during char combustion as opposed to volatilisation. This is likely due to the different chemical makeup of olive cake which predominantly contains the hard olive stones and more heterogeneous fleshy tissue materials, both of which contain low levels of structural polysaccharide material and are high in lignin like compounds. This leads to a reduction in the mass loss during pyrolysis which occurs over a wider temperature window due to the differing reactivities of chemical side groups, the loss of which drives the devolatilisation process (this is in similarity to the combustion of isolated lignin compounds – profiles being shown in Figure 8-7). This increases the importance of char oxidation process in determining the dynamics of the fuel during combustion.

On demineralisation olive becomes less reactive to devolatilisation, however, the bulk of mass loss during conversion is shifted from the char combustion to the devolatilisation phase due to the loss of mineral matter enhanced charring which lowers the total char yield. The char reactivity of delignified olive pellets is considerably higher than the raw fuel, occurring at significantly lower temperatures. This may be due to the combined influence of increases in volatile matter yield which encourages the formation of active char surface area and the removal of mineral matter during delignification – in order to explain this phenomenon the phosphorous content of the fuel has been determined and is relatively high (0.46 wt% db), phosphorous being known to be active in the inhibition of char oxidation processes (Fuentes et al., 2008).

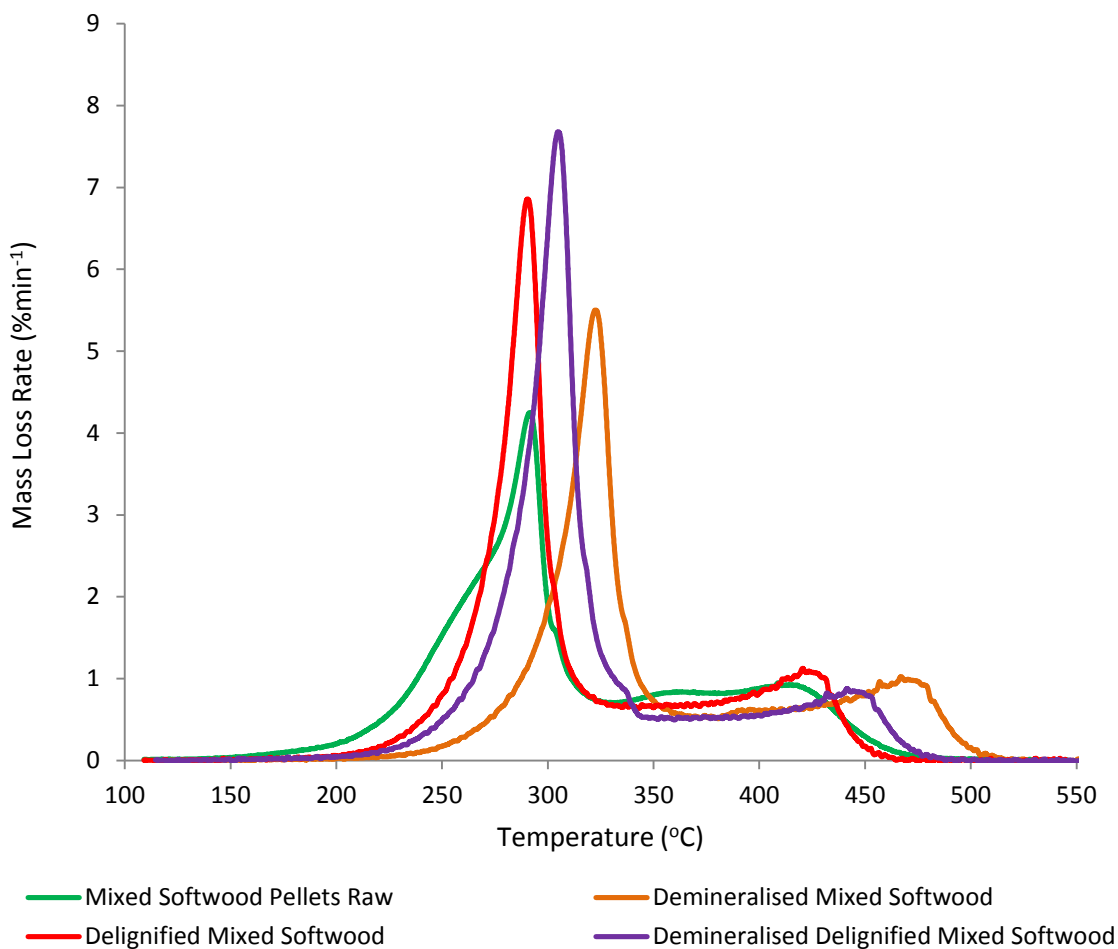


Sample	Devolatilisation Peak		Char Conversion Peak	
	Temperature (°C)	Deriv. Weight (%min ⁻¹)	Temperature (°C)	Deriv. Weight (%min ⁻¹)
Raw Eucalyptus Pellets	295.4	3.92	425.2	1.12
Delignified Eucalyptus	282.7	5.94	449.3	0.68
Demineralised Eucalyptus	289.6	5.02	447.4	0.55
Demineralised Delignified Eucalyptus	291.5	7.38	448.2	0.40

Figure 8-5 Eucalyptus Pellet Fraction Non-isothermal Combustion Profiles

The combustion profiles of all delignified and demineralised eucalyptus pellet samples show increased devolatilisation reactivity of the samples and reduced peak mass loss temperatures for devolatilisation when compared to the raw feedstock. This change is in contrast to the majority of other biomass samples which show a generally increasing trend in devolatilisation peak mass loss temperatures following loss of mineral matter either through organosolv pulping or HCl demineralisation practices. This effect is thought to be due to the competing influences of K and Ca on the reactivity of biomass to devolatilisation. Raw eucalyptus pellets contain very low alkali/alkaline earth mineral content, however this content is dominated by Ca with 0.09 wt% db as opposed to K with only 0.05. Loss of mineral matter thus results in the preferential removal of Ca (in fact calcium tends to concentrate in the delignified organosolv residue with Ca content of 0.19 wt% db). It has been reported in the literature that similar removal of Ca has resulted in some cases to a similar decrease in the temperature of peak devolatilisation mass loss rate (Jiang et al., 2013) which indicates an inhibitory effect of Ca minerals on the devolatilisation process.

The trend observed for eucalyptus fraction char conversion reactions is common to that of pine, corn stover and wheat straw fuels with raw biomass chars being considerably more reactive than delignified analogues, demineralisation increasing the temperature associated with peak char combustion rates. In this case the demineralised delignified and demineralised raw fuels show very similar char oxidative reactivities.



Sample	Devolatilisation Peak		Char Conversion Peak	
	Temperature (°C)	Deriv. Weight (%min ⁻¹)	Temperature (°C)	Deriv. Weight (%min ⁻¹)
Raw Mixed Softwood Pellets	291.4	4.25	408.9	0.95
Delignified Mixed Softwood	291.5	6.79	396.9	0.83
Demineralised Mixed Softwood	322.4	5.50	467.0	1.05
Demineralised Delignified Mixed Softwood	304.6	7.67	434.0	0.409

Figure 8-6 Mixed Softwood Pellet Fraction Non-isothermal Combustion Profiles

Mixed Softwood pellet combustion profiles show similar trends with demineralisation increasing the temperatures at which both peak devolatilisation and char oxidation occur. The char combustion profile of raw softwood shows a lengthy, even char oxidation profile with demineralisation causing char oxidation to occur over a narrower band of higher temperatures due to the removal of catalytic effects which will alter the rate of individual particle combustion rates depending upon the distribution of AAEM species across the sample. This can give rise to varied reactivity of char particle depending upon their individual content mineral content which causes each to combust at a different temperature giving the burning profile an elongated appearance.

Again demineralised delignified char reacts at a lower temperature than the demineralised raw analogue with a 33°C difference in the temperature of peak oxidation.

The combustion profiles of lignin have also been determined and are shown in Figure 8-7.

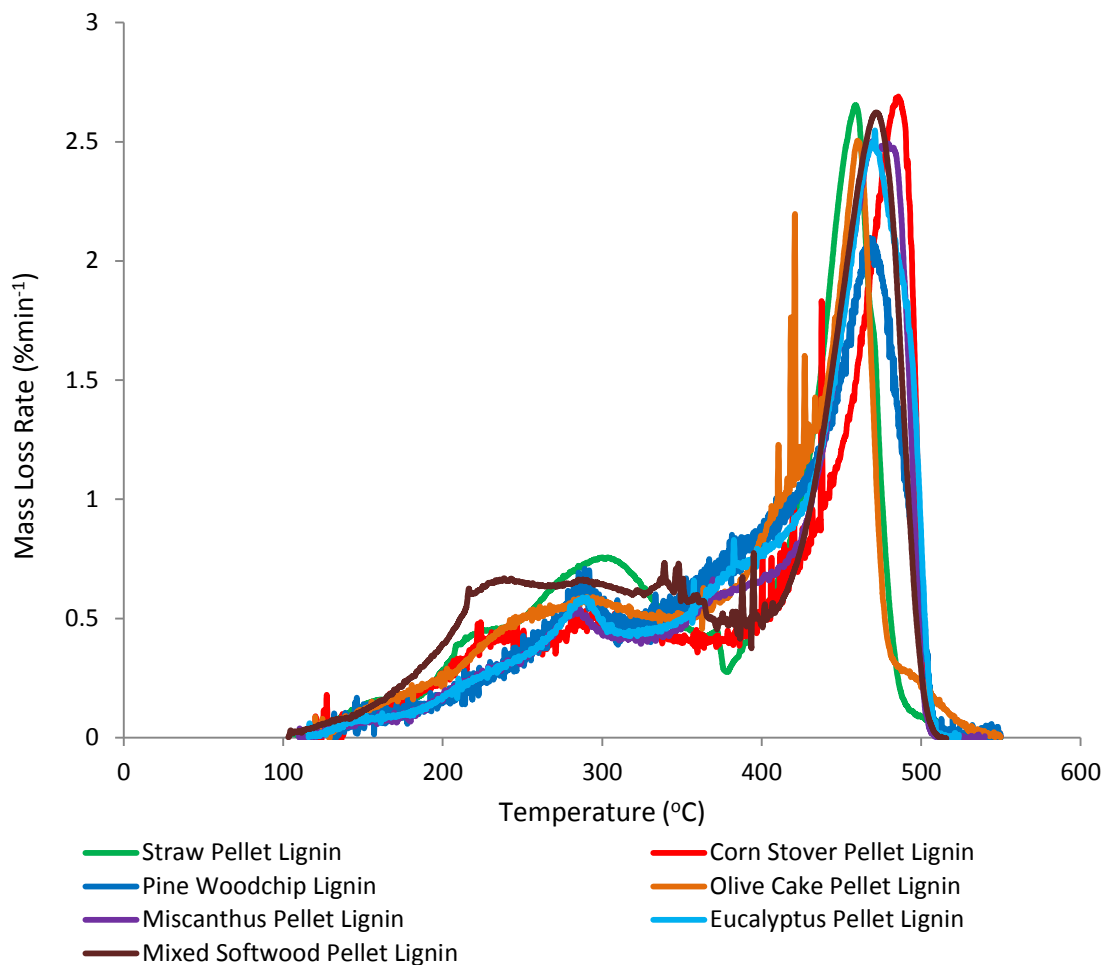


Figure 8-7 Lignin Non-isothermal Combustion Profiles

Lignin combustion profiles differ from raw and delignified fuels due to its differing structural composition. Whereas the profiles of whole fuels show clear volatile combustion and char oxidation stages the profile of isolated lignins show a gradual volatile loss on heating from 100°C which is far less rapid (average peak volatile combustion rates being only 0.509 wt%min⁻¹ for all lignins). This reduction in the rate of volatile loss is caused by the dramatically reduced total levels of volatile matter evolved for lignin (as evidenced in Chapter 6) and the nature of lignin pyrolysis which occurs via the loss of varied lignin side chain functionalities which, due to their highly varied chemical nature, are evolved at a broad range of temperatures. This in contrast to raw

fuel devolatilisation, where the bulk of mass loss occurs through decomposition of relatively homogenous polysaccharidal material which contributes the bulk of volatile matter.

The increased char generation from lignin fuels increases the importance of the char conversion phase and this is seen in far greater char oxidation mass losses as a portion of the mass of the fuel for lignins (averaging $2.49 \text{ wt}\% \text{min}^{-1}$ for all lignin samples). In addition to this the reactivity of lignin derived chars appear to be considerably less than that of demineralised raw and delignified fuel analogues with peak char oxidation rate being reached at 482.4°C on average, much higher than other demineralised samples.

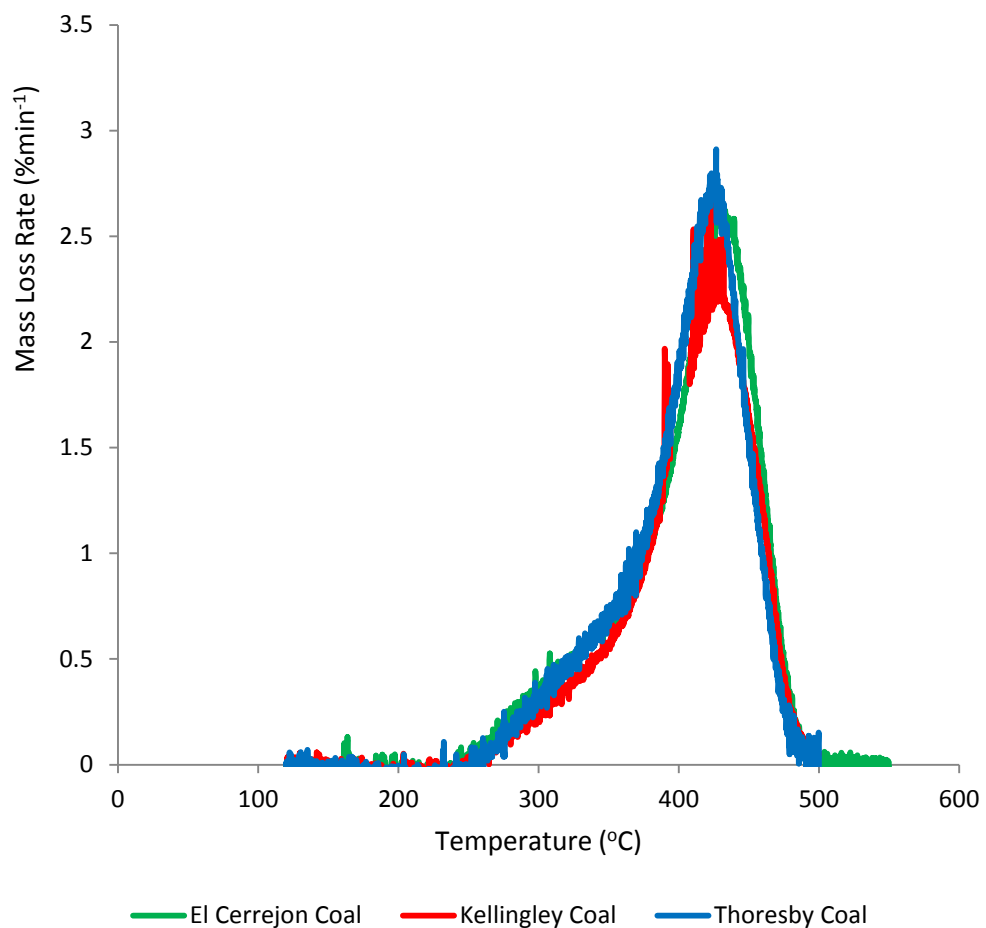


Figure 8-8 Reference Coal Non-Isothermal Combustion Profiles

The burning profiles of coals obtained using the TGA show little or do differentiation between devolatilisation and char combustion reactions with both volatile and char combustion occurring simultaneously over a relatively wide temperature window. This trend has been observed previously by Moran et al., 1986 who observed that, although it was impossible to recognise or extrapolate any kinetic parameter for individual conversion process during the slow heat combustion of coal in the TGA the profile and characteristic ignition, peak conversion rate and time to reach 90% conversion could all be used as a simple, rapid analysis of the combustion reactivity of the coal in question. This being the case the above profiles should give some clear indication of the relative reactivity of the reference coals utilised, however, due to the very low heating rate applied ($2.5\text{ }^{\circ}\text{Cmin}^{-1}$) all three coals react in an almost identical manner. Given the similarity in their combustion profiles it was determined to utilise only one reference coal for DTF testing, Kellingley coal being chosen for analysis.

There are a number of general trends observable in the above combustion profiles of lignocellulosic biomass samples. The difference in devolatilisation behaviour observed between raw, delignified, demineralised and demineralised delignified samples are summarised in the following statements:

- ▶ Where considerable mineral matter content is present, demineralisation of the biomass gives rise to a decrease in the reactivity of the fuel with respect to devolatilisation with consequent increases in the temperature at which maximum devolatilisation mass loss rates are observed
- ▶ The intensity of the devolatilisation mass loss peak tends to increase significantly with both demineralisation and delignification of the biomass. For delignified fuels this is due to the concentration of cellulose in the sample at the expense of lignin. In the case of sample demineralisation this is attributable

both to a decrease in the char yields generated and the removal of any catalytic influence of alkali/alkaline earth mineral species on localised devolatilisation processes which are seen to produce a prolonged volatile combustion profile across an extended range of temperatures

- ▶ Char conversion is heavily catalysed by presence of AAEM species, demineralisation acting to significantly increase the temperature of char combustion even where the initial concentration of active minerals is fairly low. The possibility of this reduction in char reactivity being due to the removal of hemicellulose has been largely discounted; a number of demineralised samples show clear hemicellulose shoulders in the combustion profile even where these are dominated by overlapping mineral catalysed cellulose decomposition in the raw fuel
- ▶ In all cases the demineralised delignified samples produced chars of greater reactivity than demineralised raw fuels during non-isothermal combustion, undergoing char peak char conversion at appreciably lower temperatures. Given that significant mineral interactions have been discounted due to the very low levels of mineral matter remaining in demineralised fuels this has been attributed to the reduced reactivity of lignin chars which have been shown to combust at far higher temperature than that of demineralised whole fuels or their delignified analogues

Overall the screening of samples using non-isothermal TGA methods has revealed that both demineralisation and delignification practices greatly alter the reactivity of lignocellulosic fuel chars to the point that they are likely to significantly influence char reactivity under PF firing conditions. As such an investigation into the influences of lignin derived aromatic carbon and mineral matter on simulated PF firing chars was continued using the same set of fuel samples.

8.2. Isothermal Char Reactivity of HTF Chars and

Assessment of Lignin Reactivity

As it proved impossible to produce very high heating rate chars in the DTF using lignin samples, due to their softening behaviour at low temperature, slow heating rate experiments have been conducted using a horizontal tube furnace (HTF) to generate chars using pure lignin samples and demineralised raw and delignified analogues for corn stover pellet and pine woodchip fuels. The reactivity and characteristics of lignin chars generated in the HTF have been assessed against that of respective raw and delignified counterparts allowing an assessment of the likely influence of increased lignin content on char combustion performance of the parent fuel in the absence considerable of mineral matter catalysis.

Burnout profiles are shown in Figures 8-9 and 8-10.

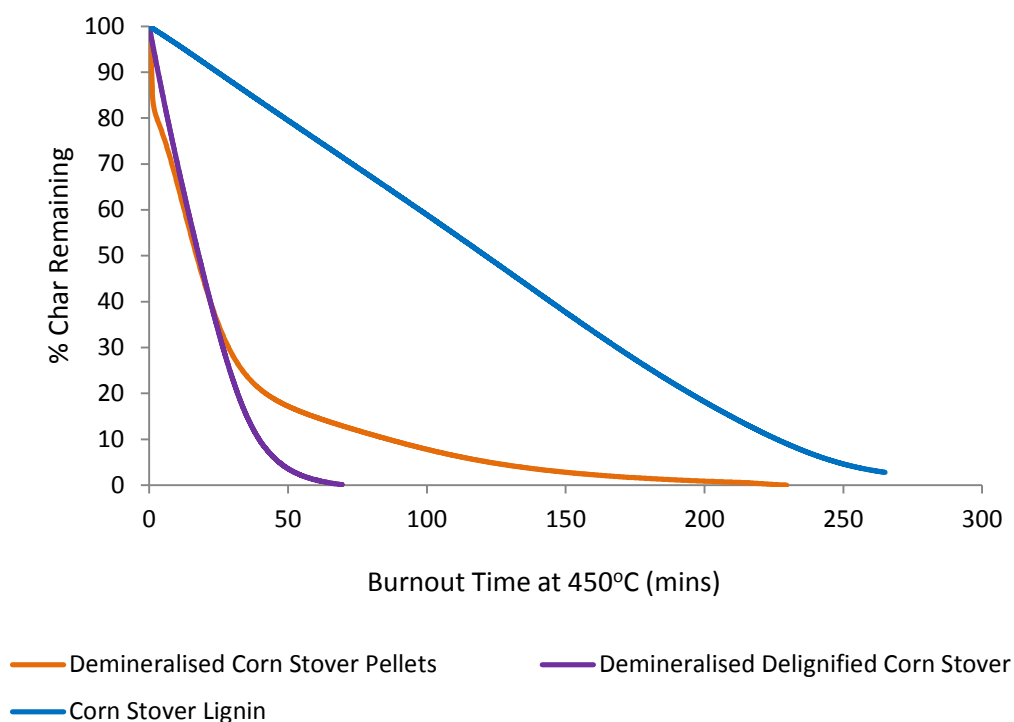


Figure 8-9 Char Burnout Profiles for Demineralised Corn Stover Fraction HTF Chars

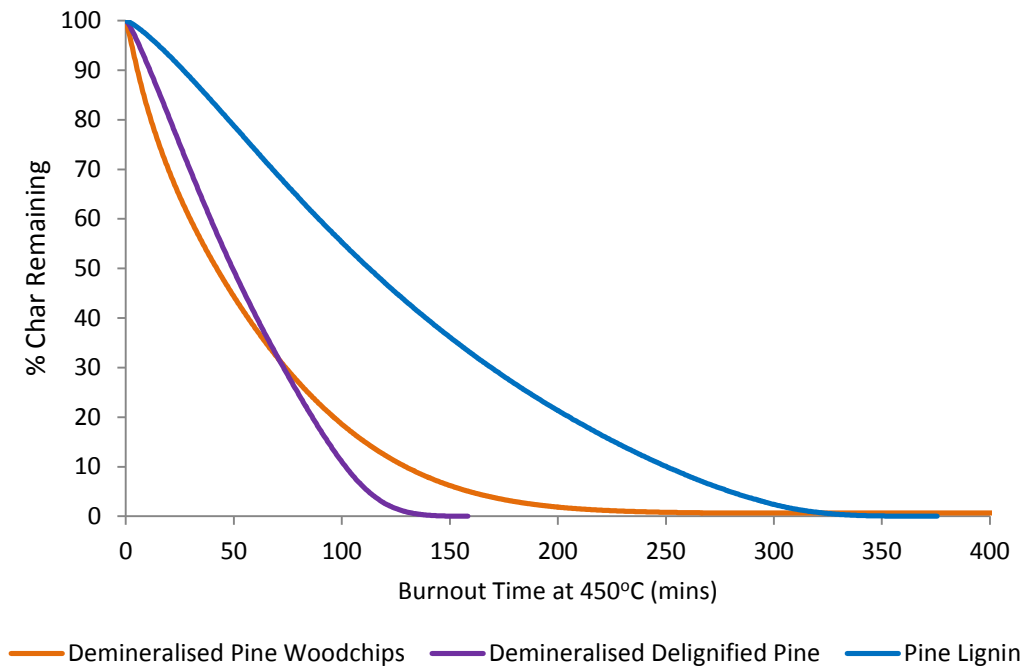


Figure 8-10 Char Burnout Profiles for Demineralised Pine Woodchip Fraction HTF Chars

For both demineralised corn stover and pine fraction chars generated in the HTF the lignin char is observed to be the least reactive by a substantial margin taking over 200 minutes to reach 90% conversion under isothermal combustion conditions at 450°C. Demineralised delignified fuels are somewhat more reactive than their demineralised raw counterparts and this has been attributed to the removal of lignin derived aromatic carbon which produces char of significantly reduced activity due principally to the reduction in porosity and surface area following the formation of a melt during pyrolysis and charring reactions (although lignin char does also appear to contain a reduced quantity of oxygen in comparison to other chars).

The relative fractional weight conversion factor, α has been calculated using equation 8.1 below:

Equation 8.1

$$\alpha = \frac{m_o - m_t}{m_o - m_f}$$

Where α is the fraction weight conversion factor ranging from 1 for no conversion to 0 for full conversion, m_o is the total initial mass of the char sample prior to combustion, m_t is the mass of char remaining at time t and m_f is the final mass following full conversion of combustible fractions within the char sample (i.e. the ash content)

α is used to trace the combustion of the char regardless of quantity of char utilised and thus provides a valid comparison of char reactivities between fuels with varying char yields.

Using the above characteristic char burnout profiles both the time to reach 90% char conversion (t_{90}) and the apparent first order rate constant (k_a) have been derived by applying first order kinetics for char conversion between 5 and 95%, k being determined graphically from the gradient of a plot of $-\ln(1-\alpha)$ versus t .

In addition to this, following conversion of the reaction rate constant to a carbon consumption rate constant by compensating for the partial pressure of oxygen the activation energy (E_a) and pre-exponential function (A) were derived using Arrhenius plots of $\ln k_a$ vs. $1/T$ as described in Section 3.4.1..

Apparent kinetic parameters of HTF char derived from isothermal combustion results are shown in Table 8-1.

Sample	Ea (kJmol ⁻¹)	A (min ⁻¹ AtmO ₂ ⁻¹)	t90 (mins)	k _{a450} (min ⁻¹)
Demineralised Corn Stover Pellets	77.1	3.12x10 ⁵	86.1	0.0243
Demineralised Delignified Corn Stover	67.6	3.12x10 ⁵	39.6	0.0532
Corn Stover Lignin	139.3	7.36x10 ⁷	226.1	0.0092
Demineralised Pine Woodchips	143.1	5.27x10 ⁹	142.7	0.0151
Demineralised Delignified Pine	134.5	4.09x10 ⁹	134.5	0.0161
Pine Lignin	163.1	2.66x10 ¹⁰	250.2	0.0086

Table 8-1 HTF Char Isothermal Combustion Kinetic Parameters

As anticipated the 90% conversion time increases with increasing aromatic carbon content for demineralised fuels, glassy lignin chars exhibiting extended burnout times in comparison to other fuels. The bulk of this difference in apparent char reaction rate is likely due to the differences in char surface area of slow heating chars which appears to be driven by the aromaticity of the fuel, reactivity decreasing in the order demineralised delignified fuel > demineralised fuel >>> isolated lignin. The activation energy required for combustion is also higher for lignin chars due to their condensed, unreactive nature.

8.3. Isothermal Char Reactivity of Rapid Heating DTF Chars

The following Figures 8-11 to 16 show plots of the conversion of chars generated under simulated PF rapid heating entrained flow pyrolysis conditions in the DTF.

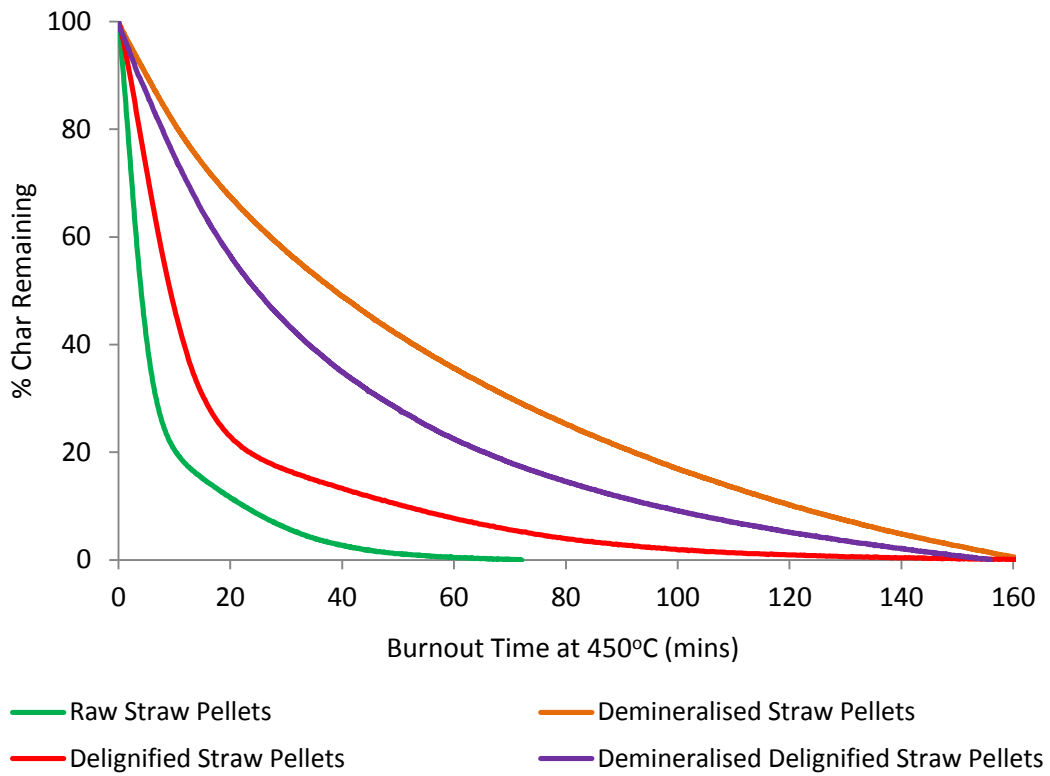


Figure 8-11 Char Burnout Profiles for Wheat Straw Pellet Fraction DTF Chars

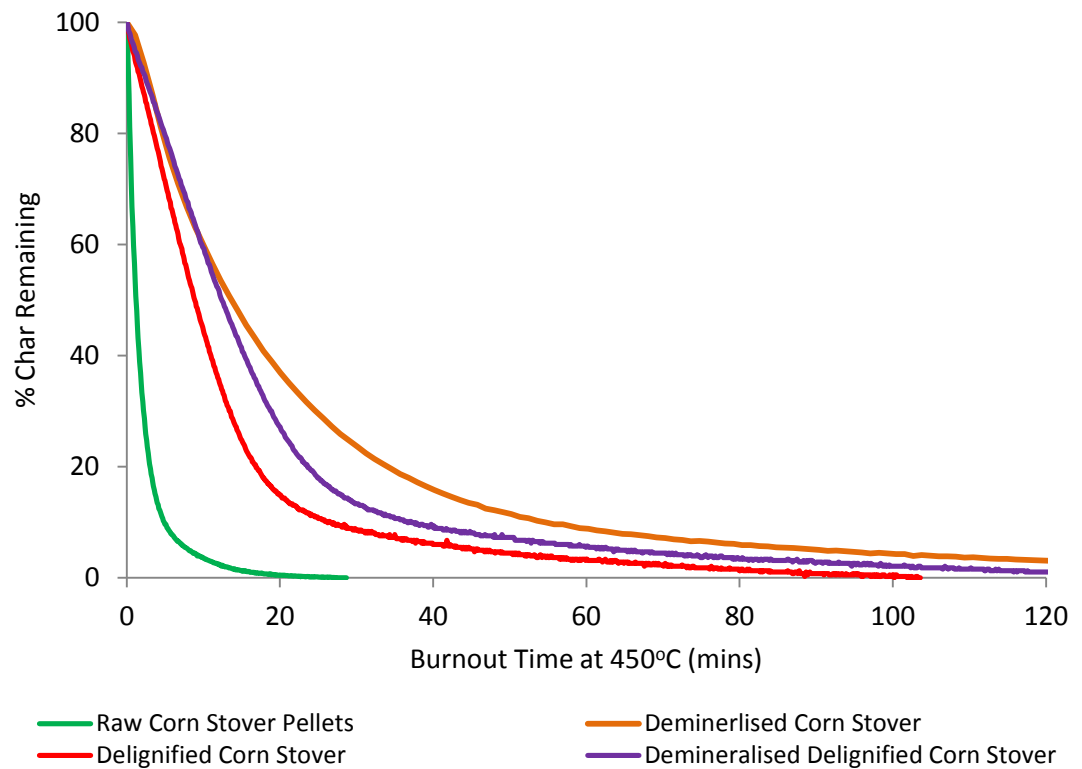


Figure 8-12 Char Burnout Profiles for Corn Stover Pellet Fraction DTF Chars

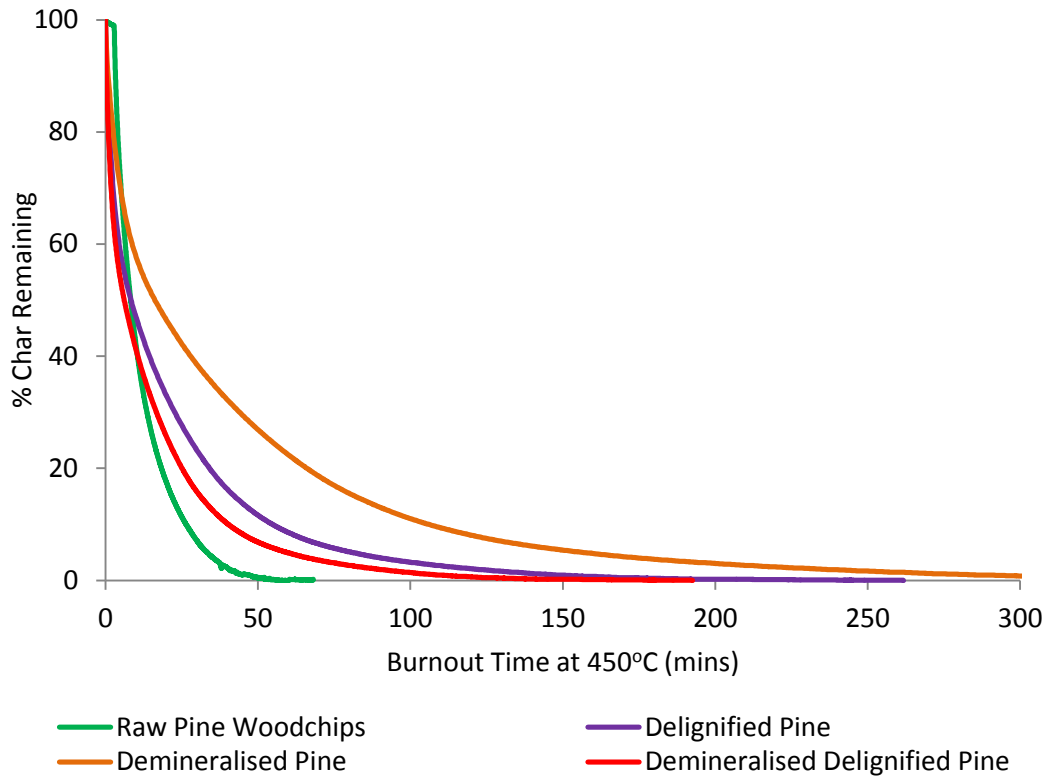


Figure 8-13 Char Burnout Profiles for Pine Woodchip Fraction DTF Chars

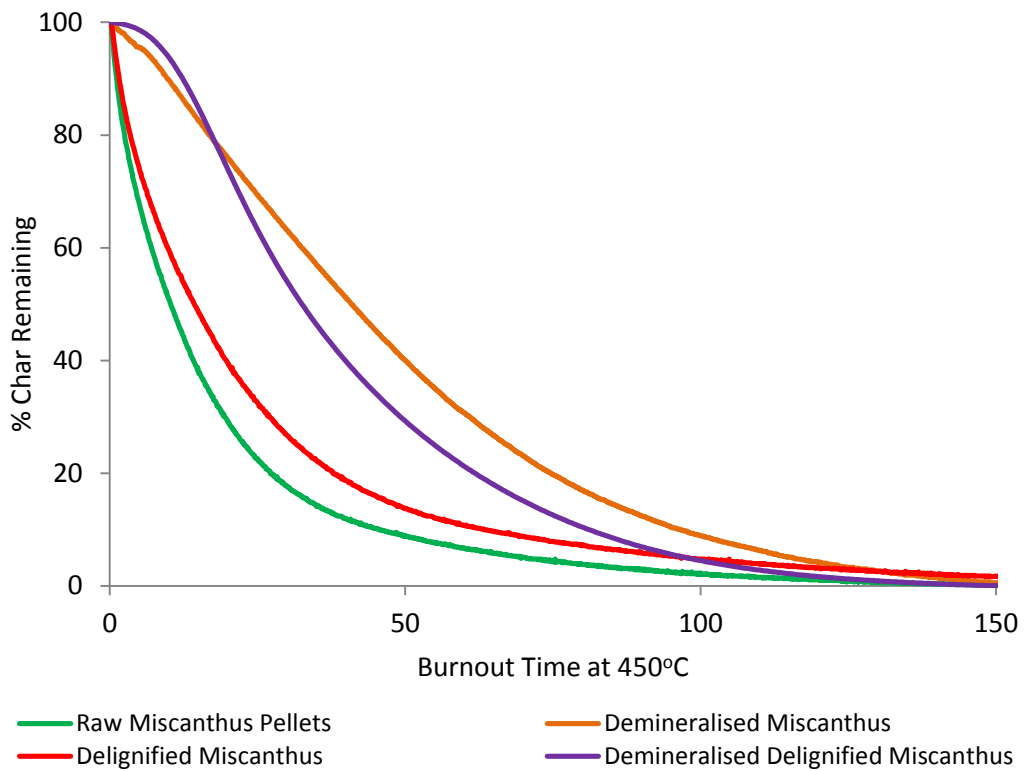


Figure 8-14 Char Burnout Profiles for Miscanthus Pellet Fraction DTF Chars

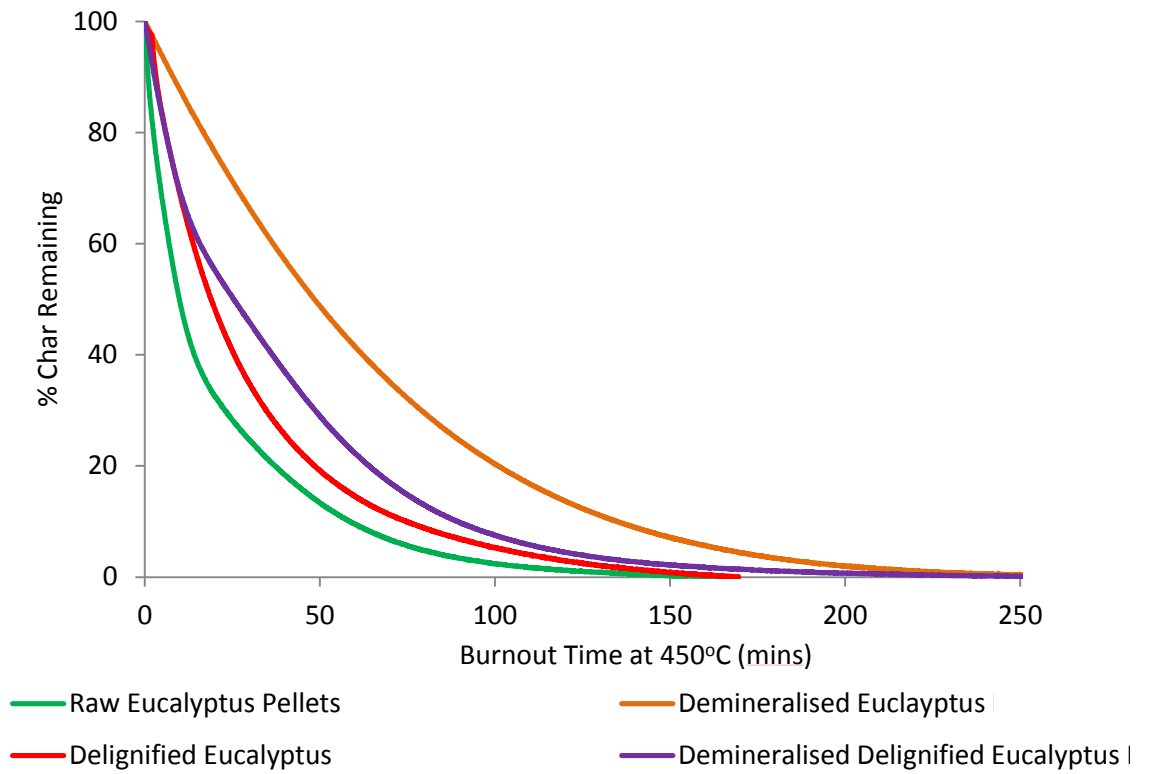


Figure 8-15 Char Burnout Profiles for Eucalyptus Pellet Fraction DTF Chars

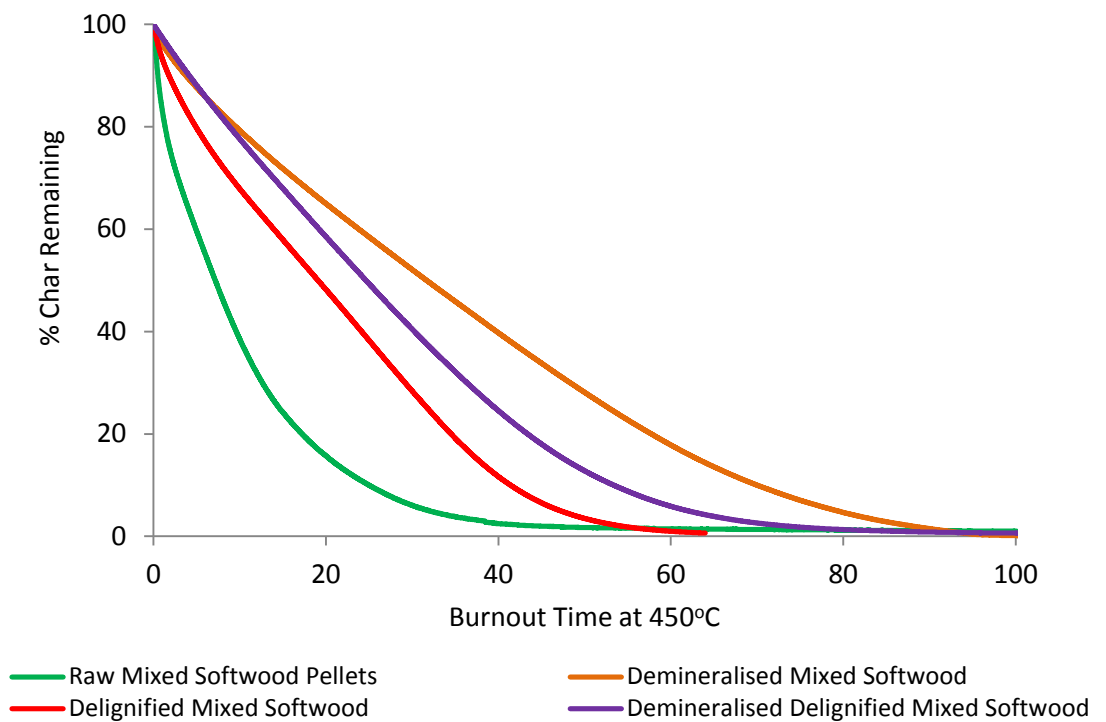


Figure 8-16 Char Burnout Profiles for Mixed Softwood Pellet Fraction DTF Chars

Apparent pseudo first order kinetic parameters have been established for DTF chars similarly to HTF chars, Arrhenius plots of $\ln k_a$ vs. reciprocal temperature being shown in Figures 8-17 – 8-28 for all fuels.

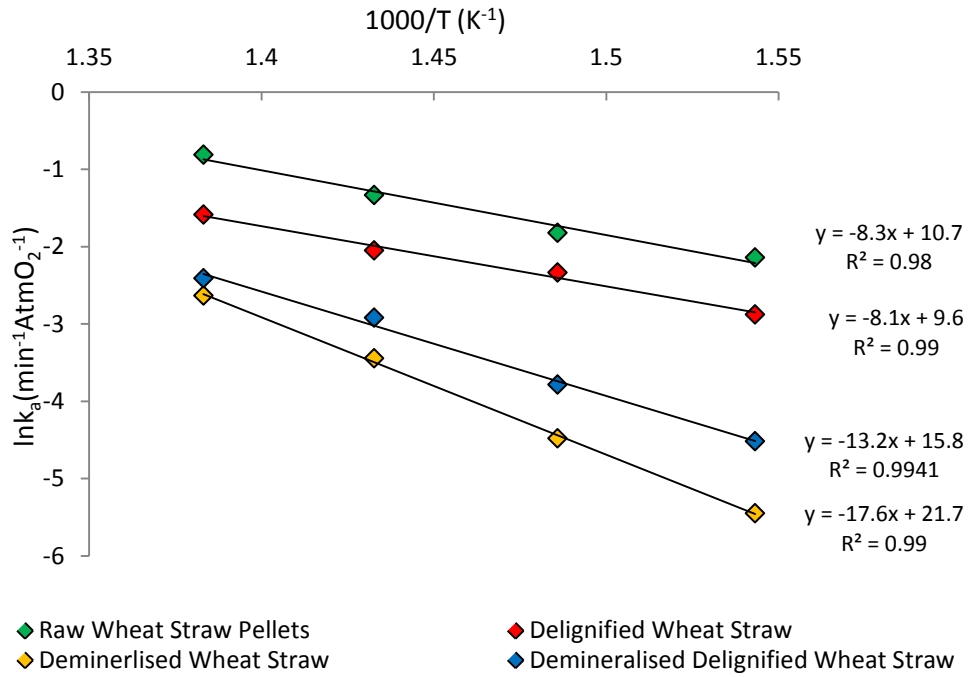


Figure 8-17 Arrhenius Plots for Wheat Straw Pellet Fraction DTF Chars

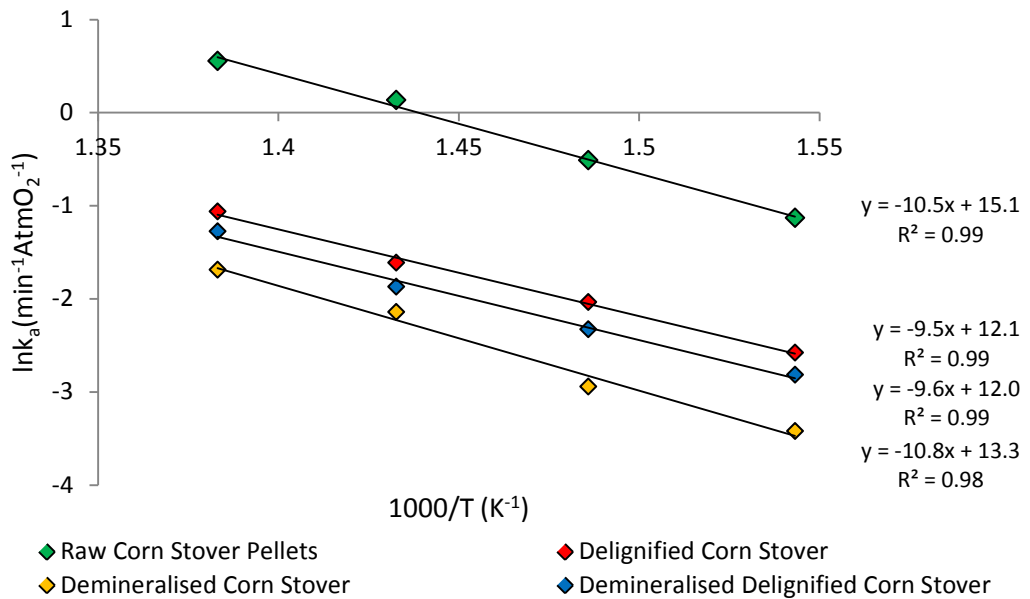


Figure 8-18 Arrhenius Plots for Corn Stover Pellet Fraction DTF Chars

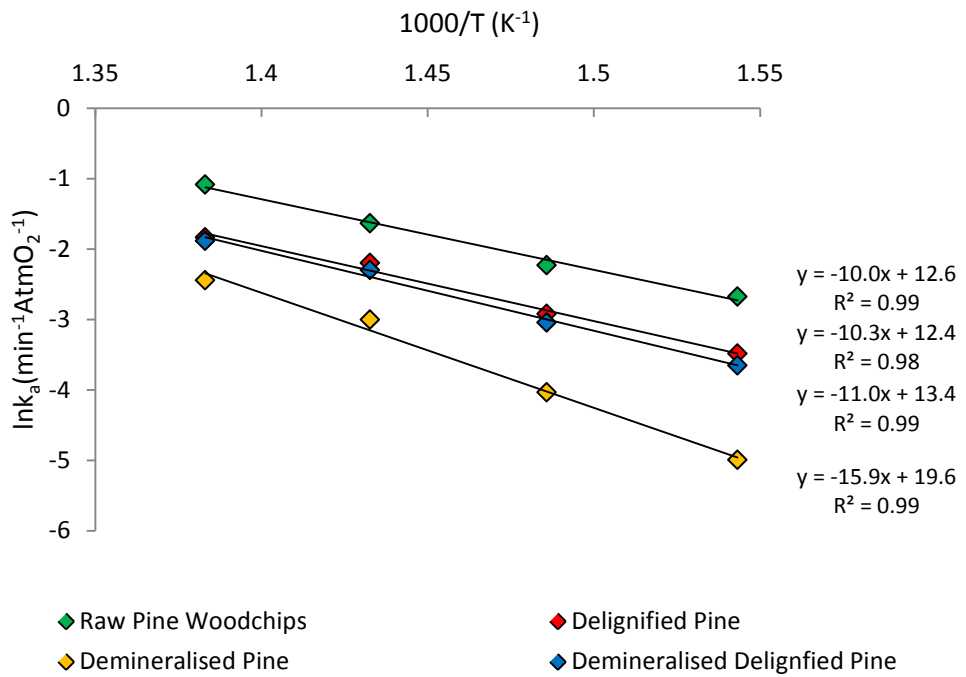


Figure 8-19 Arrhenius Plots for Pine Woodchip Fraction DTF Chars

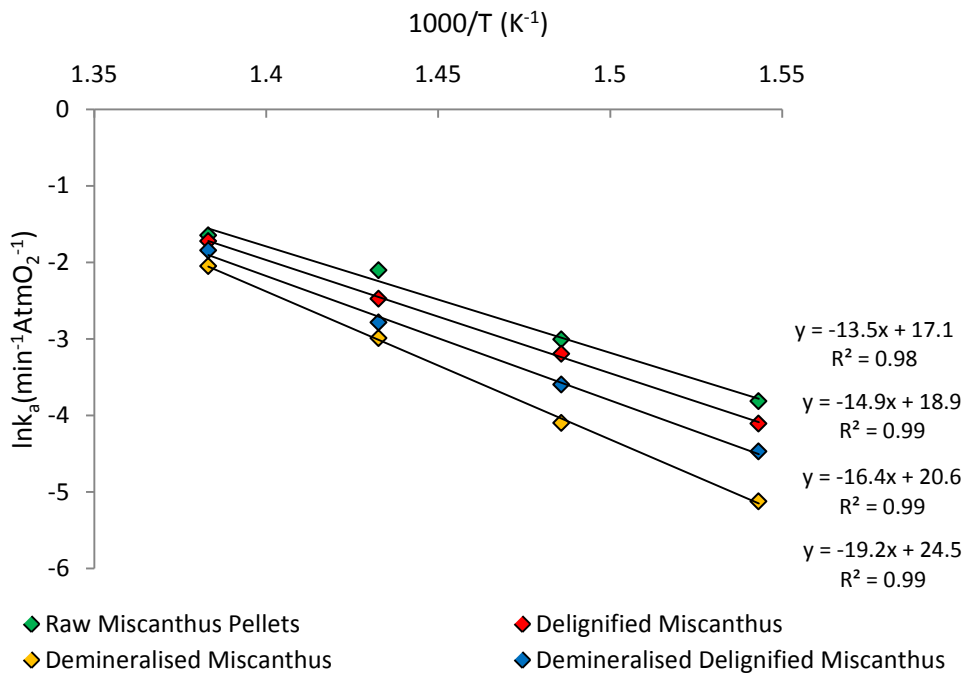


Figure 8-20 Arrhenius Plots for Miscanthus Pellet Fraction DTF Chars

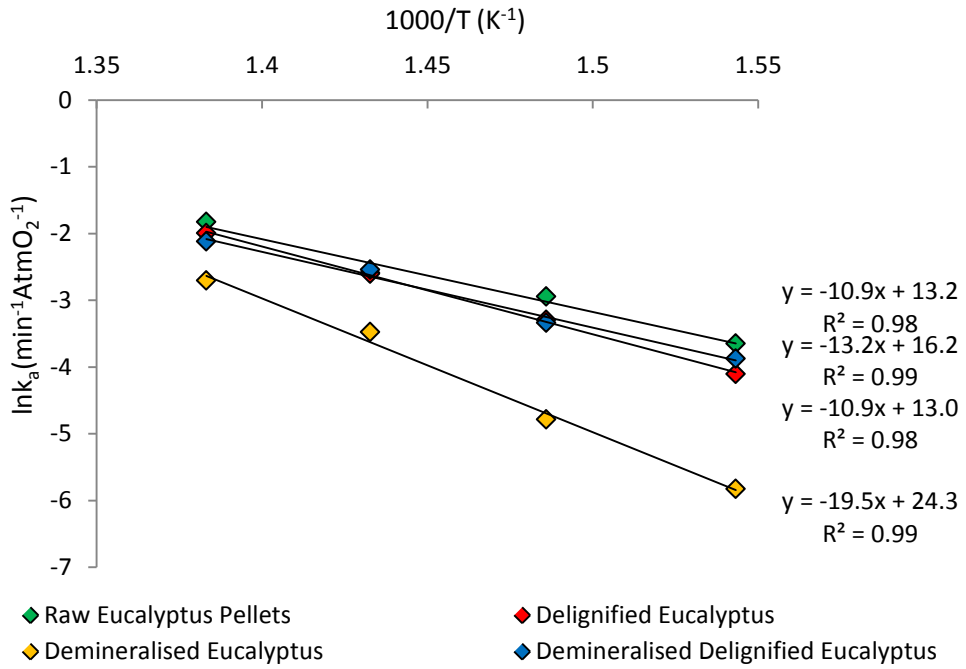


Figure 8-21 Arrhenius Plots for Eucalyptus Pellet Fraction DTF Chars

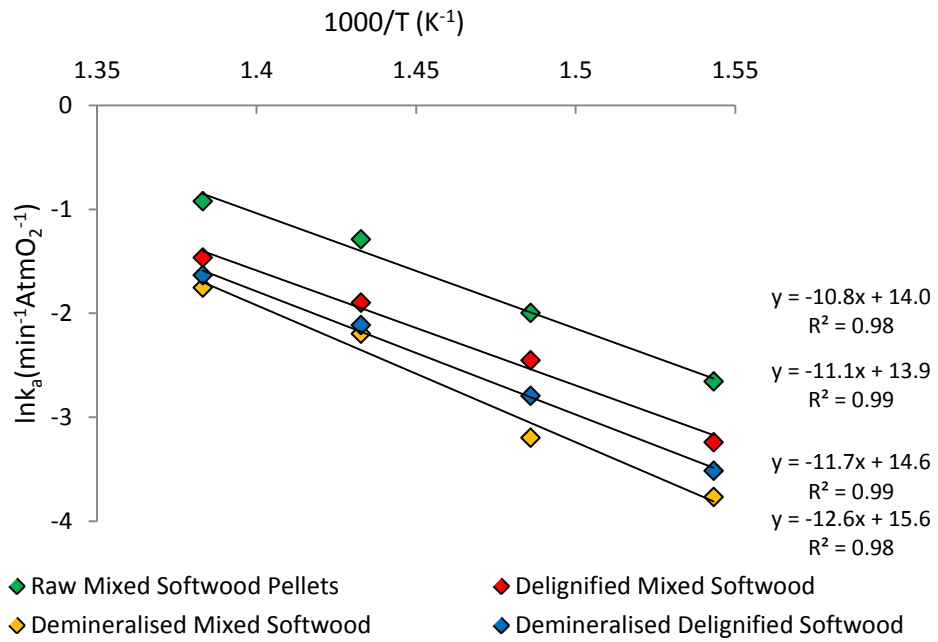


Figure 8-22 Arrhenius Plots for Mixed Softwood Pellet Fraction DTF Chars

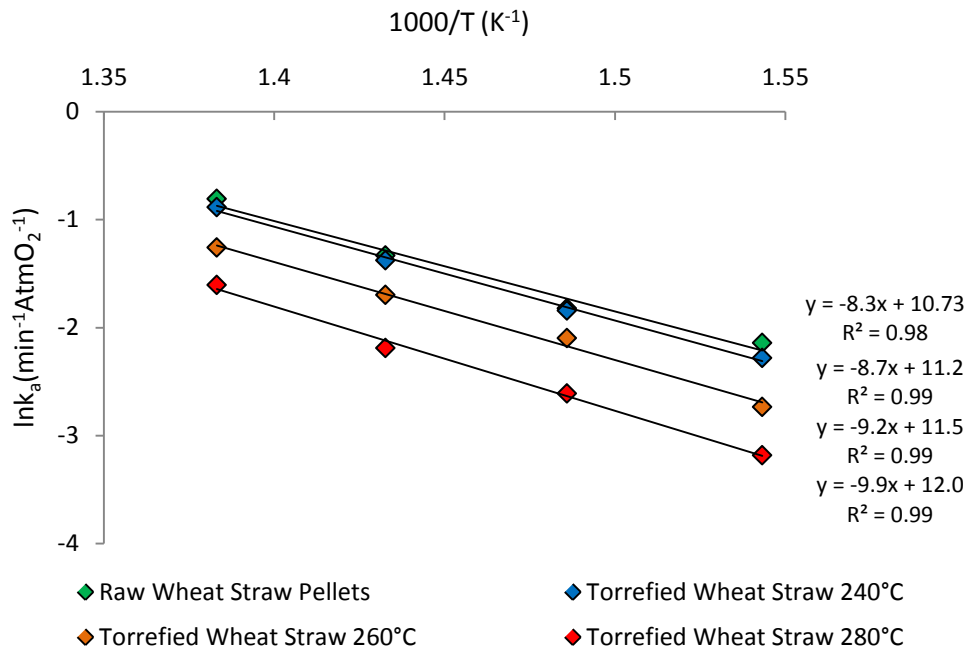


Figure 8-23 Arrhenius Plots for Raw and Torrefied Wheat Straw Pellet DTF Chars

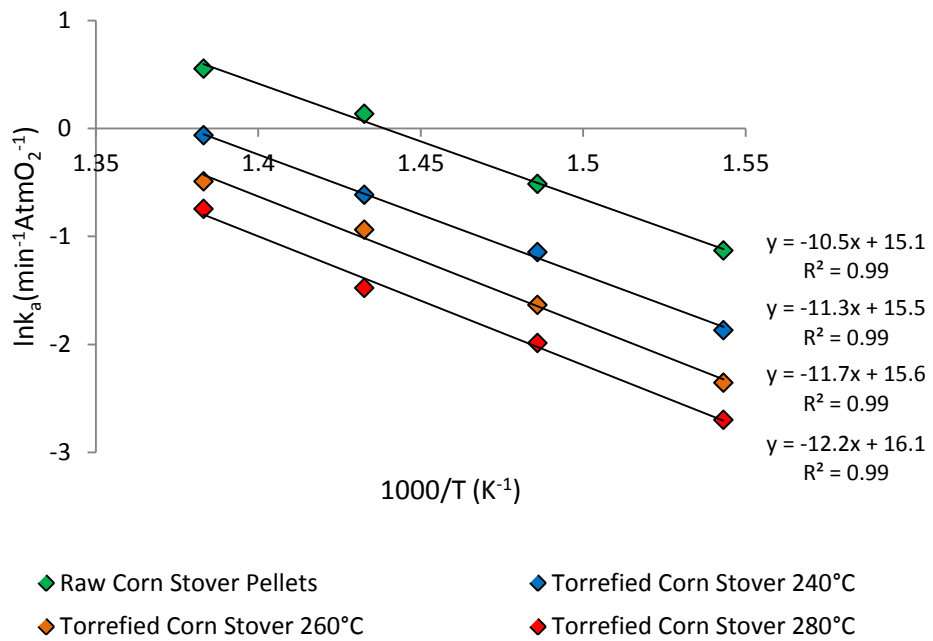


Figure 8-24 Arrhenius Plots for Raw and Torrefied Corn Stover Pellet DTF Chars

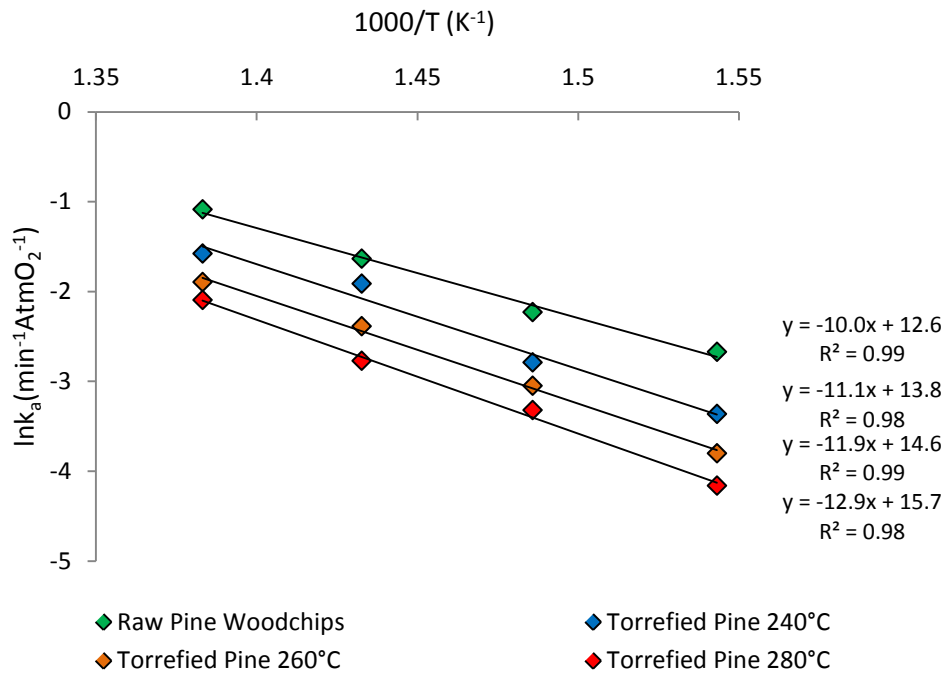


Figure 8-25 Arrhenius Plots for Raw and Torrefied Pine Woodchip DTF Chars

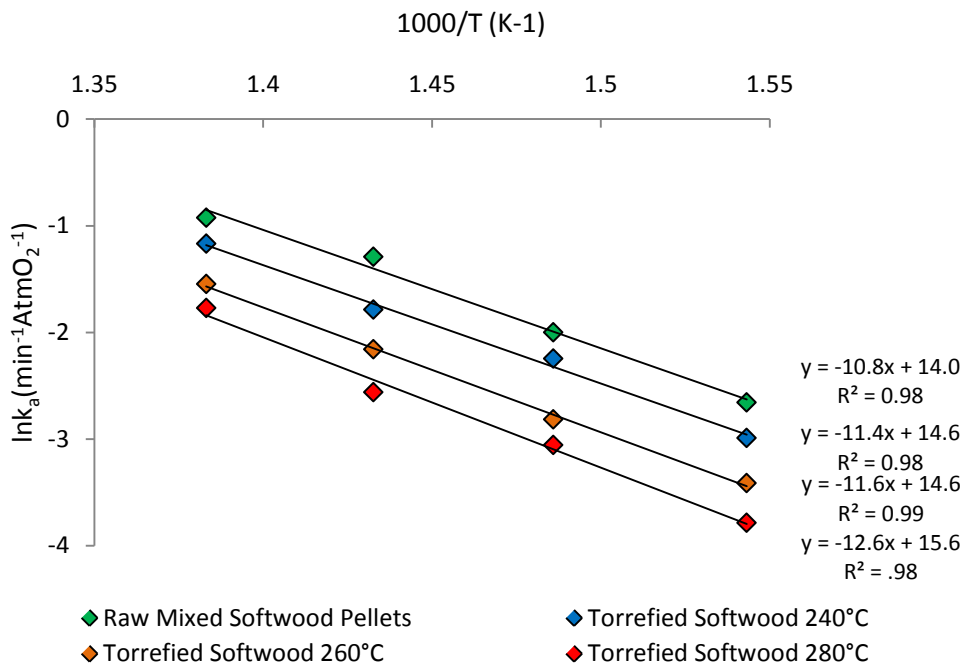


Figure 8-26 Arrhenius Plots for Raw and Torrefied Mixed Softwood Pellet DTF Chars

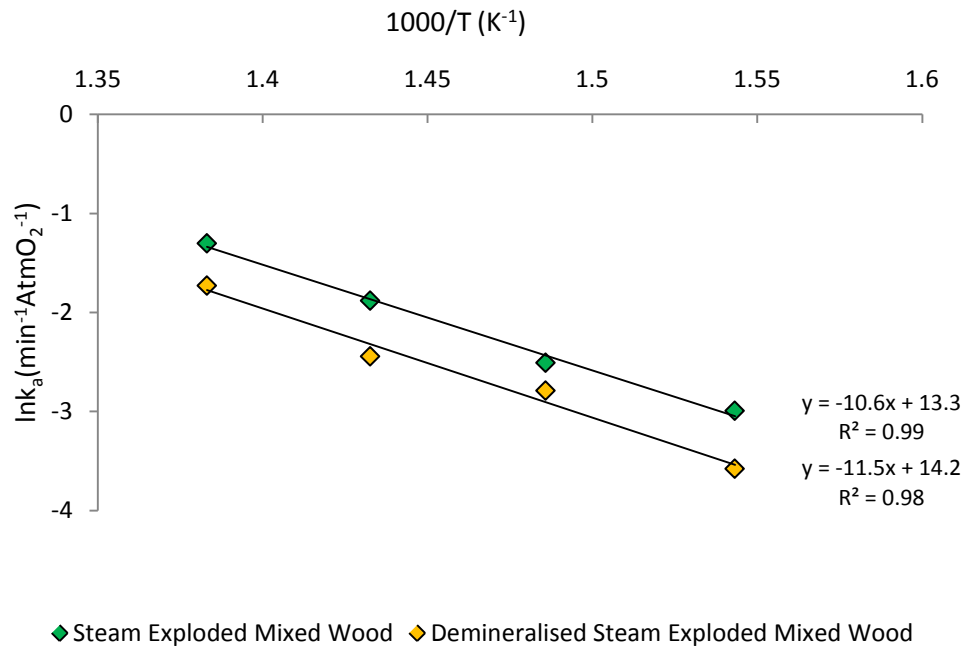


Figure 8-27 Arrhenius Plots for Steam Exploded Mixed Wood Pellet DTF Chars

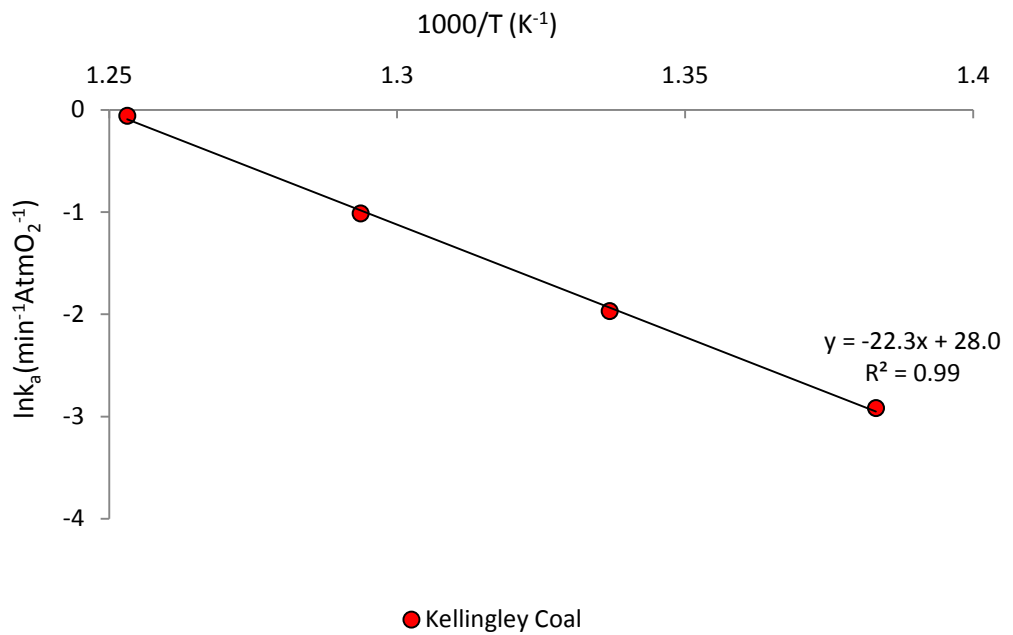


Figure 8-28 Arrhenius Plots for Kellingley Coal DTF Chars

Table 8-2 shows t_{90} during isothermal combustion at 450°C, k_a at 450°C, E_a and A for all of the fuels analysed.

Sample	$t_{90_{450}}$ (mins)	k_{a450} (s^{-1})	k_{a450} (min^{-1})	k_{a450} ($min^{-1}AtmO_2^{-1}$)	E_a ($kJmol^{-1}$)	A ($s^{-1}AtmO_2^{-1}$)
Wheat Straw Pellets	22.5	1.55×10^{-3}	0.093	0.45	69.20	7.42×10^7
Delignified Wheat Straw	50.2	7.16×10^{-4}	0.043	0.21	67.10	2.41×10^7
Corn Stover Pellets	4.9	6.07×10^{-3}	0.364	1.74	87.43	6.01×10^4
Delignified Corn Stover	26.5	1.21×10^{-3}	0.072	0.35	78.86	2.88×10^3
Pine Woodchips	28.4	1.18×10^{-3}	0.071	0.34	82.52	5.16×10^3
Delignified Pine Woodchips	54.8	5.59×10^{-4}	0.034	0.16	85.69	4.14×10^3
Miscanthus Pellets	45.5	6.74×10^{-4}	0.040	0.19	112.61	4.40×10^5
Delignified Miscanthus	63.3	6.25×10^{-4}	0.037	0.18	123.93	2.68×10^6
Eucalyptus Pellets	58.5	5.62×10^{-4}	0.034	0.16	90.53	9.31×10^3
Delignified Eucalyptus	74.7	4.75×10^{-4}	0.028	0.14	109.56	1.87×10^5
Mixed Softwood Pellets	25.7	1.39×10^{-3}	0.083	0.40	89.98	2.10×10^4
Delignified Mixed Softwood	49.7	8.06×10^{-4}	0.048	0.23	92.27	1.79×10^4
Torrefied Wheat Straw 240°C	36.8	1.44×10^{-3}	0.086	0.41	72.43	1.17×10^3
Torrefied Wheat Straw 260°C	40.4	9.91×10^{-4}	0.059	0.28	76.66	1.64×10^3
Torrefied Wheat Straw 280°C	48.2	7.02×10^{-4}	0.042	0.20	81.93	2.78×10^3
Torrefied Corn Stover 240°C	12.8	3.60×10^{-3}	0.216	1.03	93.74	9.25×10^4
Torrefied Corn Stover 260°C	20.2	2.47×10^{-3}	0.148	0.71	96.94	1.03×10^5
Torrefied Corn Stover 280°C	28.4	1.82×10^{-3}	0.109	0.52	101.45	1.69×10^5
Torrefied Pine 240°C	51.7	7.19×10^{-4}	0.043	0.21	92.57	1.68×10^4
Torrefied Pine 260°C	69.3	5.24×10^{-4}	0.031	0.15	98.97	3.54×10^4
Torrefied Pine 280°C	85.4	4.29×10^{-4}	0.026	0.12	107.41	1.18×10^5
Torrefied Mixed Softwood 240°C	30.6	1.09×10^{-3}	0.065	0.31	94.56	3.52×10^4
Torrefied Mixed Softwood 260°C	52.4	7.44×10^{-4}	0.045	0.21	96.82	3.51×10^4
Torrefied Mixed Softwood 280°C	58.6	5.93×10^{-4}	0.036	0.17	104.56	1.02×10^5
Steam Explosion Mixed Woods	37.9	9.50×10^{-4}	0.057	0.27	87.90	1.02×10^4
Demineralised Wheat Straw Pellets	121.9	2.51×10^{-4}	0.015	0.07	146.24	4.42×10^7
Demineralised Delignified Wheat Straw	101.7	3.14×10^{-4}	0.019	0.09	109.56	1.24×10^5
Demineralise Corn Stover Pellets	59.9	6.46×10^{-4}	0.039	0.19	89.99	9.78×10^3
Demineralised Delignified Corn Stover	34.6	9.74×10^{-4}	0.058	0.28	79.95	2.78×10^3
Demineralised Pine Woodchips	110.5	3.04×10^{-4}	0.018	0.09	132.58	5.50×10^6
Demineralised Delignified Pine Woodchips	67.9	5.31×10^{-4}	0.032	0.15	91.79	1.09×10^4
Demineralised Miscanthus Pellets	96.6	4.50×10^{-4}	0.027	0.13	112.61	7.24×10^8
Demineralised Delignified Miscanthus	81.1	5.52×10^{-4}	0.033	0.16	123.93	1.82×10^7
Demineralised Eucalyptus Pellets	134.9	2.34×10^{-4}	0.014	0.07	162.24	5.88×10^8
Demineralised Delignified Eucalyptus	89.4	4.19×10^{-4}	0.025	0.12	91.02	7.54×10^3
Demineralised Mixed Softwood Pellets	64.1	6.04×10^{-4}	0.036	0.17	104.51	1.02×10^5
Demineralised Delignified Mixed Softwood	52.4	6.81×10^{-4}	0.041	0.20	107.32	1.84×10^5
Demineralised Steam Explosion Mixed Wood	61.8	6.18×10^{-4}	0.037	0.18	95.90	2.50×10^4

Table 8-2 Isothermal Combustion Kinetics of DTF Chars

8.3.1. The Influence of Aromatic Carbon and Mineral Matter Content on Apparent Char Combustion Reaction Rate

There are a number of clearly evident trends associating the char burnout rates of DTF chars under isothermal combustion such that the apparent first order rate constant and thus time taken to reach 90% conversion decreases in the order raw biomass > delignified biomass > demineralised delignified biomass > demineralised biomass for all samples assessed. This is comparable to the behaviours exhibited under slow heating rate non-isothermal combustion and is indicative not only of the varying physical structure of the char formed but also its mineralogy and chemical composition.

Plots of apparent rate constant at 450°C vs. K+Ca content for non-demineralised samples and BET surface area for demineralised samples are shown in Figures 8-29 and 8-30.

As anticipated global char reactivity is dependent on both with the AAEM content of non-demineralised fuels and BET surface area of the char for demineralised analogues, indicating the importance of surface area development in determining char reactivity of the biomass chars in the absence of mineral matter influences. For non-demineralised samples the catalytic effects act to considerably increase reaction rates above those expected given the depression of surface area development evidenced with increasing AAEM content. The effect of increasing K+Ca content on char oxidation rate only appears to begin to have a noticeable influence in samples with content above ~0.5 wt% db K+Ca. Below this increasing AAEM content has little influence on reactivity, apparent pseudo-first order rate constants actually appear to decrease with increasing K+Ca (Figure 8-29) most likely due to the reduction in char surface area. Plotting apparent first order rate constant vs. the K content of the fuel alone (Figure 8-30) gives a more consistent correlation of mineral content and reactivity. This is likely due to the

increased activity of K as a char combustion catalyst over Ca driven by differences in interfacial contact between the catalyst species and char structure which can play an instrumental role in determining catalytic effectiveness.

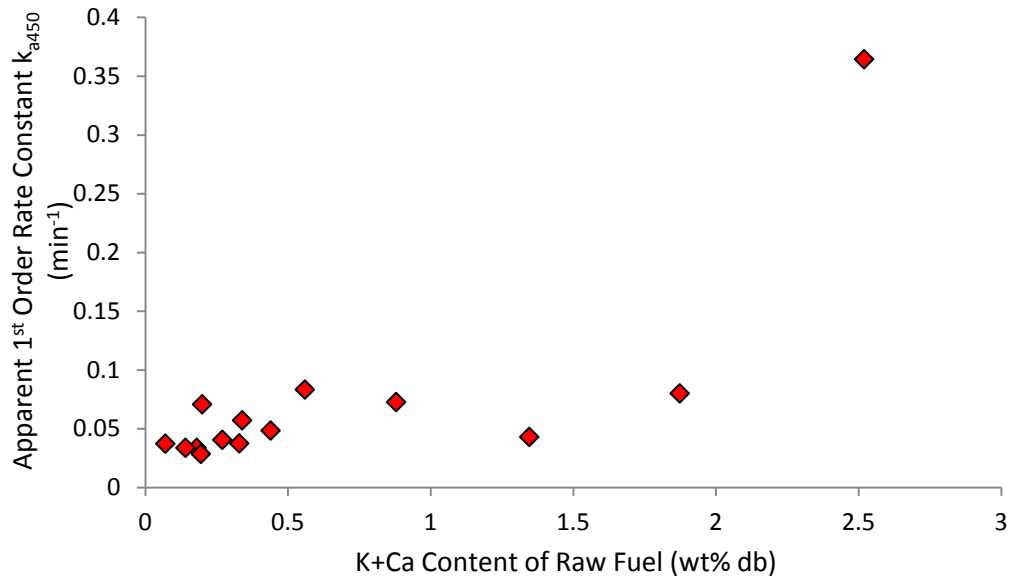


Figure 8-29 DTF Char k_a vs. K+Ca for Non-demineralised Samples

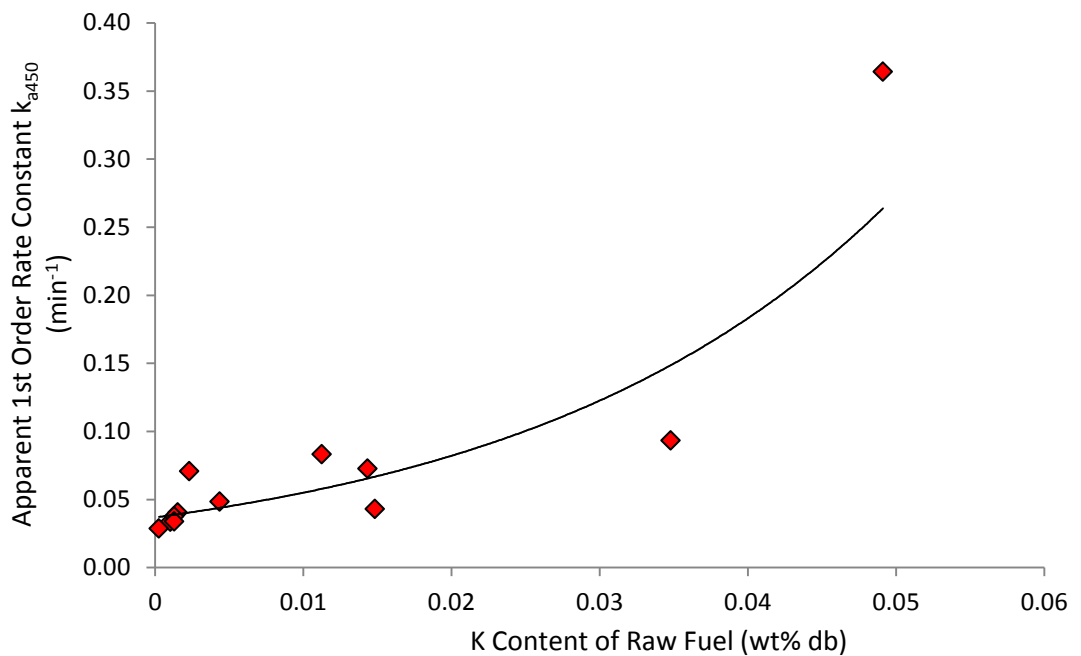


Figure 8-30 DTF Char k_a vs. K for Non-demineralised Samples

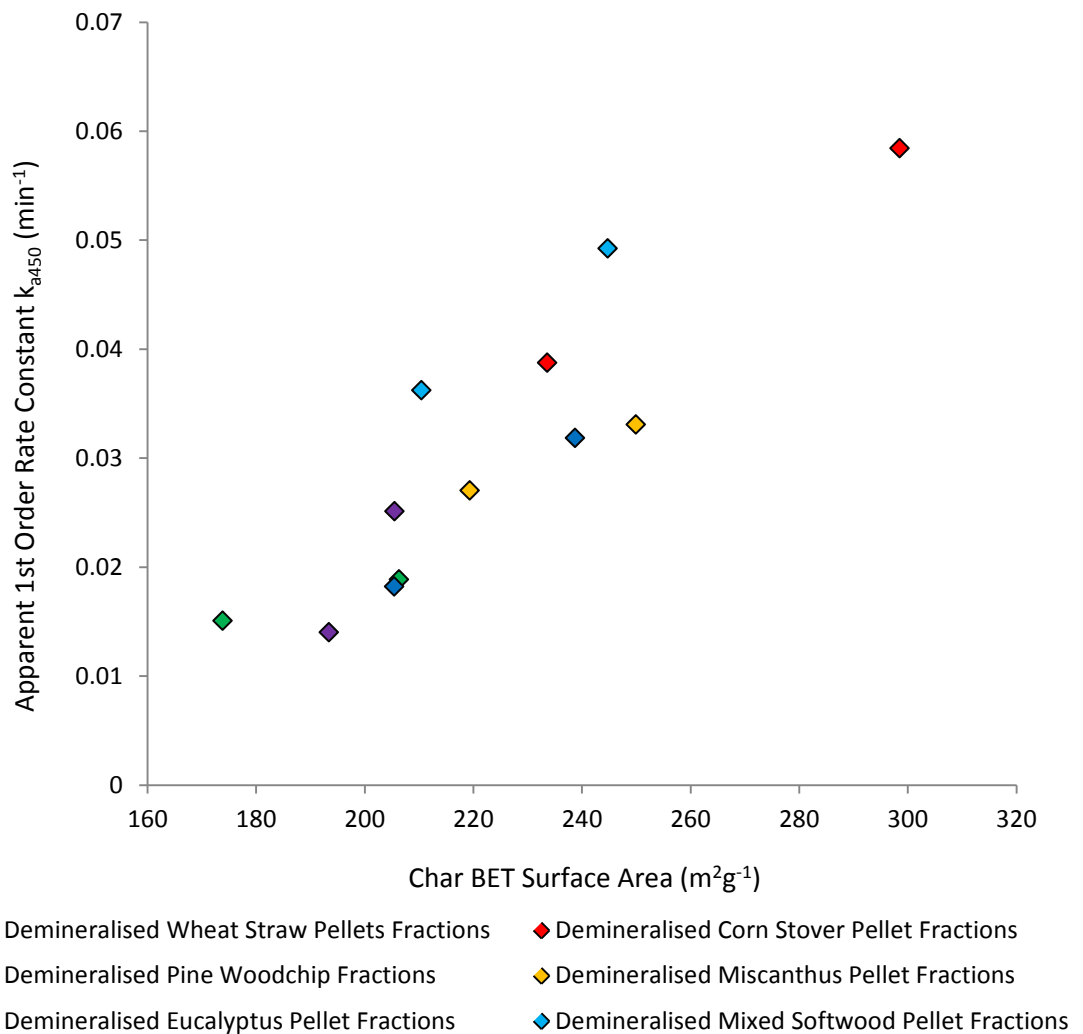


Figure 8-31 DTF Char k_a vs. BET Surface Area for Demineralised Samples

The relationship between surface area and apparent reactivity for demineralised fuels is more consistent (as shown in Figure 8-31), increased surface area giving rise to a comparable increase in the char combustion rate. This is due to the proportionality of combustion rate and surface area under regime I low temperature, chemical rate controlled combustion conditions which were utilised throughout for isothermal combustion purposes. Given the correlation of aromatic carbon content and char surface area for demineralised fuels as shown in Figure 7-16, the reduction in reactivity with increasing aromatic carbon content is likely due to the increase in lignin derived

char which has been shown to produce slow burning, low surface area chars under slow heating. As the quantity of aromatic carbon increases the propensity to form thicker walled, fused chars is enhanced resulting in a reduction in char surface area and combustion rates. The close relation of surface area and raw fuel aromatic carbon content also offers the potential to directly correlate fuel aromatic carbon content with the global reactivity of demineralised fuels as shown in Figure 8-32.

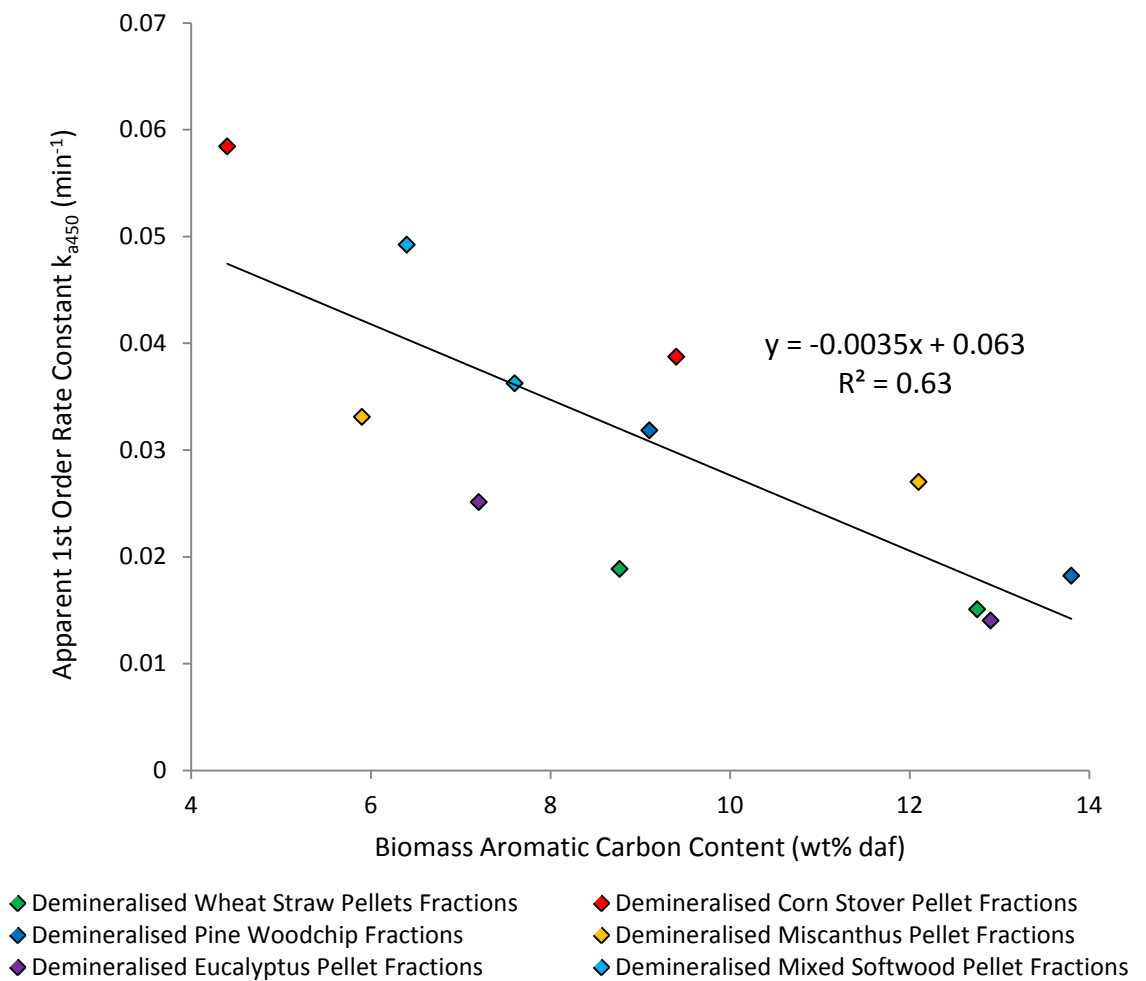


Figure 8-32 DTF Char k_a vs. Biomass Aromatic Carbon Content for Demineralised Samples

8.3.2. The Influence of Torrefaction on Apparent Char Combustion

Reaction Rate

The reactivity of torrefied biomass fuels decreases with increasing torrefaction temperature, this decrease being likewise associated with the increasing aromaticity of the samples as shown in Figure 8-32.

The straight line equation expressed in Figure 8-31 correlating pseudo first order rate constant and raw fuel aromatic carbon content in the absence of mineral matter interaction does offer the potential to predict global reaction rate with quantification of the aromatic carbon content of the fuel. However, the differing influence of K+Ca content on apparent reactivity for individual fuels precludes the generation of meaningful predictive calculations for all lignocellulosic fuels.

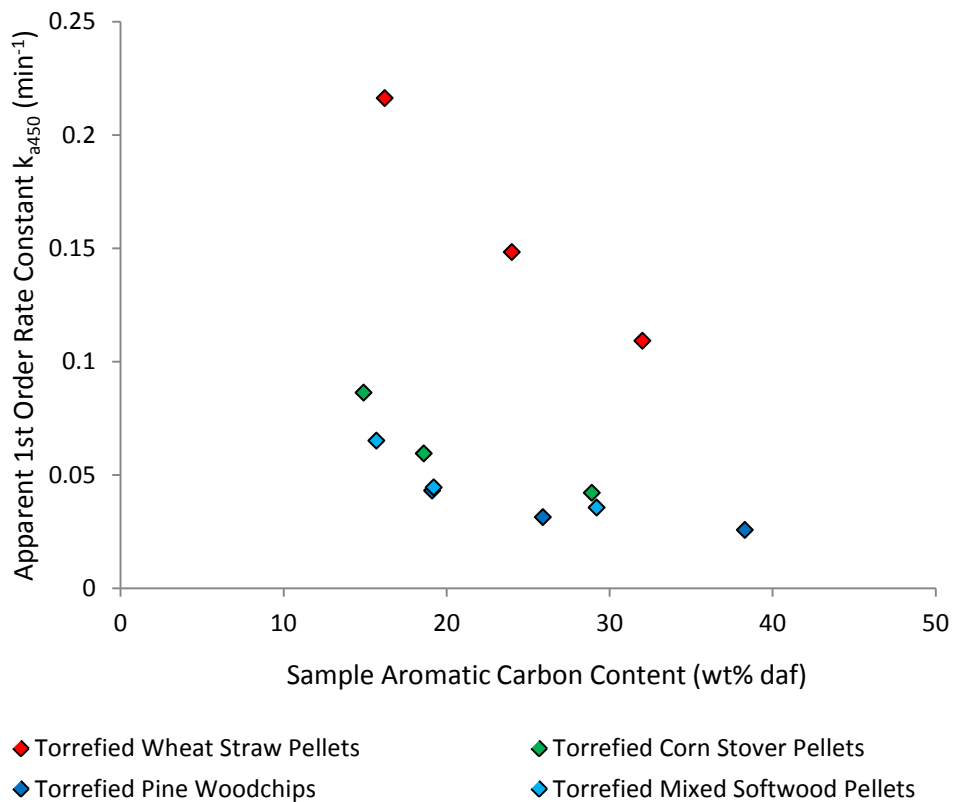


Figure 8-33 DTF Char k_a vs. Aromatic Carbon Content of Torrefied Biomass Samples

As has been reported consistently within existing literature (Jones et al., 2012; Li et al., 2015) the reactivity of all torrefied samples was shown to be lower than raw fuels, reaction rates decreasing with increasing torrefaction temperature. For torrefied wheat straw, pine and softwood samples the decrease in reactivity with torrefaction are similar, the initial reactivity difference between raw fuels and those torrefied at 240°C are most apparent, the reactivity decreases becoming less with increasing torrefaction degree. These alterations are in line with the mass losses exhibited during torrefaction. Reactivity decreases are most marked in the case of corn stover pellets, however this is predominantly due to the high rate of char combustion for this fuel both prior to and following torrefaction.

8.3.3. Intrinsic Char Combustion Reaction Rates

In order to fully appreciate the respective roles played by active char pore surface area and intrinsic chemical reaction rates in determining the overall rate of char combustion and assess the influence of mineral matter and aromatic carbon content on these factors the first order rate constant has been normalised to account for the differing surface areas of the associated chars, these intrinsic rate constants (k_i) being expressed in $\text{g}/\text{m}^2\cdot\text{min}$ and being presented in Table 8-3.

Comparable plots to those reported for apparent reaction rate have been produced for intrinsic rates with plots of intrinsic rate constant vs. K+Ca content for non-demineralised samples and aromatic carbon for demineralised samples are shown in Figures 8-34 and 8-35.

Sample	k_{i450} (g/m ² .min)
Wheat Straw Pellets	9.61x10 ⁻⁴
Delignified Wheat Straw	3.04x10 ⁻⁴
Corn Stover Pellets	3.24x10 ⁻³
Delignified Corn Stover	4.32x10 ⁻⁴
Pine Woodchips	3.83x10 ⁻⁴
Delignified Pine Woodchips	1.78x10 ⁻⁴
Miscanthus Pellets	2.08x10 ⁻⁴
Delignified Miscanthus	1.88x10 ⁻⁴
Eucalyptus Pellets	2.43x10 ⁻⁴
Delignified Eucalyptus	1.37x10 ⁻⁴
Mixed Softwood Pellets	5.99x10 ⁻⁴
Delignified Mixed Softwood	3.19x10 ⁻⁴
Torrefied Wheat Straw 240°C	7.25x10 ⁻⁴
Torrefied Wheat Straw 260°C	5.41x10 ⁻⁴
Torrefied Wheat Straw 280°C	4.53x10 ⁻⁴
Torrefied Corn Stover 240°C	2.21x10 ⁻³
Torrefied Corn Stover 260°C	1.79x10 ⁻³
Torrefied Corn Stover 280° C	1.66x10 ⁻³
Torrefied Pine 240°C	3.00x10 ⁻⁴
Torrefied Pine 260°C	2.57x10 ⁻⁴
Torrefied Pine 280°C	2.27x10 ⁻⁴
Torrefied Mixed Softwood 240°C	5.79x10 ⁻⁴
Torrefied Mixed Softwood 260°C	4.83x10 ⁻⁴
Torrefied Mixed Softwood 280°C	4.63x10 ⁻⁴
Steam Explosion Mixed Woods	4.65x10 ⁻⁴
Demineralised Wheat Straw Pellets	8.68x10 ⁻⁵
Demineralised Delignified Wheat Straw	9.14x10 ⁻⁵
Demineralise Corn Stover Pellets	1.66x10 ⁻⁴
Demineralised Delignified Corn Stover	1.96x10 ⁻⁴
Demineralised Pine Woodchips	8.87x10 ⁻⁵
Demineralised Delignified Pine Woodchips	1.33x10 ⁻⁴
Demineralised Miscanthus Pellets	1.23x10 ⁻⁴
Demineralised Delignified Miscanthus	1.32x10 ⁻⁴
Demineralised Eucalyptus Pellets	7.26x10 ⁻⁵
Demineralised Delignified Eucalyptus	1.22x10 ⁻⁴
Demineralised Mixed Softwood Pellets	1.72x10 ⁻⁴
Demineralised Delignified Mixed Softwood	1.67x10 ⁻⁴
Demineralised Steam Explosion Mixed Wood	2.51x10 ⁻⁴

Table 8-3 Intrinsic Rate Constant of DTF Chars

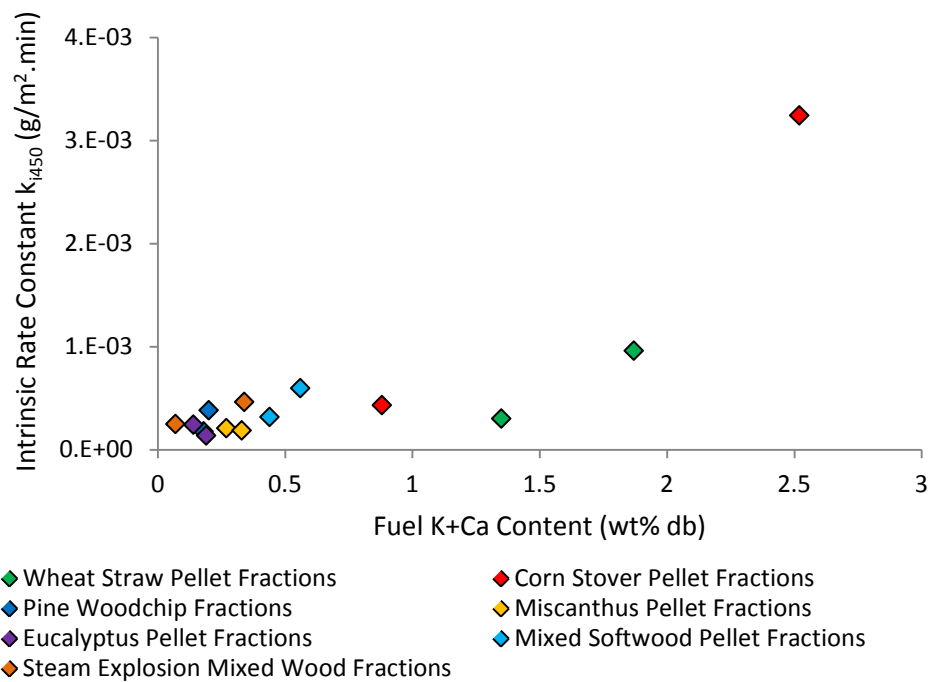


Figure 8-34 DTF Char k_i vs. K+Ca for Non-demineralised Samples

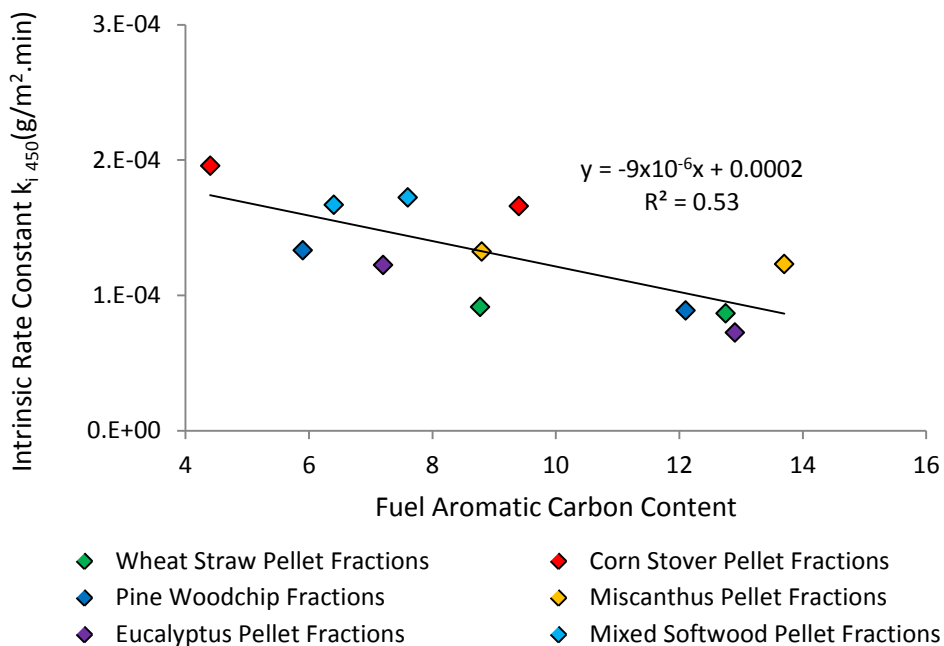


Figure 8-35 DTF Char k_i vs. Biomass Aromatic Carbon Content for Demineralised Samples

The relation between AAEM content and intrinsic reactivity is considerably more consistent than that derived for apparent reaction rate constant. Although wheat straw pellet fractions are again somewhat less reactive than anticipated this effect is significantly less than was observed for apparent reactivity. Although in the above plot the influence of alkali metals does not appear to appear to significantly increase the intrinsic char reaction rate for all those samples containing below 0.6 wt% db K+Ca content, this may be due to a number of causes including the distribution of minerals, which may exist as discrete inorganic inclusions at these low levels rather than dispersed nutritional minerals as in higher mineral matter biomass or the redistribution and volatilisation of these minerals during pyrolysis. The relationship appears to be near exponential with increasing levels of K+Ca giving increasing enhancements of the reaction rate.

A linear decreasing trend is seen between intrinsic rate constant and aromatic carbon content of demineralised fuels indicating the inherent un-reactiveness of chars derived from fuels containing higher portions of lignin. This trend is consistent across all demineralised biomass and their demineralised delignified analogues.

Given the consistent straight line relationship expressed in Figure 8-34 linking intrinsic reactivity and fuel aromatic carbon content in the absence of mineral interactions there is potential to predict the intrinsic reactivity of the fuel from aromatic carbon content.

Using this relationship to calculate an assumed intrinsic rate constant for non-demineralised fuels allows the influence of AAEM catalysis on intrinsic reactivity to be quantified. Figures calculated using this method are shown in Table 8-4, the difference between observed and calculated figures being plotted against fuel K+Ca content in Figure 8-36.

Sample	Observed k_{i450} (g/m ² .min at 450°C)	Calculated k_{i450} (g/m ² .min at 450°C)	Observed - Calculated k_{i450} (g/m ² .min at 450°C)
Wheat Straw Pellets	9.61x10 ⁻⁴	2.86x10 ⁻⁴	6.75x10 ⁻⁴
Delignified Wheat Straw	3.04x10 ⁻⁴	2.64x10 ⁻⁴	3.96x10 ⁻⁵
Corn Stover Pellets	3.24x10 ⁻³	3.02x10 ⁻⁴	2.94x10 ⁻³
Delignified Corn Stover	4.32x10 ⁻⁴	2.48x10 ⁻⁴	1.85x10 ⁻⁴
Pine Woodchips	3.83x10 ⁻⁴	3.44x10 ⁻⁴	3.92x10 ⁻⁵
Delignified Pine Woodchips	1.78x10 ⁻⁴	3.00x10 ⁻⁴	-1.22x10 ⁻⁴
Miscanthus Pellets	2.08x10 ⁻⁴	3.25x10 ⁻⁴	-1.17x10 ⁻⁴
Delignified Miscanthus	1.88x10 ⁻⁴	2.65x10 ⁻⁴	-7.67x10 ⁻⁵
Eucalyptus Pellets	2.43x10 ⁻⁴	3.57x10 ⁻⁴	-1.14x10 ⁻⁴
Delignified Eucalyptus	1.37x10 ⁻⁴	2.72x10 ⁻⁴	-1.35x10 ⁻⁴
Mixed Softwood Pellets	5.99x10 ⁻⁴	2.87x10 ⁻⁴	3.12x10 ⁻⁴
Delignified Mixed Softwood	3.19x10 ⁻⁴	2.74x10 ⁻⁴	4.48x10 ⁻⁵

Table 8-4 Observed and Calculated k_{i450}

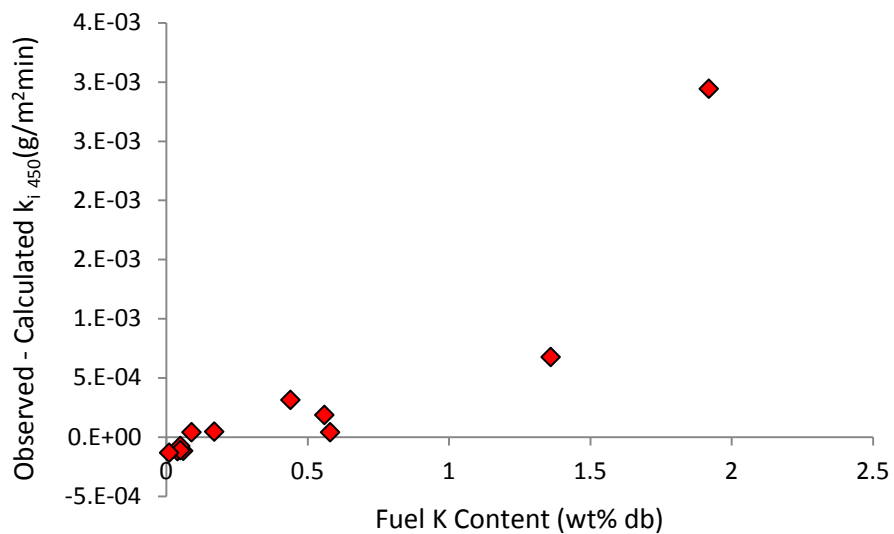
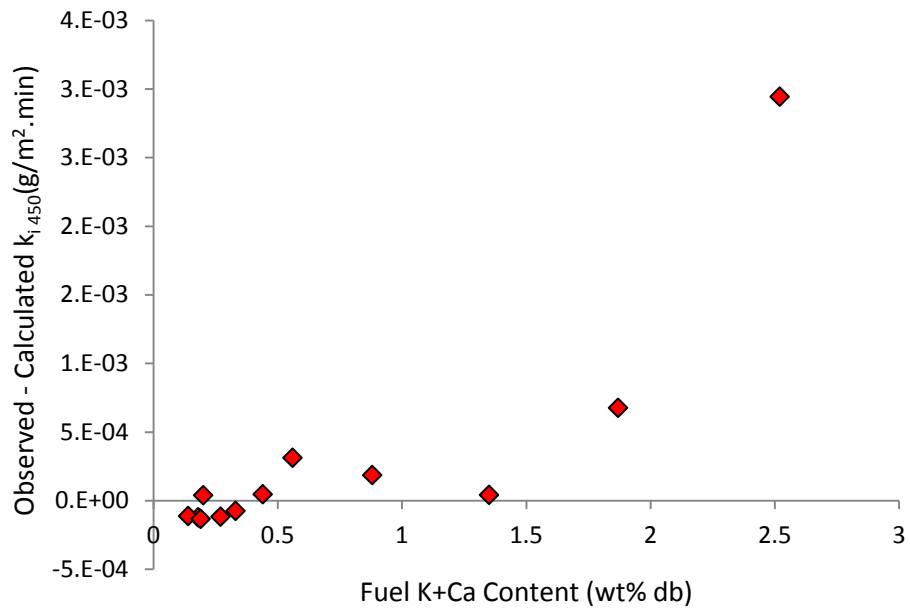


Figure 8-36 Observed-Calculated k_i vs. Fuel K+Ca and K Content

Again a somewhat more consistent relationship is seen to link intrinsic rate constant with the K content of the fuels rather than K+Ca. It is clear that for all biomass at lower K contents the prediction of intrinsic rate constant based purely upon the aromatic carbon results in relatively close correlation, however, as the K content rises, especially for raw wheat straw and corn stover pellet biomass this correlation is lost as the

influence of catalytic mineral matter takes precedent in determining reaction rate over the aromatic carbon content.

A Plot of intrinsic rate constant vs. aromatic carbon content for torrefied fuels (Figure 8-37) shows that similarly reducing rate can be seen for all torrefied fuels with increasing aromaticity and thus increasing torrefaction temperature.

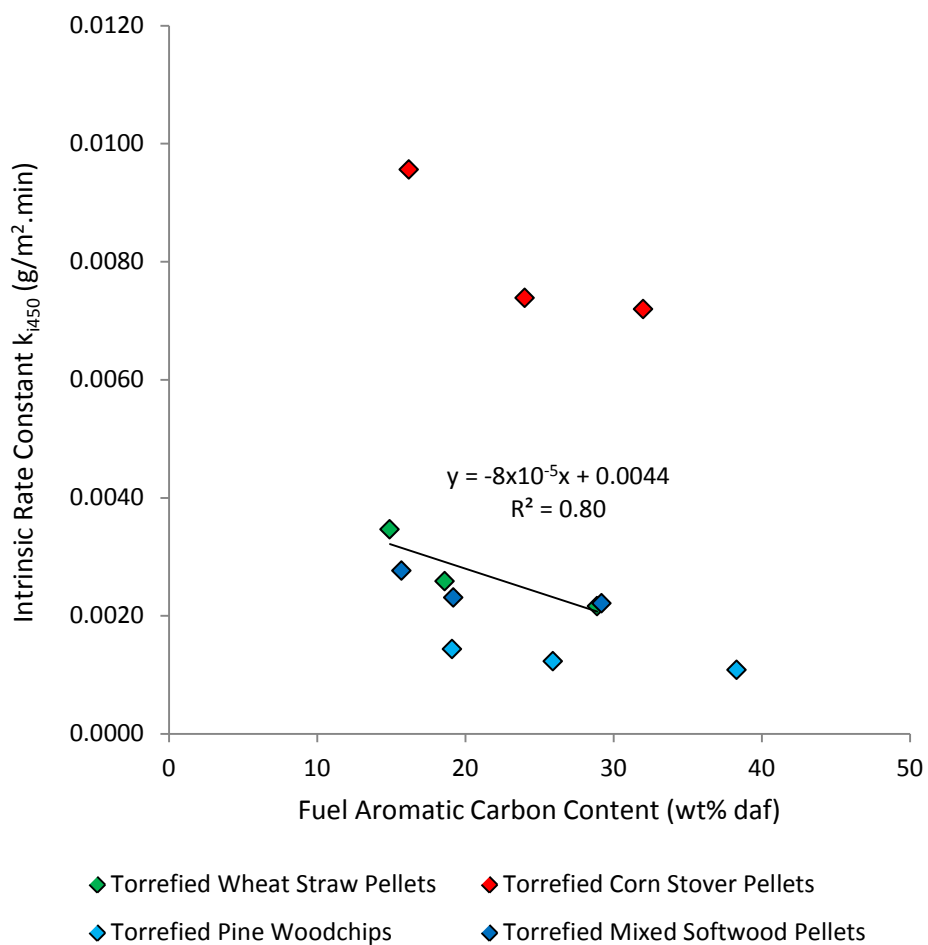


Figure 8-37 Torrefied Biomass DTF Char Combustion k_i vs. Fuel Aromatic Carbon

Torrefied fuels do appear to deactivate at higher rates than non torrefied counterparts with increase aromaticity. One potential explanation for this enhanced deactivation of aromatic derived char structures is the form of aromatic carbon entering the pyrolysis

process. For raw fuels this aromatic carbon is derived solely from lignin structures within which it is associated with a portion of aliphatic side groups, however, for torrefied fuels, especially at higher torrefaction temperatures, a significant proportion of the fuels aromatic carbon is sourced from the aromatisation of aliphatic components of the fuel precipitated by lengthy residences at moderately elevated temperature. These aromatic carbons may be of more highly condensed nature with higher depletion of oxygenated functionality than lignin, causing them to produce condensed and intrinsically unreactive chars when compared to lignin derived aromatic groups.

8.4. DTF Char Re-firing

In order to study the progression of char combustion under realistic boiler conditions a selection of samples from two different biomass fuels and one reference coal were re-fired in the DTF as described in Chapter 3.

The fuels chosen for re-firing were Kellingley coal, wheat straw pellets and eucalyptus pellets alongside their associated fractions prepared through delignification and demineralisation (raw biomass fuel, demineralised biomass fuel, organosolv residue and demineralised organosolv residue). Several DTF devolatilisation runs were completed for each fuel in order to obtain the required char sample mass for re-firing (each re-firing experiment being completed using between 4 and 8 grams of char sample depending upon the initial volatile matter yield of the fuel in question). These samples were passed through the DTF at 1100°C under a gas atmosphere containing 5 volume% oxygen in nitrogen over residence times of 50, 100, 200, 400 and 600 ms.

A portion of each char sample collected following DTF devolatilisation was isothermally combusted in the TGA at 450°C in order to establish the reproducibility of char burnout

behaviour and ash content of the individual char generation experiments. Any char which was believed to differ considerably in either of these key parameters were excluded from subsequent re-firing experiments.

It was observed that variability both in char combustion rate and the level of fuel devolatilisation as represented by the char ash content was more significant for the chars generated from biomass fuels than for Kellingley coal derived chars. This observation is most likely due to the greater inhomogeneity of biomass fuels compared to coal, the differing shape profile of the pulverised biomass which may influence the flow pattern of the fuel within the furnace given the near laminar nature of DTF gas flows caused by gas flow redirection and mixing which occurs in the gas box located at the work tube entrance (Brewster et al., 1995) and alter the residence time within the reactor and the extremely volatile nature of the biomass in contrast to coal.

The levels of char conversion achieved for each DTF residence time are shown in Table 8-5 and illustrated as plots of mass % char conversion on a daf basis vs. the DTF re-firing residence time utilised in Figures 8-38 and 8-39.

DTF R-firing Residence Time (ms)	Char Burnout (wt% daf)				
	50	100	200	400	600
Raw Wheat Straw Pellets	42	60	81	91	95
Demineralised Wheat Straw	18	35	61	84	92
Delignified Wheat Straw	37	58	77	93	96
Demineralised Delignified Wheat Straw	22	47	74	87	91
Raw Eucalyptus Pellets	31	53	74	90	95
Demineralised Eucalyptus	17	36	58	80	89
Delignified Eucalyptus	25	51	79	90	94
Demineralised Delignified Eucalyptus	19	50	69	84	91
Kellingley Coal	12	27	48	68	79

Table 8-5 DTF Re-firing Char Conversions

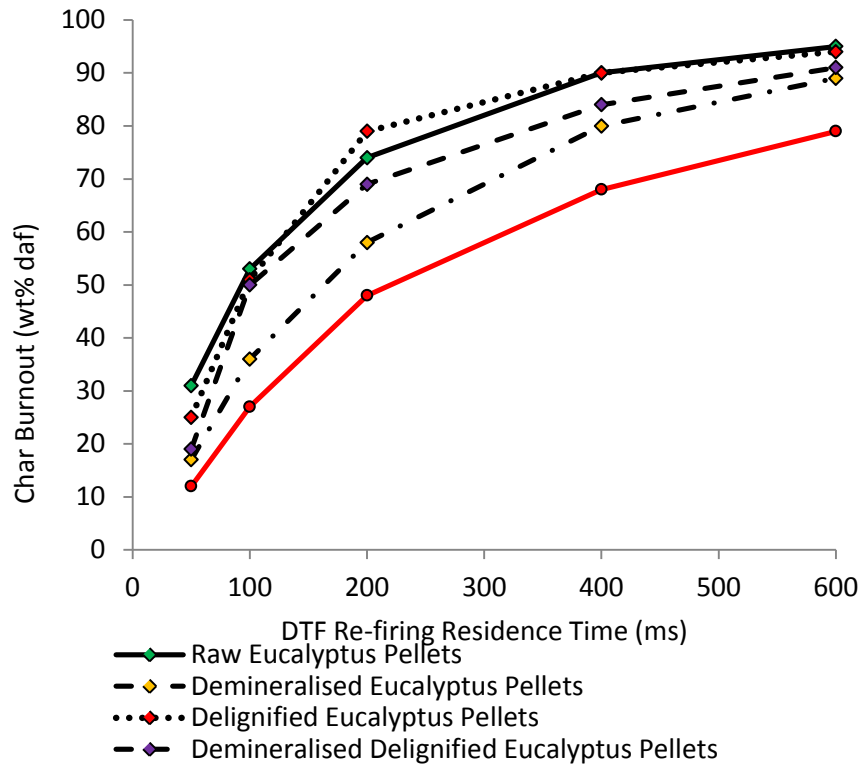


Figure 8-38 Wheat Straw Fractions Char Re-firing Burnout vs. Re-firing Residence Time

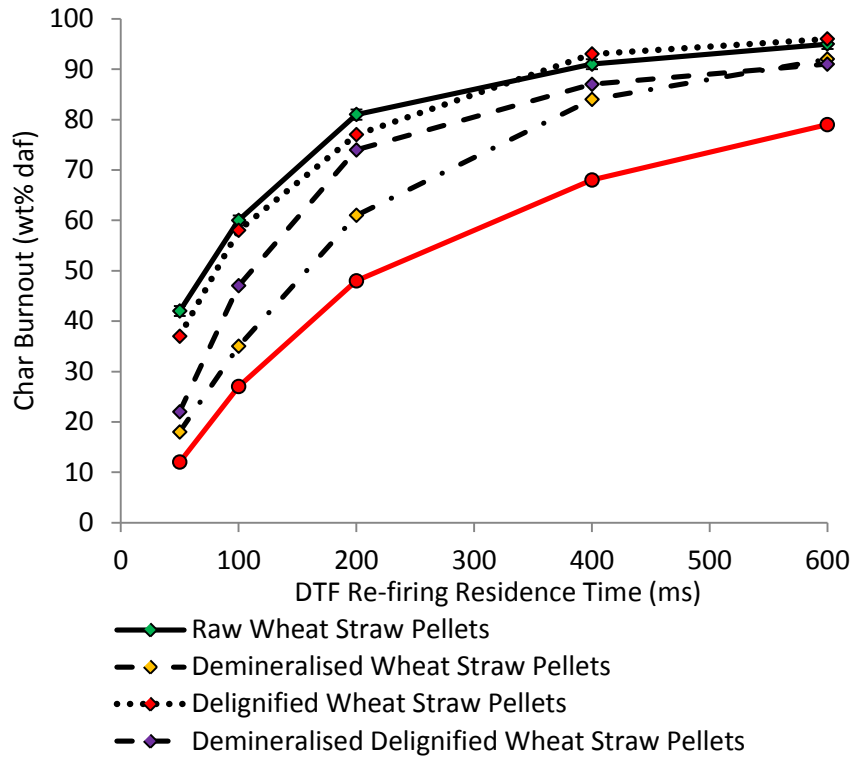


Figure 8-39 Eucalyptus Fractions Char Re-firing Burnout vs. Re-firing Residence Time

On re-firing in the DTF all biomass fraction chars are seen to combust at a higher rate and more completely than Kellingley coal chars. This result clearly indicates the enhanced reactivity of biomass chars in comparison to coal under simulated boiler conditions even where the overall size of biomass which were prepared using fuels of size fraction 125-250 μm are significantly in excess of that of coal of smaller size 75-105 μm . This enhancement in char reactivity regardless of the size of the biomass char is important given the generally increased particle sizes obtained when grinding biomass in utility scale pulverisation equipment when compared to coal. Given the increased reactivity of the biomass chars this increase in char size and thus increased residence time requirement to achieve high levels of char conversion may be partially offset by the increased reactivity of the char, however as evidenced by Steer et al., 2013 increases in the mill sieve sizes used and thus the particle sizes of the biomass must still be controlled in order to minimise increases in unburned carbon content of fly ash during co-firing (in this case 25% by energy input of miscanthus pellets) biomass with coal in a utility scale PF furnace.

Wheat straw fractions also appear to be considerably more reactive than eucalyptus pellet counterparts reaching higher levels of char conversion more rapidly. This confirms the results obtained using TGA isothermal char combustion experiments which showed straw samples to burnout at a higher rate than eucalyptus analogues. All biomass chars attained considerable degrees of conversion after 600 ms, over 90% conversion being achieved in all cases except for demineralised eucalyptus pellets which exhibited 89%. Kellingley chars attained only 79% of conversion following 600 ms at 1100°C (this is in stark contrast to the conversions achieved at 1300°C DTF temperatures which produced 93% burnout of Kellingley coal chars).

It can be seen that the difference between char burnout achieved for coal and demineralised biomass fuel with re-firing residences of 50 ms is far less than the final difference in burnout % at 600 ms, in fact for both demineralised wheat straw and demineralised eucalyptus pellets the char burnout achieved following 50 ms of combustion are only 5 and 7% greater than that of Kellingley char. This reduction in the difference between coal and biomass char burnout at lower residence time is thought to be due to differences in the prevailing particle sizes of biomass and coal chars with the biomass chars being of large particle size (this having been confirmed through optical analysis) and thus requiring additional time for the heating of the chars to the point that considerable combustion reactions are able to occur. As residence time in the high temperature, oxidising DTF environment increases the increased rate of biomass char burnout in comparison to coal becomes evident and the burnout profiles of all biomass samples shift considerable from that of coal whereby the char conversion % increases significantly. Further to this, as the residence time increases the conversion degrees undergone by the biomass fuels which, at low residence times, are relatively spread appear to converge

It can be seen that for the fractions of both wheat straw and eucalyptus pellets the order of char reactivity roughly follows that of the reactivity profiles obtained through isothermal combustion in the TGA. Both demineralised raw and demineralised delignified samples showed considerably reduced levels of char conversion at each residence time. There is however one major exception to this rule whereby the burnout for chars of organosolv residue samples, which have not been subjected to further demineralisation supersede those of the raw biomass chars following 100 ms for delignified eucalyptus and 400 ms for delignified wheat straw. This observation is in evident contrast to the results obtained through isothermal TGA combustion which

consistently resulted in a ranking of reactivity in the order raw biomass > delignified biomass > delignified demineralised biomass > demineralised biomass.

In order to more consistently assess the reaction rate of DTF chars during combustive re-firing the specific rate of oxidation has been determined as $\frac{1}{W} \left(\frac{dW}{dt} \right)$ where W is the char weight at any time t (in this case taken as the mass of char remaining at the close of the preceding time step which is assumed to be equal to the mass at commencement of the re-firing time step in question) and dW/dt is the instantaneous rate of char weight loss (in this case no instantaneous rate can be determined from the DTF and thus the char mass at the beginning and end of each individual time step are used to define a rate of mass loss across the time step) and are reported in Table 8-6.

DTF Re-firing Residence Time Intervals (ms)	Char Burnout Rate Per Unit Mass of Char Burning (ms ⁻¹)				
	0-50	50-100	100-200	200-400	400-600
Raw Wheat Straw Pellets	0.0084	0.0062	0.0026	0.0007	0.0006
Demineralised Wheat Straw Pellets	0.0036	0.0041	0.0040	0.0029	0.0025
Delignified Wheat Straw Pellets	0.0074	0.0067	0.0045	0.0035	0.0021
Demineralised Delignified Wheat Straw Pellets	0.0044	0.0064	0.0051	0.0025	0.0015
Raw Eucalyptus Pellets	0.0062	0.0064	0.0045	0.0031	0.0025
Demineralised Eucalyptus Pellets	0.0034	0.0046	0.0034	0.0026	0.0023
Delignified Eucalyptus Pellets	0.0050	0.0069	0.0057	0.0026	0.0020
Demineralised Delignified Eucalyptus Pellets	0.0038	0.0077	0.0038	0.0024	0.0022
Kellingley Coal	0.0024	0.0034	0.0029	0.0019	0.0017

Table 8-6 Char Burnout Rate on DTF Char Re-firing

Plotting these reaction rates against the level of conversion at the commencement of the residence time step within which they occur is able to give a profile of the char conversion rate with on-going conversion % of the char and are presented in Figure 8-40 and 8-41 for wheat straw and eucalyptus fractions respectively with the profile for Kellingley coal being included for reference.

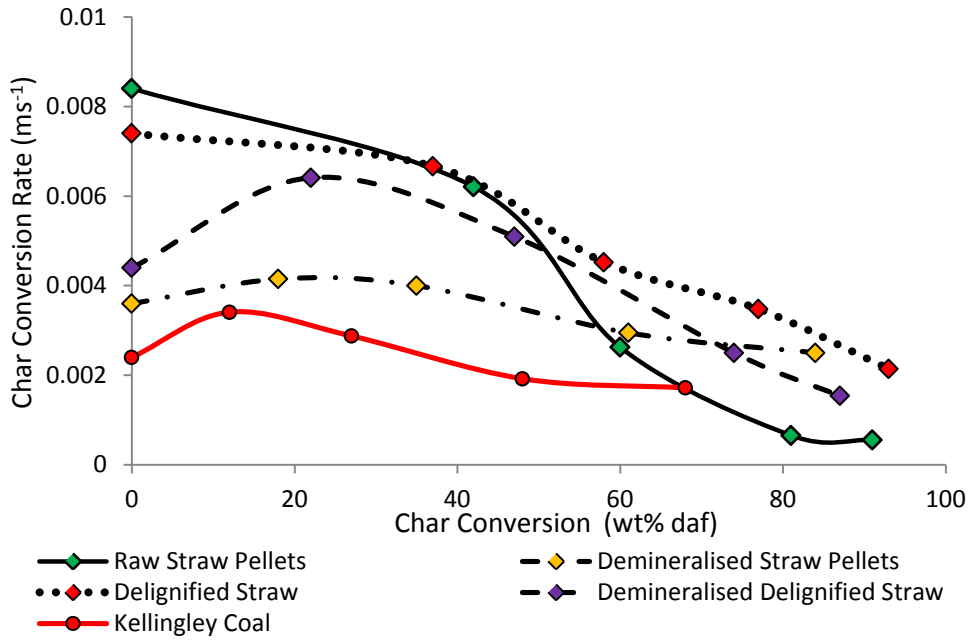


Figure 8-40 Wheat Straw Pellet Fraction DTF Char Re-firing Char Conversion Rate vs.

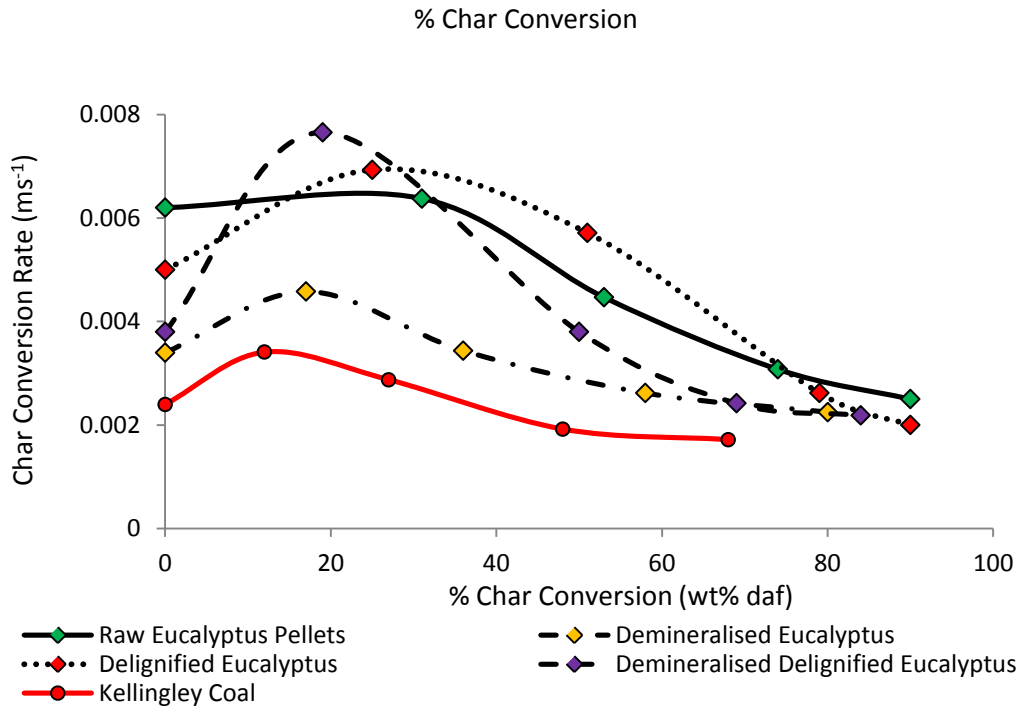


Figure 8-41 Eucalyptus Pellet Fraction DTF Char Re-firing Char Conversion Rate vs.

% Char Conversion

With the exception of raw and delignified straw pellet fuels all other biomass chars and that of Kellingley coal appear to exhibit maxima in the rate of char oxidation after a certain degree of char conversion. These variations in char combustion rate as a function of conversion are consistent with those observed by Kulaots et al., 2002, Tyler et al., 1976 and Zygourakis 2000 for pulverised coal chars obtained from utility boiler flyash, graphitic carbon and entrained flow reactor pulverised coal chars respectively, all of which reported a similar maxima being reached in the rate of char combustion as combustive conversion progresses with coal conversion rates peaking at ~10-40% conversion. An increase in the conversion percentage at which this peak in the char combustion rate is reached was observed with transition from higher levels of chemical kinetic control to greater predominance of diffusion control of the combustion rate. This is consistent with an increase in the overall chemical reactivity of the char whereby the increased rate of reaction on the char surface gives rise to rapid oxygen depletion and the increased retardation of oxygen diffusion into the particle.

Due to the rapid nature of char oxidation reactions occurring under DTF temperatures of 1100°C, oxygen is quickly consumed as it reaches the internal and external surface of the char, limiting its ability to diffuse entirely into all available pores. This gives rise to diffusion limitations occurring in micropore and macropore structures shielding a portion of the internal surface area of the char from the oxidising environment prevalent toward the exterior of the particle limiting combustion reactions to the outer regions of the char where diffusion of oxygen has been successful and the particles external surface. Under these regime II conditions the available surface area per unit mass of the char; the chemical reactivity and the bulk and particle surface concentration of oxygen are all significant in governing the overall reaction rate of char conversion. As the particle undergoes conversion, the surface area can be increased both through the growth of accessible pores and through the opening of previously shielded pore

structures in a “pore opening mechanism” which has been proposed to explain the evolution of char reactivity with increasing conversion under regime II combustion conditions. As the char carbon matrix is consumed, the external surface recedes and previously inaccessible internal pores open to the particle exterior and become available for reaction with oxygen. Pore opening during oxidation of a number of biomass chars has been observed by Senneca 2007 who suggests that the increase in macro and mesopore availability is responsible for the dramatic increases in overall char surface area following 10% combustive conversion. This opening of internal pores increases the total internal surface area available for reaction and, thus, enhances the overall reaction rate. The opening of the internal porous structure of the char gives enhanced importance to both the openness of the char structure and the thickness of the char walls. The time taken for the internal structure of the char to be opened to the oxidising external environment will reduce with decreasing wall thickness, thus thin walled chars with relatively open internal porosity are likely to give increased char conversion rates at lower levels of burnoff compared to those of thicker walled, closed chars. The increases in the reaction rate with burnoff are considerably more noticeable for demineralised delignified straw and eucalyptus samples; this is thought to most likely due to their greater surface area, as measured using nitrogen adsorption, which encourages the development of accessible surface area by enhancing the number of pores opened as burnoff progresses.

In addition to the increase in surface area with initial char combustion the particle temperature also increases due to the exothermicity of the oxidation reaction. This is known to further increase the rate of char combustion following the first 10-20% of char conversion (Wornat et al., 1996).

Plots of BET surface area for straw fraction chars against levels of burnoff are shown in Figure 8-42 and closely follow that proposed by Williams et al., 2012 for biomass chars during high temperature combustion generated using a pore tree model. This supports the supposition that the growth of char surface area does occur during combustion, alongside which the increasing availability of pores previously closed to the oxidising environment due to pore diffusion limitations both act to increase char combustion rates as a function of burnoff during the initial stages of combustion.

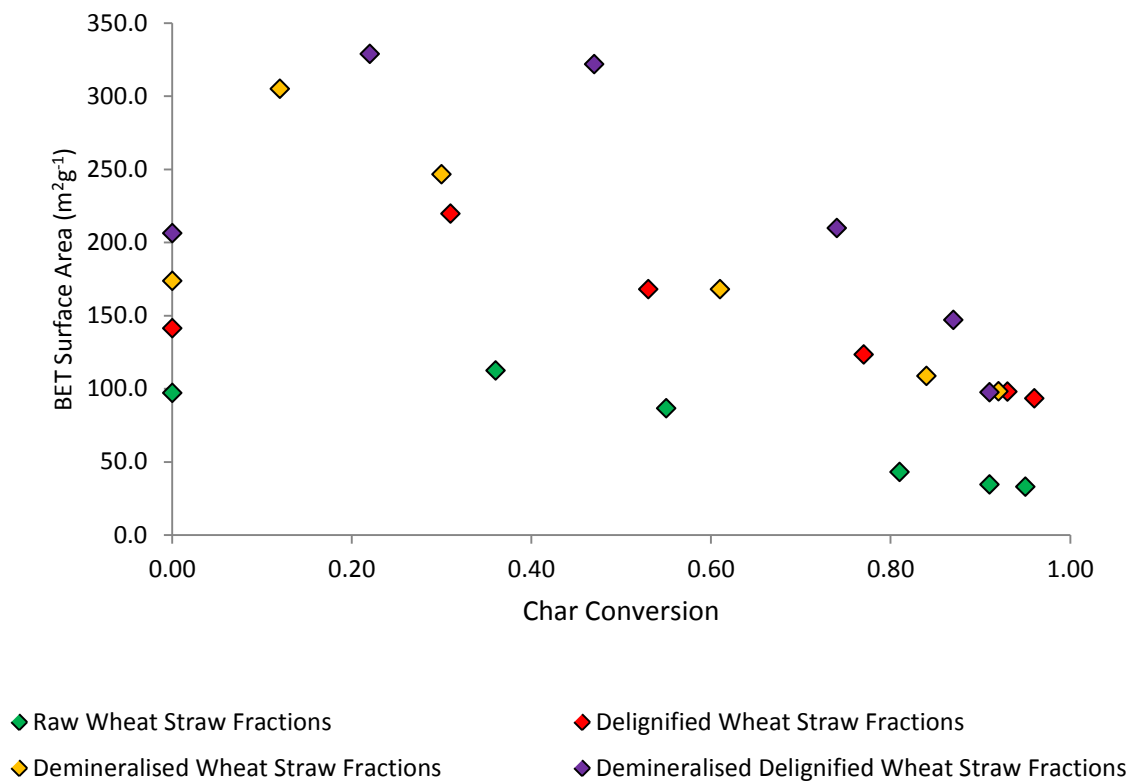


Figure 8-42 Straw Pellet Fraction Char BET Surface Area vs. DTF Re-firing Char Conversion

Following the peak in conversion rate, combustion appears to slow considerably for all fuels such that at high levels of conversion the rate of reaction is low. This is consistent both with a loss of active sites as the pore surface area is progressively consumed and the preferential oxidation of more reactive char structures during the early stages in char burnout. Those char particles which exhibit high surface area and localised

alkali/alkaline mineral concentrations undergoing rapid oxidation with depletion of amorphous carbon structures which results in more rapid initial conversion and progressive deactivation of the char (Lu et al., 2002). In addition to this the particle temperature is known to decrease as the exothermicity of the reaction decreases towards the end of char burnout.

Wornat et al., 1996 observed a similar trend with the influences of mixed chemical and diffusion controlled combustion regimes for char combustion of pine and switchgrass chars in an entrained flow reactor with direct measurement of particle temperature using luminosity. Their observation of particle combustion occurring over a wide range of particle temperatures evenly distributed between the theoretical lower limits of pure chemical control (highly unreactive particles) and the upper temperature limits of diffusion controlled combustion (highly reactive particles) has been postulated to be due to the highly heterogeneous nature of the chars in questions with a wide distribution of char morphologies and mineral matter distributions. The most reactive particles were seen to burn more rapidly and at the higher temperatures during this study, less reactive particles combusting slowly and at more moderate temperatures. As combustion proceeds, the rapid depletion of carbon from the most reactive particles leaves ash-rich particles with much reduced reactivity.

A series of studies have also attributed progressive char deactivation to the preferential loss of oxygen and hydrogen (Jenkins et al., 1973), loss of disordered, active site rich amorphous carbon (Smith, 1956), and volatilisation of catalytic AAEMs (Spiro et al., 1983; Radović et al., 1983; Yuh and Wolf, 1983) all of which contribute to the loss of reactivity during the later stages of combustion.

It is thus apparent that the behaviour of the char during combustion differs significantly under TGA and DTF conditions. Given the high temperature experienced by the oxidising

char particles within the DTF any combustion reaction is likely to occur with significant influence of pore diffusion limitations where the rate of reaction is largely controlled by a combination of chemical reaction rate and diffusion of oxygen within the char particle. Under such conditions the physical structure of the char particle and both its internal/external surface area and its development during combustion play an increased role in determining the reactivity of the char as conversion progresses.

Figures 8-43 and 8-44 show plots of $\ln[\% \text{ char remaining}]$ against DTF re-firing residence time in proof of the fact that the reactions occurring are non-first order with respect to reactant concentrations due both to changes in surface area and intrinsic reactivity with degree of conversion. None of these characteristic plots represent close correlation to the linear, with upwardly mobile trend being observed at higher conversions due to the reduction in reaction rate.

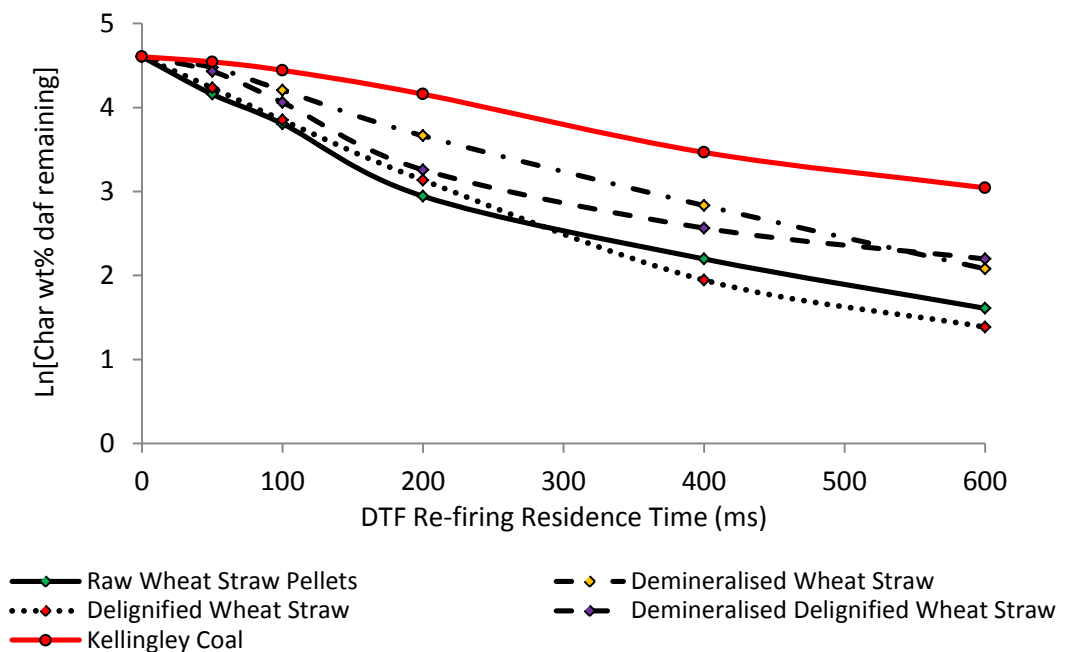


Figure 8-43 $\ln[\text{Char Remaining}]$ vs. DTF Re-firing Time for Wheat Straw Pellet Fractions

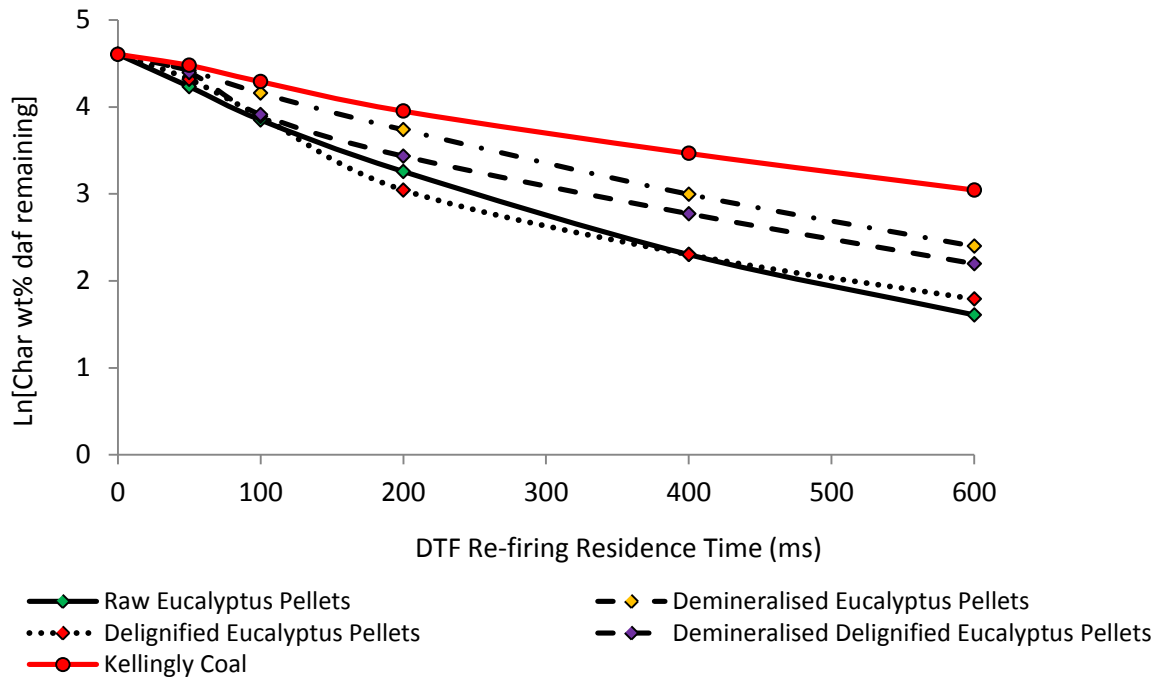


Figure 8-44 Ln[Char Remaining] vs. DTF Re-firing Time for Eucalyptus Pellet Fractions

Isothermal char reactivity experiments have been conducted for wheat straw samples to confirm the ordering of reactivity observed under DTF conditions whereby the char samples collected following individual re-firing residence times in the DTF conform to the observed trends in reactivity shown in Figures 8-39 and 8-40. Arrhenius plots for these isothermal combustion experiments are shown in Figures 8-44 – 8-47. In order to assess the evolution of intrinsic char chemical reactivity in the absence of surface area influences the BET surface area for chars having undergone varying degrees of combustive conversion have been measured and utilised to normalise apparent first order rate constant, expressing conversion rate on a unitised surface area basis ($\text{g}/\text{m}^2 \cdot \text{min}$). Kinetic parameters are summarised in Table 8-7.

	Char Conversion	Ea (kJ/mol)	A ($\text{min}^{-2}\text{AtmO}_2^{-1}$)	k_{a450} (min^{-1})	BET Surface Area (m^2g^{-1})	K_{i450} ($\text{g}/\text{m}^2\cdot\text{min}$)
Raw Wheat Straw Pellets	0.00	69.20	4.45×10^4	0.093	97.0	9.61×10^{-4}
	0.36	83.63	3.76×10^5	0.070	112.5	6.18×10^{-4}
	0.55	107.52	1.05×10^7	0.040	86.6	4.59×10^{-4}
	0.81	123.03	5.92×10^7	0.016	43.1	3.72×10^{-4}
	0.91	142.35	1.04×10^9	0.011	34.6	3.21×10^{-4}
	0.95	143.65	1.02×10^9	0.009	32.9	2.78×10^{-4}
Delignified Wheat Straw Pellets	0.00	67.10	7.41×10^6	0.043	141.4	3.04×10^{-4}
	0.31	79.08	1.34×10^5	0.052	219.6	2.38×10^{-4}
	0.53	78.77	9.80×10^4	0.042	167.9	2.49×10^{-4}
	0.77	90.81	6.96×10^5	0.037	123.4	2.97×10^{-4}
	0.93	103.73	5.62×10^6	0.034	97.9	3.52×10^{-4}
	0.96	105.16	5.73×10^6	0.031	93.3	3.28×10^{-4}
Demineralised Wheat Straw	0.00	146.24	2.65×10^9	0.015	173.8	8.68×10^{-5}
	0.12	153.76	1.36×10^{10}	0.019	304.9	6.34×10^{-5}
	0.30	151.95	8.16×10^9	0.018	246.5	7.35×10^{-5}
	0.61	155.26	7.64×10^9	0.011	167.9	6.36×10^{-5}
	0.84	172.39	1.13×10^{11}	0.008	108.6	7.55×10^{-5}
	0.92	179.85	2.98×10^{11}	0.006	98.1	6.47×10^{-5}
Demineralised Delignified Wheat Straw	0.00	109.56	7.41×10^6	0.019	206.3	9.14×10^{-5}
	0.22	127.77	2.19×10^8	0.028	328.9	8.61×10^{-5}
	0.47	139.03	1.31×10^9	0.024	321.9	7.54×10^{-5}
	0.74	135.34	4.51×10^8	0.016	209.9	7.49×10^{-5}
	0.87	132.97	2.23×10^8	0.011	146.9	7.64×10^{-5}
	0.91	135.33	2.60×10^8	0.009	97.6	9.20×10^{-5}

Table 8-7 DTF Char Re-firing Kinetic Parameters

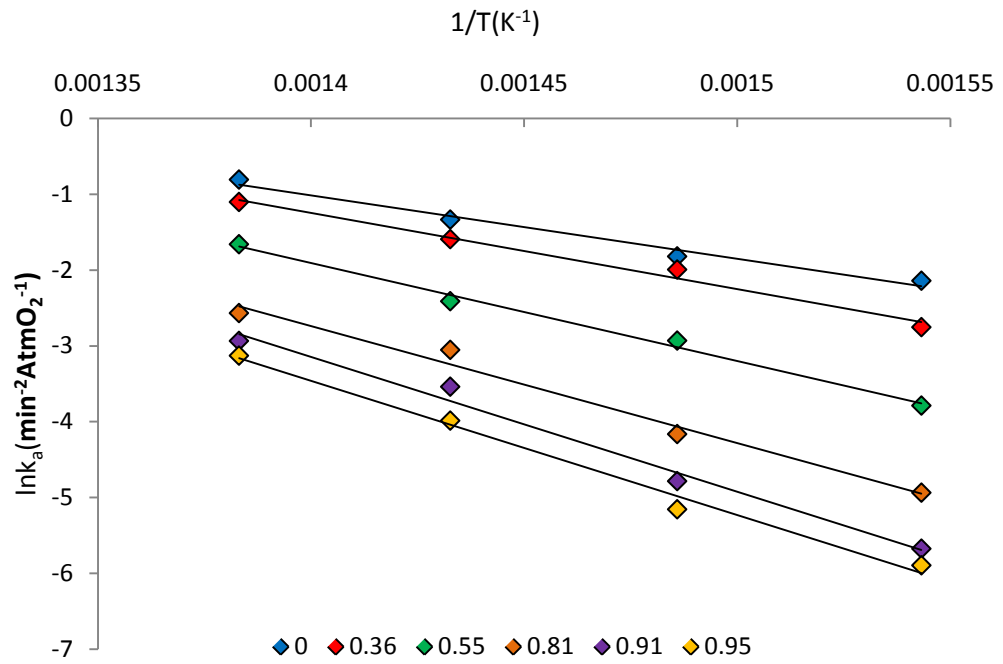


Figure 8-45 Delignified Wheat Straw Char Re-firing Arrhenius Plots

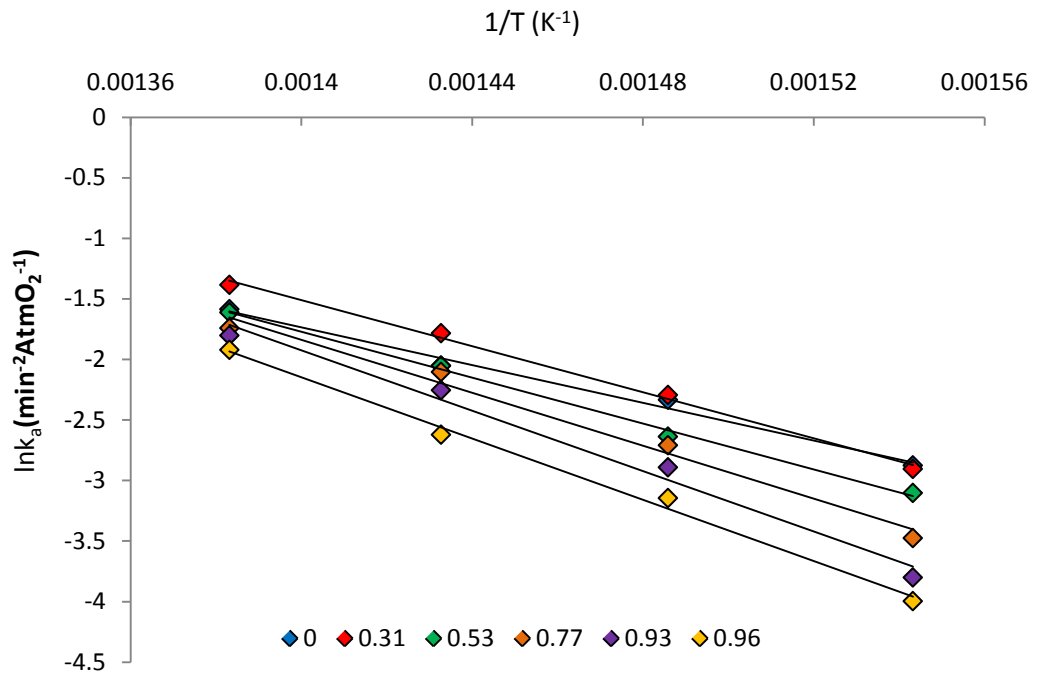


Figure 8-46 Delignified Wheat Straw Char Re-firing Arrhenius Plots

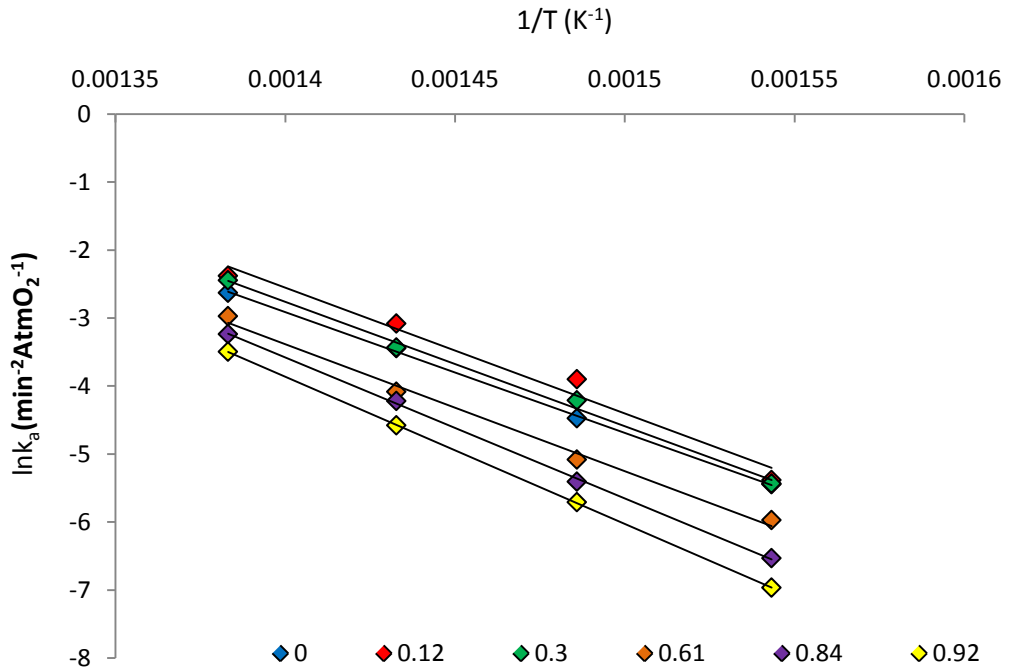


Figure 8-47 Demineralised Wheat Straw Char Re-firing Arrhenius Plots

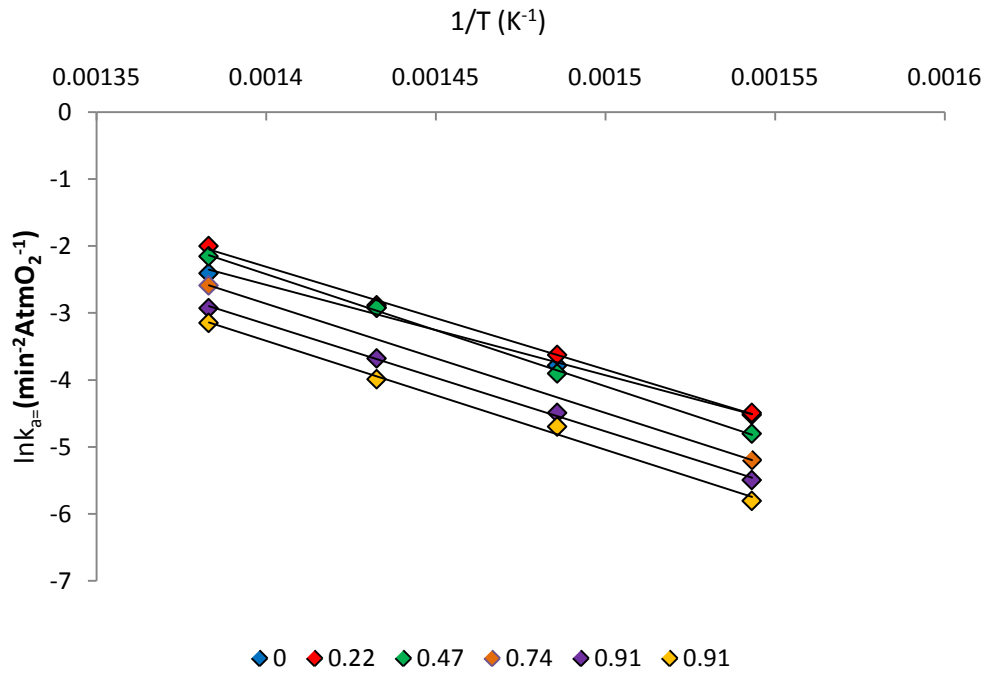


Figure 8-48 Demineralised Delignified Wheat Straw Char Re-firing Arrhenius Plots

Plots of the activation energy and intrinsic rate constant can be seen in Figures 8-49 and 8-50.

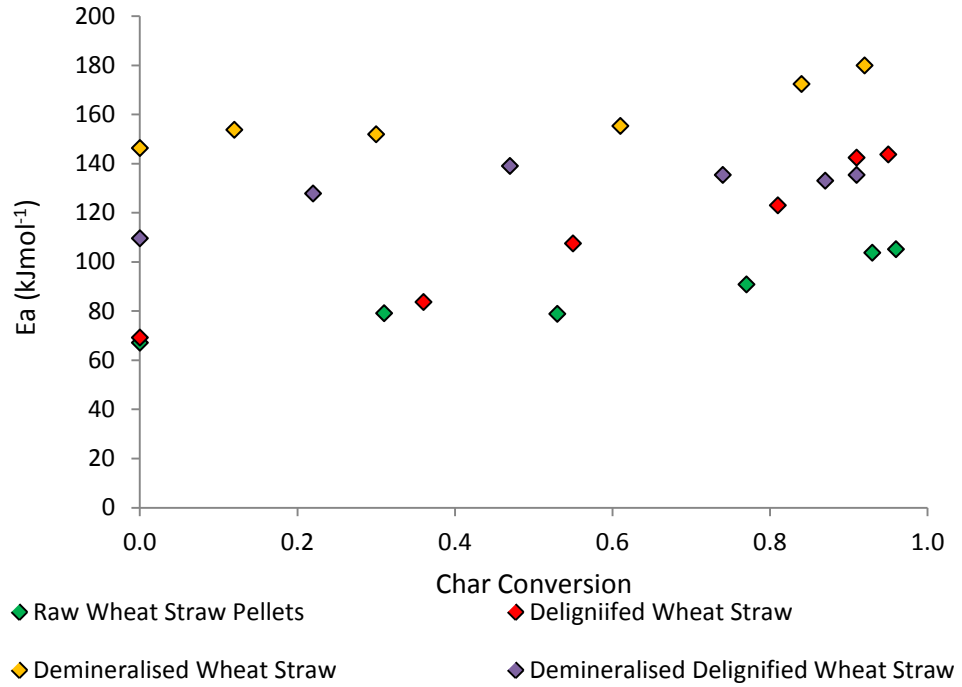


Figure 8-49 E_a vs. Char Conversion for Wheat Straw DTF Re-firing

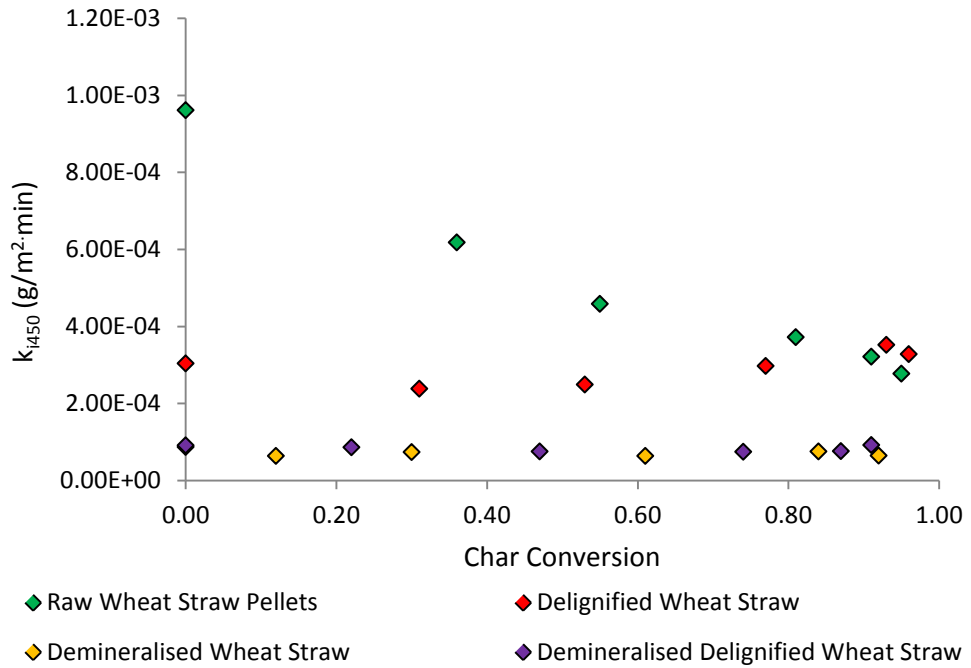


Figure 8-50 k_i vs. Char Conversion for Wheat Straw DTF Re-firing

It is clearly shown that as the degree of conversion increases as does the activation energy of char combustion which can be linked with the level of condensation of the char and its chemical recalcitrance which increases during combustive conversion (Yip et al., 2011).

The intrinsic reactivity of raw wheat straw chars decrease considerably with increasing conversion, however a relatively flat trend in k_i is observed for all other fractions. This is partly due to the much lower initial intrinsic rate constant for partially demineralised fuels but may also indicate that these chars are considerably more homogenous in terms of their chemical reactivity during high temperature combustion and thus do not undergo as significant a deactivation as high mineral matter fuels. This may be linked with the loss of AAEM matter components during combustion and their coalescence to form discrete ash rich particles. Given the low levels of change in intrinsic rate constant for low AAEM containing fuels any alteration in the rate of char oxidation at varying levels of combustive conversion will be driven predominantly by changes experienced in surface area. This is not true of high ash raw wheat straw which adopts a continuously decreasing trend in reactivity throughout DTF re-firing combustion which is in contrast to the observed developments in BET surface area which show an initial increase in surface area during the early stages of combustion, the observed reduction in oxidation rate thus being driven predominantly by intrinsic deactivation of the char.

8.5. Summary

The reactivity of whole fuels and their chars generated under slow and rapid heating pyrolysis have been assessed alongside those subject to varying degrees of combustion residence time in a DTF.

The key findings of this study are summarised as:

- ▶ The combustion reactivity of biomass chars measured during TGA slow heating rate combustion and following rapid heating entrained flow pyrolysis in a drop tube furnace have been consistently ranked from most to least reactive as raw biomass > delignified biomass > demineralised delignified biomass > demineralised biomass. This finding is a result of the influences exerted by the aromatic carbon and mineral matter content of biomass fuels have in determining the combustive reactivity of chars, especially when generated under conditions which simulate those experienced in PF fired boiler plant. It is proposed that fuels with higher lignin and thus aromatic carbon contents produce chars of reduced apparent and intrinsic reactivity, are most likely to form thick walled char structures and may thus contribute to the percentage of unburned fuel in boiler flyash. This may lead to loss in boiler efficiency and possibly increased overall particle emissions depending upon particulate abatement plat utilised.
- ▶ The influence of aromatic carbon on fuel reactivity has been quantitatively studied and, where active mineral matter contents are low, the reactivity of the biomass fuel char is driven by changes in the lignin and aromatic carbon contents, higher proportions of which within the fuel give rise to reductions in the surface area of the char which drives decreases in the apparent global char conversion rate. More aromatic rich fuels also appear to produce chars of reduced intrinsic reactivity (accounting for changes in char surface area) which also drives reduction in the rate of char conversion processes under boiler like conditions of mixed chemical and diffusion rate limitation. Where appreciable AAEM mineral matter is observed this tends to drive the overall rate of char conversion through catalysis of oxidation reactions which have been observed

to be linked predominantly with the K content of the fuel (Ca content having reduced influence on char conversion processes)

- ▶ Char combustion dynamics under boiler like conditions have been studied using the DTF such that the evolution of porous biomass structure and the influence of progressive combustion on the kinetics of biomass chars have been studied. It is shown that chars generally follow the ranking of reactivity derived using isothermal combustion of devolatilised fuels. However, the conversion of those samples which generate larger degrees of surface area during the combustion process, in this case delignified and demineralised delignified fuels, tend to supersede those of chars which appear more reactive during the initial stages of combustion, typically being those of higher AAEM content which tend to show consistent, most severe deactivation with progressing combustion.

Chapter 9: Conclusions and Future Work

In light of recent industrial interest in the adoption of biomass fuels as an alternative to coal in large scale thermochemical conversion driven power generation infrastructure this investigation has concentrated on the combustion behaviour of varied biomass fuels under pulverised fuel firing conditions. The principle aim has been the derivation of easily utilised classifications of varied biomass fuels for the prediction of combustion behaviours through both devolatilisation and char combustion phases. The study has focussed upon a quantification of the well-known influences of both organic and inorganic composition of biomass fuels on their thermal decomposition behaviours and subsequent char conversion reactivities. Special emphasis has been placed on the role played by lignin derived aromatic carbon and alkali/alkaline earth mineral species concentrations.

A new classification system for prediction of the volatile matter/char yield generated under both slow and rapid heating environments has been derived. The system proposed utilises determination of fuel aromatic carbon content (derived using ^{13}C NMR spectroscopy and elemental analysis) and mineral matter analysis (using ICP-MS), both commonly utilised for coal combustion characterisation. From these an accurate prediction of biomass char yield is made through empirical correlation between char yield, aromatic carbon and K+Ca content with R^2 correlation coefficients for predictions of 0.96 and 0.98 and average error levels of 7.8 and 8.4% for slow and rapid heat rate pyrolysis conditions respectively. The empirical formulae and their derivation are described in detail in Chapter 6 and are included below.

For slow heating pyrolysis:

$$\textit{Slow Heating Char Yield} = (1 \times \textit{Aromatic Carbon}) + (16.1 \times (K + Ca))$$

Where slow heating char yield is the char yield wt% on a dry ash free basis (daf), aromatic carbon is the wt% daf aromatic carbon content of the biomass and K+Ca is the wt% K+Ca content of the raw fuel on a dry basis.

This relationship applies up to a K+Ca content of 0.6 wt% db, beyond this a fixed additional char yield of 9.76 wt% daf can be applied as a quantification of the influence of enhanced char yield due to mineral activity as the second term in the above equation.

For rapid heating entrained flow pyrolysis the empirical prediction of char yield is conducted as follows:

$$\text{Rapid Heating Char Yield} = (0.58 \times \text{Aromatic Carbon}) + (2.43 \times (K + Ca))$$

In addition to the predictive calculation of char yield, the influence of biomass aromatic carbon and mineral matter content on the physical form PF chars produced following high heating rate pyrolysis has been investigated. The effect of these components has been evaluated both qualitatively, using microscopy, and quantitatively, using char BET surface area determinations, in Chapter 7. In both cases the reduction in lignin derived aromatic carbon content following organosolv delignification was shown to result in a decrease in the char wall thickness with consequent increase in BET surface area. The tendency of isolated lignins to form fused, low surface area chars has been demonstrated and it has been concluded that this behaviour is the principle driver for reductions in surface area for demineralised fuels with increasing aromaticity.

Mineral components of the biomass encourage the retention of the original biological structure of the char generated under rapid heating simulated PF firing pyrolysis conditions by limiting the formation of mobile intermediate phases during pyrolysis.

There also appears to be a negative correlation between char surface area and inherent

mineral content. This influence has been shown to mirror the effect of potassium and calcium in enhancing char yields, char yield enhancements correlating well with char surface area reductions. It has been suggested in recent literature that this reduction in surface area is due to the blocking of pore surface by molten ash, however, the possibility of a link between encouragement of char formation and reduction in char surface area have been discussed.

Although direct prediction of biomass char reactivities is more difficult, due to the complex behaviour of active minerals and their loss during pyrolysis, the reactivity of rapid heating chars has been studied in detail in Chapter 8. There is clear evidence that both apparent and inherent char reactivity decreases with increasing biomass aromatic carbon content. K is also evidenced as the principle contributor to catalytic char oxidation reactions which are shown to dramatically increase oxidation rates.

Overall both aromatic carbon and alkali/alkaline metal content of biomass fuels have been shown to drive the behaviour of these varied fuels during each phase of combustion by dictating pyrolysis yields, char nature and char reactivity. The quantification of these fuel components is believed to be a powerful tool in prediction of combustion performance of varied biomass fuels for use in combustion.

The performance of solid biomass fuels during the dynamic processes undergone during PF combustion will determine the overall efficiency of the combustion process, the generation of pollutant species and the optimised design and operation of combustion related equipment.

It is hoped that the experimental results described in this body of work will enable plant owners, equipment designers, scientists and engineers to more fully appreciate the driving forces determining the devolatilisation and char combustion behaviours of a

range of biomass fuels which are highly varied in their nature. This will allow biomass fuels to be more accurately characterised such that informed fuel selection can be made alongside pertinent design and adoption of conversion technologies can be made.

9.1. Future Work

Although significant progress has been made in further understanding the combustive conversion of biomass fuels there remains a wealth of information which is yet to be determined. As such a number of future studies originating directly from the work undertaken during this engineering doctoral study are proposed as follows.

9.1.1. Ignition and Flame Stability Study

It is well evidenced for coals that as the volatile matter content increases the ignition and flame stability characteristics of coals increases due to the rapid evolution of substantial portions of the fuel as a combustible gas able to support the devolatilisation and ignition of incoming coal particles (Su et al., 2001 – a comprehensive study of existing knowledge regarding coal ignition). It was thus believed that the adoption of biomass as a fuel during co-firing and 100% PF combustion applications was envisaged to also offer similar benefits with regards to the establishment of strong, stable and attached flames. This has not however been the case with the incorporation of increasing proportions of biomass in the fuel mix giving rise to detached and unstable flames at biomass inputs above 20% by energy (Lu et al., 2008). Although the influence of biomass particle size and moisture are become well understood in these circumstances, the volume of volatile matter released during initial devolatilisation may exclude oxygen from the near burner zone and give rise to decreases in flame stability which are critical in maintaining the safe operation of burner equipped power plant. It is envisaged that the predictive correlation described in this investigation (see Chapter 6)

may be used in conjunction with visible drop tube combustor studies to further correlate the aromatic carbon and mineral matter content of the fuels with ignition delay point and likely flame stability impacts.

9.1.2. Computerised Modelling Studies

Computerised modelling is a commonly utilised tool within industry used to further understand the combustion of biomass fuels in industrial PF boilers. In order to provide consistent, accurate and reliable model outputs, essential data regarding the behaviour of solid fuels under simulated PF firing conditions must be experimentally determined including the kinetic reactivity of chars, their volatile matter yields under high heating rate, high temperature condition and other varied physical and chemical properties.

A number of these key parameters have been determined in this study including the kinetic factors of char combustion, the development of char porosity during combustion, the evolution of apparent and intrinsic char reactivity. The assessment and modification of existing models may be conducted in conjunction with the development of new codes which might be able to accommodate aromatic carbon and mineral matter determinations in more accurately determining combustion behaviours of biomass fuels, thus aiding in the accurate determination of the differing conversion dynamics of varied biomass fuels and their influence on overall plant operating factors.

Any such study may assist boiler operators more accurately assess the potential impacts of altering the fuel mix whilst providing detailed information for more pertinent design and optimisation of boiler equipment.

Chapter 10: References

- AARNA, I. & SUUBERG, E. M. 1998. Changes in reactive surface area and porosity during char oxidation. Symposium (International) on Combustion, 27, 2933-2939.
- AGBLEVOR, F., BESLER, S. & MONTANE, D. 1995. Influence of inorganic compounds on char formation and quality of fast pyrolysis oils. American Chemical Society, Washington, DC (United States).
- AGRAWAL, R. K. 1988. Kinetics of reactions involved in pyrolysis of cellulose I. The three reaction model. The Canadian Journal of Chemical Engineering, 66, 403-412.
- ALONSO, M. J. G., BORREGO, A. G., ALVAREZ, D., PARRA, J. B. & MENÉNDEZ, R. 2001(a). Influence of pyrolysis temperature on char optical texture and reactivity. Journal of Analytical and Applied Pyrolysis, 58–59, 887-909.
- ALONSO, M., BORREGO, A., ALVAREZ, D. & MENENDEZ, R. 2001(b). A reactivity study of chars obtained at different temperatures in relation to their petrographic characteristics. Fuel Processing Technology, 69, 257-272.
- APAYDIN-VAROL, E. & PÜTÜN, A. E. 2012. Preparation and characterization of pyrolytic chars from different biomass samples. Journal of Analytical and Applied Pyrolysis, 98, 29-36.
- ARGYROPOULOS, D. S., JURASEK, L., KRIŠTOFOVÁ, L., XIA, Z., SUN, Y. & PALUŠ, E. 2002. Abundance and Reactivity of Dibenzodioxocins in Softwood Lignin. Journal of Agricultural and Food Chemistry, 50, 658-666.
- ARIAS, B., PEVIDA, C., RUBIERA, F. & PIS, J. 2007. Changes in coal char reactivity and texture during combustion in an entrained flow reactor. Journal of Thermal Analysis and Calorimetry, 90, 859-863.

ASMADI, M., KAWAMOTO, H. & SAKA, S. 2011(b). Pyrolysis and Secondary Reaction Mechanisms of Softwood and Hardwood Lignins at the Molecular Level Zero-Carbon Energy Kyoto 2010. In: YAO, T. (ed.). Springer Japan.

AVILA, C., PANG, C. H., WU, T. & LESTER, E. 2011. Morphology and reactivity characteristics of char biomass particles. *Bioresource Technology*, 102, 5237-5243.

BACKREEDY, R. I., JONES, J. M., POURKASHANIAN, M. & WILLIAMS, A. 2003. Burn-out of pulverised coal and biomass chars. *Fuel*, 82, 2097-2105.

BAILEY, J. G., TATE, A., DIESEL, C. F. K. & WALL, T. F. 1990. A char morphology system with applications to coal combustion. *Fuel*, 69, 225-239.

BALAT, M. 2008. Mechanisms of Thermochemical Biomass Conversion Processes. Part 1: Reactions of Pyrolysis. *Energy Sources, Part A: Recovery, Utilization, and Environmental Effects*, 30, 620-635.

BASU, P. 2010. Chapter 2 - Biomass Characteristics. In: BASU, P. (ed.) *Biomass Gasification and Pyrolysis*. Boston: Academic Press.

BAXTER, L. L., MILES, T. R., MILES JR, T. R., JENKINS, B. M., MILNE, T., DAYTON, D., BRYERS, R. W. & ODEN, L. L. 1998. The behavior of inorganic material in biomass-fired power boilers: field and laboratory experiences. *Fuel Processing Technology*, 54, 47-78.

BEN, H. & RAGAUSKAS, A. J. 2012. Torrefaction of Loblolly pine. *Green Chemistry*, 14, 72-76.

BENNER, R., HATCHER, P. G. & HEDGES, J. I. 1990. Early diagenesis of mangrove leaves in a tropical estuary: Bulk chemical characterization using solid-state ¹³C NMR and elemental analyses. *Geochimica et Cosmochimica Acta*, 54, 2003-2013.

BERGMAN, P. C., BOERSMA, A., ZWART, R. & KIEL, J. 2005. Torrefaction for biomass co-firing in existing coal-fired power stations. Energy Centre of Netherlands, Report No. ECN-C-05-013.

BERGMAN, P. C. & KIEL, J. H. Year. Torrefaction for biomass upgrading. In: Proc. 14th European Biomass Conference, Paris, France, 2005. 17-21.

BIAGINI, E., BARONTINI, F. & TOGNOTTI, L. 2006. Devolatilization of Biomass Fuels and Biomass Components Studied by TG/FTIR Technique. *Industrial & Engineering Chemistry Research*, 45, 4486-4493.

BIAGINI, E., NARDUCCI, P. & TOGNOTTI, L. 2008. Size and structural characterization of lignin-cellulosic fuels after the rapid devolatilization. *Fuel*, 87, 177-186.

BIAGINI, E., SIMONE, M. & TOGNOTTI, L. 2009. Characterization of high heating rate chars of biomass fuels. *Proceedings of the Combustion Institute*, 32, 2043-2050.

BIAGINI, E. & TOGNOTTI, L. 2006. Comparison of devolatilization/char oxidation and direct oxidation of solid fuels at low heating rate. *Energy & Fuels*, 20, 986-992.

BORREGO, A. G., GARAVAGLIA, L. & KALKREUTH, W. D. 2009. Characteristics of high heating rate biomass chars prepared under N₂ and CO₂ atmospheres. *International Journal of Coal Geology*, 77, 409-415.

BOURKE, J., MANLEY-HARRIS, M., FUSHIMI, C., DOWAKI, K., NUNOURA, T. & ANTAL, M. J. 2007. Do all carbonized charcoals have the same chemical structure? 2. A model of the chemical structure of carbonized charcoal. *Industrial & Engineering Chemistry Research*, 46, 5954-5967.

BREWSTER, B. S., SMOOT, L. D., BARTHELSON, S. H. & THORNOCK, D. E. 1995. Model comparisons with drop tube combustion data for various devolatilization submodels. *Energy & Fuels*, 9, 870-879.

BRIDGEMAN, T., JONES, J., SHIELD, I. & WILLIAMS, P. 2008. Torrefaction of reed canary grass, wheat straw and willow to enhance solid fuel qualities and combustion properties. *Fuel*, 87, 844-856.

BRIDGEMAN, T., JONES, J., WILLIAMS, A. & WALDRON, D. 2010. An investigation of the grindability of two torrefied energy crops. *Fuel*, 89, 3911-3918.

BRITISH COAL CORPORATION, C. R. E., ENERGÍA, C. E. D. G. D. & ENERGÍA, C. E. D. G. D. 1991. Studies on the Production of Nitrogen Oxides and Ash Deposition from Pulverised Coal, in Relation to Utilisation in Low NO_x Burners: Contract No 7720-EC/845, Commission of the European Communities. Directorate-General Telecommunications, Information Industries and Innovation.

BROSSE, N., SANNIGRAHI, P. & RAGAUSKAS, A. 2009. Pretreatment of *Miscanthus x giganteus* Using the Ethanol Organosolv Process for Ethanol Production. *Industrial & Engineering Chemistry Research*, 48, 8328-8334.

CAI, H. Year. Effect of maceral content on volatile release and char combustion reactivity. In: *Fuel and Energy Abstracts*, 1998. 46.

CHOI, C. Y., MUNTEAN, J. V., THOMPSON, A. R. & BOTTO, R. E. 1989. Characterization of coal macerals using combined chemical and NMR spectroscopic methods. *Energy & Fuels*, 3, 528-533.

CHOUDHURY, N., BISWAS, S., SARKAR, P., KUMAR, M., GHOSAL, S., MITRA, T., MUKHERJEE, A. & CHOUDHURY, A. 2008. Influence of rank and macerals on the burnout behaviour of pulverized Indian coal. *International Journal of Coal Geology*, 74, 145-153.

CLIFTON-BROWN, J. C., STAMPFL, P. F. & JONES, M. B. 2004. Miscanthus biomass production for energy in Europe and its potential contribution to decreasing fossil fuel carbon emissions. *Global change biology*, 10, 509-518.

CLOKE, M. & LESTER, E. 1994. Characterization of coals for combustion using petrographic analysis: a review. *Fuel*, 73, 315-320.

CLOKE, M., WU, T., BARRANCO, R. & LESTER, E. 2003. Char characterisation and its application in a coal burnout model. *Fuel*, 82, 1989-2000.

THE COMMITTEE ON CLIMATE CHANGE, 2015. Meeting carbon budgets - progress in reducing the UK's emissions 2015 report to parliament committee on climate change June 2015. The Committee on Climate Change; 7 Holbein Place London SW1W 8NR

COPELAND, J. & TURLEY, D. 2008. National and regional supply/demand balance for agricultural straw in Great Britain. National Non-Food Crops Centre, York.

CRELLING, J. C., HIPPO, E. J., WOERNER, B. A. & WEST, D. P. 1992. Combustion characteristics of selected whole coals and macerals. *Fuel*, 71, 151-158.

CRELLING, J. C., SKORUPSKA, N. M. & MARSH, H. 1988. Reactivity of coal macerals and lithotypes. *Fuel*, 67, 781-785.

DARVELL, L. I., JONES, J. M., GUDKA, B., BAXTER, X. C., SADDAWI, A., WILLIAMS, A. & MALMGREN, A. 2010. Combustion properties of some power station biomass fuels. *Fuel*, 89, 2881-2890.

DAVINI, P., GHETTI, P., BONFANTI, L. & DE MICHELE, G. 1996. Investigation of the combustion of particles of coal. *Fuel*, 75, 1083-1088.

DAVIDSON, P., GALLUZZO, N., STALLARD, G., JENNISON, K., BROWN, R., JONAS, T., PAVLISH, J., MITAS, D., LOWE, D. & ARROYO, J. 1990. Development and application of the Coal Quality Impact Model: CQIM trademark. Electric Power Research Inst., Palo Alto, CA (USA); Black and Veatch, Kansas City, MO (USA).

DEPARTMENT OF ENERGY AND CLIMATE CHANGE (DECC), 2009. National renewable energy action plan for the United Kingdom article 4 of the renewable energy directive 2009/28/EC. The Stationery Office Limited: London

DEPARTMENT OF ENERGY AND CLIMATE CHANGE (DECC), 2011(a). UK renewable energy roadmap. The Stationery Office Limited: London.

DEPARTMENT OF ENERGY AND CLIMATE CHANGE (DECC), 2011(b). Digest of United Kingdom energy statistics 2011. A National Statistics Publication, The Stationery Office Limited: London.

DEPARTMENT OF ENERGY AND CLIMATE CHANGE (DECC), 2013. Electricity market reform – contract for difference: contract and allocation overview. A National Statistics Publication, The Stationery Office Limited: London.

DEGROOT, W. F. & SHAFIZADEH, F. 1984. The influence of exchangeable cations on the carbonization of biomass. *Journal of Analytical and Applied Pyrolysis*, 6, 217-232.

DEMIRBAŞ, A. 2003. Relationships between lignin contents and fixed carbon contents of biomass samples. *Energy Conversion and Management*, 44, 1481-1486.

DÍAZ-TERÁN, J., NEVSKAIA, D. M., FIERRO, J. L. G., LÓPEZ-PEINADO, A. J. & JEREZ, A. 2003. Study of chemical activation process of a lignocellulosic material with KOH by XPS and XRD. *Microporous and Mesoporous Materials*, 60, 173-181.

DI BLASI, C. 2009. Combustion and gasification rates of lignocellulosic chars. *Progress in Energy and Combustion Science*, 35, 121-140.

DI BLASI, C. & LANZETTA, M. 1997. Intrinsic kinetics of isothermal xylan degradation in inert atmosphere. *Journal of Analytical and Applied Pyrolysis*, 40–41, 287-303.

DRAX GROUP PLC. 2014. Preliminary results 12 months ended 31 December 2013. DRAX Group plc.

DUFOUR, A., CASTRO-DIAZ, M., BROSSE, N., BOUROUKBA, M. & SNAPE, C. 2012. The Origin of Molecular Mobility During Biomass Pyrolysis as Revealed by In situ ¹H NMR Spectroscopy. *ChemSusChem*, 5, 1258-1265.

EHRBURGER, P., ADDOUN, A., ADDOUN, F. & DONNET, J.-B. 1986. Carbonization of coals in the presence of alkaline hydroxides and carbonates: Formation of activated carbons. *Fuel*, 65, 1447-1449.

EOM, I. Y., KIM, J. Y., KIM, T. S., LEE, S. M., CHOI, D., CHOI, I. G. & CHOI, J. W. 2012. Effect of essential inorganic metals on primary thermal degradation of lignocellulosic biomass. *Bioresource Technology*, 104, 687-694.

ESSENHIGH, R. H., MISRA, M. K. & SHAW, D. W. 1989. Ignition of coal particles: a review. *Combustion and Flame*, 77, 3-30.

FAHMI, R., BRIDGWATER, A. V., DARVELL, L. I., JONES, J. M., YATES, N., THAIN, S. & DONNISON, I. S. 2007. The effect of alkali metals on combustion and pyrolysis of *Lolium* and *Festuca* grasses, switchgrass and willow. *Fuel*, 86, 1560-1569.

FARROW, T. S. 2013. *A fundamental study of biomass oxy-fuel combustion and co-combustion*. University of Nottingham.

FARROW, T. S., SUN, C. & SNAPE, C. E. 2015. Impact of CO₂ on biomass pyrolysis, nitrogen partitioning, and char combustion in a drop tube furnace. *Journal of Analytical and Applied Pyrolysis*.

FENG, B. & BHATIA, S. K. 2003. Variation of the pore structure of coal chars during gasification. *Carbon*, 41, 507-523.

FISHER, E. M., DUPONT, C., DARVELL, L. I., COMMANDRÉ, J. M., SADDAWI, A., JONES, J. M., GRATEAU, M., NOCQUET, T. & SALVADOR, S. 2012. Combustion

and gasification characteristics of chars from raw and torrefied biomass. *Bioresource Technology*, 119, 157-165.

FLETCHER, T. H. 1989. Time-Resolved Temperature Measurements of Individual Coal Particles During Devolatilization. *Combustion Science and Technology* 63(1-3): 89-105.

FUENTES, M. E., NOWAKOWSKI, D. J., KUBACKI, M. L., COVE, J. M., BRIDGEMAN, T. G. & JONES, J. M. 2008. Survey of influence of biomass mineral matter in thermochemical conversion of short rotation willow coppice. *Journal of the Energy Institute*, 81, 234-241.

GANI, A. & NARUSE, I. 2007. Effect of cellulose and lignin content on pyrolysis and combustion characteristics for several types of biomass. *Renewable Energy*, 32, 649-661.

GARLOCK, R. J., BALAN, V., DALE, B. E., RAMESH PALLAPOLU, V., LEE, Y. Y., KIM, Y., MOSIER, N. S., LADISCH, M. R., HOLTZAPPLE, M. T., FALLS, M., SIERRA-RAMIREZ, R., SHI, J., EBRIK, M. A., REDMOND, T., YANG, B., WYMAN, C. E., DONOHOE, B. S., VINZANT, T. B., ELANDER, R. T., HAMES, B., THOMAS, S. & WARNER, R. E. 2011. Comparative material balances around pretreatment technologies for the conversion of switchgrass to soluble sugars. *Bioresource Technology*, 102, 11063-11071.

GAVALAS, G. R. 1980. Analysis of char combustion including the effect of pore enlargement. *Combustion Science and Technology*, 24, 197-210.

GONZÁLEZ-VILA, F. J., TINOCO, P., ALMENDROS, G. & MARTIN, F. 2001. Pyrolysis–GC–MS Analysis of the Formation and Degradation Stages of Charred Residues from Lignocellulosic Biomass. *Journal of Agricultural and Food Chemistry*, 49, 1128-1131.

- GUERRERO, M., RUIZ, M. P., ALZUETA, M. U., BILBAO, R. & MILLERA, A. 2005. Pyrolysis of eucalyptus at different heating rates: studies of char characterization and oxidative reactivity. *Journal of Analytical and Applied Pyrolysis*, 74, 307-314.
- GUERRERO, M., RUIZ, M. P., MILLERA, Á., ALZUETA, M. U. & BILBAO, R. 2008. Characterization of Biomass Chars Formed under Different Devolatilization Conditions: Differences between Rice Husk and Eucalyptus. *Energy & Fuels*, 22, 1275-1284.
- HALL, D. O., RAO, K. & BIOLOGY, I. O. 1999. *Photosynthesis*, Cambridge University Press.
- HAMES, B., SCARLATA, C. & SLUITER, A. 2008. Determination of protein content in biomass. National Renewable Energy Laboratory, Golden, CO, USA.
- HAMILTON, L. H. 1981. Char morphology and behaviour of Australian vitrinites of various ranks pyrolysed at various heating rates. *Fuel*, 60, 909-913.
- HARMSSEN, P., HUIJGEN, W., BERMUDEZ, L. & BAKKER, R. 2010. Literature review of physical and chemical pretreatment processes for lignocellulosic biomass. ECN.
- HASAN KHAN TUSHAR, M. S., MAHINPEY, N., KHAN, A., IBRAHIM, H., KUMAR, P. & IDEM, R. 2012. Production, characterization and reactivity studies of chars produced by the isothermal pyrolysis of flax straw. *Biomass and Bioenergy*, 37, 97-105.
- HAYHURST, A. & LAWRENCE, A. 1995. The devolatilization of coal and a comparison of chars produced in oxidizing and inert atmospheres in fluidized beds. *Combustion and Flame*, 100, 591-604.

HAYKIRI-ACMA, H., YAMAN, S. & KUCUKBAYRAK, S. 2011. Burning characteristics of chemically isolated biomass ingredients. *Energy Conversion and Management*, 52, 746-751.

HILL, S. J., GRIGSBY, W. J. & HALL, P. W. 2013. Chemical and cellulose crystallite changes in *Pinus radiata* during torrefaction. *Biomass and Bioenergy*, 56, 92-98.

HM GOVERNMENT, 2009. The UK low carbon transition plan: national strategy for climate and energy. The Stationery Office Limited: London.

HOSOYA, T., KAWAMOTO, H. & SAKA, S. 2009. Role of methoxyl group in char formation from lignin-related compounds. *Journal of Analytical and Applied Pyrolysis*, 84, 79-83.

HOWARD, J. B. 1981. Fundamentals of Coal Pyrolysis and Hydrolysis. In: ELLIOTT, M. A. (ed.) *Chemistry of Coal Utilization*. John Wiley & Sons.

HURT, R. H., DAVIS, K. A., YANG, N. Y., HEADLEY, T. J. & MITCHELL, G. D. 1995. Residual carbon from pulverized-coal-fired boilers. 2. Morphology and physicochemical properties. *Fuel*, 74, 1297-1306.

HURT, R. H., SAROFIM, A. F. & LONGWELL, J. P. 1991. The role of microporous surface area in the gasification of chars from a sub-bituminous coal. *Fuel*, 70, 1079-1082.

JANSE, A. M. C., DE JONGE, H. G., PRINS, W. & VAN SWAAIJ, W. P. M. 1998. Combustion Kinetics of Char Obtained by Flash Pyrolysis of Pine Wood. *Industrial & Engineering Chemistry Research*, 37, 3909-3918.

JARVIS, M. W., HAAS, T. J., DONOHOE, B. S., DAILY, J. W., GASTON, K. R., FREDERICK, W. J. & NIMLOS, M. R. 2011. Elucidation of Biomass Pyrolysis Products Using a Laminar Entrained Flow Reactor and Char Particle Imaging. *Energy & Fuels*, 25, 324-336.

JENKINS, B., BAXTER, L. & MILES, T. 1998. Combustion properties of biomass. *Fuel Processing Technology*, 54, 17-46.

JENKINS, R. G., NANDI, S. P. & WALKER JR, P. L. 1973. Reactivity of heat-treated coals in air at 500 °C. *Fuel*, 52, 288-293.

JENSEN, P. A., FRANDBSEN, F. J., DAM-JOHANSEN, K. & SANDER, B. 2000. Experimental Investigation of the Transformation and Release to Gas Phase of Potassium and Chlorine during Straw Pyrolysis. *Energy & Fuels*, 14, 1280-1285.

JIANG, L., HU, S., SUN, L.-S., SU, S., XU, K., HE, L.-M. & XIANG, J. 2013. Influence of different demineralization treatments on physicochemical structure and thermal degradation of biomass. *Bioresource Technology*, 146, 254-260.

JONES, J., BRIDGEMAN, T., DARVELL, L., GUDKA, B., SADDAWI, A. & WILLIAMS, A. 2012. Combustion properties of torrefied willow compared with bituminous coals. *Fuel Processing Technology*, 101, 1-9.

JONES, J. M., DARVELL, L. I., BRIDGEMAN, T. G., POURKASHANIAN, M. & WILLIAMS, A. 2007. An investigation of the thermal and catalytic behaviour of potassium in biomass combustion. *Proceedings of the Combustion Institute*, 31, 1955-1963.

JONES, J. M., KUBACKI, M., KUBICA, K., ROSS, A. B. & WILLIAMS, A. 2005. Devolatilisation characteristics of coal and biomass blends. *Journal of Analytical and Applied Pyrolysis*, 74, 502-511.

JONES, R. B., MCCOURT, C. B., MORLEY, C. & KING, K. 1985. Maceral and rank influences on the morphology of coal char. *Fuel*, 64, 1460-1467.

JONES, R. B., ROBERTSON, S. D., CLAGUE, A. D. H., WIND, R. A., DUIJVESTIJN, M. J., VAN DER LUGT, C., VRIEND, J. & SMIDT, J. 1986. Dynamic nuclear polarization ¹³C n.m.r. of coal. *Fuel*, 65, 520-525.

- JONES, R. W., REINOT, T. & MCCLELLAND, J. F. 2010. Molecular analysis of primary vapor and char products during stepwise pyrolysis of poplar biomass. *Energy and Fuels*, 24, 5199-5209.
- JOSEPH, S., PEACOCKE, C., LEHMANN, J. & MUNROE, P. 2009. Developing a biochar classification and test methods. *Biochar for environmental management: Science and technology*, 107-126.
- KALIYAN, N. & MOREY, R. V. 2006. Factors affecting strength and durability of densified products. *In: 2006 ASAE Annual Meeting, 2006. American Society of Agricultural and Biological Engineers*, 1.
- KASTANAKI, E. & VAMVUKA, D. 2006. A comparative reactivity and kinetic study on the combustion of coal–biomass char blends. *Fuel*, 85, 1186-1193.
- KLEMM, D., HEUBLEIN, B., FINK, H. P. & BOHN, A. 2005. Cellulose: fascinating biopolymer and sustainable raw material. *Angewandte Chemie International Edition*, 44, 3358-3393.
- KOPPEJAN, J. & VAN LOO, S. 2012. *The handbook of biomass combustion and co-firing*, Routledge.
- KÜLAOTS, I., HSU, A. & SUUBERG, E. M. 2007. The role of porosity in char combustion. *Proceedings of the Combustion Institute*, 31, 1897-1903.
- LAURENDEAU, N. M. 1978. Heterogeneous kinetics of coal char gasification and combustion. *Progress in Energy and Combustion Science*, 4, 221-270.
- LAM, P. S. 2011. *Steam explosion of biomass to produce durable wood pellets*. UNIVERSITY OF BRITISH COLUMBIA (VANCOUVER).
- LEE, G. & WHALEY, H. 1983. Modification of combustion and fly-ash characteristics by coal blending. *Journal of the Institute of Energy*, 56, 190-197.

LEE, J. W., KIDDER, M., EVANS, B. R., PAIK, S., BUCHANAN III, A., GARTEN, C. T. & BROWN, R. C. 2010. Characterization of biochars produced from cornstovers for soil amendment. *Environmental Science & Technology*, 44, 7970-7974.

LE MANQUAIS, K. 2011. *Combustion enhancing additives for coal firing*. University of Nottingham.

LESTER, E., ALVAREZ, D., BORREGO, A. G., VALENTIM, B., FLORES, D., CLIFT, D. A., ROSENBERG, P., KWIECINSKA, B., BARRANCO, R., PETERSEN, H. I., MASTALERZ, M., MILENKOVA, K. S., PANAITESCU, C., MARQUES, M. M., THOMPSON, A., WATTS, D., HANSON, S., PREDEANU, G., MISZ, M. & WU, T. 2010. The procedure used to develop a coal char classification—Commission III Combustion Working Group of the International Committee for Coal and Organic Petrology. *International Journal of Coal Geology*, 81, 333-342.

LI, X., HAYASHI, J.-I. & LI, C.-Z. 2006. FT-Raman spectroscopic study of the evolution of char structure during the pyrolysis of a Victorian brown coal. *Fuel*, 85, 1700-1707.

LIGHTMAN, P. & STREET, P. J. 1968. Microscopic examination of heat treated pulverised coal particles. *Fuel*, 47, 7-28.

LIU, Q., WANG, S., ZHENG, Y., LUO, Z. & CEN, K. 2008. Mechanism study of wood lignin pyrolysis by using TG–FTIR analysis. *Journal of Analytical and Applied Pyrolysis*, 82, 170-177.

LONG, J., SONG, H., JUN, X., SHENG, S., LUN-SHI, S., KAI, X. & YAO, Y. 2012. Release characteristics of alkali and alkaline earth metallic species during biomass pyrolysis and steam gasification process. *Bioresource Technology*, 116, 278-284.

LU, G., YAN, Y., CORNWELL, S., WHITEHOUSE, M. & RILEY, G. 2008. Impact of co-firing coal and biomass on flame characteristics and stability. *Fuel*, 87, 1133-1140.

LU, G., YAN, Y., CORNWELL, S., WHITEHOUSE, M. & RILEY, G. 2008. Impact of co-firing coal and biomass on flame characteristics and stability. *Fuel*, 87, 1133-1140.

LU, L., KONG, C., SAHAJWALLA, V. & HARRIS, D. 2002. Char structural ordering during pyrolysis and combustion and its influence on char reactivity. *Fuel*, 81, 1215-1225.

LV, G. & WU, S. 2012. Analytical pyrolysis studies of corn stalk and its three main components by TG-MS and Py-GC/MS. *Journal of Analytical and Applied Pyrolysis*, 97, 11-18.

MACIEL, G. E., BARTUSKA, V. J. & MIKNIS, F. P. 1979. Characterization of organic material in coal by proton-decoupled ¹³C nuclear magnetic resonance with magic-angle spinning. *Fuel*, 58, 391-394.

MAROTO-VALER, M. M., ANDRÉSEN, J. M., ROCHA, J. D. & SNAPE, C. E. 1996. Quantitative solid-state ¹³C nmr measurements on cokes, chars and coal tar pitch fractions. *Fuel*, 75, 1721-1726.

MCKENDRY, P. 2002. Energy production from biomass (part 2): conversion technologies. *Bioresource Technology*, 83, 47-54.

MCNAMEE, P., DARVELL, L. I., JONES, J. M. & WILLIAMS, A. The combustion characteristics of high-heating-rate chars from untreated and torrefied biomass fuels. *Biomass and Bioenergy*.

MELKIOR, T., JACOB, S., GERBAUD, G., HEDIGER, S., LE PAPE, L., BONNEFOIS, L. & BARDET, M. 2012. NMR analysis of the transformation of wood constituents by torrefaction. *Fuel*, 92, 271-280.

- MIKNIS, F. P., SULLIVAN, M., BARTUSKA, V. J. & MACIEL, G. E. 1981. Cross-polarization magic-angle spinning ¹³ C NMR spectra of coals of varying rank. *Organic Geochemistry*, 3, 19-28.
- MILLIGAN, J. B., THOMAS, K. M. & CRELLING, J. C. 1997. Temperature-programmed combustion studies of coal and maceral group concentrates. *Fuel*, 76, 1249-1255.
- MOSIER, N., WYMAN, C., DALE, B., ELANDER, R., LEE, Y. Y., HOLTZAPPLE, M. & LADISCH, M. 2005. Features of promising technologies for pretreatment of lignocellulosic biomass. *Bioresource Technology*, 96, 673-686.
- MUNIR, S., DAOOD, S. S., NIMMO, W., CUNLIFFE, A. M. & GIBBS, B. M. 2009. Thermal analysis and devolatilization kinetics of cotton stalk, sugar cane bagasse and shea meal under nitrogen and air atmospheres. *Bioresource Technology*, 100, 1413-1418.
- NARAYAN, R. & ANTAL, M. J. 1996. Thermal Lag, Fusion, and the Compensation Effect during Biomass Pyrolysis. *Industrial & Engineering Chemistry Research*, 35, 1711-1721.
- NOWAKOWSKI, D. J. & JONES, J. M. 2008. Uncatalysed and potassium-catalysed pyrolysis of the cell-wall constituents of biomass and their model compounds. *Journal of Analytical and Applied Pyrolysis*, 83, 12-25.
- OKA, N., MURAYAMA, T., MATSUOKA, H., YAMADA, S., YAMADA, T., SHINOZAKI, S., SHIBAOKA, M. & THOMAS, C. 1987. The influence of rank and maceral composition on ignition and char burnout of pulverized coal. *Fuel Processing Technology*, 15, 213-224.
- OLSSON, J. G., JÄGLID, U., PETTERSSON, J. B. C. & HALD, P. 1997. Alkali Metal Emission during Pyrolysis of Biomass. *Energy & Fuels*, 11, 779-784.

OREM, W. H. & FINKELMAN, R. B. 2003. Coal Formation and Geochemistry. In: TUREKIAN, H. D. H. K. (ed.) Treatise on Geochemistry. Oxford: Pergamon.

OTTAWAY, M. 1982. Use of thermogravimetry for proximate analysis of coals and cokes. *Fuel*, 61, 713-716.

PAN, X., GILKES, N., KADLA, J., PYE, K., SAKA, S., GREGG, D., EHARA, K., XIE, D., LAM, D. & SADDLER, J. 2006. Bioconversion of hybrid poplar to ethanol and co-products using an organosolv fractionation process: optimization of process yields. *Biotechnology and bioengineering*, 94, 851-861.

PAN, X., XIE, D., YU, R. W. & SADDLER, J. N. 2008. The bioconversion of mountain pine beetle-killed lodgepole pine to fuel ethanol using the organosolv process. *Biotechnology and bioengineering*, 101, 39-48.

PARK, J., MENG, J., LIM, K. H., ROJAS, O. J. & PARK, S. 2013. Transformation of lignocellulosic biomass during torrefaction. *Journal of Analytical and Applied Pyrolysis*, 100, 199-206.

PENG, Y. & WU, S. 2010. The structural and thermal characteristics of wheat straw hemicellulose. *Journal of Analytical and Applied Pyrolysis*, 88, 134-139.

PERLACK, R. D., WRIGHT, L. L., TURHOLLOW, A. F., GRAHAM, R. L., STOKES, B. J. & ERBACH, D. C. 2005. Biomass as feedstock for a bioenergy and bioproducts industry: the technical feasibility of a billion-ton annual supply. DTIC Document.

PERRY, S., HAMBLY, E., FLETCHER, T., SOLUM, M. & PUGMIRE, R. 2000. Solid-state ¹³C NMR characterization of matched tars and chars from rapid coal devolatilization. *Proceedings of the Combustion Institute*, 28, 2313-2319.

POTTMAIER, D., COSTA, M., FARROW, T., OLIVEIRA, A. A. M., ALARCON, O. & SNAPE, C. 2013. Comparison of Rice Husk and Wheat Straw: From Slow and Fast Pyrolysis to Char Combustion. *Energy & Fuels*, 27, 7115-7125.

RADLEIN, D. S. T. A. G., GRINSHUPUN, A., PISKORZ, J. & SCOTT, D. S. 1987. On the presence of anhydro-oligosaccharides in the sirups from the fast pyrolysis of cellulose. *Journal of Analytical and Applied Pyrolysis*, 12, 39-49.

RADOVIĆ, L. A. R., WALKER JR, P. L. & JENKINS, R. G. 1983. Effect of lignite pyrolysis conditions on calcium oxide dispersion and subsequent char reactivity. *Fuel*, 62, 209-212.

RADOVIĆ, L. R., WALKER JR, P. L. & JENKINS, R. G. 1983. Importance of carbon active sites in the gasification of coal chars. *Fuel*, 62, 849-856.

RAGAUSKAS, A. J., WILLIAMS, C. K., DAVISON, B. H., BRITOVSEK, G., CAIRNEY, J., ECKERT, C. A., FREDERICK, W. J., HALLETT, J. P., LEAK, D. J., LIOTTA, C. L., MIELENZ, J. R., MURPHY, R., TEMPLER, R. & TSCHAPLINSKI, T. 2006. The Path Forward for Biofuels and Biomaterials. *Science*, 311, 484-489.

RANZI, E., CUOCI, A., FARAVELLI, T., FRASSOLDATI, A., MIGLIAVACCA, G., PIERUCCI, S. & SOMMARIVA, S. 2008. Chemical Kinetics of Biomass Pyrolysis. *Energy & Fuels*, 22, 4292-4300.

RAVEENDRAN, K. & GANESH, A. 1998. Adsorption characteristics and pore-development of biomass-pyrolysis char. *Fuel*, 77, 769-781.

RAVEENDRAN, K., GANESH, A. & KHILAR, K. C. 1995. Influence of mineral matter on biomass pyrolysis characteristics. *Fuel*, 74, 1812-1822.

RENTEL, K. 1987. Marie-Therese Mackowsky Memorial Issue The combined maceral-microlithotype analysis for the characterization of reactive inertinites. *International Journal of Coal Geology*, 9, 77-86.

RHÉN, C., ÖHMAN, M., GREF, R. & WÄSTERLUND, I. 2007. Effect of raw material composition in woody biomass pellets on combustion characteristics. *Biomass and Bioenergy*, 31, 66-72.

ROCKWOOD, D. L., RUDIE, A. W., RALPH, S. A., ZHU, J. & WINANDY, J. E. 2008. Energy product options for Eucalyptus species grown as short rotation woody crops. *International Journal of Molecular Sciences*, 9, 1361-1378.

ROSENBERG, P., PETERSEN, H. I. & THOMSEN, E. 1996. Combustion char morphology related to combustion temperature and coal petrography. *Fuel*, 75, 1071-1082.

RUIZ, H. A., RUZENE, D. S., SILVA, D. P., DA SILVA, F. F. M., VICENTE, A. A. & TEIXEIRA, J. A. 2011. Development and characterization of an environmentally friendly process sequence (autohydrolysis and organosolv) for wheat straw delignification. *Applied biochemistry and biotechnology*, 164, 629-641.

RUSSELL, J. A., MILLER, R. K. & MOLTON, P. M. 1983. Formation of aromatic compounds from condensation reactions of cellulose degradation products. *Biomass*, 3, 43-57.

SAMI, M., ANNAMALAI, K. & WOOLDRIDGE, M. 2001. Co-firing of coal and biomass fuel blends. *Progress in Energy and Combustion Science*, 27, 171-214.

SATHE, C., PANG, Y. & LI, C.-Z. 1999. Effects of Heating Rate and Ion-Exchangeable Cations on the Pyrolysis Yields from a Victorian Brown Coal. *Energy & Fuels*, 13, 748-755.

SELIG, M. J., VIAMAJALA, S., DECKER, S. R., TUCKER, M. P., HIMMEL, M. E. & VINZANT, T. B. 2007. Deposition of lignin droplets produced during dilute acid pretreatment of maize stems retards enzymatic hydrolysis of cellulose. *Biotechnology progress*, 23, 1333-1339.

SENNECA, O., CHIRONE, R. & SALATINO, P. 2004. Oxidative pyrolysis of solid fuels. *Journal of Analytical and Applied Pyrolysis*, 71, 959-970.

- SHARMA, R. K., WOOTEN, J. B., BALIGA, V. L., LIN, X., GEOFFREY CHAN, W. & HAJALIGOL, M. R. 2004. Characterization of chars from pyrolysis of lignin. *Fuel*, 83, 1469-1482.
- SHAW, M. D., KARUNAKARAN, C. & TABIL, L. G. 2009. Physicochemical characteristics of densified untreated and steam exploded poplar wood and wheat straw grinds. *Biosystems Engineering*, 103, 198-207.
- SHEN, D. K., GU, S. & BRIDGWATER, A. V. 2010. Study on the pyrolytic behaviour of xylan-based hemicellulose using TG-FTIR and Py-GC-FTIR. *Journal of Analytical and Applied Pyrolysis*, 87, 199-206.
- SHUANGNING, X., ZHIHE, L., BAOMING, L., WEIMING, Y. & XUEYUAN, B. 2006. Devolatilization characteristics of biomass at flash heating rate. *Fuel*, 85, 664-670.
- SIMONE, M., BIAGINI, E., GALLETI, C. & TOGNOTTI, L. 2009. Evaluation of global biomass devolatilization kinetics in a drop tube reactor with CFD aided experiments. *Fuel*, 88, 1818-1827.
- SIMONS, G. A. 1983. The role of pore structure in coal pyrolysis and gasification. *Progress in Energy and Combustion Science*, 9, 269-290.
- SJOSTROM, E. 2013. *Wood chemistry: fundamentals and applications*, Elsevier.
- SMITH, I. Year. The combustion rates of coal chars: a review. In: *Symposium (International) on Combustion*, 1982. Elsevier, 1045-1065.
- SMITH, K. L., SMOOT, L. D., FLETCHER, T. H. & PUGMIRE, R. J. 2013. *The structure and reaction processes of coal*, Springer Science & Business Media.
- SMITH, W. & POLLEY, M. 1956. The Oxidation of Graphitized Carbon Black. *The Journal of Physical Chemistry*, 60, 689-691.

SMOOT, L. D. 1993. Fundamentals of coal combustion: for clean and efficient use, Elsevier.

SOLOMON, P. R. 1981. Relation between coal aromatic carbon concentration and proximate analysis fixed carbon. *Fuel*, 60, 3-6.

SOLOMON, P. R., SERIO, M. A. & SUUBERG, E. M. 1992. Coal pyrolysis: experiments, kinetic rates and mechanisms. *Progress in Energy and Combustion Science*, 18, 133-220.

SPACKMAN, W. 1958. SECTION OF GEOLOGY AND MINERALOGY: THE MACERAL CONCEPT AND THE STUDY OF MODERN ENVIRONMENTS AS A MEANS OF UNDERSTANDING THE NATURE OF COAL*. *Transactions of the New York Academy of Sciences*, 20, 411-423.

SPIRO, C. L., MCKEE, D. W., KOSKY, P. G. & LAMBY, E. J. 1983. Catalytic CO₂-gasification of graphite versus coal char. *Fuel*, 62, 180-184.

STACH, E. 1982. *Stach's Textbook of Coal Petrology*, Borntraeger.

STEER, J., MARSH, R., GRIFFITHS, A., MALMGREN, A. & RILEY, G. 2013. Biomass co-firing trials on a down-fired utility boiler. *Energy Conversion and Management*, 66, 285-294.

STEFANIDIS, S. D., KALOGIANNIS, K. G., ILIOPOULOU, E. F., MICHAILOF, C. M., PILAVACHI, P. A. & LAPPAS, A. A. 2014. A study of lignocellulosic biomass pyrolysis via the pyrolysis of cellulose, hemicellulose and lignin. *Journal of Analytical and Applied Pyrolysis*, 105, 143-150.

STOPES, M. C. 1935. On the petrology of banded bituminous coals. *Fuel*, 14, 4-13.

STREET, P. J., WEIGHT, R. P. & LIGHTMAN, P. 1969. Further investigations of structural changes occurring in pulverized coal. *Fuel*, 48, 343-365.

SU, S., POHL, J. H., HOLCOMBE, D. & HART, J. 2001. A proposed maceral index to predict combustion behavior of coal. *Fuel*, 80, 699-706.

SU, S., POHL, J. H., HOLCOMBE, D. & HART, J. A. 2001. Techniques to determine ignition, flame stability and burnout of blended coals in p.f. power station boilers. *Progress in Energy and Combustion Science*, 27, 75-98.

SUÁREZ-RUIZ, I., FLORES, D., MENDONÇA FILHO, J. G. & HACKLEY, P. C. 2012. Review and update of the applications of organic petrology: Part 1, geological applications. *International Journal of Coal Geology*, 99, 54-112.

SULLIVAN, A. L. & BALL, R. 2012. Thermal decomposition and combustion chemistry of cellulosic biomass. *Atmospheric Environment*, 47, 133-141.

SUZUKI, S., SHINTANI, H., PARK, S.-Y., SAITO, K., LAEMSAK, N., OKUMA, M. & IYAMA, K. 1998. Preparation of binderless boards from steam exploded pulps of oil palm (*Elaeis guineensis* Jaxq.) fronds and structural characteristics of lignin and wall polysaccharides in steam exploded pulps to be discussed for self-bindings. *Holzforschung-International Journal of the Biology, Chemistry, Physics and Technology of Wood*, 52, 417-426.

TEICHMÜLLER, M. 1989. The genesis of coal from the viewpoint of coal petrology. *International Journal of Coal Geology*, 12, 1-87.

SUTTON, D., KELLEHER, B. & ROSS, J. R. 2001. Review of literature on catalysts for biomass gasification. *Fuel Processing Technology*, 73, 155-173.

THOMAS, C. G., GOSNELL, M. E., GAWRONSKI, E., PHONT-ANANT, D. & SHIBAOKA, M. 1993. The behaviour of inertinite macerals under pulverised fuel (pf) combustion conditions. *Organic Geochemistry*, 20, 779-788.

TOLVANEN, H., KOKKO, L. & RAIKO, R. 2013. Fast pyrolysis of coal, peat, and torrefied wood: Mass loss study with a drop-tube reactor, particle geometry analysis, and kinetics modeling. *Fuel*, 111, 148-156.

UNITED NATIONS FRAMEWORK; CONVENTION ON CLIMATE CHANGE (UNFCCC), 2005. Clarifications on definition of biomass and consideration of changes in carbon pools due to a CDM project activity." EB20 Report, Appendix 8.

VAN DER STELT, M. J. C., GERHAUSER, H., KIEL, J. H. A. & PTASINSKI, K. J. 2011. Biomass upgrading by torrefaction for the production of biofuels: A review. *Biomass and Bioenergy*, 35, 3748-3762.

VAN DAM, J. E., VAN DEN OEVER, M. J., TEUNISSEN, W., KEIJSERS, E. R. & PERALTA, A. G. 2004. Process for production of high density/high performance binderless boards from whole coconut husk: Part 1: Lignin as intrinsic thermosetting binder resin. *Industrial Crops and Products*, 19, 207-216.

VANHOLME, R., DEMEDTS, B., MORREEL, K., RALPH, J. & BOERJAN, W. 2010. Lignin Biosynthesis and Structure. *Plant Physiology*, 153, 895-905.

VASSILEV, S. V., BAXTER, D., ANDERSEN, L. K. & VASSILEVA, C. G. 2010. An overview of the chemical composition of biomass. *Fuel*, 89, 913-933.

VASSILEV, S. V., BAXTER, D., ANDERSEN, L. K., VASSILEVA, C. G. & MORGAN, T. J. 2012. An overview of the organic and inorganic phase composition of biomass. *Fuel*, 94, 1-33.

VILLAVERDE, J. J., LI, J., EK, M., LIGERO, P. & DE VEGA, A. 2009. Native Lignin Structure of *Miscanthus x giganteus* and Its Changes during Acetic and Formic Acid Fractionation. *Journal of Agricultural and Food Chemistry*, 57, 6262-6270.

VLEESKENS, J. Year. Combustion efficiency and petrographic properties. In: International conference on coal science, 1983. 599-602.

WANG, B., SUN, L., SU, S., XIANG, J., HU, S. & FEI, H. 2012. Char Structural Evolution during Pyrolysis and Its Influence on Combustion Reactivity in Air and Oxy-Fuel Conditions. *Energy & Fuels*.

WANG, J., ZHANG, M., CHEN, M., MIN, F., ZHANG, S., REN, Z. & YAN, Y. 2006. Catalytic effects of six inorganic compounds on pyrolysis of three kinds of biomass. *Thermochimica Acta*, 444, 110-114.

WANG, Z., PECHA, B., WESTERHOF, R. J., KERSTEN, S. R., LI, C.-Z., MCDONALD, A. G. & GARCIA-PEREZ, M. 2014. Effect of cellulose crystallinity on solid/liquid phase reactions responsible for the formation of carbonaceous residues during pyrolysis. *Industrial & Engineering Chemistry Research*, 53, 2940-2955.

WHITE, J. E., CATALLO, W. J. & LEGENDRE, B. L. 2011. Biomass pyrolysis kinetics: A comparative critical review with relevant agricultural residue case studies. *Journal of Analytical and Applied Pyrolysis*, 91, 1-33.

WILLIAMS, A., BACKREEDY, R., HABIB, R., JONES, J. M. & POURKASHANIAN, M. 2002. Modelling coal combustion: the current position. *Fuel*, 81, 605-618.

WILLIAMS, A., JONES, J. M., MA, L. & POURKASHANIAN, M. 2012. Pollutants from the combustion of solid biomass fuels. *Progress in Energy and Combustion Science*, 38, 113-137.

WOOTEN, J. B., SEEMAN, J. I. & HAJALIGOL, M. R. 2004. Observation and Characterization of Cellulose Pyrolysis Intermediates by ¹³C CPMAS NMR. A New Mechanistic Model. *Energy & Fuels*, 18, 1-15.

WORNAT, M. J., HURT, R. H., DAVIS, K. A. & YANG, N. Y. C. 1996. Single-particle combustion of two biomass chars. *Symposium (International) on Combustion*, 26, 3075-3083.

WORNAT, M. J., HURT, R. H., YANG, N. Y. C. & HEADLEY, T. J. 1995. Structural and compositional transformations of biomass chars during combustion. *Combustion and Flame*, 100, 131-143.

- XU, M. & SHENG, C. 2012. Influences of the Heat-Treatment Temperature and Inorganic Matter on Combustion Characteristics of Cornstalk Biochars. *Energy & Fuels*, 26, 209-218.
- YANG, H., YAN, R., CHEN, H., LEE, D. H. & ZHENG, C. 2007. Characteristics of hemicellulose, cellulose and lignin pyrolysis. *Fuel*, 86, 1781-1788.
- YANG, H., YAN, R., CHEN, H., ZHENG, C., LEE, D. H. & LIANG, D. T. 2006. In-Depth Investigation of Biomass Pyrolysis Based on Three Major Components: Hemicellulose, Cellulose and Lignin. *Energy & Fuels*, 20, 388-393.
- YIP, K., NG, E., LI, C.-Z., HAYASHI, J.-I. & WU, H. 2011. A mechanistic study on kinetic compensation effect during low-temperature oxidation of coal chars. *Proceedings of the Combustion Institute*, 33, 1755-1762.
- YOUNG, B. & SMITH, I. 1989. The combustion of Loy Yang brown coal char. *Combustion and Flame*, 76, 29-35.
- YUH, S. J. & WOLF, E. E. 1983. FTIR studies of potassium catalyst-treated gasified coal chars and carbons. *Fuel*, 62, 252-255.
- ZILM, K. W., PUGMIRE, R. J., LARTER, S. R., ALLAN, J. & GRANT, D. M. 1981. Carbon-13 CP/MAS spectroscopy of coal macerals. *Fuel*, 60, 717-722.
- ZOLIN, A., JENSEN, A., JENSEN, P. A., FRANSEN, F. & DAM-JOHANSEN, K. 2001. The Influence of Inorganic Materials on the Thermal Deactivation of Fuel Chars. *Energy & Fuels*, 15, 1110-1122.